Biological Research

is the continuation since 1992 of
ARCHIVOS DE BIOLOGÍA Y MEDICINA EXPERIMENTALES
founded in 1964
Founding Editor:
Jorge Mardones
Past Editors:
Tito Ureta,
Patricio Zapata,
Manuel Krauskopf
Jorge Garrido

This Journal is the official organ of the SOCIEDAD DE BIOLOGÍA DE CHILE
Legal personality Nº 2.521 (4.6.54)
RUT 70-397.400-7
Legal address: Canadá 308
Santiago 9, Chile
(Legal Advisor and Representative)
Jaime Altamirano P.

This journal is partly subsidized by the "Funds for Publication of Scientific Journals" of the National Comission of Scientific and Technological Research (CONICYT), Chile

Yearly subscription US$ 250
Payable to
Sociedad de Biología de Chile

Correspondence to
BIOLOGICAL RESEARCH
Sociedad de Biología de Chile
Canadá 253, piso 3º, Dpto. F.
PO Box 16164, Santiago, Chile
Fax (56-2) 225 8427
Phone (56-2) 209 3503
E-mail socbiol@biologiachile.cl
Internet: www.biologiachile.cl

Indexed by Scielo, Medline, Biosis, Embase, Lilacs, Periodica, Research Alert, Science Citation Index Expanded (ISI), Web of Science (ISI)

Abstracted in Biological Abstracts, Excerpta Medica, Index Medicus and Medlars

ISSN: 0716-9760
ISSN electronic version: 0717-6287

Editor-in-Chief

Dr. Manuel J. Santos
Pontificia Universidad Católica de Chile
Santiago, Chile.

Associate Editors

Dr. Ricardo Moreno Pontificia Universidad Católica de Chile, Chile.
Dr. Gloria Montenegro Pontificia Universidad Católica de Chile, Chile.
Dra. Victoria Velarde Pontificia Universidad Católica de Chile, Chile.
Dra. Rosalba Lagos Universidad de Chile, Chile.
Dr. Christian González Universidad de Chile, Chile.
Dr. Mauricio González Universidad de Chile, Chile

Assistants to the Editors

Yolanda Zambrano (Production)
Sociedad de Biología de Chile
Lafayete Eaton (Editing Proofreading)
Sociedad de Biología de Chile

Editorial Board

Oscar Burrone International Centre for Genetic Engineering and Biotechnology (ICGEB) Trieste, Italy.
Enrique Brandan Pontificia Universidad Católica de Chile, Chile.
Néstor Bianchi Instituto Multidisciplinario de Biología Celular (IMBICE) La Plata, Argentina
Philipe Bouvet École Normale Supérieure du Lyon, France.
Francisco Bozinovic Pontificia Universidad Católica de Chile, Chile.
Juan José Cazzulo Universidad Nacional San Martín, Argentina.
Víctor Cifuentes Universidad de Chile, Chile.
Inés Contreras Universidad de Chile, Chile
Leopoldo De Meis Universidad Federal Río de Janeiro, Brazil.
Sonia Dietrich Institute of Botany, São Paulo, Brazil.
Raúl Fernández Donoso Universidad de Chile, Chile.
Gonzalo Gajardo Universidad de Los Lagos, Chile.
Joan Guinovart Universidad de Barcelona, Spain.
Cecilia Hidalgo Universidad de Chile, Chile.
Luis Felipe Hinojosa Universidad de Chile, Chile.
Carlos Hirschberg Boston University, U.S.A.
Tsuneo Imanaka Toyama University, Japan.
Nibaldo Inestrosa Pontificia Universidad Católica de Chile, Chile.
Ramón Latorre Centro de Neurociencia de Valparaíso, Chile.
Sergio Lavandero Universidad de Chile, Chile.
Lisette Leyton Universidad de Chile, Chile.
Martín Montecino Universidad de Concepción, Chile.
Juan Olate Universidad de Concepción, Chile.
Adrián Palacios Universidad de Valparaíso, Chile.
Manuel Rieber Instituto Venezolano de Investigaciones Científicas (IVIC), Venezuela.
Gloria Riquelme Universidad de Chile, Chile.
Flavio Salazar O. Universidad de Chile, Chile.
José Luis Santos Universidad de Chile, Chile.
M.A.Q. Siddiqui State University of New York, U.S.A.
Eugenio Spencer Universidad de Santiago de Chile, Chile.
Marc Thiry Université de Liège, Belgium.
Carlos Valenzuela Universidad de Chile, Chile
Pablo Valenzuela Fundación Ciencia para la Vida, Chile.
Claudio Vásquez Universidad de Santiago de Chile, Chile.

Directorio Sociedad de Biología de Chile 2013-2014

Mesa Directiva

Dra. Rosalba Lagos
Presidenta
Facultad de Ciencias
Universidad de Chile
Las Palmeras 3425
Fono: 56-2-9787348
rolagos@uchile.cl

Dr. Rodrigo Iturriaga
Vicepresidente
Facultad de Ciencias Biológicas
P. Universidad Católica de Chile
Alameda 340
Fono: 56-2-23542852
riturriaga@bio.puc.cl

Dr. Patricio Ojeda
Past president
Facultad de Ciencias Biológicas
P. Universidad Católica de Chile
Alameda 340
Fono: 56-2-3542879
pojeda@bio.puc.cl

Dr. Héctor Toledo
Tesorero
Facultad de Medicina
Universidad de Chile
Independencia 1027
Fono: 56-2-9786053
htoledo@med.uchile.cl

Dr. Gino Corsini A.
Secretario
Facultad de Medicina
Universidad Diego Portales
Av. Ejército 141
Fono: 56-2-2676 2931
gino.corsini@mail.udp.cl

Dr. Ricardo Moreno
Director
Facultad de Ciencias Biológicas
P. Universidad Católica de Chile
Alameda 340
Fono: 56-2-23542885
rmoreno@bio.puc.cl

Dr. Alejandro Roth
Director
Facultad de Ciencias
Universidad de Chile
Las Palmeras 3425
Fono: 56-2-2978 7407
alejroth@uchile.cl

Presidentes de Sociedades Afiliadas

Sociedad de Ecología de Chile
Dr. Marco Lardies
Universidad Adolfo Ibáñez
Fono 56-2-3311583
marco.lardies@uai.cl

Sociedad de Biología Celular de Chile
Dr. Mauricio González
INTA
Universidad de Chile
Fono: 56-2-29781511
E-mail: mgonzale@inta.uchile.cl

Sociedad de Bioquímica y Biología Molecular de Chile
Dr. Sergio Lavandero
Facultad de Ciencias Químicas y Farmacéuticas
Universidad de Chile
Fono: 56-2-29782903
E-mail: slavander@uchile.cl

Sociedad de Reproducción y Desarrollo
Dra. Ilona Concha
Facultad de Ciencias
Universidad Austral de Chile
Fono: 56-63-221795
E-mail:conchagrabinger@uauch.cl

Sociedad de Botánica de Chile
Dra. Gloria Rojas Villegas
Museo Nacional de Historia Natural
Teléfono: 56-02-6804619
E-mail:grojas@mnhn.cl

Sociedad de Farmacología de Chile
Dr. Juan Carlos Prieto
Facultad de Medicina
Universidad de Chile
Fono 56-2-9786044
E-mail: jprieto@med.uchile.cl

Sociedad Chilena de Ciencias Fisiológicas
Dr. Julio Alcayaga
Facultad de Ciencias
Universidad de Chile
Fono: 56-2-9787366
E-mail: jalcayag@uchile.cl

Sociedad de Microbiología de Chile
Dr. Nicolas Guiliani
Facultad de Ciencias
Universidad de Chile
Fono: 56-2-29787241
E-mail:nguilian@uchile.cl

Sociedad de Genética de Chile
Dr. Mauricio Moraga
Facultad de Medicina
Universidad de Chile
Fono: 56-2 29786599
E-mail: mmoraga@med.uchile.cl

Sociedad Chilena de Inmunología
Dr. Angel Oñate
Facultad de Ciencias Biológicas
Universidad de Concepción
Fono: 56-41-2204118
E-mail: aonate@udec.cl

Sociedad Chilena de Evolución
Dr. Marco Méndez
Facultad de Ciencias
Universidad de Chile
Fono: 56-2-29781552
E-mail: mmendez@uchile.cl

Sociedad Chilena de Neurociencia
Dr. Alan Neely
Facultad de Ciencias,
Universidad de Valparaíso
Fono: 56-32-2508040
E-mail: alan.neely@uv.cl

Secciones

Sección Zoología
Mauricio Canals

Biological Research

2013 - vol. 46 - nº 1

Review Article

Biol Res 46: 5-11, 2013

Exosomes: mediators of communication in eukaryotes

María A. Lopez-Verrilli[1]* and Felipe A. Court[1,2]*

[1] Millennium Nucleus for Regenerative Biology, P. Catholic University of Chile, Santiago, Chile
[2] NeuroUnion Biomedical Foundation, Santiago, Chile

ABSTRACT

In addition to the established mechanisms of intercellular signaling, a new way of communication has gained much attention in the last decade: communication mediated by exosomes. Exosomes are nanovesicles (with a diameter of 40-120 nm) secreted into the extracellular space by the multivesicular endosome after its outer membrane fuses with the plasma membrane. Once released, exosomes modulate the response of the recipient cells that recognize them. This indicates that exosomes operate in a specific manner and participate in the regulation of the target cell. Remarkably, exosomes occur from unicellular organisms to mammals, suggesting an evolutionarily conserved mechanism of communication. In this review we describe the cascade of exosome formation, intracellular traffic, secretion, and internalization by recipient cells, and review their most relevant effects. We also highlight important steps that are still poorly understood.

Key words: Exosome, nanovesicle, intercellular communication.

INTRODUCTION

Cell-cell communication is imperative for life. There are different pathways of intercellular communication, such as the expression of signalling molecules on plasma membranes or the secretion of soluble ligands (Grimmelikhuijzen and Hauser, 2012), gap junctions and tunneling nanotubes that allow electrical and metabolic coupling among cells (Abounit and Zurzolo, 2012; Orellana et al., 2012). In addition to these modes of communication, cells release membrane vesicles into the extracellular environment that affect target cells (Simons and Raposo, 2009).

In the 1980s, the groups of Stahl and Johnstone described the secretion of nano-sized vesicles during reticulocyte maturation (Harding et al., 1983; Pan et al., 1985). These vesicles were named exosomes and were thought to be necessary to remove unneeded proteins from cells (Johnstone et al., 1987). Later, Raposo et al. described that exosomes had antigen-presenting capacity (Raposo et al., 1996). Thereafter, the study of functional effects of exosomes has grown steadily (Simons and Raposo, 2009; Thery et al., 2009; Record et al., 2011; Pant et al., 2012).

Exosome release has been shown in eukaryotes, from microorganisms up to mammals. For example, they are secreted by protists like *Dictyostelium discoideum* (Lavialle et al., 2009) and *Trypanosoma cruzi* (Bayer-Santos et al., 2012), fungi (Rodrigues et al., 2011), plants (Regente et al., 2012), and animals from invertebrates such as *Drosophila melanogaster* (Korkut et al., 2009; Beckett et al., 2012; Gross et al., 2012) and *Caenorhabditis elegans* (Liegeois et al., 2006) to vertebrates (Record et al., 2011).

As depicted in figure 1, four sequential steps have been described in the literature for exosome-mediated communication. To date, this cascade comprising exosome formation, intracellular traffic, secretion and internalization by recipient cells, has been best characterized in immune cells (Thery et al., 2009; Bobrie et al., 2011) while the information in other cell types is fragmented. Considering this, we propose that communication mediated by exosomes between cells must have been conserved throughout evolution, although how this pathway may have evolved is not yet known. In this review we aim to illustrate the current state of knowledge of this particular way of cellular communication.

EXOSOME-MEDIATED COMMUNICATION

1. Exosome biogenesis

Multivesicular endosomes (MVE, also called multivesicular bodies or MVB) give rise to exosomes as follows. The membrane of late endosomes invaginates and forms small vesicles that are pinched off into the endosomal space. These are the intralumenal vesicles (ILV) and the whole is the MVE (Fig. 1A). Notice that the internal face of an ILV membrane corresponds to the cytoplasmic face of the endosome limiting membrane, and the content of the ILV is originated from the cytosol prior to ILV formation. This anatomical fact has functional relevance for exosomes. A set of MVEs fuse their limiting membranes to the plasma membrane and the ILVs with their cargo into the extracellular space. These secreted vesicles are exosomes (Fig. 1B-C) (Simons and Raposo, 2009).

Formation of ILVs in the late endosome involves the endosomal sorting complex required for transport (ESCRT) proteins (Babst, 2011). ESCRT proteins are components of four ESCRT complexes, ESCRT-0, ESCRT-I, ESCRT-II, and ESCRT-III (Hanson et al., 2009). Each of these complexes is sequentially and transiently recruited to the forming MVE until a vesicle is fully shaped and released as an ILV into the endosomal space (Hurley and Emr, 2006). However, increasing evidence suggests that some lipids such as ceramide may play a key role in ILV formation, independently of ESCRT complexes (Trajkovic et al., 2008; Babst, 2011).

As mentioned above, a set of MVE fuse with the plasma membrane while other MVEs follow a degradative route and

* Corresponding authors: María A. Lopez-Verrilli and Felipe A. Court , Department of Physiology, Faculty of Biology, Pontificia Universidad Católica de Chile, Av. B. O'Higgins 340/Casilla 114-D, Santiago 8331150, Chile. Phone: (00562) 686 2899, Fax: (00562) 354 1850, e-mail: alejanddra@gmail.com; fcourt@bio.puc.cl

Received: December 24, 2012. In Revised form: January 29, 2013. Accepted: February 1, 2013

fuse with lysosomes. This pathway leads to the degradation of ILVs content. Which are the mechanisms that guide MVE fusion with the plasma membrane or with lysosomes? Evidence to date is incomplete but supports the existence of different populations of MVEs (White et al., 2006) and/or different subpopulations of ILVs within a pool of common MVEs. Accordingly, MVEs rich in Rab7 GTPase and ILVs containing phosphatidylinositol-3-phosphate and ubiquitinated proteins are sorted to lysosomes (Vanlandingham and Ceresa, 2009). Conversely, MVEs rich in Rab11 GTPase and ILVs with high amounts of ceramide are sorted for exosome secretion (Zerial and McBride, 2001; Savina et al., 2005). Rab GTPases coordinate intracellular traffic, such as vesicle formation, transport and fusion with the target membranes (Zerial and McBride, 2001). In this way, the recruitment of specific Rabs and their effectors to MVEs membrane directs their final destination towards degradation or exosome secretion.

2. Loading of exosomes

In eukaryotes, most secreted proteins use the endoplasmic reticulum/Golgi-dependent secretory pathway (Keller and Simons, 1997). These proteins have a signal peptide which directs their fate towards the exocytic route (Nickel, 2005). However, proteins that follow unconventional secretory pathways, such as the exosome-mediated route, do not use this signal peptide. What commands the secretion of cellular components within vesicles and how are molecules sorted into exosomes? Ubiquitination is the best characterized signal that commands protein sorting into ILVs, for both cytosolic proteins and the cytosolic tail of membrane receptors (Baietti et al., 2012). Ubiquitinated-proteins interact sequentially with the ESCRT complex and with specific domains of late endosomes. This leads to the invagination of the late endosome membrane together with the tagged-protein and the final formation of an ILV (Babst, 2011; MacDonald et al., 2012). However, some non-ubiquitinated proteins such as the transferrin receptor interact with the ESCRT complex and are sorted into exosomes, suggesting that different protein interactions can provide access to ESCRT processing (Marsh and van Meer, 2008). In fact, an alternative mechanism to ubiquitin-tagging has been recently described for a plasma membrane receptor (Baietti et al., 2012). Syndecans –transmembrane proteins that offer heparin sulphate to the cell surface– recruit the fibroblast growth factor receptor into MVEs. To achieve this, the cytosolic domain of syndecan interacts with the adaptor protein syntenin which in turn connects syndecans to Alix, an auxiliary component of the ESCRT machinery. This syndecan-syntenin-Alix pathway leads to the exosome secretion of fibroblast growth factor receptor (Baietti et al., 2012). It remains to be explored whether this new pathway is sufficient to recruit other plasma receptors, such as the transferrin receptor, into exosomes.

Finally, tetraspanins –evolutionarily conserved transmembrane proteins– have been proposed to mediate molecule sorting into ILVs (Rana and Zoller, 2011). Tetraspanins form microdomains in the cell surface by interacting between themselves and a large variety of transmembrane and cytosolic proteins and participate in

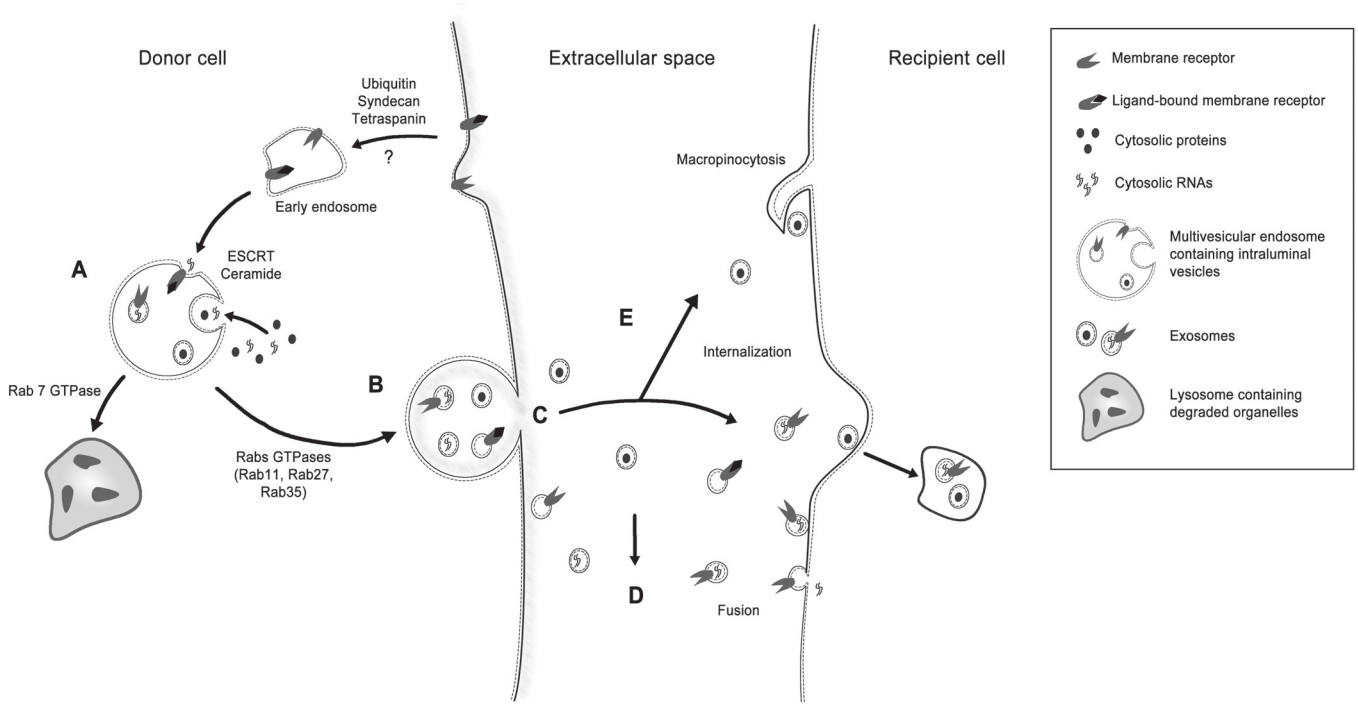

Figure 1. Sequential steps necessary for exosome-mediated communication. Intralumenal vesicles (ILV) are formed after the invagination of the multivesicular endosome membrane. These ILVs are loaded with specific cargo originated from the plasma membrane and/or the cytoplasm (A). Notice that the internal face of an ILV membrane corresponds to the cytoplasmic face of the endosome limiting membrane, and the ILV is loaded with cytosolic components. Upon fusion of the MVE with the plasma membrane (B), ILV are secreted as exosomes (C). Exosomes can be lost (D) or taken up by target cells (E) by fusion, or internalization mediated by surface molecules or by macropinocytosis. Additional abbreviation: ESCRT, endosomal sorting complex required for transport.

vesicular traffic (Levy and Shoham, 2005). Although this field is quite speculative to date, exosomes from all cell types are enriched in tetraspanins, thus they are plausible candidates to mediate selective cargo recruitment into these vesicles.

The sorting process of protein complexes into ILVs is a highly regulated mechanism. Most proteins secreted by exosomes derive from parent cell membranes, the cytosol or the Golgi, but rarely the endoplasmic reticulum or mitochondria. Some of the proteins sorted into ILV participate in antigen presentation (MHC-I, MHC-II), cell adhesion (integrins), cell structure and motility (actins, tubulin, myosin, etc.), stress regulators (heat shock proteins 70 and 90), metabolic enzymes (b-enolase, peroxidases, pyruvate kinase) proteins of ESCRT machinery, proteins of the signalling cascade (kinases), tetraspanins (CD9, CD63, CD81, CD82), proteins involved in transcription and protein synthesis (histones, ribosomal proteins, ubiquitin), and proteins involved in trafficking and membrane fusion (Rabs, annexins) (Lakkaraju and Rodriguez-Boulan, 2008). Additionally, cytosolic proteins remain in the lumen of exosomes and those derived from the plasma membrane remain in the vesicle membrane, maintaining the same topology they had in the cell, with potential roles in sequestering soluble ligands (Pan et al., 1985; Thery et al., 2009).

Although exosomes were originally described in 1980's, interest in these vesicles was renewed in recent years when exosomes were reported to contain functional mRNA and microRNA (Valadi et al., 2007). The functional consequences of transfer of genetic material include the induction, amplification and/or modulation of immune responses, as well as acquisition of new functional properties in other recipient cells. For example, glioblastoma cells carrying EGFRvIII mRNA have been shown to stimulate tubule formation in endothelial cells and proliferation of glioblastoma cells, thereby promoting acquisition of the angiogenic phenotype and metastatic abilities (Skog et al., 2008). Exosomes have been shown to be highly enriched in defined mRNA species compared to their distributions in the donor cell (Skog et al., 2008). This fact supports the existence of a sorting mechanism, but it has not been characterized so far.

Exosomes contain not only proteins and nucleic acids but also a specific lipid composition; they are rich in cholesterol, sphingomyelin and ceramide; and they also exhibit phosphatidylserine (Thery et al., 2009). Interestingly, bioactive lipids such as prostaglandins are also sorted into exosomes (Subra et al., 2010). ExoCarta –a free to use web-database of proteins, RNA and lipids identified in exosomes– has been compiled and reveals molecules that are more often found in exosomes and those that are specific to certain cell types (http://www.exocarta.org) (Mathivanan and Simpson, 2009).

In conclusion, the effort to characterize the composition of exosomes has been largely successful but the data on a mechanism to recruit the cargo have been meager. This shows a clear need to characterize the interactions between proteins, lipids and RNAs that allow specific cargo packaging into exosomes.

3. Secretion of exosomes

The secretion of exosomes has been described both *in vivo* and *in vitro* as a non-conventional secretory mechanism (Nickel, 2005). As mentioned above, once the MVEs fuse with the plasma membrane, ILVs are secreted as exosomes (Fig. 1C). Electron microscopy analysis of exosomes show a cup-shaped morphology and a size between 40-120 nm (Simons and Raposo, 2009). Exosomes have been isolated *in vitro* but also *in vivo* in bodily fluids such as blood, urine, breast milk, amniotic fluid, malignant ascites, bronchoalveolar lavage fluid and synovial fluid (Record et al., 2011).

Exosomes are released both constitutively and in a regulated manner. For example, B cells secrete detectable levels of exosomes only following the activation of a cell surface receptor (Saunderson et al., 2008) while most tumor cells constitutively secrete exosomes (Record et al., 2011). Importantly, distinct subpopulations of exosomes are secreted from polarized cells; apical and basolateral exosomes (Tauro et al., 2012). This indicates that exosome secretion can be even more complex, since a different mechanism may coexist in the cell to target exosome release to the appropriate membrane.

Intracellular calcium is a physiological second messenger in the secretion of exosomes (Savina et al., 2003; Faure et al., 2006). In murine macrophages, dendritic and neuroblastoma cells, activation of $P2X_7$ receptors (purinergic receptor P2X) by ATP increases intracellular calcium and also secretion of exosomes (Qu et al., 2009; Emmanouilidou et al., 2010). Pharmacological elevation of intracellular calcium also induces exosome secretion in cortical neurons, oligodendrocytes and erythroleukemia cells (Savina et al., 2003; Faure et al., 2006; Fruhbeis et al., 2012), which confirms the role of calcium as second order messenger. Together with a cytosolic calcium increase, the expression of Rab11 GTPase is needed for exosome secretion in erythroleukemia cells *in vitro* (Savina et al., 2005). In fact, calcium dependent-exosome secretion is enhanced when cells with low endogenous levels of the Rab11 are manipulated to overexpress this GTPase (Savina et al., 2005). Although the direct link between calcium and Rabs is missing, two other Rab proteins have been implicated in the fusion of MVE membrane to the plasma membrane of mammalian cells. For example, Rab35 is involved in the secretion of myelin protein-enriched exosomes in oligodendroglial cells and Rab27a/b but not Rab11 mediates MVE transport and docking to the plasma membrane in HeLa cells *in vitro* (Hsu et al., 2010; Ostrowski et al., 2010). Finally, in the motor nerve endings of the fly *D. melanogaster* exosome secretion is regulated by Rab11 but not by Rab27 or Rab35, while secretion of vesicles loaded with neurotransmitter required Rab3, which suggests a specific pathway for exosomes (Koles et al., 2012). These results reflect the variety of secretory pathways during exosome formation within a cell and in diverse cell types (Koles et al., 2012). Collectively, calcium and specific Rab GTPases participate in the fusion of MVEs to the plasma membrane as a step in the secretion of exosomes. Taken together, this evidence indicates that exosome secretion, besides being constitutive, is also regulated.

Eukaryotic cells have developed elaborate mechanisms of quality control within their classical ER/Golgi-dependent secretory pathway. It is likely that a quality control is also operating in the exosome pathway. However, the molecular machinery involved in the transport of MVEs to the plasma membrane, their docking and fusion to release exosomes is poorly understood.

4. Exosome uptake by recipient cells

Once in the extracellular space, exosomes may be eliminated (Fig. 1D). This fate is illustrated by their presence in urine

(Miranda et al., 2010). The biological significance of this elimination, if any, has not been explored. By contrast, exosomes have important effects on target cells (Fig. 1E). Interaction of exosomes with target cells follows two alternatives; endocytosis of the whole vesicle or and/or fusion with the plasma membrane. Membrane vesicles of all cellular origins express adhesion molecules on their surface, which could favor their endocytosis by recipient cells (Record et al., 2011). For example, surface molecules such as integrins, tetraspanins and phosphatidylserine in exosomes form complexes with cell surface molecules and participate in the attachment of exosomes, as studied in dendritic cells (Thery et al., 2009). In these cells, the whole exosome is internalized and sorted into recycling endosomes and then through late endosomes/lysosomes (Morelli et al., 2004). Co-incubation of exosomes and dendritic cells with specific antibodies to block various adhesion molecules reduces exosome internalization by these cells (Morelli et al., 2004). By this mechanism, dendritic cells process and then present to T lymphocytes peptides derived from the internalized exosomes. Alternatively, exosomes can be selectively internalized by macropinocytosis, a mechanism where macromolecules are taken by actin-membrane ruffles, and that does not necessarily depend on receptor-ligand interaction (Fitzner et al., 2011). On the other hand, fusion of exosomes has been shown to be a lipid-dependent process, in which a high content of sphingomyelin/ganglioside GM3 in exosomes is responsible for the increased fusion efficiency in tumor cells (Parolini et al., 2009), while

TABLE I

Representative findings of functional effects of exosomes in eukaryotes

Organism	Exosome source	Effect	References
Protists	Dictyostelium discoideum	Exosomes-like vesicles are secreted by D. discoideum migrating cells and coordinate cell migration. These vesicles have been proposed for drug carriers in cancer therapy.	(Kriebel et al. 2008; Lavialle et al. 2009)
	Leishmania donovani, Trypanosoma cruzi	Exosomes deliver parasite cargo into host cells and modulate the immune response.	(Silverman et al. 2010; Bayer-Santos et al. 2012)
Fungi	Histoplasma capsulatum, Cryptococcus neoformans	Fungal species secrete extracellular vesicles with similar composition to exosomes. These vesicles are involved in host-pathogen interactions.	(Albuquerque et al. 2008; Rodrigues et al. 2008)
Plants	Sunflower seeds, barley leaves	Isolation and characterization of exosomes from seed and leaved fluids.	(An et al. 2007; Regente et al. 2009)
Animals	Caenorhabditis elegans	Polarized secretion of morphogens mediated by exosomes.	(Liegeois et al. 2006)
	Drosophila melanogaster	Wnt morphogens secretion during development.	(Korkut et al. 2009; Beckett et al. 2012; Gross et al. 2012)
	Mammalian cells	Antigen presenting capacity	First functional effect: (Raposo et al. 1996) Others: (Mittelbrunn et al. 2011; Huan et al. 2012)
		Exosomes contain mRNA and microRNA that can be transferred to other cells where they are functional.	First antecedent: (Valadi et al. 2007) Others: (Lasser et al. 2011; Gallo et al. 2012)
		"Trojan horses" for pathogens propagation:	
		– Prions	– (Fevrier et al. 2004; Vella et al. 2008)
		– Virus	– (Barreto et al. 2010; Lenassi et al. 2010)
		– Bacteria	– (Yang et al. 2012)
		Spread of neurodegenerative diseases.	(Emmanouilidou et al. 2010; Saman et al. 2012)
		Antitumoral effects.	(Zhang et al. 2011; Lv et al. 2012)
		Pro-angiogenic, pro-metastasic.	(Al-Nedawi et al. 2008; Peinado et al. 2012)
		Biomarkers for cancer diagnosis and prognosis.	(Skog et al. 2008; Miranda et al. 2010; Khan et al. 2012)
		Future therapy models.	(Alvarez-Erviti et al. 2011; Zhuang et al. 2011)
		Tolerogenic pre-transplantation and anti-cancer vaccines	(Hartman et al. 2011; Rountree et al. 2011; Viaud et al. 2011; Li et al. 2012)

cholesterol-rich microdomains are necessary for dendritic cell exosome fusion with target cells (Montecalvo et al., 2012).

In any case, an important unanswered question in the field is how exosomes deliver their intralumenal content into the cytosol of the recipient cells.

5. Effect of exosome cargo on recipient cells

Since the discovery that exosomes participate in the cascade of antigen presentation (Raposo et al., 1996), this novel mechanism of intercellular communication has been implicated in various essential processes such as development (Korkut et al., 2009), immune responses (Thery et al., 2009), cancer and tumor metastasis (Peinado et al., 2012), and in the transmission of infectious agents like prions and viruses (Fevrier et al., 2004; Lenassi et al., 2010). Table I provides an overview of the most relevant findings of exosome functional effects in eukaryotes to date. It is worth mentioning that studies on exosomes other than mammalian cells are scant but still support the role of exosomes as a conserved mechanism of communication throughout evolution.

Finally, exosomes are promising tools to target drugs or biological material to specific cells across different biological barriers (O'Loughlin et al., 2012; Pant et al., 2012). For example, Alvarez-Erviti et al. (2011) obtained neuronal-targeted exosomes from genetically modified dendritic cells *in vitro* and loaded them with specific siRNA. After intravenous injection, these exosomes loaded with siRNA knocked down their target gene in brain neurons (Alvarez-Erviti et al., 2011). Thus, the possibility to deliver agents in a specific manner to defined target cells opens a wide avenue of research, even to overcome important challenges such as biological barriers, or tolerance to vesicles by using those derived from patient cells.

CONCLUSION

In this review we illustrate the sequential steps for exosome-mediated communication and compile the evidence supporting this role in eukaryotes. Although exosomes have been described in many cells from a wide variety of organisms, many important gaps remain concerning their formation cascade and their physiological relevance. Addressing these questions implies important challenges, such as the development of sensitive techniques to purify these nano-vesicles from small volumes of fluids and to determine precisely how and with what types of cells exosomes interact *in vivo*. The disclosure and growth of this research area will help to address these issues and lead to major advances in understanding exosomal functions as means for cell-to-cell communication.

ACKNOWLEDGMENTS

This work was supported by grants from FONDECYT no. 1110987 (FAC) and no. 3110014 (MALV) and Millenium Nucleus Nº P-07-011-F.

REFERENCES

ABOUNIT S, ZURZOLO C (2012) Wiring through tunneling nanotubes--from electrical signals to organelle transfer. J Cell Sci 125:1089-98.

ALBUQUERQUE PC, NAKAYASU ES, RODRIGUES ML, FRASES S, CASADEVALL A, ZANCOPE-OLIVEIRA RM, ALMEIDA IC, NOSANCHUK JD (2008) Vesicular transport in Histoplasma capsulatum: an effective mechanism for trans-cell wall transfer of proteins and lipids in ascomycetes. Cell Microbiol 10:1695-710.

AL-NEDAWI K, MEEHAN B, MICALLEF J, LHOTAK V, MAY L, GUHA A, RAK J (2008) Intercellular transfer of the oncogenic receptor EGFRvIII by microvesicles derived from tumour cells. Nat Cell Biol 10:619-24.

ALVAREZ-ERVITI L, SEOW Y, YIN H, BETTS C, LAKHAL S, WOOD MJ (2011) Delivery of siRNA to the mouse brain by systemic injection of targeted exosomes. Nat Biotechnol 29:341-5.

AN Q, VAN BEL AJ, HUCKELHOVEN R (2007) Do plant cells secrete exosomes derived from multivesicular bodies? Plant Signal Behav 2:4-7.

BABST M (2011) MVB vesicle formation: ESCRT-dependent, ESCRT-independent and everything in between. Curr Opin Cell Biol 23:452-7.

BAIETTI MF, ZHANG Z, MORTIER E, MELCHIOR A, DEGEEST G, GEERAERTS A, IVARSSON Y, DEPOORTERE F, COOMANS C, VERMEIREN E, ZIMMERMANN P, DAVID G (2012) Syndecan-syntenin-ALIX regulates the biogenesis of exosomes. Nat Cell Biol 14:677-85.

BARRETO A, RODRIGUEZ LS, ROJAS OL, WOLF M, GREENBERG HB, FRANCO MA, ANGEL J (2010) Membrane vesicles released by intestinal epithelial cells infected with rotavirus inhibit T-cell function. Viral Immunol 23:595-608.

BAYER-SANTOS E, AGUILAR-BONAVIDES C, RODRIGUES SP, CORDERO EM, MARQUES AF, VARELA-RAMIREZ A, CHOI H, YOSHIDA N, DA SILVEIRA JF, ALMEIDA IC (2012) Proteomic analysis of Trypanosoma cruzi secretome: characterization of two populations of extracellular vesicles and soluble proteins. J Proteome Res 107:9.

BECKETT K, MONIER S, PALMER L, ALEXANDRE C, GREEN H, BONNEIL E, RAPOSO G, THIBAULT P, BORGNE RL, VINCENT JP (2012) Drosophila S2 Cells Secrete Wingless on Exosome-Like Vesicles but the Wingless Gradient Forms Independently of Exosomes. Traffic (in Press).

BOBRIE A, COLOMBO M, RAPOSO G, THERY C (2011) Exosome secretion: molecular mechanisms and roles in immune responses. Traffic 12:1659-68.

EMMANOUILIDOU E, MELACHROINOU K, ROUMELIOTIS T, GARBIS SD, NTZOUNI M, MARGARITIS LH, STEFANIS L, VEKRELLIS K (2010) Cell-produced alpha-synuclein is secreted in a calcium-dependent manner by exosomes and impacts neuronal survival. J Neurosci 30:6838-51.

FAURE J, LACHENAL G, COURT M, HIRRLINGER J, CHATELLARD-CAUSSE C, BLOT B, GRANGE J, SCHOEHN G, GOLDBERG Y, BOYER V, KIRCHHOFF F, RAPOSO G, GARIN J, SADOUL R (2006) Exosomes are released by cultured cortical neurones. Mol Cell Neurosci 31:642-8.

FEVRIER B, VILETTE D, ARCHER F, LOEW D, FAIGLE W, VIDAL M, LAUDE H, RAPOSO G (2004) Cells release prions in association with exosomes. Proc Natl Acad Sci U S A 101:9683-8.

FITZNER D, SCHNAARS M, VAN ROSSUM D, KRISHNAMOORTHY G, DIBAJ P, BAKHTI M, REGEN T, HANISCH UK, SIMONS M (2011) Selective transfer of exosomes from oligodendrocytes to microglia by macropinocytosis. J Cell Sci 124:447-58.

FRUHBEIS C, FROHLICH D, KRAMER-ALBERS EM (2012) Emerging roles of exosomes in neuron-glia communication. Front Physiol 3:119.

GALLO A, TANDON M, ALEVIZOS I, ILLEI GG (2012) The majority of microRNAs detectable in serum and saliva is concentrated in exosomes. PLoS One 7:e30679.

GRIMMELIKHUIJZEN CJ, HAUSER F (2012) Mini-review: the evolution of neuropeptide signaling. Regul Pept 177 Suppl:S6-9.

GROSS JC, CHAUDHARY V, BARTSCHERER K, BOUTROS M (2012) Active Wnt proteins are secreted on exosomes. Nat Cell Biol 14:1036-45.

HANSON PI, SHIM S, MERRILL SA (2009) Cell biology of the ESCRT machinery. Curr Opin Cell Biol 21:568-74.

HARDING C, HEUSER J, STAHL P (1983) Receptor-mediated endocytosis of transferrin and recycling of the transferrin receptor in rat reticulocytes. J Cell Biol 97:329-39.

HARTMAN ZC, WEI J, GLASS OK, GUO H, LEI G, YANG XY, OSADA T, HOBEIKA A, DELCAYRE A, LE PECQ JB, MORSE MA, CLAY TM, LYERLY HK (2011) Increasing vaccine potency through exosome antigen targeting. Vaccine 29:9361-7.

HSU C, MOROHASHI Y, YOSHIMURA S, MANRIQUE-HOYOS N, JUNG S, LAUTERBACH MA, BAKHTI M, GRONBORG M, MOBIUS W, RHEE J, BARR FA, SIMONS M (2010) Regulation of exosome secretion by Rab35 and its GTPase-activating proteins TBC1D10A-C. J Cell Biol 189:223-32.

HUAN J, HORNICK NI, SKINNER AM, GOLOVIZNINA NA, ROBERTS CT, KURRE P (2013) RNA trafficking by acute myeloid leukemia exosomes. Cancer Res 73:918-29.

HURLEY JH, EMR SD (2006) The ESCRT complexes: structure and mechanism of a membrane-trafficking network. Annu Rev Biophys Biomol Struct 35:277-98.

JOHNSTONE RM, ADAM M, HAMMOND JR, ORR L, TURBIDE C (1987) Vesicle formation during reticulocyte maturation. Association of plasma membrane activities with released vesicles (exosomes). J Biol Chem 262:9412-20.

KELLER P, SIMONS K (1997) Post-Golgi biosynthetic trafficking. J Cell Sci 110 (Pt 24):3001-9.

KHAN S, JUTZY JM, VALENZUELA MM, TURAY D, ASPE JR, ASHOK A, MIRSHAHIDI S, MERCOLA D, LILLY MB, WALL NR (2012) Plasma-derived exosomal survivin, a plausible biomarker for early detection of prostate cancer. PLoS One 7:e46737.

KOLES K, NUNNARI J, KORKUT C, BARRIA R, BREWER C, LI Y, LESZYK J, ZHANG B, BUDNIK V (2012) Mechanism of evenness interrupted (Evi)-exosome release at synaptic boutons. J Biol Chem 287:16820-34.

KORKUT C, ATAMAN B, RAMACHANDRAN P, ASHLEY J, BARRIA R, GHERBESI N, BUDNIK V (2009) Trans-synaptic transmission of vesicular Wnt signals through Evi/Wntless. Cell 139:393-404.

KRIEBEL PW, BARR VA, RERICHA EC, ZHANG G, PARENT CA (2008) Collective cell migration requires vesicular trafficking for chemoattractant delivery at the trailing edge. J Cell Biol 183:949-61.

LAKKARAJU A, RODRIGUEZ-BOULAN E (2008) Itinerant exosomes: emerging roles in cell and tissue polarity. Trends Cell Biol 18:199-209.

LASSER C, ALIKHANI VS, EKSTROM K, ELDH M, PAREDES PT, BOSSIOS A, SJOSTRAND M, GABRIELSSON S, LOTVALL J, VALADI H (2011) Human saliva, plasma and breast milk exosomes contain RNA: uptake by macrophages. J Transl Med 9:9.

LAVIALLE F, DESHAYES S, GONNET F, LARQUET E, KRUGLIK SG, BOISSET N, DANIEL R, ALFSEN A, TATISCHEFF I (2009) Nanovesicles released by Dictyostelium cells: a potential carrier for drug delivery. Int J Pharm 380:206-15.

LENASSI M, CAGNEY G, LIAO M, VAUPOTIC T, BARTHOLOMEEUSEN K, CHENG Y, KROGAN NJ, PLEMENITAS A, PETERLIN BM (2010) HIV Nef is secreted in exosomes and triggers apoptosis in bystander CD4+ T cells. Traffic 11:110-22.

LEVY S, SHOHAM T (2005) The tetraspanin web modulates immune-signalling complexes. Nat Rev Immunol 5:136-48.

LI X, LI JJ, YANG JY, WANG DS, ZHAO W, SONG WJ, LI WM, WANG JF, HAN W, ZHANG ZC, YU Y, CAO DY, DOU KF (2012) Tolerance induction by exosomes from immature dendritic cells and rapamycin in a mouse cardiac allograft model. PLoS One 7:e44045.

LIEGEOIS S, BENEDETTO A, GARNIER JM, SCHWAB Y, LABOUESSE M (2006) The V0-ATPase mediates apical secretion of exosomes containing Hedgehog-related proteins in Caenorhabditis elegans. J Cell Biol 173:949-61.

LV LH, WAN YL, LIN Y, ZHANG W, YANG M, LI GL, LIN HM, SHANG CZ, CHEN YJ, MIN J (2012) Anticancer drugs cause release of exosomes with heat shock proteins from human hepatocellular carcinoma cells that elicit effective natural killer cell antitumor responses in vitro. J Biol Chem 287:15874-85.

MACDONALD C, BUCHKOVICH NJ, STRINGER DK, EMR SD, PIPER RC (2012) Cargo ubiquitination is essential for multivesicular body intralumenal vesicle formation. EMBO Rep 13:331-8.

MARSH M, VAN MEER G (2008) Cell biology. No ESCRTs for exosomes. Science 319:1191-2.

MATHIVANAN S, SIMPSON RJ (2009) ExoCarta: A compendium of exosomal proteins and RNA. Proteomics 9:4997-5000.

MIRANDA KC, BOND DT, MCKEE M, SKOG J, PAUNESCU TG, DA SILVA N, BROWN D, RUSSO LM (2010) Nucleic acids within urinary exosomes/microvesicles are potential biomarkers for renal disease. Kidney Int 78:191-9.

MITTELBRUNN M, GUTIERREZ-VAZQUEZ C, VILLARROYA-BELTRI C, GONZALEZ S, SANCHEZ-CABO F, GONZALEZ MA, BERNAD A, SANCHEZ-MADRID F (2011) Unidirectional transfer of microRNA-loaded exosomes from T cells to antigen-presenting cells. Nat Commun 2:282.

MONTECALVO A, LARREGINA AT, SHUFESKY WJ, STOLZ DB, SULLIVAN ML, KARLSSON JM, BATY CJ, GIBSON GA, ERDOS G, WANG Z, MILOSEVIC J, TKACHEVA OA, DIVITO SJ, JORDAN R, LYONS-WEILER J, WATKINS SC, MORELLI AE (2012) Mechanism of transfer of functional microRNAs between mouse dendritic cells via exosomes. Blood 119:756-66.

MORELLI AE, LARREGINA AT, SHUFESKY WJ, SULLIVAN ML, STOLZ DB, PAPWORTH GD, ZAHORCHAK AF, LOGAR AJ, WANG Z, WATKINS SC, FALO LD, JR., THOMSON AW (2004) Endocytosis, intracellular sorting, and processing of exosomes by dendritic cells. Blood 104:3257-66.

NICKEL W (2005) Unconventional secretory routes: direct protein export across the plasma membrane of mammalian cells. Traffic 6:607-14.

O'LOUGHLIN AJ, WOFFINDALE CA, WOOD MJ (2012) Exosomes and the emerging field of exosome-based gene therapy. Curr Gene Ther 12:262-74.

ORELLANA JA, SANCHEZ HA, SCHALPER KA, FIGUEROA V, SAEZ JC (2012) Regulation of intercellular calcium signaling through calcium interactions with connexin-based channels. Adv Exp Med Biol 740:777-94.

OSTROWSKI M, CARMO NB, KRUMEICH S, FANGET I, RAPOSO G, SAVINA A, MOITA CF, SCHAUER K, HUME AN, FREITAS RP, GOUD B, BENAROCH P, HACOHEN N, FUKUDA M, DESNOS C, SEABRA MC, DARCHEN F, AMIGORENA S, MOITA LF, THERY C (2010) Rab27a and Rab27b control different steps of the exosome secretion pathway. Nat Cell Biol 12:19-30; sup pp 1-13.

PAN BT, TENG K, WU C, ADAM M, JOHNSTONE RM (1985) Electron microscopic evidence for externalization of the transferrin receptor in vesicular form in sheep reticulocytes. J Cell Biol 101:942-8.

PANT S, HILTON H, BURCZYNSKI ME (2012) The multifaceted exosome: biogenesis, role in normal and aberrant cellular function, and frontiers for pharmacological and biomarker opportunities. Biochem Pharmacol 83:1484-94.

PAROLINI I, FEDERICI C, RAGGI C, LUGINI L, PALLESCHI S, DE MILITO A, COSCIA C, IESSI E, LOGOZZI M, MOLINARI A, COLONE M, TATTI M, SARGIACOMO M, FAIS S (2009) Microenvironmental pH is a key factor for exosome traffic in tumor cells. J Biol Chem 284:34211-22.

PEINADO H, ALECKOVIC M, LAVOTSHKIN S, MATEI I, COSTA-SILVA B, MORENO-BUENO G, HERGUETA-REDONDO M, WILLIAMS C, GARCIA-SANTOS G, GHAJAR C, NITADORI-HOSHINO A, HOFFMAN C, BADAL K, GARCÍA BA, CALLAHAN MK, YUAN J, MARTINS VR, SKOG J, KAPLAN RN, BRADY MS, WOLCHOK JD, CHAPMAN PB, KANG Y, BROMBERG J, LYDEN D (2012) Melanoma exosomes educate bone marrow progenitor cells toward a pro-metastatic phenotype through MET. Nat Med 18:883-91.

QU Y, RAMACHANDRA L, MOHR S, FRANCHI L, HARDING CV, NUNEZ G, DUBYAK GR (2009) P2X7 receptor-stimulated secretion of MHC class II-containing exosomes requires the ASC/NLRP3 inflammasome but is independent of caspase-1. J Immunol 182:5052-62.

RANA S, ZOLLER M (2011) Exosome target cell selection and the importance of exosomal tetraspanins: a hypothesis. Biochem Soc Trans 39:559-62.

RAPOSO G, NIJMAN HW, STOORVOGEL W, LIEJENDEKKER R, HARDING CV, MELIEF CJ, GEUZE HJ (1996) B lymphocytes secrete antigen-presenting vesicles. J Exp Med 183:1161-72.

RECORD M, SUBRA C, SILVENTE-POIROT S, POIROT M (2011) Exosomes as intercellular signalosomes and pharmacological effectors. Biochem Pharmacol 81:1171-82.

REGENTE M, CORTI-MONZON G, MALDONADO AM, PINEDO M, JORRIN J, DE LA CANAL L (2009) Vesicular fractions of sunflower apoplastic fluids are associated with potential exosome marker proteins. FEBS Lett 583:3363-6.

REGENTE M, PINEDO M, ELIZALDE M, DE LA CANAL L (2012) Apoplastic exosome-like vesicles: a new way of protein secretion in plants? Plant Signal Behav 7:544-6.

RODRIGUES ML, NAKAYASU ES, OLIVEIRA DL, NIMRICHTER L, NOSANCHUK JD, ALMEIDA IC, CASADEVALL A (2008) Extracellular vesicles produced by Cryptococcus neoformans contain protein components associated with virulence. Eukaryot Cell 7:58-67.

RODRIGUES ML, NOSANCHUK JD, SCHRANK A, VAINSTEIN MH, CASADEVALL A, NIMRICHTER L (2011) Vesicular transport systems in fungi. Future Microbiol 6:1371-81.

ROUNTREE RB, MANDL SJ, NACHTWEY JM, DALPOZZO K, DO L, LOMBARDO JR, SCHOONMAKER PL, BRINKMANN K, DIRMEIER U, LAUS R, DELCAYRE A (2011) Exosome targeting of tumor antigens expressed by cancer vaccines can improve antigen immunogenicity and therapeutic efficacy. Cancer Res 71:5235-44.

SAMAN S, KIM W, RAYA M, VISNICK Y, MIRO S, JACKSON B, MCKEE AC, ALVAREZ VE, LEE NC, HALL GF (2012) Exosome-associated tau is secreted in tauopathy models and is selectively phosphorylated in cerebrospinal fluid in early Alzheimer disease. J Biol Chem 287:3842-9.

SAUNDERSON SC, SCHUBERTH PC, DUNN AC, MILLER L, HOCK BD, MACKAY PA, KOCH N, JACK RW, MCLELLAN AD (2008) Induction of exosome release in primary B cells stimulated via CD40 and the IL-4 receptor. J Immunol 180:8146-52.

SAVINA A, FADER CM, DAMIANI MT, COLOMBO MI (2005) Rab11 promotes docking and fusion of multivesicular bodies in a calcium-dependent manner. Traffic 6:131-43.

SAVINA A, FURLAN M, VIDAL M, COLOMBO MI (2003) Exosome release is regulated by a calcium-dependent mechanism in K562 cells. J Biol Chem 278:20083-90.

SILVERMAN JM, CLOS J, DE'OLIVEIRA CC, SHIRVANI O, FANG Y, WANG C, FOSTER LJ, REINER NE (2010) An exosome-based secretion pathway is responsible for protein export from Leishmania and communication with macrophages. J Cell Sci 123:842-52.

SIMONS M, RAPOSO G (2009) Exosomes--vesicular carriers for intercellular communication. Curr Opin Cell Biol 21:575-81.

SKOG J, WURDINGER T, VAN RIJN S, MEIJER DH, GAINCHE L, SENA-ESTEVES M, CURRY WT, JR., CARTER BS, KRICHEVSKY AM, BREAKEFIELD XO (2008) Glioblastoma microvesicles transport RNA and proteins that promote tumour growth and provide diagnostic biomarkers. Nat Cell Biol 10:1470-6.

SUBRA C, GRAND D, LAULAGNIER K, STELLA A, LAMBEAU G, PAILLASSE M, DE MEDINA P, MONSARRAT B, PERRET B, SILVENTE-POIROT S, POIROT M, RECORD M (2010) Exosomes account for vesicle-mediated transcellular transport of activatable phospholipases and prostaglandins. J Lipid Res 51:2105-20.

TAURO BJ, GREENING DW, MATHIAS RA, MATHIVANAN S, JI H, SIMPSON RJ (2013) Two distinct populations of exosomes are released from LIM1863 colon carcinoma cell-derived organoids. Mol Cell Proteomics 12:587-98.

THERY C, OSTROWSKI M, SEGURA E (2009) Membrane vesicles as conveyors of immune responses. Nat Rev Immunol 9:581-93.

TRAJKOVIC K, HSU C, CHIANTIA S, RAJENDRAN L, WENZEL D, WIELAND F, SCHWILLE P, BRUGGER B, SIMONS M (2008) Ceramide triggers budding of exosome vesicles into multivesicular endosomes. Science 319:1244-7.

VALADI H, EKSTROM K, BOSSIOS A, SJOSTRAND M, LEE JJ, LOTVALL JO (2007) Exosome-mediated transfer of mRNAs and microRNAs is a novel mechanism of genetic exchange between cells. Nat Cell Biol 9:654-9.

VANLANDINGHAM PA, CERESA BP (2009) Rab7 regulates late endocytic trafficking downstream of multivesicular body biogenesis and cargo sequestration. J Biol Chem 284:12110-24.

VELLA LJ, GREENWOOD DL, CAPPAI R, SCHEERLINCK JP, HILL AF (2008) Enrichment of prion protein in exosomes derived from ovine cerebral spinal fluid. Vet Immunol Immunopathol 124:385-93.

VIAUD S, PLOIX S, LAPIERRE V, THERY C, COMMERE PH, TRAMALLONI D, GORRICHON K, VIRAULT-ROCROY P, TURSZ T, LANTZ O, ZITVOGEL L, CHAPUT N (2011) Updated technology to produce highly immunogenic dendritic cell-derived exosomes of clinical grade: a critical role of interferon-gamma. J Immunother 34:65-75.

WHITE IJ, BAILEY LM, AGHAKHANI MR, MOSS SE, FUTTER CE (2006) EGF stimulates annexin 1-dependent inward vesiculation in a multivesicular endosome subpopulation. Embo J 25:1-12.

YANG C, CHALASANI G, NG YH, ROBBINS PD (2012) Exosomes released from Mycoplasma infected tumor cells activate inhibitory B cells. PLoS One 7:e36138.

ZERIAL M, MCBRIDE H (2001) Rab proteins as membrane organizers. Nat Rev Mol Cell Biol 2:107-17.

ZHANG H, XIE Y, LI W, CHIBBAR R, XIONG S, XIANG J (2011) CD4(+) T cell-released exosomes inhibit CD8(+) cytotoxic T-lymphocyte responses and antitumor immunity. Cell Mol Immunol 8:23-30.

ZHUANG X, XIANG X, GRIZZLE W, SUN D, ZHANG S, AXTELL RC, JU S, MU J, ZHANG L, STEINMAN L, MILLER D, ZHANG HG (2011) Treatment of brain inflammatory diseases by delivering exosome encapsulated anti-inflammatory drugs from the nasal region to the brain. Mol Ther 19:1769-79.

Biol Res 46: 13-20, 2013

Expression of resistin, CXCR3, IP-10, CCR5 and MIP-1 α in obese patients with different severity of asthma

Sara Rojas-Dotor[1], Nora H. Segura-Méndez[2], Ken Miyagui-Namikawa[2] and Rafael Mondragón-González[3]

[1] Unidad de Investigación Médica en Inmunología. Hospital de Pediatría. Centro Medico Nacional SXXI, Instituto Mexicano del Seguro Social, México D.F. México.
[2] Departamento de Alergología e Inmunología Clínica. Centro Medico Nacional SXXI, IMSS, México D.F. México.
[3] Unidad de Investigación Médica en Inmunoquímica. Centro Medico Nacional SXXI, IMSS, México D.F. México.

ABSTRACT

Asthma studies suggest that alteration in the inflammation pattern may be associated with the severity of asthma. The aim of this study was to compare *in vitro* the expression of chemokines, chemokine receptors and cytokine production from CD4+ T human lymphocytes of asthmatic, both obese and non-obese patients with different severity levels of asthma. Lymphocytes were labeled with monoclonal anti-human CXCR3/IP-10, MIP-1α/CCR5 antibodies and were analyzed by flow cytometry. Cell culture supernatants were used to measure production of interleukin IL-6 and resistin by ELISA. CXCR3/IP-10 expression increased in non-obese patients with mild persistent asthma (2.2%, p<0.05), moderate persistent asthma (3%, p<0.003) and severe persistent asthma (4%, p<0.004); this effect was stronger in obese patients with severe persistent asthma (35%, p<0.004). MIP-1 α / CCR5 increased in non-obese patients with intermittent asthma (0.65%, p<0.05) and severe asthma (1.4%, p<0.03); in obese patients, this expression was greater in intermittent asthma (8%, p<0.05) and severe persistent asthma (12%, p<0.04). Resistin production strongly increased in obese patients with intermittent (976 ng/ml) and severe persistent asthma (795 ng/ml). IL-6 increased in both lean and obese persons; however, the highest value was registered in the group of severe persistent obese asthmatics (992 pg/ml). Obesity *per se* increased the inflammatory profile of chemokines / cytokines secreted by cells of the blood, increasing the inflammatory status in asthmatic patients. Resistin showed characteristics of a pro-inflammatory cytokine mainly in severely obese asthmatics.

Key Words: Asthma classification, severity, chemokines (MIP-1α, IP-10), CC chemokine receptors (CXCR3, CCR5), interleukin-6, resistin.

INTRODUCTION

Allergic asthma is caused by a complex interaction among different types of immune cells in the airways. After exposure to the allergen, different cells such as alveolar macrophages, adipocytes, lymphocytes and eosinophils secrete different interleukins (IL)-6, -10, -4 and IL-13). These cytokines activate an inflammatory cascade and attract chemokines (IP-10, MIP1-α etc.) to activate chemokine receptors such as CXCR3 and CCR5, a crucial process of cellular infiltration in the lungs (Huber et al., 2008). Chemokines that cause inflammation include inhibitory protein 10 (IP)-10, also known as CXCL-10, macrophage inflammatory proteins 1α and 1β (MIP-1 α-1 β or CCL3); these bind to CXCR3 and CCR5 respectively, and the chemokines that inhibit inflammation, such as monocyte chemoattractant protein 3 (MCP-3) or CCL7 and I-139 bind to CCR4 or CCR8 respectively (Barnes, 2000). Many of these mediators are synthesized and secreted by fat tissue cells, which cause an increase in the inflammatory response to the allergen in these patients (Fantuzzi, 2005). Resistin, a mediator also known as specific secretor factor in adipose tissue, is involved in insulin resistance induced by obesity and diabetes. Several studies have shown that resistin in humans, in contrast to its production by adipocytes in mice, is synthesized predominantly by mononuclear cells, both within and outside adipose tissue; it facilitates cellular infiltration and increases the width of fat tissues (Tilg and Moschen, 2006; Steppan, et al., 2001; Curat et al., 2006). Some studies in humans have failed to confirm the relationship between the circulating levels of resistin and the body mass index (BMI) and its role in insulin sensitivity (Bastard et al., 2002; Fasshauer and Paschke, 2003). However, some studies have reported increased resistin levels in overweight subjects and type 2 diabetes (McTernan et al., 2002; Vidal-Puig and Orahilly, 2001). Resistance to a cortisone-based treatment seems to be a failure in inhibiting cytokine production by lymphocytes, suggesting that different inflammatory cytokines which are associated with chemokines and chemokine receptors in the airways may be present in patients with different degrees of severity of asthma (Shannon et al., 2008). Asthma and obesity are public health concerns that have high impact and an increasing prevalence in recent years (Shore, 2007, 2008). Prospective studies have demonstrated that obesity is a risk factor for the development and exacerbation of asthma, and a positive correlation between body mass index and the development of asthma has been observed (Segura et al., 2007).

Other studies have shown that severe asthma has a higher prevalence in overweight patients compared to normal weight patients and that body mass index (BMI) is positively associated with clinical asthma severity. In addition, patients with more severe asthma have higher BMI than those with milder asthma (Saint-Pierre et al., 2006). Obesity has mechanical effects on lung function; it leads to a systemic pro-inflammatory status, thereby potentially increasing airway inflammation, and is associated with a number of co-morbid factors which might interfere with asthma control. Obesity does not cause airflow obstruction, but can result in pulmonary restriction and reduction in airway diameter, which could

Corresponding author: Sara Rojas-Dotor Ph. D. Unidad de Investigación Médica en Inmunología, Hospital de Pediatría, CMN-SXXI, IMSS. Mailing address: Avenida Cuauhtémoc 330, Col. Doctores, C. P. 06720, México D. F. Zip code 06720. Tel/fax +52 (55) 5627-6943.. E-mail: srdotor@yahoo.com.mx

Received: January 26, 2012. In Revised form: July 2, 2012. Accepted: September 12, 2012

contribute to airway hyper-responsiveness. Mouse asthma models have demonstrated that obesity and cytokines can enhance airway hyper-responsiveness, airway inflammation and allergic responses, but it is unclear whether obesity-associated inflammatory mechanisms are relevant in human asthma (Beuther, 2009). The aim of this study was to compare, *in vitro*, the expression of chemokines, chemokine receptors and cytokine production by peripheral blood lymphocytes from healthy subjects and patients with different severity of asthma, with or without obesity.

METHODS

Subjects

All patients and volunteers gave their written informed consent for interviewing and blood sampling. The study was conducted according to the recommendations of the Declaration of Helsinki and approved by the local Ethics Committee. The sample consisted of fifty asthmatic patients, diagnosed with allergic asthma according to The Global Initiative for Asthma (GINA, 2008), which establishes a practical system of classification considering clinical and functional aspects such as frequency of diurnal and nocturnal respiratory symptoms and lung function; their combination allows us to classify asthma severity as: a) intermittent asthma, in which the main symptoms of breathlessness of varying intensity and duration, bronchial spasms, cough, mucus secretions, and wheezing occur less than once a week, maximum volume exhaled in the first second of a forced expiration (FEV_1) equal to or greater than 80% of predicted with less than 20% variability, b) mild persistent asthma, which consists of symptoms that occur at night, more than once a week, FEV_1 greater than or equal to 80% of predicted with lower variability of 20-30%, c) moderate persistent asthma, with exacerbated symptoms that affect activity and sleep and with the use of short-acting β2 agonists on a daily application, FEV_1 from 60 to 80% of predicted with greater than 30% variability, and d) severe persistent asthma, with daytime and nighttime symptoms that are frequently exacerbated and the use of short-acting β2 agonists with daily application, FEV_1 less than or equal to 60% of predicted with greater than 30% variability. We included clinical symptoms, spirometry and skin prick tests. In addition, we applied the following criteria: a) inclusion; age between 18 and 65 years for both sexes, obese and non obese (14 obese men and 12 women, 10 non-obese men and 14 women, 12 healthy subjects), residents of the metropolitan area of Mexico City, b) exclusion; patients with pulmonary diagnosis other than allergic asthma, history of immunotherapy in the past year, history of immunodeficiency or autoimmune diseases, smoking history and / or patients who have cooked with wood, confirmed pregnancy, who have used topical or systemic antihistamine-based therapies within two weeks prior to entering the study , who have received astemisol within the last two months prior to the execution of the skin prick test for mites, the presence of hives or dermographism, asthma attacks at any stage and residence less than a year in Mexico City. Patients were divided into three groups according to their body mass index (BMI) following the guidelines established by the World Health Organization (WHO) (Pauwels et al., 2001): obesity (BMI ≥ 30 kg/m^2), and non-obese (BMI < 30 kg/m^2) and healthy. After the taking the blood sample, the patients were treated with a combination therapy based on mometasone / formoterol (260 μg) (Merck, California., USA) and oriented to control environmental factors (dust, pollen, cigarette smoke etc) that trigger asthma exacerbation. Healthy non-smoking subjects without obesity, hypertension, diabetes, or any other metabolic symptoms were used as controls.

Isolation of mononuclear cells from healthy subjects and patients with asthma

Fifteen ml of venous heparinized blood were obtained from asthmatic patients, both obese and non-obese, and healthy non-smoking adult volunteer donors (n= 62) of both sexes. The blood was diluted 1:3 with phosphate buffered saline (PBS; 0.15 M phosphate buffer). Blood was layered over 3 ml of Ficoll-Hypaque (Sigma Chemical Co., St. Louis, Missouri, USA) with gradient (δ = 1.077) and centrifuged at 1500 rpm for 30 min at 21 °C (Böyum, 1968). The cellular interface peripheral blood mononuclear cells (PBMC) were collected and washed twice with PBS. Cell viability was determined using Trypan blue dye (Sigma Chemical Co., St Louis, MO); exclusion was ≥ 90%.

Cell culture

Lymphocytes (5 x 10^5) were incubated for 24 h at 37 °C, 5% CO_2 without stimulation in 24-well plates with RPMI-1640 medium supplemented with 10% fetal calf serum (FCS), 2 mM L-glutamine, 100 U/ml streptomycin, 5 μg/ml gentamicin and 1 mM sodium pyruvate (Gibco Laboratories, Grand Island, NY). Cells were harvested and centrifuged at 1500 rpm. The cell culture supernatants were collected and stored at -70 °C until use.

Cell Purification

The cellular interface peripheral blood mononuclear cells (PBMC) were removed and washed two times with PBS. CD4+ T cells were purified using the CD4+ T cell isolation kit II, as an indirect magnetic labeling system for the isolation of untouched CD4+ T cells from human PBMCs (Miltenyi Biotec, Germany), and LS column and MidiMACS separator. Briefly, 1 x 10^7 PBMC cells were placed in propylene tubes with 80 μl PBS-albumin-EDTA and 20 μl cocktail of biotin-conjugated antibodies against CD8, CD11b, CD16, CD19, CD36, CD56, CD123, TCRγ/δ and CD235a (Glycophorin A) and were incubated for 10 min at 4 °C. These cells were subsequently labeled magnetically with Anti-Biotin MicroBeads for depletion. The CD4+ lymphocytes obtained were 95% pure. Acquisition of 10,000 events was conducted in flow cytometry FACSaria (BD Biosciences, Palo Alto, CA). For analysis Cell Quest software, version 3.1 (Becton Dickson, San Jose, CA) was used.

Immunofluorescent staining for chemokine and chemokine receptors

Lymphocytes were stained with monoclonal anti-human anti-MIP1α, anti- CCR5 or anti-IP-10, anti-CXCR3 antibodies coupled to fluorescein isothiocyanate (FITC) or phycoerythrin (PE), respectively. Unconjugated isotype-matched control monoclonal antibodies were detected using anti-mouse IgG1-FITC or -PE antibodies (PharMingen, San Diego, CA, USA).

Briefly, 5 X 10^5 CD4+ T cells from each group were incubated in 24-well plates for 24 h; after incubation, cells were centrifuged for 5 min at 400 g and supernatants were aspirated without disturbing the pellets. Cells were washed with PBS/0.5% albumin/2mM EDTA. They were then marked with mAb and incubated for 20 min at 4 °C in the dark, and fixed with 1% p-formaldehyde (Sigma Chemical Co., St. Louis, MO) according to the manufacturer's instructions (PharMingen). Acquisition of 10,000 events was conducted in flow cytometry FACSaria (BD). For analysis, FACS Diva 6.1 software was used Miltenyi, et al., 1990.

Quantification of resistin and IL-6

Resistin and IL-6 in the cell culture supernatants were measured using commercially available enzyme-linked immunosorbent assay kits (ELISA) (Peprotech®, Rocky Hill, NJ).

Statistical analysis

The statistical analysis was performed using the SPSS® software, version 14.0 (SPSS Inc., Chicago. Illinois, USA) and MS Excel 2007. Quantitative data was expressed as mean and standard deviation (SD). Statistical comparison among groups was performed using the Mann-Whitney U tests. Differences were considered as statistically significant when $p<0.05$. The relationship between in resistin production and the in IL-6 production were analyzed using normal distribution histograms with confidence intervals of 95%.

RESULTS

CXCR3 and IP-10 expression

CXCR3 and IP-10 expressions were compared among obese and non-obese patients with with different degrees of severity of asthma (intermittent, mild persistent, moderate persistent, and severe persistent asthma), as well as with healthy subjects. In non-obese patients, CXCR3 and IP-10 expressions were not significantly different in intermittent asthmatic compared to controls (healthy subjects); this expression, however, increased gradually in patients with mild persistent asthma, moderate persistent asthma and severe persistent asthma, with statistically significant differences among groups (2.2%, 3% and 4% respectively; $p< 0.004$) (Fig. 1a). In obese patients with intermittent asthma, mild persistent asthma, moderate persistent asthma and severe persistent asthma CXCR3 and IP-10 were significantly over-expressed (19%, 16%, 13% and 35% respectively; $p<0.04$) compared to healthy subjects and non-obese patients (Fig. 1b). Meanwhile, the expression was significantly lower in moderate persistent obese asthmatic (13%, $p< 0.05$) and was the highest for obese patients with severe asthma (35%, $p<0.001$) (Fig.1b).

MIP-1α and CCR5 expression

The expression of MIP-1α and CCR5 in non-obese asthmatic patients was significantly increased in patients with intermittent asthma and severe persistent asthma (0.6% and 1.4%, $p< 0.05$ and $p< 0.03$ respectively) compared to healthy subjects. Expression levels in mild persistent asthmatic and moderate persistent asthmatic were lowest (0.3% and 0.4%, $p<0.04$ and $p<0.05$ respectively) as shown in Figure 2a. MIP-1α and CCR5 expressions in obese, asthmatic patients increased significantly (8%, 6%, 7% and 12%, $p< 0.04$ respectively) in all groups compared to healthy subjects (Fig. 2b). There were considerable differences in the severe persistent asthmatic group (12%, $p< 0.04$) compared to other groups (Fig. 2b). We also observed over-expression of MIP-1α and CCR5 in obese patients compared to non-obese patients.

Production of cytokines IL-6 and resistin in obese and non-obese asthmatics patients compared to healthy subjects

The concentration of resistin strongly increased in obese patients with intermittent asthma and severe persistent asthma (976 ng/ml and 795 ng/ml, respectively) (Fig. 3). Therefore, there was an increase in the production of resistin in obese patients compared to lean patients: Intermittent 976 *vs.* 190 ng/ml, moderate persistent 480 *vs.* 378 ng/ml and severe persistent 795 *vs.* 612 ng/ml; except for the lean subjects with mild persistent asthma 715 *vs.* 417 ng/ml as shown in Figure 3. All obese patients, regardless of the degree of their disease, showed high levels of IL-6 compared to lean patients: intermittent asthma (742 *vs.* 600 pg/ml), mild persistent asthma (776 *vs.* 552 pg/ml), moderate persistent asthma (902 *vs.* 712 pg/ml) and severe persistent asthma (992 *vs.* 839 pg/ml) (Fig. 3).

DISCUSSION

The coordinated expression and binding of chemokines to their receptors seem to be differentially regulated in specific stages of asthma. In this study, CXCR3/ IP-10 and CCR5/ MIP-1α were overexpressed in obese patients with severe persistent asthma, which is in agreement with the reported of Brasier (2008) in patients with severe persistent asthma who underwent bronchoalveolar lavage.

We also showed that obesity *per se* increased the inflammatory status of asthmatic patients, probably due to the chemotactic effect of chemokines secreted by the blood cells of asthmatics. Additionally, cell activation may modify the expression of chemokines and chemokine receptors, which, in alternate fashion, are essential for leukocyte recruitment during inflammation. Once activated, T lymphocytes acquire different migratory capacities and are, in fact, the key factor for an efficient immune-response regulation. Interestingly, we found an association between increased expression of CXCR3 / IP-10 and severity of disease in non-obese asthmatic patients, while in obese patients increased expression of these markers was only observed in intermittent obese asthmatics and obese individuals with severe persistent asthma. The classification of asthma severity was very useful to us to relate the different levels of asthma severity to the expression of inflammatory markers studied; however, asthma, as a chronic inflammatory disease shows variations in clinical manifestations and the degree of airflow obstruction, so its severity may change over time in the same patient, indicating that not all inflammatory markers correlate with levels severity of asthma, as reported in the intermittent asthma group, especially in obese patients.

The elevated expression of these molecules in humans in primary and more severe stages of the disease had not been previously reported. We show that higher BMI scores

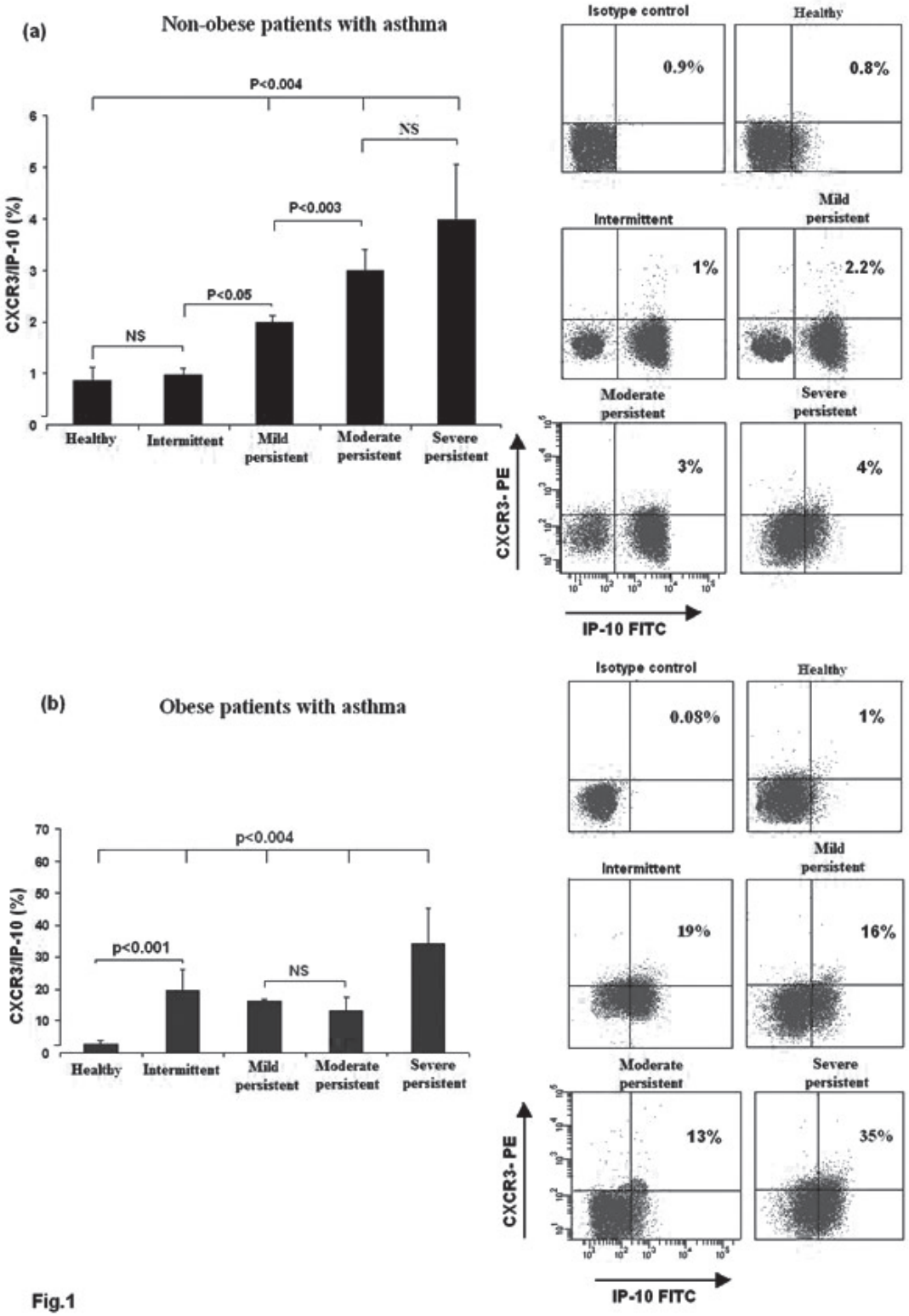

Fig 1: Expression of IP-10 and CXCR3 in lymphocyte populations obtained from healthy subjects, non-obese patients with asthma and obese patients with asthma

Five x 10^5 CD4+ lymphocytes were obtained from human peripheral blood (a) non-obese and (b) obese patients with intermittent, mild persistent, moderate persistent and severe persistent asthma and healthy subjects. The cells were isolated by the method of Böyum and purified to CD4 + T cells by the negative selection technique and were cultured for 24 h. They were stained with fluorochromo-conjugated (FITC or PE) anti human IP-10 and CXCR3 monoclonal antibodies. 10,000 events were analyzed by flow cytometry. The quadrants were set with the isotype control (FITC or PE-conjugated mouse IgG). Bold histograms and numbers in the dot plots represent the mean ± SD of positively stained cells from at least six independent experiments. The statistical differences between the groups were calculated using the Mann-Whitney U test. $p < 0.05$ was considered significant.

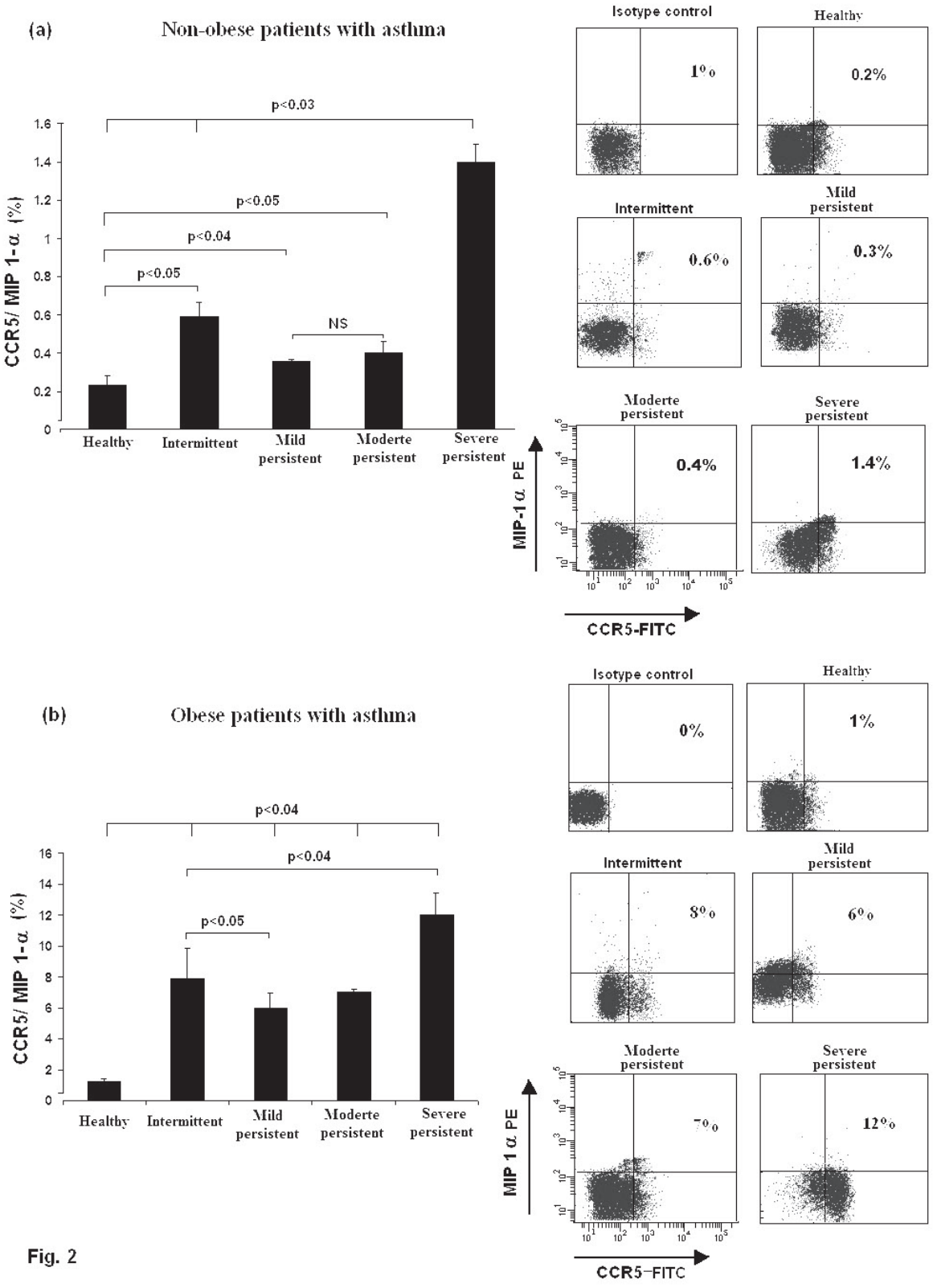

Fig. 2

Fig 2: MIP1 α and CCR5 expression in lymphocytes from peripheral blood

Five x 10^5 CD4+ lymphocytes were obtained from non-obese and obese patients with intermittent, mild persistent, moderate persistent and severe persistent asthma and healthy subjects and were cultured in 24-well plates in a humidified chamber at 37 °C and 5% CO_2 for 24 h. Cells were stained with fluorochromo-conjugated (FITC or PE) anti human MIP 1-α and CCR5 monoclonal antibodies. At least 10,000 events were analyzed by flow cytometry. Black bars and bold numbers in the dot plots represent the mean ± SD from five independent experiments. The quadrants were set with mouse IgG isotype control. The statistical differences between the groups were calculated using the Mann-Whitney U test ($p < 0.05$).

and elevated CXCR3/IP-10 expression levels (up to 9 times) are associated with increased asthma severity added to the condition of obesity. These findings highlight the importance of controlling theinflammation taking into account the role of obesity and it provides support for the assumptions that obesity-induced inflammation may contribute to greater asthma severity. The strong correlation between CXCR3 expression and Th1 differentiation led us to the hypothesis, subsequently verified in mouse models, that CXCR3 and its ligands regulate the migration of Th1 cells into sites of Th1-driven inflammation (Lin et al., 2011); it also correlates with a study in which the expression of CXCR3 and its ligand IP-10 (CXCL10) was induced by IFN-γ in mice challenged with an allergen in the lung (Gangur et al., 1998). High levels of IP-10 and CXCR3 have been reported in co-cultured cells in the presence of INF-γ in patients with chronic obstructive disease. IP-10 differs from other chemokines in its apparent specificity to activate T lymphocytes. We believe that it is also relevant in regulating the production and synthesis pattern of cytokines. These data imply that CCR5 and CXCR3 could be a potent therapeutic target of asthma for inhibiting the recruitment of T-cells to the airways.

Some limitations of the study deserve further discussion. To identify cells that express on their cell surface characteristic inflammatory markers we have often used invasive techniques such as bronchoalveolar lavage fluid, which was not performed in this study. Based upon the principle that cells migrate selectively to the inflammatory focus through chemokines and their receptors, a peripheral blood sample is less painful for the patient. In addition, the chemokine system *in vivo* is extremely redundant due to the large number of different chemokines, the overlap in chemokine function and the pleiotrophy of chemokine–receptor interaction. One of the challenges in this field is to identify which receptors play major roles in specific inflammatory conditions. The current findings suggest that the Th2-linked (CC) receptors are not the only potential targets for asthma therapy. The Th1-linked (CC) receptors, especially CCR5 and CXCR3, may also be valid targets. It was demonstrated that these markers play an important role in migratory behavior of peripheral blood T cells and influence the activation of T helper cells; however, we must be cautious in extrapolating these results to other population of lymphocytes such as CD8+ T cells and regulatory T cells.

The levels of many cytokines and other mediators may be elevated in obese patients and many be involved in systemic inflammation, such as interleukin 6, TNF-α, and reactive C protein. Our data showed high concentrations of resistin and IL-6 in overweight asthmatic patients compared to healthy individuals, consistent with what has been reported in the literature (Bokarewa et al., 2005). In a previous study it was demonstrated that an increase in resistin is associated with the severity of asthma, which results in an increased expression of adhesion molecules such as VCAM-1 and ICAM-1, as well as pro-inflammatory cytokines IL-6 and TNF-α, which trigger damage (Mondragón-González et al., 2007). IL-6 also activates β1-integrin, which is a component of the VLA-4 complex and the ligand for fibronectin and VCAM-1, and thereby could influence cell attachment (Clahsen and Schaper, 2008). In this study, a strong increase in resistin and IL-6 levels was observed in obese patients with severe persistent asthma, while in thin patients with the same disease the production of these cytokines was significantly lower. Generally in overweight

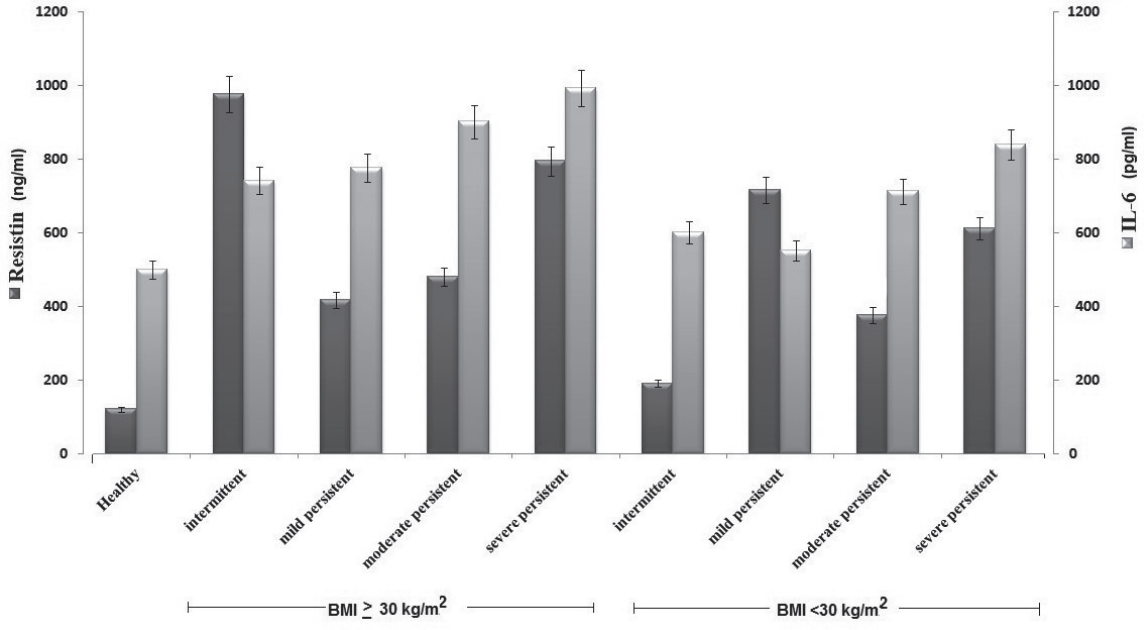

Fig 3: Resistin and IL-6 production by lymphocyte cells obtained from healthy subjects, lean patients and obese patients with different levels of severity of asthma

Cell culture supernatants were analyzed by ELISA to determine IL-6 and resistin production. The bars represent the average of three independent experiments in each group and the healthy subjects (control group). Quantitative data were expressed as normal distribution histograms with confidence intervals of 95%.

or obese individuals a considerable increase in adipocytes occurs, which increases IL-6 and resistin levels, and these in turn activate endothelial cells to stimulate migration of leukocytes and accumulation of leukocytes in the fatty adipose tissue. Under these conditions the increase in fatty tissue and expression of inflammatory cytokines contribute to the chronic inflammatory status, and they are characteristics of obesity. We observed this phenotype in intermittent asthma and severe asthma patients compared to the other asthma groups and healthy subjects. The production level of resistin in obese intermittent patients was elevated.This may be because resistin behaves as a prototype inflammatory cytokine, favoring the inflammatory process, and it also may have an additive effect with the inflammation that affects obesity. In lean patients the increased production of resistin was observed in patients with moderate persistent asthma and severe persistent asthma; of severity exacerbation of clinical symptoms was present at these levels. The relation between high concentrations of resistin and asthma severity obtained in our study agrees with the results obtained in *in vivo* studies (Mishra et al., 2007), in which it was found that resistin and IL-13 cause inflammation in airways and pulmonary remodeling in the lung of mice, resulting in the deposit of perivascular and peribronchial collagen fibers. Additionally, IL-6 and resistin could be induced by different allergens independent of Th2-cells, with biological and clinical adverse effects in patients with exacerbated asthma (Wolpe et al., 1998). In obese patients there is a condition of chronic systemic inflammation, which also means that if they have asthma, it is more severe than in lean persons and is difficult to control. In this study we found that the greater the overlap of groups, for example in severe persistent asthmatic obese it was poorer its final clinical status. In addition, obese asthmatics, regardless of the degree of severity of the disease showed high levels of IL-6, compared to healthy and non-obese patients. Hence there is a direct relationship between obesity, production of IL-6 and resistin, and cells migrating from the bloodstream the to inflammatory focus. We have previously reported that asthmatic patients with a BMI ≥ 30 had a high concentration of leptin, especially women. In the current study, we showed that concentrations of IL-6 and resistin, together with obesity, can be considered as indicators of asthma severity.

CONCLUSION:

Obesity *per se* increased the inflammatory profile of chemokines / cytokines secreted by cells of the blood by increasing the inflammatory status of asthma. Resistin shows characteristics of a pro-inflammatory cytokine, mainly in severely obese asthmatics. Chemokine receptors and their ligands, such as CXCR3/IP-10 and CCR5/MIP-1α, should be considered key inflammatory molecules in obese patients with different levels of asthma severity.

ACKNOWLEDGMENTS

This research was supported by the Consejo Nacional de Ciencia y Tecnología (CONACYT), México (No. 38104-M). The authors wish to thank American Journal Experts for the critical review of the English of the manuscript. The authors are grateful to laboratory technician José de la Luz Romero Preciado of the Blood Bank in Centro Médico Nacional Siglo-XXI-IMSS, México, D. F. México.

REFERENCES

BARNES, PJ (2000) Chronic obstructive pulmonary disease. N Engl J Mol 343: 269-280.

BASTARD JP, MAACHI M, VAN NHIEU JT, JARDEL C, BRUCKERT E, GRIMALDI A, ROBERT JJ, CAPEAU J, HAINQUE B (2002) Adipose tissue IL-6 content correlates with resistance to insulin activation of glucose uptake both *in vivo* and *in vitro*. J Clin Endocrinol Metab 7: 2084-2089.

BATEMAN ED, HURD SS, BARNES PJ, BOUSQUET J, DRAZEN JM, FITZGERALD M, GIBSON P, OHTA K, OBYRNE P, PEDERSEN SE, PIZZICHINI E, SULLIVAN SD, WENZEL SE, ZAR HJ (2008) Global strategy for asthma management and prevention: GINA executive summary. Eur Respir J 31: 143-178.

BEUTHER DA (2009) Obesity and asthma. Clin Chest Med 3: 479-88.

BOKAREWA M, NAGAEV I, DAHLBERGL, SMITH U, TARKOWSKI A (2005) Resistin, an adipokine with potent proinflammatory properties. J Immunol 174: 5789–5795.

BÖYUM A (1968) Isolation of mononuclear cells and granulocytes from human blood. Isolation of monuclear cells by one centrifugation and of granulocytes by combining centrifugation and sedimentation at 1 g. Scand J Clin Lab Invest 97: 77-89.

BRASIER AR, VICTOR S, BOETTICHER G, JU H, LEE C, BLEECKER ER, CASTRO M, BUSSE WW, CALHOUN WJ (2008) Molecular phenotyping of severe asthma using pattern recognition of bronchoalveolar lavage–derived cytokines. J Allergy Clin Immunol 121: 30-37.

CLAHSEN T, SCHAPER F (2008) Interleukin-6 acts in the fashion of classical chemokine on monocytic cells by inducing integrin activation, cell adhesion, actin polymerization, chemotaxis, and transmigration. J Leukoc Biol 84 : 1521-1529.

CURAT CA, WEGNER V, SENGENES C, MIRANVILLE A, TONUS C, BUSSE R. BOULOUMIE A (2006) Macrophages in human visceral adipose tissue: Increased accumulation in obesity and a source of resistin and visfatin. Diabetologia 49: 744-747.

FANTUZZI G (2005) Adipose tissue, adipokines and inflammation. J Allergy Clin Immunol 115: 911-919.

FASSHAUER M, PASCHKE R (2003) Regulation of adipocytokines and insulin resistance. Diabetologia 46: 1594-1603.

GANGUR V, SIMONS FE, HAYGLASS KT (1998) Links Human IP-10 selectively promotes dominance of polyclonally activated and environmental antigen-driven IFN-gamma over IL-4 responses. FASEB J 12: 705-713.

HUBER J, KIEFER FW, ZEYDA M, LUDVIK B, SILBERHUMER GR, PRAGER G, ZLABINGER GJ,. STULNIG T M (2008) CC chemokine and CC chemokine receptor profiles in visceral and subcutaneous adipose tissue are altered in human obesity. J Clin Endocrinol Metab 93: 3215-3221.

LIN Y, YAN H, XIAO Y, PIAO H, XIANG R, JIANG L, CHEN H, HUANG K, GUO Z, ZHOU W, LU B, GAO J (2011) Attenuation of antigen-induced airway hyperresponsiveness and inflammation in CXCR3 knockout mice. Respir Res12:123.

MCTERNAN CL, MCTERNAN PG, HARTE AL, LEVICK PL, BARNETT AH, KUMAR S (2002) Resistin, central obesity and type 2 diabetes. Lancet 359: 46-47.

MISHRA A, WANG M, SCHLOTMAN J, NIKOLAIDIS NM, DEBROSSE CW, KAROW ML, ROTHENBERG ME (2007) Resistin-like molecule-beta is an allergen-induced cytokine with inflammatory and remodeling activity in the murine lung. Am J Physiol Lung Cell Mol Physiol 293: 303-304.

MONDRAGÓN-GONZÁLEZ R, SEGURA-MÉNDEZ NH, DEL RIVERO-HERNÁNDEZ L, RODRÍGUEZ-VELASCO GJ, CRUZ-LÓPEZ M (2007) Association between adipocines and cellular adhesion molecules in asthmatic adults with or without obesity compared with healthy adults. Arch Alerg Inmunol Clin 38: 155-158.

PAUWELS RA, BUIST AS, MA P, JENKINS CR, HURD SS; GOLD Scientific Committee (2001) Global strategy for the diagnosis, management, and prevention of chronic obstructive pulmonary disease: National Heart, Lung, and Blood Institute and World Health Organization Global Initiative for Chronic Obstructive Lung Disease (GOLD): Executive summary. Respir Care 46: 798-825.

SAINT-PIERRE P, BOURDIN A, CHANEZ P, DAURES JP, GODARD P (2006) Are overweight asthmatics more difficult to control? Allergy 61: 79–84.

SEGURA MN, MURILLO GE, ROJAS-DOTOR S, RICO G, MARTÍNEZ HL, SANDOVAL SC (2007). Inflammatory markers associated with asthma and body mass index. Rev Alerg Mex 54: 96-200.

SHANNON J, ERNST P, YAMAUCHI Y, OLIVENSTEIN R, LEMIERE C, FOLEY S, CICORA L, LUDWIG M, HAMID Q, MARTIN JG (2008) Differences in airway cytokine profile in severe asthma compared to moderate asthma. Chest 133: 420-426.

SHORE SA (2007) Obesity and asthma: Implications for treatment. Curr Opin Pulm Med 13: 56–62.

SHORE SA (2008) Obesity and asthma: Possible mechanisms. J Allergy Clin Immunol 121: 1087-1093.

STEPPAN CM, BAILEY ST, BHAT S, BROWN EJ, BANERJEE RR, WRIGHT CM, PATEL HR, AHIMA RS, LAZAR MA (2001) The hormone resistin links obesity to diabetes. Nature, 409: 307-312.

TILG H. MOSCHEN AR (2006) Adipocytokines: Mediators linking adipose tissue, inflammation and immunity. Natures Reviews Immunology 6: 772-783.

VIDAL-PUIG A, ORAHILLY (2001) Resistin: A new link between obesity and insulin resistance? Clin Endocrinol 55: 437-438.

WOLPE SD, DAVATELIS G, SHERRY B, BEUTLER B, HESSE DG, NGUYEN HT, MOLDAWER LL, NATHAN CF, LOWRY SF, CERAMI A (1998) Macrophages secrete a novel heparin-binding protein with inflammatory and neutrophil chemokinetic properties. J Exp Med 167: 570-581.

Biol Res 46: 21-26, 2013

The monthly rhythm of incidence and age at menarche: thirty five years of research. The circa-vacation-study expectancy rhythm of incidence and age at menarche

Carlos Y. Valenzuela
Programa de Genética Humana, ICBM, Facultad de Medicina, Universidad de Chile, Independencia 1027, Casilla 70061, Santiago, Chile

ABSTRACT

The hypothesis that the vacation-study-expectancy scholar regime produces most of the monthly rhythm of the age at menarche (AaM) was tested. Studies on monthly menarche incidence (MI) refuted climatic factors as a main factor in this rhythm, and indicated that the main factor of this rhythm is the succession of expectancies of study (Stu-months) or vacation (Vac-months) months within a year. Thus the hypothesis of seasonal circa-annual rhythm should be modified to the circa-[vacation (fiesta)]-[study (non-fiesta)]-expectancies rhythm for the MI and age at menarche annual rhythms. In several countries Vac-months had higher MI than Stu-months. The high MI of Vac-months was followed by a large decrease when girls started their studies and a MI increase occurred as vacations approached. The hypothesis proposes that at the end of vacations and at the beginning of the study period the AaM should be lowest, and then the mean of AaM should increase because of the menarche delay of girls whose menarche was arrested by the initiation of school work. This pattern was found in four independent samples, from Chile, Colombia, USA and Brazil. The probability that this result be due to random fluctuation of means is extraordinarily low ($P<10^{-8}$). I conclude that the influence of the expectancy of vacation and study periods on the monthly rhythm of the age at menarche is a real process that accounts for most of this rhythm.

Key terms: age at menarche, annual rhythm, circa-vacation-study-expectancy rhythm, fiesta expectancy, menarche incidence

INTRODUCTION

In the early 1970s I undertook a longitudinal follow up study on human growth and development. This study was part of an international program coordinated by the International Center for Childhood (UN) whose main office was in Paris. The program included studies in USA, Europe, South America and Africa. Prof. Nathalie Masse, the Director of this Center, said that the monthly rhythm of menarche incidence was probably not due to climatic factors, because in her experience with the circa-annual monthly rhythm of menarche incidence (MI) the winter (Dec-Jan) peak of menarche often seen in the Northern Hemisphere was present as a summer peak in the Southern Hemisphere (Africa). She suggested performing the analysis in Santiago (Chile, Southern Hemisphere) to see whether this summer peak of MI was also present. We found peaks of menarche incidence in December (Dec), January (Jan) and February (Feb) (Patri et al., 1980) and a striking relationship with the month of birth and conception (Valenzuela et al 1991, 1993) showing non-climatic factors acting on this rhythm. By climatic factors is meant photoperiod, temperature, humidity, cloudiness and any other climatic factor. Then we worked in a multinational group with samples from Hungary, Colombia, India and Chile, with a wide hypothetic-deductive research to elucidate the main factors of the menarche rhythm. To refute seasonality our method assumed: 1) the consistent antithetical expectancies that should necessarily be found between Northern and Southern Hemispheres; 2) the marked differences in climatic conditions between equatorial, tropical, temperate, Arctic and Antarctic and polar earth zones; 3) the similarities of MI that should be found in months of the same season; 4) the marked or antithetical differences that should be found in MI of months belonging to antithetical seasons (summer and winter) and the similarities that should be found in months of different seasons with similar climatic conditions (autumn and spring); 5) the similarity of the rhythm that should be found in regions with the same latitude, altitude and geographical conditions. With all these expected situations we refuted conclusively the seasonality of the circa-annual rhythm of MI; for example: 1) marked rhythms were found in samples from tropical or equatorial zones where the rhythm was not expected (Chennai in India and Medellín in Colombia); 2) in all the examined samples strong differences were found among months of the same season or with the same photoperiod and temperature; it was frequent to find a peak of MI followed by a trough of MI in contiguous months (Valenzuela et al., 1996a, 1996b, 1999; Valenzuela 2004, Valenzuela 2006); 3) samples from contiguous regions belonging to different countries show different MI rhythms. One of the most striking differences in the menarche incidence (MI), between Hemispheres was found in Feb, with a peak in Santiago (summer) and a trough in Europe (winter, Valenzuela et al. 1991, 1993, 1996a, 1996b). This could be produced by climatic factors, but this is refuted because in most countries of Europe, Jan and Dec (winter months as Feb) showed a peak, but Feb showed a trough. In Santiago we observed for Dec-Jan-Feb a peak-peak-peak series, in Europe a peak-peak-trough series. This correlated very well with the quality of months being a vacation (Vac) or a study (Stu) month; in Santiago a Vac-Vac-Vac series and in Europe a Vac-Vac-Stu series occurred for Dec-Jan-Feb, respectively. This discovery was realized independently by Prof. Csoknyay in Hungary, Prof. Srikumari in India, Prof. Pineda in Colombia and by our group in Santiago, because in the four countries Stu-months and Vac-months showed lower and higher MI,

Corresponding author: Carlos Y. Valenzuela. Programa de Genética Humana. Instituto de Ciencias Biomédicas (ICBM), Facultad de Medicina, Universidad de Chile. Independencia 1027, Casilla 70061, Independencia, Chile. Fax (56-2) 7373158; Phone (56-2) 9786302. E-mail: cvalenzu@med.uchile.cl

Received: January 31, 2012. In Revised form: October 30 , 2012. Accepted: August 29, 2012

respectively (Valenzuela et al., 1996a, 1996b, 1999). We decided to test the hypothesis that Stu-months and Vac-months implied low and high MI, respectively. With four samples from Chennai (ancient Madras, India), Debrecen (Hungary), Medellín (Colombia) and Santiago (Chile) we found only 5 out of 48 months that disagreed with the hypothesis, thus the agreement was highly significant ($P<10^{-8}$, Valenzuela et al., 1999). We hypothesized that vacations associated with fiesta (or relaxation) expectancy elicited menarche and that study, associated with non-fiesta (or stress) expectancy, delayed (inhibited) menarche. This does not mean only the relationship with the school-vacation-study period, but with the socio-cultural yearly periodicity that involves students, workers, travelers and most human annual activities. This seems to explain the preliminary conclusion of Nakamura et al. (1986) in Japan that there was not a relationship of the secular changes in the monthly rhythm of MI and secondary school periods. They found annual rhythms with peaks in Apr and Aug since 1891 until now, and a third peak in Jan since 1960. They argued that by 1900 around 1% of girls attended secondary school after the age of 12. From our perspective, this is a premature conclusion because there is the possibility that general social vacations used to coincide with primary school vacations, but no data was provided to test this hypothesis. Also, the two described peaks maintained for more than 90 years agree well with social vacation-work periods. We postulated that the "annual expectancy" or a "long term expectancy" of a "climate" of celebration was the "zeitgeber" (http://en.wikipedia.org/wiki/Zeitgeber) "time giver" or "synchronizer" of the MI annual rhythm, and not the seasonal climate (Valenzuela et al., 1999; Valenzuela, 2004). Thus the following test was to examine the days of celebrations (feasts) for the girls in Medellín and Santiago for which we knew the holidays or, more precisely the days of fiesta. Very significant peaks of MI were found for the birthday and fiesta days that were significant for girls, but not for holidays without special significance for them (a revision of specific days is found in Valenzuela, 2004, where the memory bias was also tested and refuted) or in current holidays of the week (Saturday and Sunday), which did not show a peak of menarche (Valenzuela, 2004).Thus we discarded definitively the refuted hypothesis of the circa-annual seasonal monthly MI and worked with the circa-[vacation (fiesta)]-[study (non-fiesta)] expectancies rhythm as the primary cause of the circa-annual menarche rhythm. This hypothesis proposes that the calendar rhythm of general vacation (fiesta) – study (non-fiesta) lived by girls, year by year since their birth (or even prenatally, remember that the hypothesis proposes a general vacation-study rhythm for everybody not only for girls having menarche) generates a circa-annual rhythm of expectancies of fiesta-non-fiesta that leads to increase MI by the expectancy of a fiesta-period and to stop or delay menarche by the expectancy of a non-fiesta period. Vacation months are associated with a high increase of MI and study months with a trough of MI.

With this in mind, the hypothesis of influence of the fiesta-vacation versus non-fiesta-study on the age at menarche was a logical expectancy. Previously, the age at menarche was related to the season (Gueresi, 1997), but since the relationship found was rather for vacation-study periods, the study of MI and age at menarche according to seasons blurs the relationship of MI with Vac-Stu months and hides the true origin of the menarche rhythm. It seems that our refutation of the seasonal factors presented as early as 1991 (Valenzuela et al., 1991, 1993) was not accepted by researchers working in this field. Matchock et al. (2004) insisted on seasonal factors as the cause of the MI rhythm. Their data show several conclusive refutations of seasonal or climatic factors. They found that May and July (one month before and after the summer solstice, respectively, with similar photoperiod and temperature) had a significant trough ($p<0.001$) and peak ($p<0.0001$) of menarche, respectively. Also, they found that Jan and Feb, two winter months, had a significant peak ($p<0.01$) and trough ($p<0.01$), respectively. These facts refute conclusively the climatic or seasonal hypothesis; but they agree perfectly with our Vac-Stu fiesta-non-fiesta hypothesis. If Dec-Jan are months with vacations as well as Jul-Aug, and Feb (or including middle-end Jan) and Jun (or including beginning-middle Jul) is a month of study, as we know, in general, from the USA vacation-study calendar, the results of Matchock et al (2004) fit perfectly our vacation-study hypothesis. To better understand our hypothesis on the circa-vacation-study age at menarche, let us work with the Chilean school rhythm. In Dec, Jan and Feb (Vac-months) higher MI were found, but in Mar (first Stu-month) a fall in the incidence occurs. This lower incidence continues until Jun; it begins to increase until Dec, where a peak is again observed. The expected annual rhythm of the age at menarche is easy to predict from such a rhythm of incidence. In Mar until Jun lower means of menarche age should be observed (menarche refractory to study delay); the monthly mean should increase from Jun to Dec (the delayed menarche during the Stu-months) as the Vac-months approach. This pattern was seen in Santiago (temperate zone S Hemisphere), Medellín (equatorial zone, N. Hemisphere) and Riberão Preto (Brazil, temperate zone, S. Hemisphere) and published previously (Valenzuela 2004, 2006). The present study intends to test formally the hypothesis of the influence of Stu-months and Vac-month on the age at menarche. The expectancy of studies can delay menarche but it cannot suppress it definitively. Soon or later, according to the impressionableness (in face of the expectancy of fiesta or non-fiesta) of each girl, menarche is going to occur. Those girls that should have had menarche in a certain month (due to their natural sexual maturation) and were delayed by studies (stress) are going to have it in the following months at a higher age of menarche.

RATIONALE, DATA METHODS AND STATISTICS

Rationale

After examining data on the monthly MI we found that the monthly incidence rhythm accounted for the relationship of menarche and the condition Stu-month (low incidence) or Vac-month (high incidence). By assuming that the study regime decreases the MI and delays menarche of susceptible girls, we proposed a hypothesis on the monthly rhythm of the age at menarche (Valenzuela, 2006). The hypothesis proposed that the last month(s) of the long vacation period (with a high MI) and the following Stu-months (with a low MI) should present the lowest means of the age at menarche. In the last Vac-months no more delayed girls are present and in the initial Stu-months only refractory girls for the factors that delayed menarche menstruate at the earliest ages. In the following Stu-months the low incidence and mean age of menarche are maintained or grow slowly, but a tendency

to increase the mean age at menarche should be seen until a Vac-month, where a higher incidence of menarche should be observed with a high mean of menarche age (induction of delayed menarche). This increase in the menarche age occurs in the initial Vac-months until all the delayed girls have their menarche; at this point a dramatic fall in the age of menarche should be observed, conserving the high MI that is the characteristic of Vac-months. The expected random monthly incidence of menarche was calculated as the quotient between the number of days of each month and 365.25 (Feb = 28.25 days). As pointed out in the Introduction, our studies showed that it was not properly the fiesta period or holidays, but rather the expectancy of fiesta or holidays is the factor that increases the MI. It was evident that the environment or circumstances related to the expectancy of fiesta (relaxation or reward) or non-fiesta (stress or unwanted situation) could impress strongly the neuro-psycho-endocrine system, so as to change the age of circa-vital events such as menarche (Valenzuela et al., 1999; Valenzuela, 2004, 2006). I think that the expectancy of the event, and not necessarily the event itself was the cause of the rhythm, because of the left-biased bell shaped distribution of menarche around the event. This precluded a recruitment distribution where menarche increases its incidence in the previous days (or weeks or months) of the event (Vac-months) and decreases drastically after the event (Valenzuela et al., 1999; Valenzuela, 2004, 2006). We have called the factor of the rhythm fiesta as a preliminary approach. We do not know whether entering school is a stress factor, but I use this term in a colloquial mode, leaving its demonstration for further research. Hard work is necessary to discover the specific neuro-psycho-endocrine factor. It is important to remark that in Chile the two weeks of winter vacation often occurs in July, but it is not a fixed period; it is defined year to year and it may range from the last week of June to the first week of August. Thus, the winter vacation in Chile cannot produce a clear expectancy of fiesta as fixed holidays or vacations can. We found a strong confirmation of this condition examining MI in the Christian celebration of the Holy Week that is variable in the calendar year to year; as expected the Holy Week did not have a menarche peak (not published). The midyear vacations in Medellín (Colombia), Riberão Preto (Brazil) and in USA (mid-Atlantic states, Matchock et al., 2004) are fixed periods of vacation, thus the fiesta-expectancy for the mid-year vacation does really occur.

DATA AND METHODS

Published data of age at menarche from Santiago, Chile (two samples, 1978 and 1990-1), Medellín, Colombia (1990) and Riberão Preto, Brazil (1998) were studied (Tavares et al., 2000, 2004; Valenzuela, 2006). The condition of Vac-month or Stu-month is in these cited articles. The monthly incidence and the mean age at menarche in a calendar month were indicated as over (+) or under (-) the expected incidence or the total mean age, respectively. Months were classified as Vac-month if they had a week or more of vacation days, when it was indicated in the literature or if it was considered as a Vac-month by the authors; otherwise it was considered as a Stu-month. A more recent sample from USA was included (Matchock et al., 2004); however, this study did not present the age at menarche for each month but the result of the analysis clustering months by season.

STATISTICS

The agreement and disagreement with the hypothesis, given in the Rationale, was indicated for each month by (+) and (-), respectively and a sign test was applied to calculate the statistical significance, under the binomial expected probability of 0.5 for (+) and 0.5 for (-) signs. Since the condition of agreement and disagreement may be difficult to evaluate for a reader who does not know the hypothesis, an example is developed. Feb in Santiago is the last summer Vac-month, thus according to the hypothesis it should present a high MI (Vac-month) but a low mean age at menarche because it happens after two months of vacations where all the delayed girls have had their menarche. If this is found in Santiago a + sign is given to Feb; however, Feb in Medellín (Colombia) or Riberão Preto (South Brazil) is the first school month, after the Dec-Jan vacations so it should present a low MI and a low mean age at menarche. In this example the MI is mentioned to orient the reader, but it was tested in previous articles, thus in the present analysis only the expected mean age at menarche was used to assign the agreement or disagreement with the hypothesis.

RESULTS

The agreement and disagreement with the hypothesis is shown in Table 1 for samples from Santiago (1978 and 1990) and in Table 2 for samples from Medellín (1990) and Riberão Preto (1998). In Table 2 a sample from the mid-Atlantic states of USA (Matchock et al., 2004) is included to test the agreement of MI with the sample from Medellín, because the samples from the Northern Hemisphere share a very similar pattern of vacation-study regime and coincide in having the National Day in July (4^{th} for USA, and 20^{th} for Colombia). However, the samples differ completely in the climatic conditions. While in the Mid-Atlantic States of USA there are four clearly demarked seasons, in Medellín, an equatorial city with eight solar seasons, an "eternal" spring occurs. Differences between the samples also agreed with differences in vacation-study condition of months. Dec in Medellín showed the second peak of MI, but it did not show a significant increase in MI in USA; this also agrees with the hypothesis because in Medellín Dec is a full vacation month, but it is a partial vacation month in USA. Also, the mid-year vacation in Medellín includes days of Jun and finishes in Jul (at the 20^{th} Jul National Day), but the midyear vacation in USA begins in Jul and finishes in Aug; we see a shift toward Aug in the USA sample in relation to Medellín. In the comparison of samples from Medellín and USA a significant correlation was found for the MI ($r = 0.6869$; $p = 0.014$).

In Santiago, in 1978 Mar was a Vac-month and in 1990-1 it was a Stu-month; Sep was Stu-month in 1978 and Vac-month in 1990-1. The standard deviation is missing in the Brazilian sample, so the standard error could not be calculated. The standard error is important because the agreement-disagreement with the hypothesis is interpreted between two consecutive months by their significant difference (more than two standard errors) in the MI (previous analyses) or in the mean age at menarche. The Brazilian sample is rather small, so a large variance and standard error are expected in the monthly incidence of and mean age at menarche, this implies that the tendency of the monthly mean of the age at menarche cannot be precisely evaluated as it can in the other samples. In the Chilean and Colombian samples there was a complete

TABLE 1

Incidence, mean age at menarche and agreement or disagreement with the hypothesis of the influence of the vacation-study condition on the age at menarche. Chilean girls from Santiago sampled in 1990-1 and 1978 (Valenzuela et al., 1999; Valenzuela, 2006).

Age at menarche in months															
		Chilean sample 1990-1991							Chilean sample 1978						
MONTH		N	%	IS	MAM	SE	MS	AHY	N	%	IS	MAM	SE	MS	AHY
JAN	V	415	12.9	+	148.5	0.82	-	+	362	13.9	+	150.6	0.85	-	+
FEB	V	497	15.4	+	148.3	0.67	-	+	344	13.2	+	149.6	0.90	-	+
MAR	S	238	7.4	-	149.1	0.94	-	+	223	8.5	+	151.1	1.04	-	+
APR	S	141	4.4	-	150.5	1.24	-	+	160	6.1	-	150.1	1.33	-	+
MAY	S	142	4.4	-	150.8	1.22	-	+	140	5.4	-	147.9	1.34	-	+
JUN	S	184	5.7	-	149.7	1.10	-	+	187	7.2	-	149.9	1.06	-	+
JUL	V	250	7.8	-	151.3	0.88	-	+	163	6.2	-	151.5	1.13	-	+
AUG	S	221	6.9	-	153.6	0.98	+	±	180	6.9	-	152.9	1.13	+	+
SEP	V	283	8.8	+	151.6	0.88	+	+	181	6.9	-	152.6	1.15	+	+*
OCT	S	234	7.3	-	153.8	0.90	+	+	186	7.1	-	153.0	1.15	+	+
NOV	S	224	7.0	-	155.8	0.88	+	+	184	7.0	-	155.0	1.12	+	+
DEC	V	396	12.3	+	155.6	0.71	+	+	302	11.6	+	157.7	0.78	+	+
Total		3225	100		151.4	0.26			2612	100		151.9	0.31		

MONTH = V (vacation), S (Study); N = number; IS = incidence sign: + = over the expected monthly incidence; - under the expected monthly incidence; MAM = mean age at menarche; SE = standard error; MS = MAM sign; + = mean over the total mean; - = mean under the total mean; AHY = agreement (+) or disagreement (-) with the hypothesis. * In 1978 September was not a vacation month.

TABLE 2

Incidence, mean age at menarche and agreement or disagreement with the hypothesis of the influence of the vacation-study condition on the age at menarche. Samples from Medellín (Colombia, Valenzuela et al., 1999) and Riberão Preto (Brazil, Tavares et al., 2004). Monthly incidence of menarche in a USA sample (Matchock et al., 2004).

Age at menarche in months																
		Medellín sample (1990)							USA		Brazilian sample (1998)					
MONTH	VS	N	%	IS	MAM	SE	MS	AHY	N	VS	N	%	IS	MAM*	MS	AHY
JAN	V	334	9.7	+	147.9	0.75	-	+	274	V	45	9.8	+	148.0	-	+
FEB	S	207	6.0	-	146.8	0.97	-	+	160	S	35	7.6	-	144.3	-	+
MAR	S	208	6.1	-	148.1	0.97	-	+	209	S	41	8.9	+	147.0	-	+
APR	S	246	7.2	-	147.8	0.83	-	+	232	S	28	6.1	-	151.0	+	-
MAY	S	229	6.7	-	148.8	0.94	-	+	171	S	40	8.7	+	148.7	-	+
JUN	V	253	7.4	-	152.0	0.96	+	+	256	S	42	9.1	+	150.2	+	+
JUL	V	559	16.3	+	148.7	0.65	-	+	331	V	38	8.3	-	149.4	±	+
AUG	S	188	5.5	-	149.0	1.18	-	+	240	S	39	8.5	+	150.0	+	-
SEP	S	177	5.2	-	149.9	1.04	+	+	193	S	25	5.4	-	147.3	-	+
OCT	S	231	6.7	-	151.3	0.89	+	+	183	S	28	6.1	-	149.1	-	+
NOV	V	322	9.4	+	151.4	0.85	+	+	224	S	33	7.2	-	152.0	+	+
DEC	V	481	14.0	+	152.3	0.65	+	+	223	V	66	14.4	+	152.7	+	+
Total		3435	100		149.7	0.25			2696	460	100			149.4		

Nomenclature as in Table 1. MAM* = mean without standard error.

agreement with the hypothesis (36 months). In the Brazilian sample only two months disagreed with the expected situation. Thus in the total 48 months we found two disagreements, this occurs with probability $P = 4.27x10^{-12}$. As proposed in the Rationale, one of the most relevant expected results of the hypothesis is the fall in the mean age at menarche between the first month of vacations (long vacations), when a great number of girls with delayed menarche had it, and the last month of vacations or the first month of study. If we observe the mean age at menarche (in months) at Dec and February (both months belong almost to the same season) the opportunity for a contrast is optimum. This is an additional refutation of the climatic genesis of the rhythm; among the four samples we have: Chile 1978, Dec = 157.7, Feb = 149.6 (dif = 8.1 months, $P<10^{-7}$); Chile 1990-1, Dec = 155.6, Feb = 148.3 (dif = 7.3, $P<10^{-8}$); Colombia 1990, Dec = 152.3, Feb = 146.8 (dif = 5.5, $P<10^{-6}$); Brazil 1998, Dec = 152.7, Feb = 144.3 (dif = 8.4, the probability cannot be calculated because the standard deviation is not known, but this difference is surely significant, because the standard deviation in all the samples is near 14 months).

In complete agreement with our hypothesis, and in disagreement with the seasonal hypothesis, the USA sample showed a late menarche for girls having it in Dec and an early menarche in girls having it in Feb (Matchock et al., 2004).

DISCUSSION

It is important to remember that this hypothesis was proposed after seeing the distribution of the monthly incidence of menarche (MI). Thus there is no possibility of a circular epistemological procedure when we studied the age at menarche. We confirm that the beginning of studies delays menarche in some girls, who are going to have it some months later when Vac-months approach. This result was observed in the four samples (and in the USA sample, as far as MI and age at menarche in Dec and Feb are concerned); when the vacation period is coming there is an increased number of girls having menarche at older ages. This occurs at midyear in Medellín and Riberão Preto (and it is expected for USA) with fixed vacations in the middle of the school period. The pattern of MI has been also found in India and Hungary (and in USA as described), thus we can conclude that this is a very probable true cultural-biotic relationship. We confirm our proposition that this is not a seasonal circa-annual rhythm, but a circa-[vacation (fiesta)]-[study (non-fiesta)] expectancies rhythm that is a systematic periodicity repeated year after year, caused by socio-cultural events with deep significance for girls. The decay of the age at menarche from 5.5 to 8.4 months between December and February, in the four samples (and in the sample from USA, but without published values) is an extraordinary biotic process; this decay shows that the cultural-expectancy of important events for girls is a factor comparable to deep under nutrition (Leenstra et al., 2005), highly competitive physical training (Vadocz et al., 2002) or near 50 years in the secular trend of menarche age (Nakamura et al., 1986; Vecek et al., 2012; Woronkowicz et al. 2012).

Unfortunately the Brazilian sample is too small to study the influence of the daily MI or for a precise study of differences in the monthly MI (large standard errors), and the two disagreements with the hypothesis could be due to random fluctuations. It is possible that some fiesta periods are not described in the article, as for example in April and around July-August. Also, the USA study (Matchock et al., 2004) did not provide figures for monthly means of menarche with which a fine test of our hypothesis could be done. However, Dec and Feb agree perfectly with our hypothesis as far as the authors informed qualitatively in the article.

These studies uncover important socio-cultural effects on the neuro-psycho-endocrine system. It is probable that boys are also submitted to such fiesta-expectancy influences, for example growth or sexual development could be accelerated in vacations in relation to the study period; we made some observations in the longitudinal follow up study, but these were not formalized or published. Unfortunately, studies are performed in relation to seasons and this does not allow answering this question. Our study provides a solid framework for psycho-somatic, bio-socio-cultural, socio-endocrine and bio-psycho-anthropological studies. We point out one of these important socio-cultural-endocrine interactions. Dec 8 is a very important religious (Catholic) fiesta. Colombia and Chile are mostly Catholic countries in which the 8 Dec is a holiday and highly celebrated. However, while in Colombia Catholic girls receive often the first communion (an important family fiesta) on this day, the Catholic Church discontinued this practice in Chile. In Colombia several days presented significant accumulation of menarche; among them 8 Dec presented the highest significant peak of MI, but in Chile the MI on 8 Dec was not significantly different from any other day of December (Valenzuela, 2004). Again, we emphasize that it is not the first communion that elicits menarche (in the girl that receives it), but the expectancy of a national and familial fiesta that elicits menarche in girls of these families who are in the time of their first menstruation. Our study reveals that living year by year highly affective-emotional cultural rhythms imprints dynamically the brain so as to condition deeply the neuro-psycho-endocrine axis that is compelled to follow these rhythms. Some cultural elements such as religious or national festivities are shown to have more psycho-endocrine influences than previously expected.

ACKNOWLEDGEMENTS

This long research was possible by the collaboration of Prof J Csoknyay (Hungary), N Pineda (Colombia), CR Srikumari (India) and A Patri (Chile). Dr. J Csoknyay first proposed the possible influence of vacation on the menarche rhythm.

REFERENCES

BOJLEN K, BENTZON WW (1974) Seasonal variation in the occurrence of menarche. Dan Med Bull 21:161-168.

GUERESI P (1997) Monthly distribution of menarche in three Provinces of North Italy. Ann Hum Biol 24:157-168.

LEENSTRA T, PETERSEN LT, KARIUKI SK, OLOO AJ, KAGER PA, ter KUILE FO (2005) Prevalence and severity of malnutrition anda ge at menarche; cross- sectional Studies in adolescente schoolgirls in western Kenya. Eu J Clin Nut 59: 41- 48.

NAKAMURA I, SHIMURA M, NONAKA K, MIURA T (1986) Changes of recollected menarcheal age and month among women in Tokyo over a period of 90 years. Ann Hum Biol 13: 547-554.

PATRI A, VALENZUELA CY, MORALES I, SAAVEDRA I, FIGUEROA L (1980) Edad de menarquia de niñas de Escuelas Fiscales del Área Norte de Santiago. Cuad Med Soc (Chile) 21:12-20.

TAVARES CH, BARBIERI MA, BETTIOL H, BARBIERI MR, DE SOUZA L (2004) Monthly distribution of menarche among Schoolgirls from a municipality in Southeastern Brazil. Am J Hum Biol 16:17-23.

VADOCZ EA, SIEGEL SR, MALINA RM (2002) Age at menarche in competitive figure skaters: variation by competency and discipline. J Spo Sci 20: 93-100.

VALENZUELA CY (2004) Día de menarquia, expectativa de fiesta y sesgo de memoria Rev Med Chile 132:299-306.

VALENZUELA CY (2006) Confirmación de la expectativa vacación-estudio como factor principal del ritmo anual de incidencia y edad de menarquia. Rev Med Chile 134:606-612.

VALENZUELA CY, NUÑEZ E, TAPIA C (1991) Month at menarche: a re-evaluation of the seasonal hypothesis. Ann Hum Biol 18:383-393.

VALENZUELA CY, NUÑEZ E, TAPIA C (1993) Month at menarche: a re-evaluation of the seasonal hypothesis. Ann Hum Biol 20:200-202.

VALENZUELA CY, SRIKUMARI CR, GOPINATH PM, GHOSE N, GAJALAKSHMI P, CSOKNYAY J (1996) New evidence of non seasonal factors in the menarche rhythm. Biol Res 29:245-251.

VALENZUELA CY, PINEDA N, OLARTE G, VÁSQUEZ G (1996) Ritmo anual de menarquia en Medellín, Colombia. Rev Med Chile 124:437-441.

VALENZUELA CY, SRIKUMARI CR, CSOKNYAY J, PINEDA N (1999) Ritmos anuales escolar (vacaciones-estudio) y de menarquia. Rev Med Chile 127:143-150.

VECEK N, VECEK A, PETRANOVIC MZ, TOMAS Z, ARCH-VECEK B, SKARIC- JURIC T, MILICIC J (2012) Secular trend of menarche in Zagreb (Croatia) adolescents. Eu J Obst Gynecol Reprod Biol 160: 51-54.

WORONKOWICZ A, CICHOCKA BA, KOWAL M, KRYST L, SOBIECKI J (2012) Physical development of girls from Krakow in the aspect of socioeconomical changes in Poland (1938-2010). Am J Hum Biol. 2012 Jun 27. doi: 10.1002/ajhb. 22283

Biol Res 46: 27-32, 2013

Regional density of glial cells in the rat corpus callosum

Daniel Reyes-Haro*,‡, Ernesto Mora-Loyola‡, Berenice Soria-Ortiz and Jesús García-Colunga

Departamento de Neurobiología Molecular y Celular. Instituto de Neurobiología, Universidad Nacional Autónoma de México, Campus Juriquilla, Boulevard Juriquilla 3001 Juriquilla, Querétaro CP 76230, México.

ABSTRACT

Axons and glial cells are the main components of white matter. The corpus callosum (CC) is the largest white matter tract in mammals; in rodents, 99% of the cells correspond to glia after postnatal day 5 (P5). The area of the CC varies through life and regional differences related to the number of axons have been previously described. Whether glial cell density varies accordingly is unknown; thus the aim of this study was to estimate glial cell density for the genu, body and splenium -the three main regions of CC-, of P6 and P30 rats. Here we report that the density of CC glial cells reduced by ~10% from P6 to P30. Even so, the density of astrocytes showed a slight increase (+6%), probably due to differentiation of glioblasts. Interestingly, glial cell density decreased for the genu (-21%) and the body (-13%), while for the splenium a minor increase (+5%) was observed. The astrocyte/glia ratio increased (from P6 to P30) for the genu (+27%), body (+17%) and splenium (+4%). Together, our results showed regional differences in glial cell density of the CC. Whether this pattern is modified in some neuropathologies remains to be explored.

Key words: Astrocytes, corpus callosum, genu, glial cells, splenium

INTRODUCTION

The corpus callosum (CC) is the main white matter tract in the brain and is involved in interhemispheric communication. This commissure is composed of axons and glial cells, while neuronal somata make up less than 1%. After postnatal day 5 (P5), glial cells predominate, accounting for 99% of all cells (Sturrock, 1976; Aboitiz & Montiel, 2003). The size, myelination, and density of fibers in callosal subregions are related to the brain regions they connect (Doron & Gazzaniga, 2008). Thus thin unmyelinated fibers are most dense in the genu and splenium (anterior and posterior CC), where they connect association and prefrontal areas, while large diameter myelinated fibers are concentrated in the midbody of the CC, where they connect primary and secondary sensory and motor areas (Aboitiz, 1992). Interestingly, electron microscopic analysis revealed that the number of callosal axons increases from 4.4 million at birth to 11.4 million at P5 and this number is maintained until the adult stage in rats (P60) (Gravel et al., 1990), although the number of axons of the visual cortex projecting through the splenium of the rat CC decreased by 15% from P15 to P60 (Kim & Juraska, 1997). On the other hand, myelination in the CC starts with non-compacted cytoplasmic sheaths of myelin at P12, and each oligodendrocyte sheathes an average of 13 axons. Later, when the compact myelin is formed, a single oligodendrocyte sheathes, on average, 15 axons (P17) (Bjartmar et al., 1994). Considering all this information, CC regions might differ in glial cell density. Interestingly, it is not known if the glial cell density increases or remains constant through development, or if the distribution of glial cells and the astrocyte/glial cell ratios are different among different regions of the CC. Therefore, the aim of this study was to estimate glial cell densities in the CC at two ages (P6 and P30) and to determine if there are differences among callosal regions.

MATERIAL AND METHODS

Histology

Six female rats per age group (P6 and P30) were anesthetized with an overdose of sodium pentobarbital (100 mg/Kg) and then decapitated. Whole brains were removed rapidly and dissected on ice. The hemispheres were separated and fixed with 4% paraformaldehyde in phosphate buffered saline (PBS, 0.1 M, pH 7.4) for 24 h and then transferred to 30% sucrose in 0.1 M PBS at 4 ºC for cryoprotection. Sagittal sections (30 µm; two consecutive from the right hemisphere and one the from left hemisphere = 3 slides per animal) were obtained using a freezing cryostat and collected on gelatinized slides for staining with propidium red to estimate glial cell number (Fig. 1 and 2).

Immunohistofluorescence

Cryosections were blocked in PBS containing 1% bovine serum albumin, 1% goat serum, and 0.1% Triton X-100 for 1 h and labeled overnight at 4 ºC with a 1:500 dilution of anti-glial fibrillary acidic protein (monoclonal mouse anti-GFAP, Milipore, USA). After incubation with the primary antibody, samples were rinsed 3 times in PBS and labeled for 1 h at room temperature with a 1:500 dilution of Alexa 488 goat anti-mouse antibody (Invitrogen, USA). Finally, slides with sagittal sections containing the CC were washed 3 times with PBS, stained with propidium red and mounted with Vectashield (Vector laboratories, Inc, USA). Slides were examined with an epifluorescence microscope (Olympus BX60) coupled to a digital camera (Olympus DP70). Image-Pro MC for Windows was used for estimation of glial cell density. A Zeiss LSM 510 Meta confocal microscope (Zeiss, Göttingen, Germany)

Corresponding author:* Dr. Daniel Reyes-Haro. Departamento de Neurobiología Molecular y Celular. Instituto de Neurobiología, Universidad Nacional Autónoma de México, Campus Juriquilla, Boulevard Juriquilla 3001 Juriquilla, Querétaro CP 76230, México. Tel/ Fax. 52(442) 238-1064. E-mail: dharo@unam.mx

Received: July 6, 2012. In Revised form: Octobrer 30, 2012. Accepted: December 26, 2012

was used for confocal images, with wavelength 488 nm for excitation of Alexa 488 and propidium red. The emission wavelengths were 519 nm and 610 nm respectively. The z-stack images (4 to 5 consecutive confocal sections of 512 x 512) were obtained every 5 μm with stack size of X: 450 μm and Y: 450 μm and processed in Aim Image Examiner.

Glial cell counting

The population of cells immunostained by the GFAP antibody was contrasted with the number of propidium red-labeled nuclei for each slide and each CC region. Data analysis (counting) was performed using Image J software 1.41 (NIH, National Institute of Health, Bethesda, Maryland, USA).

A test square grid of 0.01 mm^2 in each section was used to estimate the number of propidium red-stained cell nuclei equivalent to the total number of glial cells including $GFAP^+$ cells corresponding to astrocytes (only process-bearing cells showing their soma in the plane of the section were counted). Six randomly chosen fields (as indicated in Figs. 1D and 2D) were counted by progressive displacement of the test square grid. The astrocyte / glial cell ratio results from the estimation of the GFAP+ cells divided by the total number of glial cells labeled with propidium red. Data are presented as the mean ± standard error of the mean (S.E.M.) and nonparametric statistics were performed with the Mann-Whitnney-U test; $p < 0.05$ was considered significant.

RESULTS

The pool of glial cells is reduced from P6 to P30

Our estimations of glial cell density began at P6 because the nuclear counts could be related to the estimation of glial cell number (99% after P5; Sturrock, 1976); P30 (considered as an adult stage) was selected for comparison. We found that the number of glial cells decreased from 1880 ± 45 / mm^2 (P6) to 1672 ± 27 / mm^2 (P30) ($p = 0.00012$, Fig. 3). On the other hand, the number of astrocytes ($GFAP^+$ cells) showed a + 7% increase, from 135 ± 1.4 / mm^2 at P6 to 144 ± 1.59 / mm^2 at P30 ($p < 0.0001$; Fig. 3). These results indicate that the pool of glial cells of CC is reduced and that a fraction of glioblasts differentiated into astrocytes between P6 and P30.

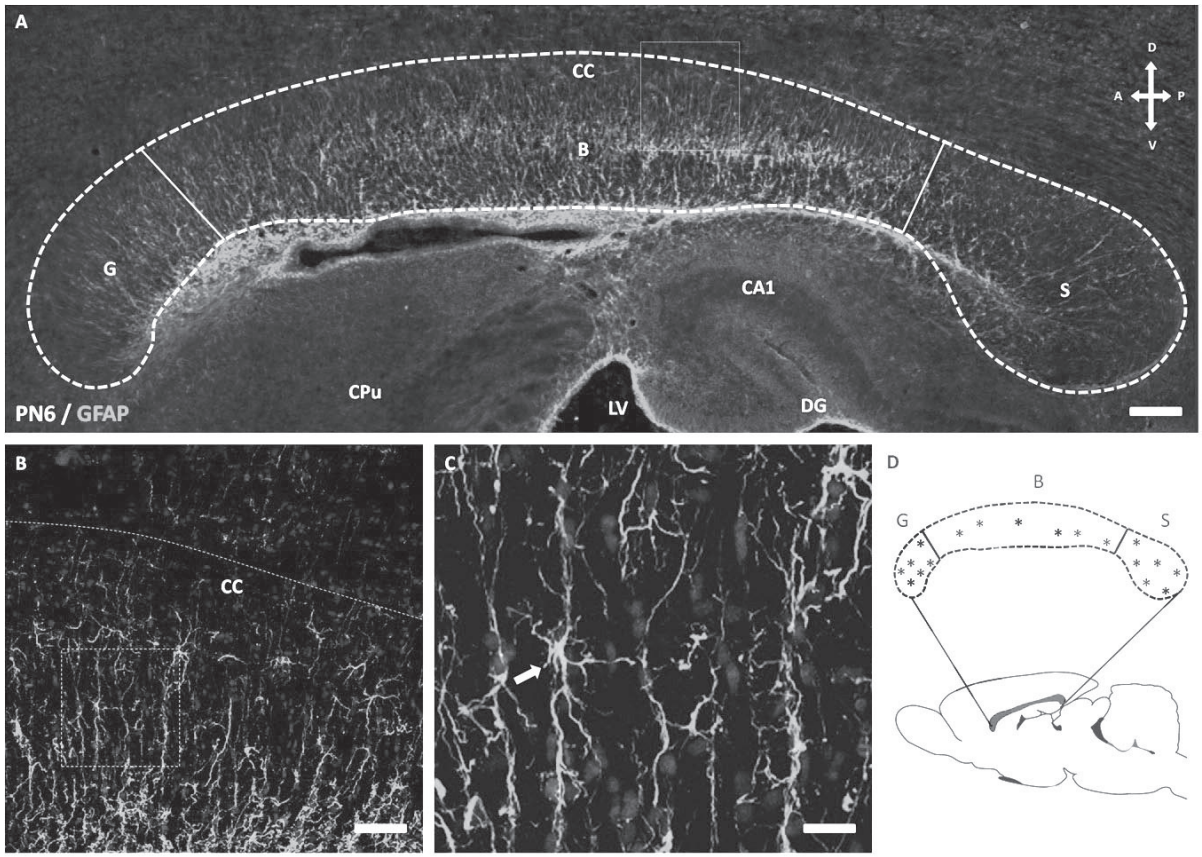

Figure 1. *The rat corpus callosum (CC) at P6. A,* Sagittal sections of the rat brain were immunostained for GFAP (18 slides from 6 brains; 3 per brain) and propidium red. The CC was dissected in 3 regions: genu (G), body (B) and splenium (S) for estimation of glial cell density (n = 18 per region). Other brain regions are indicated for anatomical reference: hippocampal CA1 region (CA1), caudate-putamen (CPu), hippocampal dentate gyrus (DG), lateral ventricle (LV). Arrows showing anatomical orientation: dorsal (D), ventral (V), anterior (A) and posterior (P). B, Zoom of the square in A to show astrocytes from CC, notice the radial projections of astrocytes. C, Zoom of the square in B to highlight radial glia (arrow). Scale bars 200 μm (A), 80 μm (B), 20 μm (C). D, The representative sites (*) used for estimation of glial cell density are highlighted in a diagram of CC. Three slides containing sagittal sections of CC where used for each brain and each region of CC included 2 selected sites per slide for estimations (6 sites per region, per rat brain).

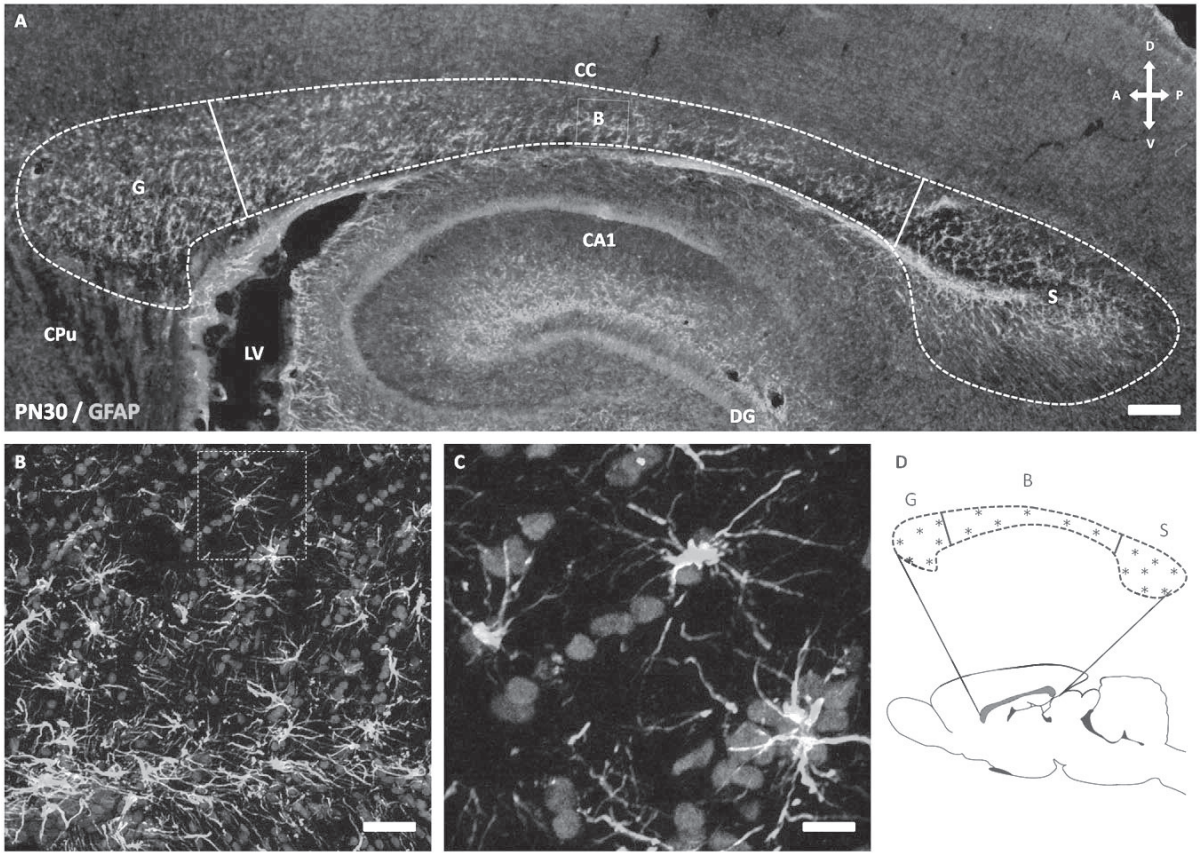

Figure 2. The rat corpus callosum (CC) at P30. *A,* Sagittal sections of the rat brain were immunostained for GFAP and propidium red (18 slides from 6 brains; 3 per brain). The CC was dissected in 3 regions: genu (G), body (B) and splenium (S) for estimation of glial cell density (n = 18 per region). Other brain regions are indicated for anatomical reference: hippocampal CA1 region (CA1), caudate-putamen (CPu), hippocampal dentate gyrus (DG), lateral ventricle (LV). Arrows showing anatomical orientation: dorsal (D), ventral (V), anterior (A) and posterior (P). B, Zoom of the square in A to show fibrous astrocytes from CC, notice that radial projections of astrocytes observed at P6 are absent at P30. C, Zoom of the square in B to highlight fibrous astrocytes (arrow). Scale bars 250 μm (A), 80 μm (B), 20 μm (C). D, The representative sites (*) used for estimation of glial cell density are highlighted in a diagram of CC. Three slides containing sagittal sections of CC where used for each brain and each region of CC included 2 selected sites per slide for estimations (6 sites per region, per rat brain).

Glial cells are more abundant in the genu

The size, myelination, and density of fibers in callosal subregions are related to the brain regions they connect (Doron & Gazzaniga, 2008). We estimated glial cell density to be greater in the genu at P6 (2319 ± 32 / mm^2) than in the body or splenium (1616 ± 14 / mm^2 and 1704 ± 14 / mm^2, respectively; $p < 0.0003$) (Fig. 4A). A similar pattern was observed at P30, but here glial cell density of the splenium was closer to that of the genu; glial cell density in the genu was 1824 ± 8 / mm^2, whereas for the body and splenium there were 1405 ± 9 and 1788 ± 13 cells / mm^2, respectively ($p < 0.001$) (Fig. 4B). Therefore, we found a higher density of glial cells in the genu than in the body or splenium, at both P6 and P30.

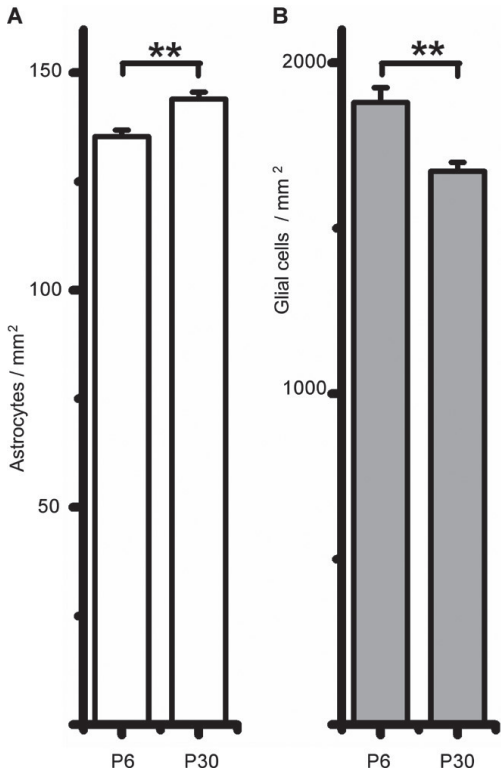

Figure 3. Estimation of glial cell density for rat CC at P6 and P30. A, The number of astrocytes per area (mm2) increased from P6 (n=52) to P30 (n=53). B, The number of glial cells decreased from P6 (n=53) to P30 (n=54). The estimation included all the regions of rat CC. Data are mean ± S.E.M. (**$p < 0.001$).

The glial cell density reduces from P6 to P30 in the genu and body

Our next step was to compare regional glial cell density between P6 and P30. The results showed that glial cell density was reduced in the genu (-21%; from 2319 ± 32 / mm^2 (P6) to 1824 ± 8 / mm^2 (P30); p<0.0001) and in the body (-18%; from 1616 ± 14 / mm^2 (P6) to 1405 ± 9 / mm^2 (P30); p<0.0001). Interestingly, the splenium showed a different pattern because a slight increase in glial cell density was observed (+5%; from 1704 ± 14 / mm^2 (P6) to 1788 ± 13 / mm^2 (P30); p=0.001) (Table 1).

Astrocyte density increases from P6 to P30

Astrocytes increased in number in the genu (+6.8%; from 147 ± 2 / mm^2 (P6) to 157 ± 2 / mm^2 (P30); p= 0.006), the body (+4.6%; from 128 ± 1 / mm^2 (P6) to 134 ± 2 / mm^2 (P30); p=0.0209) and the splenium (+9.2%; from 130 ± 1 / mm^2 (P6) to 142 ± 2 / mm^2 (P30); p<0.0001) (Table 1).

We then estimated the astrocyte / glia ratio at P6 and P30, based on GFAP immunoreactivity and nuclear staining. We consider that this ratio is a more accurate estimation because it considers the glial cell density, which varies among CC regions. Our estimations showed that the astrocyte / glia ratio increased by + 27% for the genu (from 0.0637 ± 0.0014 to 0.0858 ± 0.0008; p<0.0001), +17% for the body (from 0.0794 ± 0.0008 to 0.0951 ± 0.0014; p<0.0001) and +4% for the splenium (from 0.0766 ± 0.0008 to 0.0793 ± 0.0008; p=0.066) (Fig. 5). Overall, these results indicate that the density of astrocytes increases during postnatal development, because a fraction of glioblasts differentiate to astrocytes before P30.

DISCUSSION

The development of the CC is not homogenous through its three main regions; the genu, body, and splenium. Different changes in callosal thickness occur due to axonal myelination, redirection, and pruning (LaMantia & Rakic, 1990; Luders et al., 2010). Nevertheless, glial cell density has not been explored among CC regions during postnatal development. Here, we report that the pool of glial cells decreased from P6 to P30. During this period of development, glioblasts (the dominant cell type in CC at P5) differentiate mainly to oligodendrocytes and astrocytes (Mori & Leblond, 1970; Sturrock, 1976). Surprisingly, when the glial cell density was estimated in the three regions of the rat CC, we found that glial cell density was greater in the genu at both P6 and P30 than in the body or the splenium. The functional significance of the greater density of glial cells in the genu remains to be investigated.

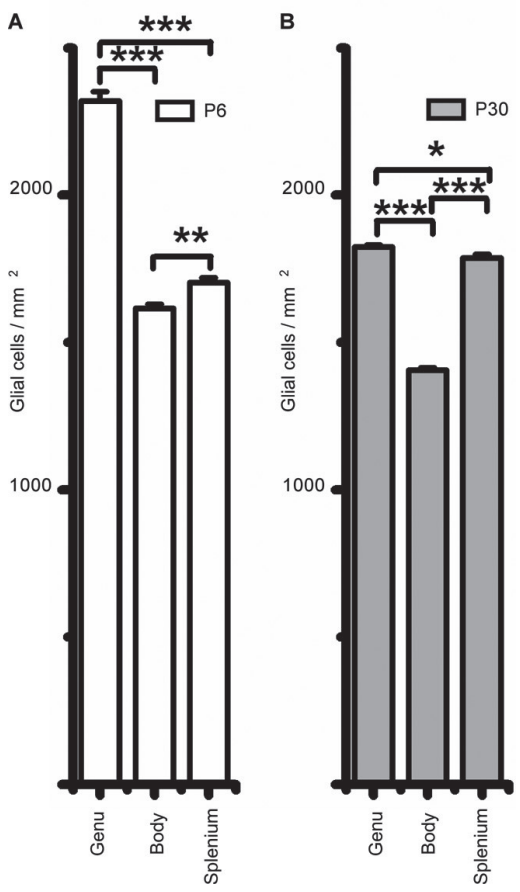

Figure 4. Regional glial cell density in rat CC at P6 and P30. The genu showed the highest density of glial cells among regions, at P6 (A; n=17 per region) and P30 (B; n=18 per region). Data are mean ± S.E.M. (*** p < 0.0001; ** p < 0.001, * p < 0.05).

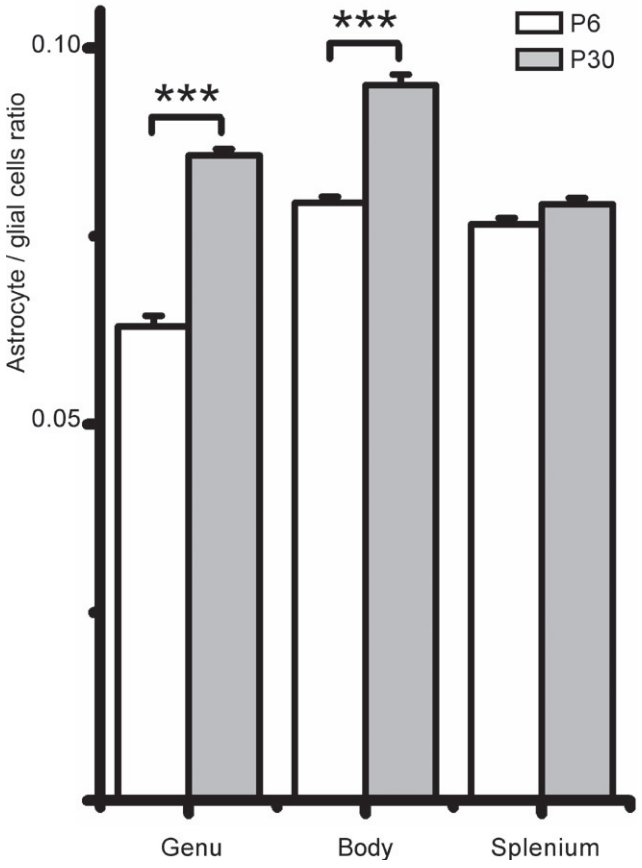

Figure 5. Astrocyte / glial cell ratio in rat CC at P6 and P30. The proportion of astrocytes among glial cells increased significantly for the genu (n=17) and the body (n=18) (P6 and P30), but not for the splenium (n=17 (P6) and n=18 (P30)). Data are mean ± S.E.M. (*** p < 0.0001).

TABLE 1

Regional changes in glial cell density from P6 to P30

Astrocytes				
Region of CC	**P6**	**P30**	**% of increase**	**p**
Genu	147 ± 2 / mm^2 (n=18)	157 ± 2 / mm^2 (n=17)	+ 6.80%	p = 0.006
Body	128 ± 1 / mm^2 (n=17)	134 ± 2 / mm^2 (n=18)	+ 4.60%	p = 0.0209
Splenium	130 ± 1 / mm^2 (n=17)	142 ± 2 / mm^2 (n=18)	+ 9.20%	p < 0.0001
Glial cells				
Region of CC	**P6**	**P30**	**% of change**	**p**
Genu	2319 ± 32 / mm^2 (n=17)	1824 ± 8 / mm^2 (n=18)	- 21.34%	p < 0.0001
Body	1616 ± 14 / mm^2 (n=17)	1405 ± 9 / mm^2 (n=18)	- 13.05%	p < 0.0001
Splenium	1704 ± 14 / mm^2 (n=17)	1788 ± 13 / mm^2 (n=18)	+ 4.92%	p = 0.01

We found that the genu had the lowest astrocyte/glia ratio, with the body and splenium having similar but larger ratios at P6. However, the splenium had the lowest ratio while the body had the highest ratio at P30. These results support the hypothesis that glial cell density varies among regions of CC. Our estimations can be compared with other studies, for example, the density of astrocytes (based on GFAP$^+$ cells) that we calculated for the CC (144 cells/mm^2; P30) is similar to that in other brain regions where astrocyte markers such as GFAP or S100β have been used (130 astrocytes/mm^2 and 160 astrocytes/mm^2) (Morgan et al., 1995; Ren et al., 1992). Our estimate of astrocytes (6-9% at P30) is slightly lower than that reported in the CC of rodents using morphological identification (13-15% at P25-P45) (Sturrock, 1976), which might be due to some astrocytes that express low levels of GFAP (Zhou et al., 2000). Accordingly, the astrocyte density estimated in different brain regions was lower using GFAP than S100β (Savchenko et al., 2000).

Overall, our results show a regional difference in glial cell density that could be related to changes in the size of the CC and the number of callosal axons (Berbel and Innocenti, 1988). This pattern could be modified when glial cell dysfunction occurs and white matter integrity is compromised (Tkachev et al.,2003; Benedetti et al., 2011). Thus, glial cell density could be affected in specific regions of the CC in some neuropathologies (Lyoo et al., 2002; Di Paola et al., 2010).

In conclusion, the glial cell density of the CC decreased while astrocyte density increased between P6 and P30. This pattern was conserved among the three regions of CC, except for the splenium where the glial cell density increased. The genu displayed the highest density of glial cells, including astrocytes. Further studies are needed to see if the density of glial cells in the CC is differentially affected in neuropathologies such as bipolar depression or schizophrenia.

AKNOWLEDGEMENTS

We are grateful to L. González-Santos, M. García-Servín, E. Ruiz-Alcibar, E. N. Hernández-Ríos for technical support, and to Dr. Dorothy Pless for reviewing the manuscript. We are in debt to Prof. R. Miledi and Dr. A. Martínez-Torres for scientific support. This work was supported by Grants from the Consejo Nacional de Ciencia y Tecnología (CONACyT) 81911 and 166964 (to JGC and DRH); from Programa de Apoyo a Proyectos de Investigación e Innovación Tecnológica de la Universidad Nacional Autónoma de México (PAPIIT-UNAM) IN204809 and IB200412 (to JGC and DRH).

REFERENCES

ABOITIZ F (1992) Brain connections: interhemispheric fiber systems and anatomical brain asymmetries in humans. Biol Res 25: 51-61.

ABOITIZ F, MONTIEL J (2003) One hundred million years of interhemispheric communication: the history of the corpus callosum. Braz J Med Biol Res 36: 409-420.

BENEDETTI F, YEH PH, BELLANI M, RADAELLI D, NICOLETTI MA, POLETTI S, FALINI A, DALLASPEZIA S, COLOMBO C, SCOTTI G, SMERALDI E, SOARES JC, BRAMBILLA P (2011) Disruption of white matter integrity in bipolar depression as possible structural marker of illness. Biol Psychiatry 69: 309-317.

BJARTMAR C, HILDEBRAND C, LOINDER K (1994) Morphological heterogeneity of rat oligodendrocytes: electron microscopic studies on serial sections. Glia 11: 235-244.

BERBEL P, INNOCENTI GM (1988) The development of the corpus callosum in cats: a light and electron-microscopic study. J Comp Neurol 276: 132-156.

DI PAOLA M, SPALLETA G, CALTAGIRONE C (2010) In vivo structural neuroanatomy of corpus callosum in Alzheimer's disease and mild cognitive impairment using different MRI techniques: a review. J Alzheimers Dis 20: 67-95.

DORON KW, GAZZANIGA MS (2008) Neuroimaging techniques offer new perspectives on callosal transfer and interhemispheric communication. Cortex 44: 1023-1029.

GRAVEL C, SASSEVILLE R, HAWKES R (1990) Maturation of the corpus callosum of the rat: II. Influence of thyroid hormones on the number and maturation of axons. J Comp Neurol 291: 147-161.

KIM JH, JURASKA JM (1997) Sex differences in the development of axon number in the splenium of the rat corpus callosum from postnatal day 15 through 60. Brain Res Dev Brain Res 102: 77-85.

LAMANTIA AS, RAKIC P (1990) Axon overproduction and elimination in the corpus callosum of the developing rhesus monkey. J Neursoci 10: 2156-2175.

LUDERS E, THOMPSON PM, TOGA AW (2010) The development of the corpus callosum in the healthy human brain. J Neurosci 30: 10985-10990.

LYOO IK, KWON JS, LEE SJ, HAN MH, CHANG CG, SEO CS, LEE SI, RENSHAW PF (2002) Decrease in genu of the corpus callosum in medication-naive, early-onset dysthymia and depressive personality disorder. Biol Psychiatry 52: 134-143.

MORI S, LEBLOND CP (1970) Electron microscopic identification of three classes of oligodendrocytes and a preliminary study of their proliferative activity in the corpus callosum of young rats. J Comp Neurol 139: 1-28.

MORGAN TE, LAPING NJ, ROZOVSKY T, ODA T, HOGAN TH, FINCH CE, PASINETTI GM (1995) Clusterin expression by astrocytes is influenced by transforming growth factor beta 1 and heterotypic cell interactions. J Neuroimmunol 58: 101-110.

REN JQ, AIKA Y, HEIZMANN CW, KOSAKA T (1992) Quantitative analysis of neurons and glial cells in the rat somatosensory cortex with special reference to GABAergic neurons and parvalbumin-containing neurons. Exp Brain Res 92: 1-14.

SAVCHENKO VL, MCKANNA JA, NIKONENKO IR, SKIBO GG (2000) Microglia and astrocytes in the adult rat brain: comparative immunocytochemical analysis demonstrates the efficacy of lipocortin 1 immunoreactivity. Neuroscience 96: 195-203.

STURROCK RR (1976) Light microscopic identification of immature glial cells in semithin sections of the developing mouse corpus callosum. J Anat 122: 521-537.

TKACHEV D, MIMMACK ML, RYAN MM, WAYLAND M, FREEMAN T, JONES PB, STARKEY M, WEBSTER MJ, YOLKEN RH, BAHN S (2003) Oligodendrocyte dysfunction in schizophrenia and bipolar disorder. Lancet 362: 798-805.

ZHOU M, SCHOOLS GP, KIMELBERG HK (2000) GFAP mRNA positive glia acutely isolated from rat hippocampus predominantly show complex current patterns. Brain Res Mol Brain Res 76: 121-131.

Biol Res 46: 33-38, 2013

Protective role of vitamins C and E in diclorvos-induced oxidative stress in human erythrocytes *in vitro*

Sema Eroğlu[1], Dilek Pandir[1,*], Fatma G. Uzun[2] and Haticç Bas[1]

[1] Bozok University, Faculty of Arts and Science, Department of Biology, Yozgat, Turkey
[2] Gazi University, Faculty of Science, Department of Biology, Ankara, Turkey

ABSTRACT

Organophosphate (OP) pesticides such as dichlorvos (DDVP) intoxication has been shown to produce oxidative stress due to the generation of free radicals, which alter the antioxidant defense system in erythrocytes. In this study, the effects of DDVP (1, 10, 100 μM) or DDVP + vitamin C (VC; 10 μM) or vitamin E (VE; 30 μM), on the levels of malondialdehyde (MDA), superoxide dismutase (SOD), catalase (CAT) and glutathione peroxidase (GPx) activities in human erythrocytes were examined *in vitro*. There were no statistical differences between all groups for 1 μM concentration of DDVP. Treatment with DDVP alone produced an increase in the level of MDA and decreased activities of antioxidant enzymes ($P < 0.05$). Groups treated with vitamins and DDVP showed protective effects of vitamins against DDVP-induced changes in antioxidant enzyme activity and lipid peroxidation (LPO) (10 μM). At 100 μM concentration of DDVP vitamins had no effect on DDVP-induced toxicity. The results show that administration of DDVP resulted in the induction of erythrocyte LPO and alterations in antioxidant enzyme activities, suggesting that reactive oxygen species (ROS) may be involved in the toxic effects of DDVP. Also the data show that the plasma level of VC and VE may ameliorate OP-induced oxidative stress by decreasing LPO in erythrocytes at certain doses of OP pesicides.

Key words: antioxidant enzyme, dichlorvos, oxidative stress, vitamin, malondialdehyde.

INTRODUCTION

Pesticides are occasionally used indiscriminately in large amounts causing environmental pollution, and therefore are a cause of concern (John et al., 2001). Environmental pollution by pesticide residues is a major environmental concern due to their extensive use in agriculture and in public health programs (Celik and Suzek, 2009). Organophosphate (OP) pesticides have been detected in the soil, water bodies, vegetables, grains and other food products (IARC, 1983). OP insecticides are some of the most useful and diverse insecticides; they have been in use for almost five decades. However, the uncontrolled use of these insecticides in agriculture and public health operation has increased the scope of ecological imbalance and thus many non-target organisms have become victims (Celik and Suzek, 2009).

Dichlorvos (DDVP) is an OP that has been in use for more than 40 years. It has been evaluated in a wide range of toxicological assays including bioassays for carcinogenicity and mutagenicity (genotoxicity). The genotoxicity evaluations have included a wide range of test systems and endpoints including assays both *in vitro* and *in vivo*. There is general agreement that DDVP is genotoxic *in vitro* (Booth et al., 2007). Literature also cites DDVP toxicity to humans which includes dose-dependent decrease in human erythrocyte cholinesterase activity and sperm motility based on the urinary concentration of dimethyl phosphate, a urine metabolite of DDVP (Okamura et al., 2005).

Recent findings indicate that toxic manifestations induced by OP may be associated with an enhanced production of reactive oxygen species (ROS) (Gultekin et al., 2000, 2001; Durak et al., 2009). Among the ROS, superoxide anions, hydroxyl radicals and hydrogen peroxide enhance the oxidative process and induce lipid peroxidative damage in cell membranes (Altuntas and Delibas, 2002). The cell has several ways to alleviate the effects of oxidative stress, either by repairing the damage or by directly decreasing the occurrence of oxidative damage by means of enzymatic and non-enzymatic antioxidants. Enzymatic and non-enzymatic antioxidants have also been shown to scavenge free radicals and ROS (Gultekin et al., 2001).

As some of the pesticides may be present in tissues of exposed humans and animals, they may produce oxidative stress in tissues. Antioxidant enzymes such as superoxide dismutase (SOD), catalase (CAT) and glutathione peroxidase (GPx) in tissues may neutralize the oxidative stress (Kalender et al., 2004). Non-enzymatic antioxidants such as vitamin E (VE) and vitamin C (VC) can also act to overcome oxidative stress, being a part of the total antioxidant system. α-Tocopherol (the main form of VE) is considered as a major lipophilic antioxidant (Vatassery, 1998). VE resides mainly in the membranes and thus helps to maintain membrane stability (Baker et al., 1996). VC and VE have been shown to possess anticarcinogenic, anticlastogenic, and antimutagenic properties in a variety of *in vivo* and *in vitro* models of pesticide exposure (Hoda and Sinha, 1993).

VC (L-ascorbic acid) is hydrophilic and a very important free-radical scavenger in extracellular fluids, trapping radicals in the aqueous phase and protecting biomembranes from peroxidative damage (Harapanhalli et al., 1996). The anticarcinogenic, anticlastogenic and even antimutagenic roles of VC have been tested in a variety of *in vivo* and *in vitro* systems exposed to radiation and pesticides (Castillo et al., 2000; Durak et al., 2009). It prevents the increased production

Corresponding author: Dr. Dilek Pandir. Bozok University, Faculty of Arts and Science, Department of Biology, 66100, Yozgat, Turkey. Phone: +90 354 242 10 21/2546. Fax: +90 354 242 10 22. E-mail: durak77@gmail.com. dilek.pandir@bozok.edu.tr

Received: June 20, 2012. In Revised form: October 8, 2012. Accepted: October 16, 2012

of free radicals induced by oxidative damage to lipids and lipoproteins in various cellular compartments and tissues (Sies et al., 1992). The antioxidative efficiency of VE can be considerably increased by co-supplementation with VC, which is a co-antioxidant for VE (Stocker, 1994; Durak et al., 2009).

The present study was undertaken to determine the possible negative effects of DDVP on erythrocytes and additionally to investigate whether there is any preventive effect of a combination of plasma level of vitamins C and E *in vitro* after DDVP administration.

METHODS

Erythrocyte preparation

Twenty ml venous blood samples were obtained in heparinized dry tubes from each of six male volunteers (range 21–26 years). All volunteers were healthy, taking no medication, non-smokers, and none of them were farm or agricultural workers. Plasma was separated by centrifugation. Erythrocyte packets were prepared by washing with cold isotonic saline. After the supernatant was removed, packed erythrocytes were suspended in phosphate buffer. The concentration of hemoglobin was determined (Drabkin, 1946).

Treatment of erythrocytes

VC (L-ascorbic acid) was supplied by Carlo Erba (Milano, Italy). VC was dissolved in distilled water (Konopacka et al., 1998). VE (DL-α-tocopherol) was supplied by Merck (Germany). VE was dissolved in corn oil (Kalender et al., 2007). The doses of VC (10 μM) and VE (30 μM) were chosen based on the levels of each vitamin in human plasma (Blasiak and Stankowska, 2001). Other chemicals were supplied by Sigma-Aldrich. DDVP (1, 10 and 100 μM) was supplied by Ankara Agricultural Protection Central. Erythrocytes were divided into non-treated control and experimental groups. The control group was incubated in 0.9% NaCl at 7.4 pH. The experimental group was divided into treatment groups: DDVP (n=6), VC (n=6), VE (n=6), VC+VE (n=6), DDVP +VC (n=6), DDVP+VE (n=6), DDVP +VC+VE (n=6) groups. MDA levels and the activities of SOD, CAT and GPx were measured by spectrophotometer (Shimadzu UV-1700, Japan).

Antioxidant enzyme assays

CAT enzyme activity was measured according to the method described by Aebi (1983) by assaying the hydrolysis of H_2O_2 and the resulting decrease in absorbance at 240 nm. Data are expressed as UCAT/mg hemoglobin. GPx activity was measured using H_2O_2 as substrate according to the method described by Paglia and Valentine (1967) of absorbance at 340 nm. Data are presented as UGPx/mg hemoglobin. Total SOD activity was determined according to the method described by Marklund and Marklund (1974) by assaying the autooxidation and illumination of pyrogallol at 440 nm. Data are expressed as USOD/mg hemoglobin.

Measurement of MDA levels

MDA content was assayed using the thiobarbituric acid (TBA) test as described by Ohkawa (1979). Absorbance was measured at 532 nm to determine the MDA content. Specific activity is presented as nmol/mg hemoglobin.

Statistical analysis

Data were analyzed by software program SPSS 11.0 for Windows. Differences were calculated using one-way analysis of variance (ANOVA), followed by Tukey's procedure for multiple comparisons. $P < 0.05$ value was taken as statistically significant. All data are expressed as means ± standard deviation (S.D).

RESULTS

There were no statistical differences between VC-treated, VE-treated and VC + VE-treated cells compared to control cells (Figs. 1-4). There were no statistical differences between all groups for 1 μM concentration of DDVP.

Antioxidant Enzyme Activities

SOD (Fig. 1), CAT (Fig. 2) and GPx (Fig. 3) activities were significantly ($P < 0.05$) decreased in the DDVP treatment group compared to control group and vitamin groups alone (10 μM and 100 μM). The activities of enzymes were significantly increased in DDVP + VC and DDVP + VE groups compared to the DDVP group (10 μM). In the DDVP + VC + VE group in CAT and GP there were significantly ($P < 0.05$) increased enzyme activities compared to the DDVP, DDVP + VC and DDVP + VE groups (10 μM). These effects were not seen in 100 μM treated groups. For enzyme activities there were no statistical differences between DDVP-treated, DDVP + VE-treated, DDVP + VC-treated and DDVP + VC + VE-treated cells at 100 μM.

MDA levels

MDA levels were significantly increased in the DDVP treatment group compared to the control and groups with only vitamins (10 μM and 100 μM). There were significant decreases in the DDVP + VC and DDVP + VE groups compared to the DDVP group (10 μM). The DDVP + VC + VE group showed a significant decrease compared to the DDVP, DDVP + VC and DDVP + VE groups (10 μM) ($P < 0.05$). These effects were not seen in 100 μM treated groups. There were no statistical differences between DDVP-treated, DDVP + VE-treated, DDVP + VC-treated and DDVP + VC + VE-treated cells at 100 μM (Fig. 4).

DISCUSSION

A large number of xenobiotics have been identified to have the potential to generate free radicals in biological systems (Kehrer, 1993). DDVP acts primarily by irreversibly inhibiting acetylcholinesterase (AChE) at cholinergic junctions of the nervous system (Petroianu et al., 2006), which produces hepatotoxicity in rats and induces oxidative stress (Gupta et al., 2005). DDVP is taken into the human body very rapidly by the lungs, stomach, or skin (Guloglu et al., 2004). DDVP has toxic effects on mammals and also on fish, birds, honeybees and non-target invertebrates (Ural and Köprücü, 2006; Ogutcu et al., 2008). High doses of DDVP stimulate LPO through increasing plasma MDA levels and decreasing erythrocyte CAT activities

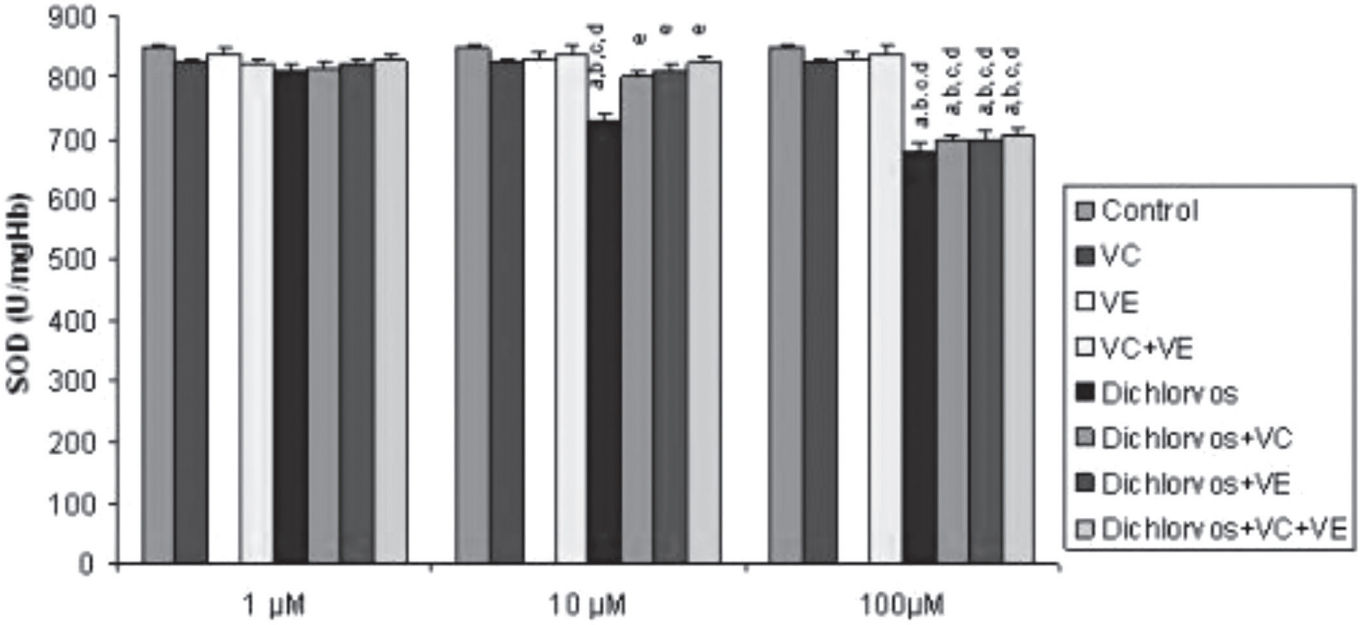

Figure 1. SOD activity in control and experimental groups of erythrocytes with dichlorvos. Comparison of nontreated control cells and other groups. [b]Comparison of VC-treated cells with VE-, VE+VC-, dichlorvos-, dichlorvos +VC-, dichlorvos +VE- and dichlorvos+VC+VE-treated cells. [c]Comparison of VE-treated cells with VE+VC-, dichlorvos-, dichlorvos+VC-, dichlorvos+VE- and dichlorvos+VC+VE-treated cells. [d]Comparison of VC+VE-treated cells with dichlorvos-, dichlorvos+VC-, dichlorvos+VE-dichlorvos+VC+VE-treated cells. [e]Comparision of dichlorvos-treated cells with dichlorvos+VC-, dichlorvos+VE- and dichlorvos +VC+VE-treated cells ($P<0.05$). Data represent the means ±SD of six samples.

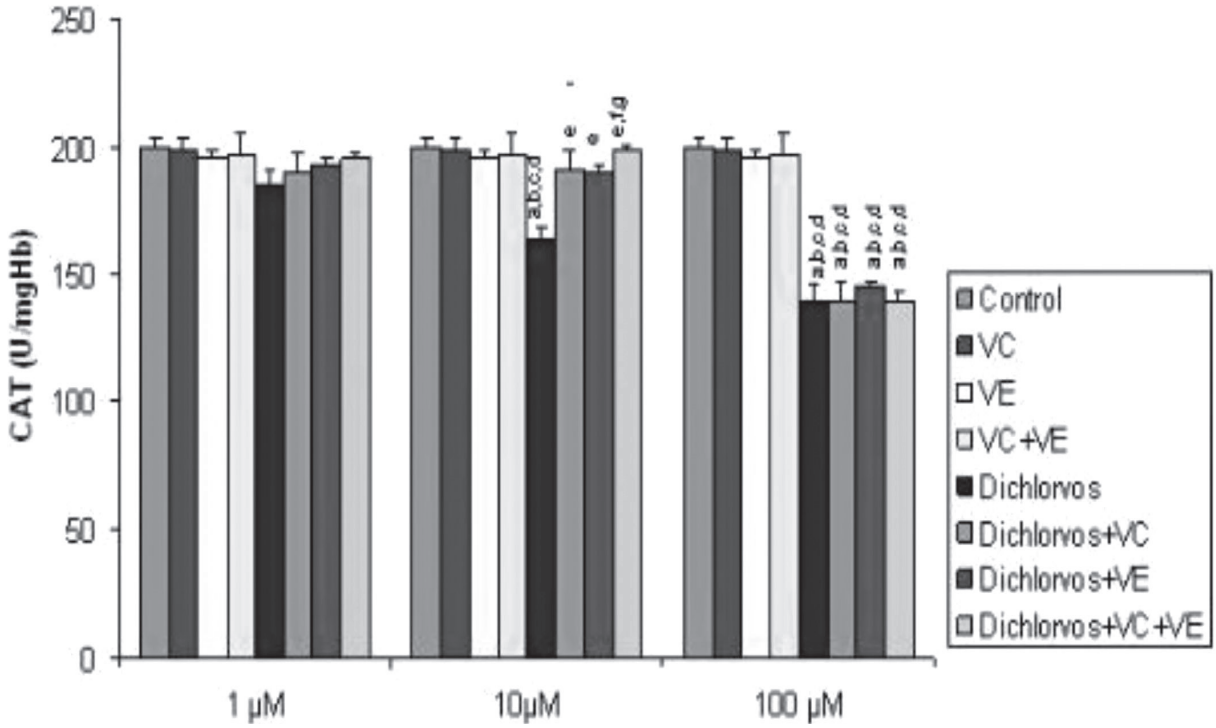

Figure 2. CAT activity in control and experimental groups of erythrocytes with dichlorvos. Comparison of nontreated control cells and other groups. [b]Comparison of VC-treated cells with VE-, VE+VC-, dichlorvos-, dichlorvos +VC-, dichlorvos +VE- and dichlorvos+VC+VE-treated cells. [c]Comparison of VE-treated cells with VE+VC-, dichlorvos-, dichlorvos+VC-, dichlorvos+VE- and dichlorvos+VC+VE-treated cells. [d]Comparison of VC+VE-treated cells with dichlorvos-, dichlorvos+VC-, dichlorvos+VE-dichlorvos+VC+VE-treated cells. [e]Comparision of dichlorvos-treated cells with dichlorvos+VC-, dichlorvos+VE- and dichlorvos +VC+VE-treated cells. [f]Comparision of dichlorvos+VC-treated cells with dichlorvos+VE- and dichlorvos +VC+VE-treated cells. [g]Comparision of dichlorvos+VE-treated cells with dichlorvos+VC+VE-treated cells ($P<0.05$). Data represent the means ±SD of six samples.

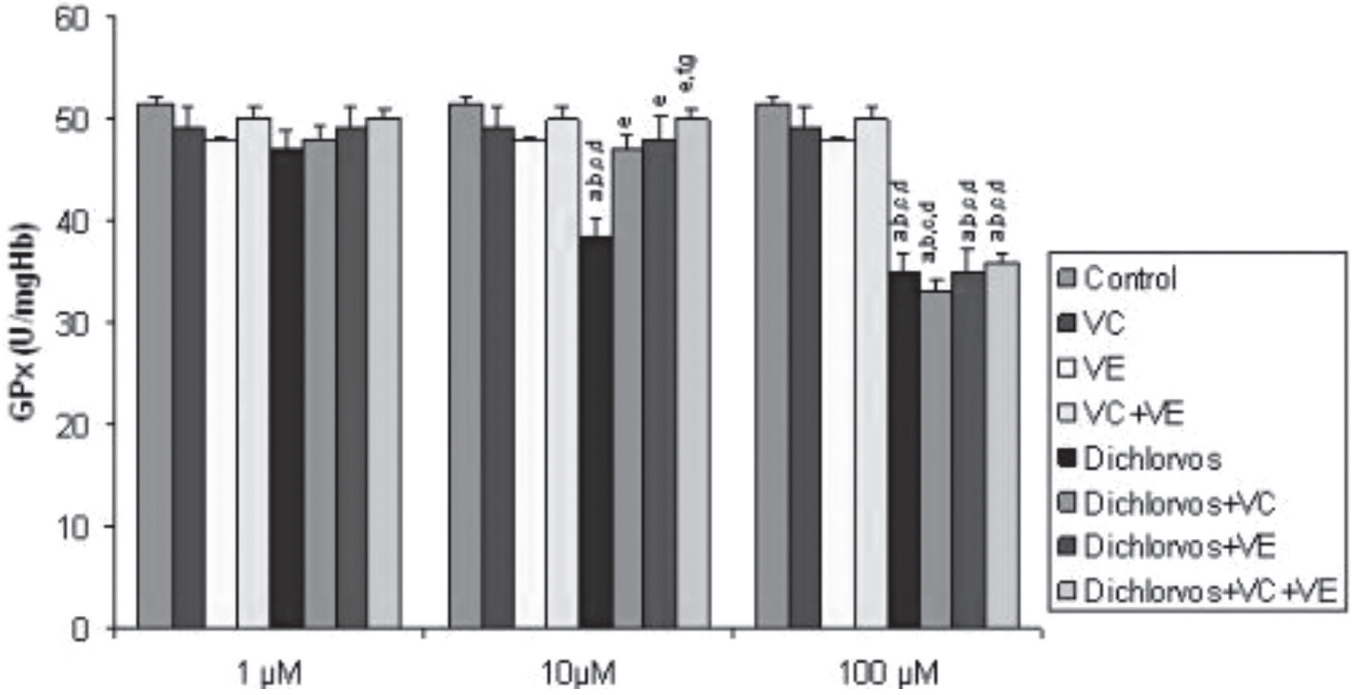

Figure 3. GPx activity in control and experimental groups of erythrocytes with dichlorvos. [a]Comparison of nontreated control cells and other groups. [b]Comparison of VC-treated cells with VE-, VE+VC-, dichlorvos-, dichlorvos +VC-, dichlorvos +VE- and dichlorvos+VC+VE-treated cells. [c]Comparison of VE-treated cells with VE+VC-, dichlorvos-, dichlorvos+VC-, dichlorvos+VE- and dichlorvos+VC+VE-treated cells. [d]Comparison of VC+VE-treated cells with dichlorvos-, dichlorvos+VC-, dichlorvos+VE-dichlorvos+VC+VE-treated cells. [e]Comparision of dichlorvos-treated cells with dichlorvos+VC-, dichlorvos+VE- and dichlorvos +VC+VE-treated cells. [f]Comparision of dichlorvos+VC-treated cells with dichlorvos+VE- and dichlorvos +VC+VE-treated cells. [g]Comparision of dichlorvos+VE-treated cells with dichlorvos+VC+VE-treated cells ($P<0.05$). Data represent the means ±SD of six samples.

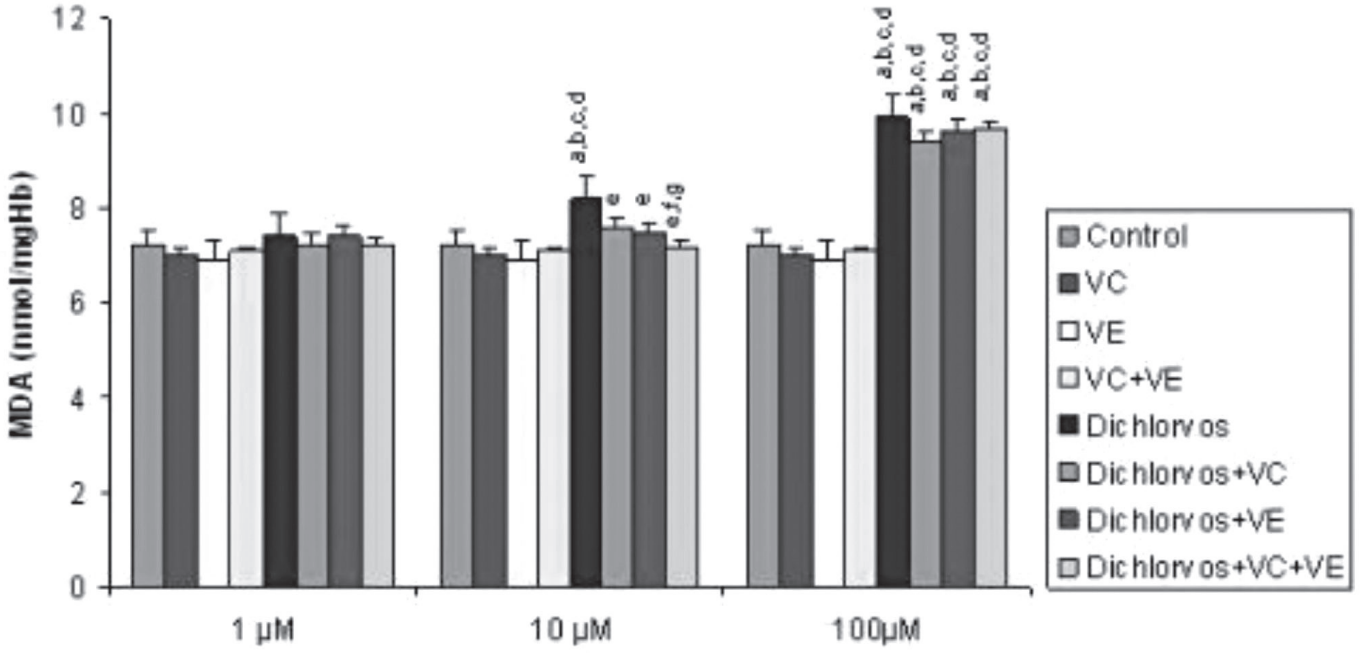

Figure 4. MDA levels in control and experimental groups of erythrocytes with dichlorvos. [a]Comparison of nontreated control cells and other groups. [b]Comparison of VC-treated cells with VE-, VE+VC-, dichlorvos-, dichlorvos +VC-, dichlorvos +VE- and dichlorvos+VC+VE-treated cells. [c]Comparison of VE-treated cells with VE+VC-, dichlorvos-, dichlorvos+VC-, dichlorvos+VE- and dichlorvos+VC+VE-treated cells. [d]Comparison of VC+VE-treated cells with dichlorvos-, dichlorvos+VC-, dichlorvos+VE-dichlorvos+VC+VE-treated cells. [e]Comparision of dichlorvos-treated cells with dichlorvos+VC-, dichlorvos+VE- and dichlorvos +VC+VE-treated cells. [f]Comparision of dichlorvos+VC-treated cells with dichlorvos+VE- and dichlorvos +VC+VE-treated cells. [g]Comparision of dichlorvos+VE-treated cells with dichlorvos+VC+VE-treated cells ($P<0.05$). Data represent the means ±SD of six samples.

in vivo (Yarsan and Cakir, 2006). In this study, treatment with DDVP significantly increased the levels of MDA and decreased the activities of antioxidant enzymes (10, 100 μM).

LPO has been suggested as one of the molecular mechanisms involved in pesticide-induced toxicity (Kehrer, 1993). Some studies have reported that OP cause LPO (Celik and Suzek, 2009; Gultekin et al., 2000; Durak et al., 2009) in vertebrates. The interaction of hemoglobin with redox drugs or xenobiotics is a source of radical production in erythrocytes (French et al., 1978, Winterbourn et al., 1978), giving rise to superoxide radicals, hydrogen peroxide and in some cases peroxy radicals, and inducing membrane LPO and hemolysis (Clemens et al., 1984). MDA is a major oxidation product of peroxidized polyunsatured fatty acids and increased MDA content is an important indicator of LPO. Xenobiotics such as pesticides cause increase of the MDA level in tissues (Banerjee et al., 2001; Hazarika et al., 2003). In this study the MDA level was increased in DDVP group, suggesting that the MDA level could be used as a marker for OP injury. This increase suggested that DDVP can accelerate the increase in free oxygen groups when administrated at 10 μM and 100 μM concentrations. The treatment with plasma levels of VE and VC attenuated the DDVP-induced increase in MDA level at 10 μM. These data show that the plasma level of VE and VC may have significant effects in reducing DDVP-based toxicity in this dose.

Oxygen is a highly reactive molecule that damages living organisms by producing reactive oxygen species (Davies, 1995); organisms contain intracellular antioxidant enzymes such as SOD, CAT and GPx, that work together to prevent oxidative damage to the cell (Bukowska, 2004). SOD catalyzes the conversion of superoxide radicals to hydrogen peroxide, while CAT converts hydrogen peroxide into water (Mansour and Mossa, 2009). The major function of GPx, which uses glutathion as a substrate, is to reduce soluble hydrogen peroxide and alkyl peroxides (Bebe and Panemangalore, 2003). These antioxidant enzymes can, therefore, alleviate the toxic effects of ROS (Mansour and Mossa, 2009). In this study, erythrocyte SOD, CAT and GPx activities were decreased in the DDVP-treated groups. The decrease in the activity of SOD in OP-treated groups may be attributed to the saturation of SOD during the process of converting O_2^- to H_2O_2. The CAT decrease may involve CAT saturation during the breakdown of free radicals and hydrogen peroxide (H_2O_2), or the inhibition of CAT by these radicals (Eraslan et al., 2007). The decrease in GPx activity may be result directly from the decreased levels of GSH following exposure, since the GPx enzyme depends on GSH for activity (Mahaboob and Kour, 2007). In this study, SOD, CAT and GPx activities significantly decreased in the at 10 μM and 100 μM DDVP-treated groups.

The widespread use of OP has long been shown to exert deleterious effects on living organisms. Oxidative damage to biomolecules is inhibited by antioxidants (Ames et al., 1993). A combination of vitamins E and C can reduce LPO caused by toxic substances (Gultekin et al., 2001). There are many studies demonstrating that VE protects cell membranes by preventing LPO. α-Tocopherol reacts with peroxyl radicals depending on its methylation state of the chromanol ring and the saturation grade of the side chain, forming tocopheroxyl radicals (Brigelius-Flohe, 2009). Tocopheroxyl radicals are converted to tocopherols by reacting with ascorbate (May et al., 1998). VE has been shown to play a role in various enzymes' activities by enabling their translocation to the membrane (Kempna et al., 2004) or affecting their transcriptional activation process (Khor and Ng, 2000). In many studies VE neutralizes LPO and unsaturated membrane lipids because of its oxygen scavenging effect (Aldana et al., 2001; John et al., 2001). Frei *et al.* (1989) have shown that VC is a powerful antioxidant preventing LPO in plasma exposed to various types of oxidative stress. VC is a significant water-soluble antioxidant in plasma which helps to reduce the effect of oxidative stress. As it is water soluble, it can easily react with free radical in extracellular body fluids (Bendich, 1990). VC exerts its antioxidant effects in both direct and indirect ways. In the direct way, VC scavenges the free radicals formed as a byproduct of metabolic reactions (Dawson et al., 1990). In an indirect way VC helps recycling of oxidized VE, thus supplying active VE fighting against LPO (Netke et al., 1997). In the present study, plasma level of VC and VE protected against DDVP-induced oxidative stress only in a 10 μM concentration of DDVP *in vitro*.

The results of the present experiment showed that DDVP induces oxidative stress in erythrocytes *in vitro* through the generation of free radicals and alteration of the cellular antioxidant defense system. Plasma levels of VC and VE protected cells against only certain doses of DDVP-induced oxidative stress.

REFERENCES

AEBI H (1983) Catalase. In: Bergmeyer, H.U. (Ed.), Methods in Enzymatic Analysis. Academic Press, New York. pp: 276-286.

ALDANA L, TSUTSUMI V, CRAIGMILL A, SILVEIRA ML, DE MEJIA EG (2001) α- tocopherol modulates liver toxicity of the pyrethroid cypermethrin. Toxicol Lett 125:107-116.

ALTUNTAS I, DELIBAS N (2002) The effects of fenthion on lipid peroxidation and some liver enzymes: the possible protective role of vitamins E and C. Turk J Med Sci 32:293-297.

AMES BN, SHGENIAGA MK, HAGEN TM (1993) Oxidants, antioxidants, and the degenerative diseases of aging. *Proc Natl Acad Sci* 90:7915-7922.

BAKER HWG, BRINDL J, IRVINE DS, AITKEN RJ (1996) Protective effect of antioxidants on the impairment of sperm motility by activated polymorphonuclear leukocytes. Fertil Steril 65:411-419.

BANERJEE BD, SETH V, AHMED RS (2001) Pesticides induced oxidative stres: perspectives and trends. Rev Environ Health 16:1-40.

BEBE FN, PANEMANGALORE M (2003) Exposure to low doses of endosulfan and chlorpyrifos modifies endogenous antioxidants in tissues of rats. J Environ Sci Health B 38:349-363.

BENDICH A (1990) Antioxidant Micro Nutrients and Immune Responses. In "Micronutrients and Immune Functions" (A. Bendich and C. E. Butterworth, eds.), Vol. 87, pp. 168-180. New York Academy of Science, New York.

BLASIAK J, STAŃKOWSKA D (2001) Genotoxicity of Malaoxon: Induction of oxidized and methylated bases and protective effect of α-Tocopherol. Pestic Biochem Physiol 71:88-96.

BOOTH ED, JONES E, ELLIOTT BM (2007) Review of the in vitro and in vivo genotoxicity of dichlorvos. Regul Toxicol Pharmacol 49:316-332.

BRIGELIUS-FLOHE R (2009) Vitamin E: The shrew waiting to be tamed. Free Radic Biol Med 46:543-554.

BUKOWSKA B (2004) 2,4,5-T and 2,4,5-TCP induce oxidative damage in human erythrocytes: the role of glutathione. Cell Biol Interact 28:557-563.

CASTILLO J, BENAVENTE-GARCIA O, LORENTE J, ALCARAZ M, REDONDO A, ORTUNO A, DEL RIO JA, (2000) Antioxidant activity and radioprotective effects against chromosomal damage induced in vivo by X rays of flavan-3-ols (procyanidins) from grape seeds (Vitis vinifera): Comparative study versus other phenolic and organic compounds. J Agricul Food Chem 48 1738-1745.

CELIK I, SUZEK H (2009) Effects of subacute exposure of dichlorvos at sublethal dosages on erythrocytes and tissue antioxidant defense systems and lipid peroxidation in rats. Ecotoxicol Environ Saf 72:905-908.

CLEMENS MR, REMMER H, WALLER HD (1984) Phenylhydrazine-induced lipid peroxidation of red blood cells in vitro and in vivomonitoring by

the production of volatile hydrocarbons. Biochem Pharmacol 33 (11) :1715–1718.

DAVIES KJ (1995). Oxidative stress: The paradox of aerobic life. Biochemical Society Symposia 61: 1–31

DAWSON EB, HARRİS WA, POWELL LC (1990) Relationship between ascorbic acid and male fertility. World Rev Nutr Diet 62:1-26.

DRABKIN DI (1946) Spectrophotometric studies. XIV. The crystallographic and optical properties of the haemoglobin of man in comparison with those of other species. J Biol Chem 164:703-723.

DURAK D, UZUN FG, KALENDER S, OGUTCU A, UZUNHISARCIKLI M, KALENDER Y (2009) Malathion-induced oxidative stress in human erythrocytes and the protective effect of vitamins C and E *in vitro*. Environmental Toxicology 24(3): 235-242.

ERASLAN G, SAYGI S, ESSİZ D, AKSOY A, GUL H, MACIT E (2007) Evaluation of aspect of some oxidative stress parameters using vitamin E, proanthocyanidin and N-acetylcysteine against exposure to cyfluthrin in mice. Pestic Biochem Phys 88:43-49.

FREI B, ENGLAND L, AMES BN (1989) Ascorbate is an outstanding antioxidant in human blood plasma. *Proc Natl Acad Sci* 86: 6377-6381.

FRENCH JK, WINTERBOURN CC, CARRELL RW (1978) Mechanism of oxyhaemoglobin breakdown on reaction with acetylphenylhydrazine. Biochemical Journal 173 (1):19–26.

GULOGLU C, ALDEMIR M, ORAK M, KARA IH (2004) Diclorvos poisoning after intramuscular injection. Am J Emerg Med 22:328-330.

GULTEKIN F, OZTURK M, AKDOGAN M (2000) The effect of organophosphate insecticide chlorpyrifos-ethyl on lipid peroxidation and antioxidant enzymes (in vitro). Arch Toxicol 74:533-538.

GULTEKIN F, DELIBAS N, YASAR S, KILINC I (2001) In vivo changes in antioxidant systems and protective role of melatonin and a combination of vitamin C and vitamin E on oxidative damage in erythrocytes induced by chlorpyrifos-ethyl in rats. Arch Toxicol 75:88-96.

GUPTA SC, SIDDIQUE HR, SAXENA DK, KAR CHOWDHURI D (2005) Hazardous effect of organophosphate compound, dichlorvos in transgenic *Drosophila melanogaster* (hsp70-lacZ): induction of hsp70, antioxidant enzymes and inhibition of acetylcholinesterase. Biochem Biophys Acta 1725: 81-92.

HARAPANHALLI RS, YAGHMAI V, GIULIANI D, HOWELL RW, RAO DV (1996) Antioxidant effects of vitamin C in mice following X- irradiation. Res Comm Mol Pathol Pharmacol 94:271-287.

HAZARIKA A, SARKAR SN, HAJARE S, KATARIA M, MALIK JK (2003) Influence of malathion pretreatment on the toxicity of anilofos in male rats: a biochemical interaction study. Toxicology 185:1-8.

HODA Q, SINHA SP (1993) Vitamin C-mediated minimisation of rogor-induced genotoxicity. Mutat Res 299:29-36.

IARC (1983) Monograph on the evaluation of carcinogenic risk of chemicals to man Vol. 30 Miscellaneous pesticides, Lyon, IARC press pp:61-72.

JOHN S, KALE M, RATHORE N, BHATNAGAR D (2001) Protective effect of vitamin E in dimethoate and malathion induced oxidative stress in rat erythrocytes. J Nut Biochem 12:500-504.

KALENDER S, KALENDER Y, OGUTCU A, UZUNHISARCIKLI M, DURAK D, AÇIKGOZ F (2004) Endosulfan-induced cardiotoxicity and free radical metabolism in rats: the protective effect of vitamin E. Toxicology 202:227-235.

KALENDER S, KALENDER Y, DURAK D, OGUTCU A, UZUNHISARCIKLI M, CEVRIMLI BS, YILDIRIM M (2007) Methyl parathion induced nephrotoxicity in male rats and protective role of vitamins C and E. Pestic Biochem Phys 88:213-218.

KEHRER JP (1993) Free radical as mediator of tissue injury and disease. Crit Rew Toxicol 23:21-48.

KEMPNA P, REITER E, AROCK M, AZZI A, ZINGG JM (2004) Inhibition of HMC-1 mast cell proliferation by vitamin E: Involvement of the protein kinase B pathway. J Biol Chem 279:50700-50709.

KHOR HT, NG TT (2000) Effects of administration of alpha-tocopherol and tocotrienols on serum lipids and liver HMG CoA reductase activity. Int J Food Sci Nutr 51: 3-11.

KONOPACKA M, WIDEL M, RZESZOWSKA WJ (1998) Modifying effect of vitamins C, E and beta carotene aganist gamma-ray-induced DNA damage in mouse cells. Mutat Res 417:85-94.

MAHABOOB KS, KOUR G (2007) Subacute oral toxicity of chlorpyriphos and protective effect of green tea extract. Pestic Biochem Phys 89:118-123.

MANSOUR SA, MOSSA AH (2009) Lipid peroxidation and oxidative stress in rat erythrocytes induced by chlorpyrifos and the protective effect of zinc. Pestic Biochem Physiol 93:34-39.

MARKLUND S, MARKLUND G (1974) Involvement of superoxide anion radical in the autoxidation of pyrogallol and a convenient assay for superoxide dismutase. Eur J Biochem 47:469-474.

MAY JM, MAY JM, QU ZC, MENDIRATTA S (1998) Protection and recycling of alpha tocopherol in human erythrocytes by intracellular ascorbic acid. Arch Biochem Biophys 349:281-289.

NETKE SP, ROOMI MW, TSAO C, NIEDZWIECKI A (1997) Ascorbic acid protects guinea pigs from acute aflatoxin toxicity. Toxicol Appl Pharmacol 143:429-435.

OGUTCU A, SULUDERE Z, KALENDER Y (2008) Dichlorvos-induced hepatotoxicity in rats and the protective effects of vitamins C and E. Environ Toxicol Pharmacol 26:355-361.

OHKAWA H, OHISHI N, TAGI K (1979) Assay for lipid peroxides in animal tissues by thiobarbituric acid reaction. Anal Chem 95: 351-362.

OKAMURA A, KAMIJIMA M, SHIBATA E, OHTANI K, TAKAGI K, UEYAMA J, WATANABE Y, OMURA M, WANG H, ICHIHARA G, KONDO T, NAKAJIMA T (2005) A comprehensive evaluation of the testicular toxicity of dichlorvos in Wistar rats. Toxicology 213:129-137.

PAGLIA DE, VALENTINE WN (1967) Studies on the quantitave and qualitative characterization of erythrocyte glutathione peroxidase. J Lab Clin Med 70:158-169.

PETROIANU GA, HASAN MY, NURULAIN SM, SHAFIULLAH M, SHEEN R, NAGELKERKE N (2006) Ranitidine in acute high-dose organophosphate exposure in rats: effect of the time-point of administration and comparison with pyridostigmine. Basic Clin Pharmacol Toxicol 99: 312-316.

SIES H, STAHL W, SUNDQUIST AR (1992) Antioxidant function of vitamin: Vitamins C & E, β-carotene and other carotenoids. Ann N Y Acad Sci 669:7-12.

STOCKER R (1994) Lipoprotein oxidation: mechanistic aspects, methodological approaches and clinical relevance. Curr Opin Lipidol 5:422-433.

URAL MS, KOPRUCU SS (2006) Acute toxicity of dichlorvos on Fingerling European Catfish, *Silurus glanis*. Bull Environ Contam Toxicol 76:871-876.

VATASSERY GT (1998) Vitamin E and other endogenous antioxidants in the central nervous system Geriatrics 53:25-27.

WINTERBOURN CC, FRENCH JK, CLARIDGE RF (1978) Superoxide dismutase as an inhibitor of reactions of semiquinone radicals. FEBS Lett 94(2): 269–272.

YARSAN E, CAKIR O (2006) Effects of dichlorvos on lipit peroxidation in mice on subacute and subchronic periods. Pestic Biochem Phys 86:106-109.

Biol Res 46: 39-45, 2013

Protective effect of silk lutein on ultraviolet B-irradiated human keratinocytes

Sutatip Pongcharoen[1*], Prateep Warnnissorn[1], Ongart Leŗtkajornsin[2], Nanteetip Limpeanchob[3] and Manote Sutheerawattananonda[4]

[1] Departments of Medicine
[2] Surgery, Faculty of Medicine
[3] Department of Pharmaceutical Practice, Faculty of Pharmaceutical Sciences, Naresuan University, Phitsanulok
[4] School of Food Technology, Institute of Agricultural Technology, Suranaree University of Technology, Nakornrajchasrima, Thailand

ABSTRACT

Carotenoids are efficient antioxidants that are of great importance for human health. Lutein and zeaxanthin are carotinoids present in high concentrations in the human retina which are involved in the photoprotection of the human eye. Lutein may also protect the skin from ultraviolet (UV)-induced damage. The present study investigated the protective effect of lutein extracted from yellow silk cocoons of *Bombyx mori* on human keratinocytes against UVB irradiation. A human keratinocyte cell line and primary human keratinocytes were used to investigate the UVB protection effects of silk lutein and plant lutein. Silk lutein showed no cytotoxicity to keratinocytes. Treatment with silk lutein prior to UVB irradiation enhanced cell viability and cell proliferation, and reduced cell apoptosis. The protective effects of silk lutein may be superior to those of plant lutein. Silk lutein may have a benefit for protection of keratinocytes against UVB-irradiation.

Key terms: Silk lutein, keratinocytes, UV, apoptosis

INTRODUCTION

Carotenoids play an important role in photosynthetic system, in which they function as light-harvesting pigments in the blue-green spectral region (Polivka and Sundstrom, 2004). Carotenoids including alpha- and beta-carotene, beta-cryptoxanthin, lutein, and zeaxanthin, found in vegetables and fruits as well as in egg yolk, are known to have anti-oxidant properties that reduce cell damage caused by free radicals (Bailey et al., 2009; Johnson, 2009; Polidori et al., 2009; Maiani et al., 2009; Santocono et al., 2007; Trevithick-Sutton et al., 2006). Carotenoid consumption may also help to decrease the risk of developing malignancies (Chang et al., 2005; Jeong et al., 2009; Pelucchi et al., 2008), associated with decreases in oxidative stress (Thomson et al., 2007; Tamimi et al., 2009) and DNA damage (Santocono et al., 2007; Yong et al., 2009).

Lutein and zeaxanthin have been reported to help in protecting the skin against ultraviolet irradiation-induced damage (Santocono et al., 2006; Roberts and Green, 2009). They reduce photoageing and photocarcinogenesis resulting from UVB irradiation (Astner et al., 2007). A previous study in humans has shown that both consumption and external application of lutein and zeaxanthin can protect the skin from oxidation. In that study, several parameters including surface lipids, hydration, photoprotective activity, elasticity, and lipid peroxidation were assessed (Palombo et al, 2007). The molecular formula of lutein is $C_{40}H_{52}O_2$ and its molecular weight is 644 daltons. The lutein molecule has double bonds, forming a more chemically reactive allylic hydroxyl end group than those extra conjugated double bonds found in zeaxanthin (Kopczynski et al., 2005).

The present study investigated the effect of lutein extracted from silk on human keratinocytes *in vitro*. We hypothesized that silk lutein may protect keratinocytes from UVB irradiation. In addition, the currently available commercial plant lutein, which is an ester form (Harikumar et al., 2008) was also tested. Silk lutein prepared from yellow silk cocoons in this present study was in a protein binding form that was a sericin-lutein complex. Sericin is one of the main protein constituents of yellow silk cocoons. The yellow pigment-binding protein of this silk lutein is similar to the pigmented tissues of the macular lutea in the retina of the eye. It is possible that absorption and transportation of protein-binding lutein within the body may be better than lutein-fatty acids esters. For these reasons, we hypothesized that the protective effect, if any, of silk lutein may be superior to lutein esters extracted from plants.

METHODS

Silk lutein

Silk lutein was prepared according to patent pending no. PCT/TH2010/000048. Yellow silk cocoons of *Bombyx mori* were degummed under high pressure and temperature to remove sericin. Degummed cocoons were extracted with a solvent mixture of hexane, ethyl alcohol, and ethyl acetate. The solution obtained was then partitioned with 10% NaCl to remove impurities from the non-aqueous phase to the aqueous phase. The non-aqueous phase was concentrated at ambient temperature and freeze-dried. Silk lutein concentration was quantified by reversed-phase HPLC (Agilent HP 1100 series) using a LiChrospher®100 reversed-phase C_{18} column as stationary and acetonitrile/methanol-ethyl acetate as mobile phases and monitored at 445 nm. The lutein was kept in the dark at -20 °C until use.

* Corresponding author: Dr. Sutatip Pongcharoen, Department of Medicine, Faculty of Medicine, Naresuan University, Phitsanulok 65000, Thailand. Tel: +66 55 965053 Fax: +66 55 965021. E-mail: sutatipp@nu.ac.th

Received: August 8, 2012. In Revised form: October 5, 2012. Accepted: October 16, 2012

Keratinocyte cell line

Human keratinocyte cell line (CCD 1102 KERTr) (the American Type Culture Collection, University Boulevard, Manassas, VA, USA) was maintained in 100 mm^2 sterile Petri dishes in Keratinocyte-serum-free medium (Gibco, NY, USA), containing 1% antibiotics, 20-30 μg/ml of bovine pituitary extract, 0.1% 300 mM $CaCl_2$, and 200 ng/ml of recombinant epidermal growth factor. The cells were incubated at 37 °C and 5% CO_2. Approximately 95% confluent cultures were passaged every 4-5 days by trypsinization with 0.25% trypsin-EDTA (Gibco) in phosphate-buffered saline (PBS: Sigma-Aldrich, MO, USA).

Primary human keratinocytes

Primary human keratinocytes were isolated from foreskins of boys less than 10 years old (n=5) and from an adult skin after an approval from the Ethical Committee on Human Rights Research Involving Human Subjects, Naresuan University. After removal of excess subcutaneous fat and dermis, the skin was cut into small pieces and soaked in 2.5 mg/ml dispase II (Roche Applied Science, Mannhiem, Germany) at 4 °C for 48 hours. Epidermal sheets were carefully separated from dermis and immediately trypsinized to obtain single cell suspensions in 0.05% trypsin-EDTA (Invitrogen, Carlsbad, CA) and neutralized with 10% fetal calf serum in DMEM (both obtained from Thermo Scientific, Waltham, MA). The trypsinized single cell suspension was cultured in Keratinocyte Serum-Free Medium (Ker SFM; Invitrogen) supplemented with 25 μg/ml bovine pituitary extract, 0.2 ng/ml epidermal growth factor and 0.4 mM $CaCl_2$, according to Rheinwald et al. (2002). Keratinocytes from the third to the fifth subcultures were used in our study. To demonstrate that almost all of the cultured cells were keratinocytes, the cells were fixed with cold ethanol while vortexing and were then stained with a marker of keratinocyte, anti-pan-cytokeratin-FITC antibody (Sigma-Aldrich) according to the manufacturer recommendation. These cultured keratinocytes were shown by FACSCalibur (BD, San Jose, CA) to be stained more than 95% with this antibody (data not shown).

Lutein administration and UVB irradiation

Keratinocyte cell lines and human keratinocytes were plated at 2×10^5 cells/60 mm^2 culture dishes for 24 hours before the plates were added with silk lutein or commercial lutein, Xanthophyll (Fluka, Sigma-Aldrich). The concentrations of both types of lutein were 0.5, 1.5, 5, and 15 μM in culture medium. The culture dishes were then incubated for another 24 hours. Then the medium containg lutein was removed by gently pipetting the medium out followed by gentle and thorough washes with PBS. The culture dishes were then supplemented with Earle's Balanced Salt Solution 1X (EBSS) (Gibco) normal complete medium before they were irradiated with UVB using a BS-03 irradiation chamber (Dr. Grobel UV-Elektronik GmbH, Ettlingen, Germany), ranging from 8 to 32 mJ/cm^2. This range of irradiation was evaluated in our preliminary studies using the same conditions of keratinocyte culture and the same number of passages, which showed that at UVB of ≥32 mJ/cm^2 most of the cells were killed (data not shown). For the keratinocyte cell line the UVB doses were 8, 16, 24, and 32 mJ/cm^2 and the lutein concentrations were 0.5, 1.5, 5, and 15μM. For human keratinocytes the UV doses were 16, 24, and 32 mJ/cm^2 and the lutein concentrations were 1.5, 5, and 15μM. After irradiation, the EBSS was gently removed and then Keratinocyte-SFM medium was added.

Cell survival assay

Trypan blue exclusion as well as MTT assays were carried out in order to determine the effect of lutein on the survival of keratinocytes. The assays were also performed to investigate the viability of keratinocytes which were treated with lutein prior to UBV-irradiation at 8 to 32 mJ/cm^2. Briefly, keratinocytes treated with silk lutein or commercial lutein, hereafter referred to as c-lutein, as above were evaluated for the total number of cells and the number of dead cells using trypan blue exclusion and MTT assays. For the UVB irradiation experiments, lutein treated cells were irradiated with UVB at 8 to 32 mJ/cm^2 before they were cultured for another 24 hours. These cells were then evaluated for the total number of live cells and dead cells by trypan blue exclusion as well as MTT assay. Briefly, for MTT assay keratinocytes were plated into 96-well flat-bottom tissue culture plates at 1.5×10^4 cells/well. After an overnight culture, lutein and c-lutein were added at the same concentrations as above. The cultures were similarly irradiated with UVB and washed as aforementioned. Two hours before the assays were terminated, freshly prepared thiazolyl blue tetrazolium bromide; MTT (Sigma) solution was added at a final concentration of 0.5 mg/ml. At the end of the culture period, the culture plates were flicked off and tapped before 100 μl/well of dimethyl sulfoxide (DMSO; Sigma) in ethanol (1:1, v/v) was added. The plates were further incubated for 5 minutes and then the absorbance was read at 595 nm using an iMark Microplate Reader (Bio-Rad, Hercules, CA, USA).

Apoptosis assay

Apoptosis assay using an annexin V-FITC apoptosis detection kit (BD Biosciences, CA, USA) was performed to assess the effect of lutein and c-lutein on the apoptosis of keratinocytes as well as to investigate the effect of cell apoptosis caused by UVB-irradation on lutein- and c-lutein-treated keratinocytes. Briefly, keratinocytes treated with silk lutein or c-lutein as above were analyzed for cell apoptosis. To do this, some culture dishes were trypsinised to stain with annexin V FITC and the remainder was irradiated with UVB at 8 to 32 mJ/cm^2. After irradiation the culture dishes were incubated for an additional 24 hours before they were trypsinised. The trysinised cells were then stained with annexin V-FITC and propidium iodide for 15 minutes before they were analyzed using FACScalibur (Becton Dickinson, CA, USA) with CellQuestPro software (BD).

Cell proliferation assay

To determine the ability of keratinocytes to proliferate after they had been exposed to lutein and c-lutein as well as to the UBV as in the survival and apoptosis assays, the BrdU-incorporation assay was performed. In these experiments the cells were cultured in 96-well flatted-bottom tissue culture plates at 1.5×10^4 cells/ml. The treated keratinocytes was added with BrdU of the Cell Proliferation ELISA, BrdU colorimetric kit (Roche Applied Science, IN, USA) 18 hours before the assay was terminated. The color products were developed according

to the manufacturer's instruction and the absorbance was read at 450nm using the iMark Microplate Reader (Bio-Rad).

Statistical analysis

Each assay using human keratinocyte cell lines was performed on at least three different occasions. For primary human keratinocytes (n=6), all samples were tested in all different occasions. Statistical differences were analyzed using two-tailed Student's *t-test* and p values of less than 0.05 were considered significant. The data are presented as mean±SD.

RESULTS

Viability of lutein treated keratinocytes and UVB-irradiated keratinocytes

The results from MTT assays showed that keratinocytes treated with lutein and c-lutein had similar viability compared to keratinocytes in culture medium alone. This means that lutein and c-lutein at this range of concentrations were not toxic to the cells (Figure 1A and 1B).

The effect of lutein on the protection of keratinocytes from UV-irradiation was tested. Silk lutein at the concentrations of 5 and 15μM protected the keratinocytes from UVB mediated cell damage, particularly at 16 and 24 mJ/cm^2 of UVB. This was shown by the ability of the keratinocyte cell line to proliferate after irradiation (Figure 2A). However, c-lutein produced no effect on keratinocyte proliferation (Figure 2B). Thus it appeared that prior treatment with silk lutein helped to protect the cells from UVB-induced cell damage. For the primary keratinocytes, silk lutein at a concentration of 15μM helped in protecting from cellular damage, which was seen in the UVB of 24 and 32 mJ/cm^2 (Figure 2C). The c-lutein at a concentration of 15μM also had a protective effect on the primary keratinocytes treated with 32 mJ/cm^2 of UVB (Figure 2D).

Apoptosis of lutein treated keratinocytes and UVB-irradiation

The results from the annexin-V assay showed that the keratinocyte cell line treated with silk lutein and c-lutein in the range of concentrations had similarly few cells undergoing necrosis (1-2%), early apoptosis (4-10%), and late apoptosis (1-3%) compared to keratinocytes in culture medium alone (Figure 3A and 3B). This means that lutein at this range of concentrations had no effect on cell apoptosis.

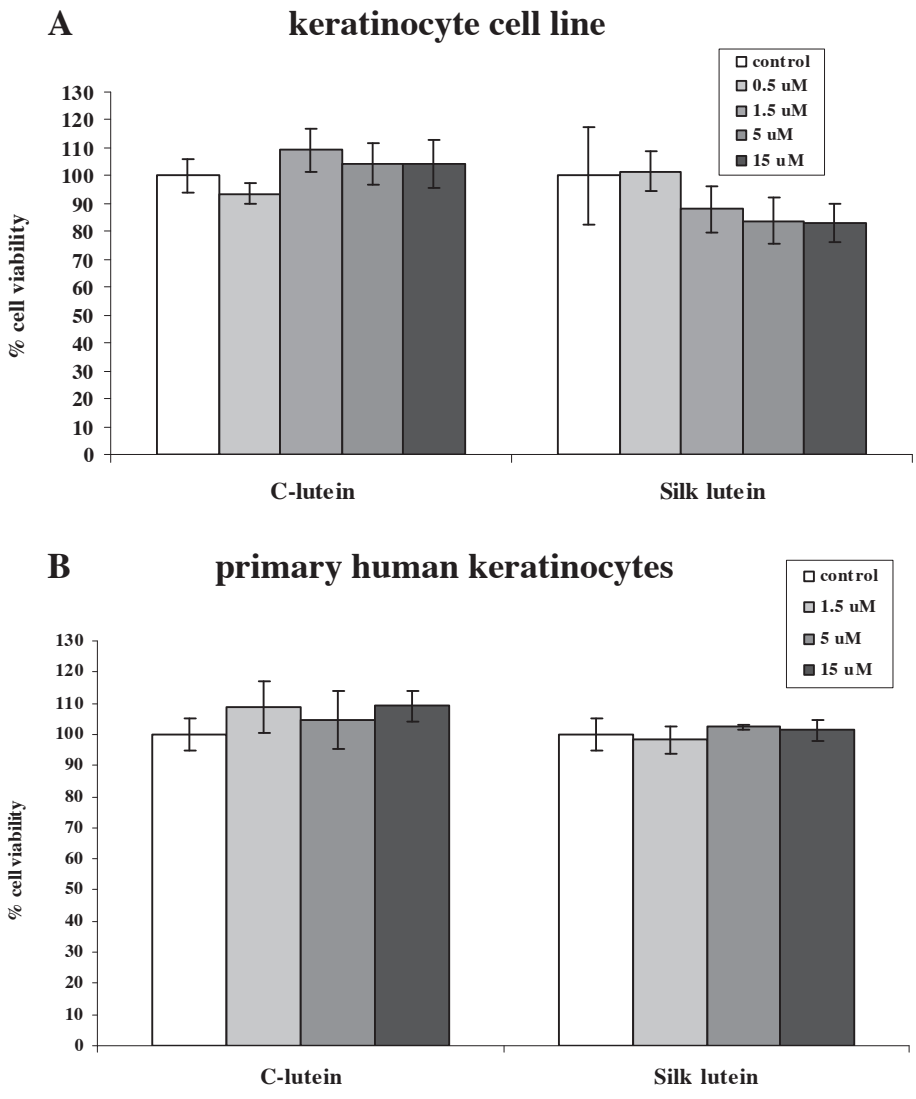

Figure 1 Effect of lutein on the viability of keratinocytes measured by MTT assay. Viability of keratinocyte cell line (A) and primary human keratinocytes (B) treated with c-lutein or silk lutein for 24 hours at concentrations ranging from 0.5 to 15 μM. Each bar represents the mean percentage of cell viability. Error bars are one standard deviation.

The keratinocyte cell line treated with either silk lutein or c-lutein at concentrations of 5 and 15μM and then irradiated with 24 mJ/cm^2 of UVB had a significant decrease in the number of cells undergoing early and late apoptosis compared to cells without prior treatment with silk lutein and c-lutein (Figure 4A and 4B). A similar effect was also seen for the primary human keratinocytes (Figure 4C and 4D).

Proliferation of lutein treated and UVB-irradiated keratinocytes

From the BrdU proliferation assays it was found that the proliferation of both the keratinocyte cell line and primary cells treated with either silk lutein or c-lutein was comparable to that of keratinocytes in culture medium alone (Figure 5A, 5B, 5C, 5D). This indicates that lutein at this range

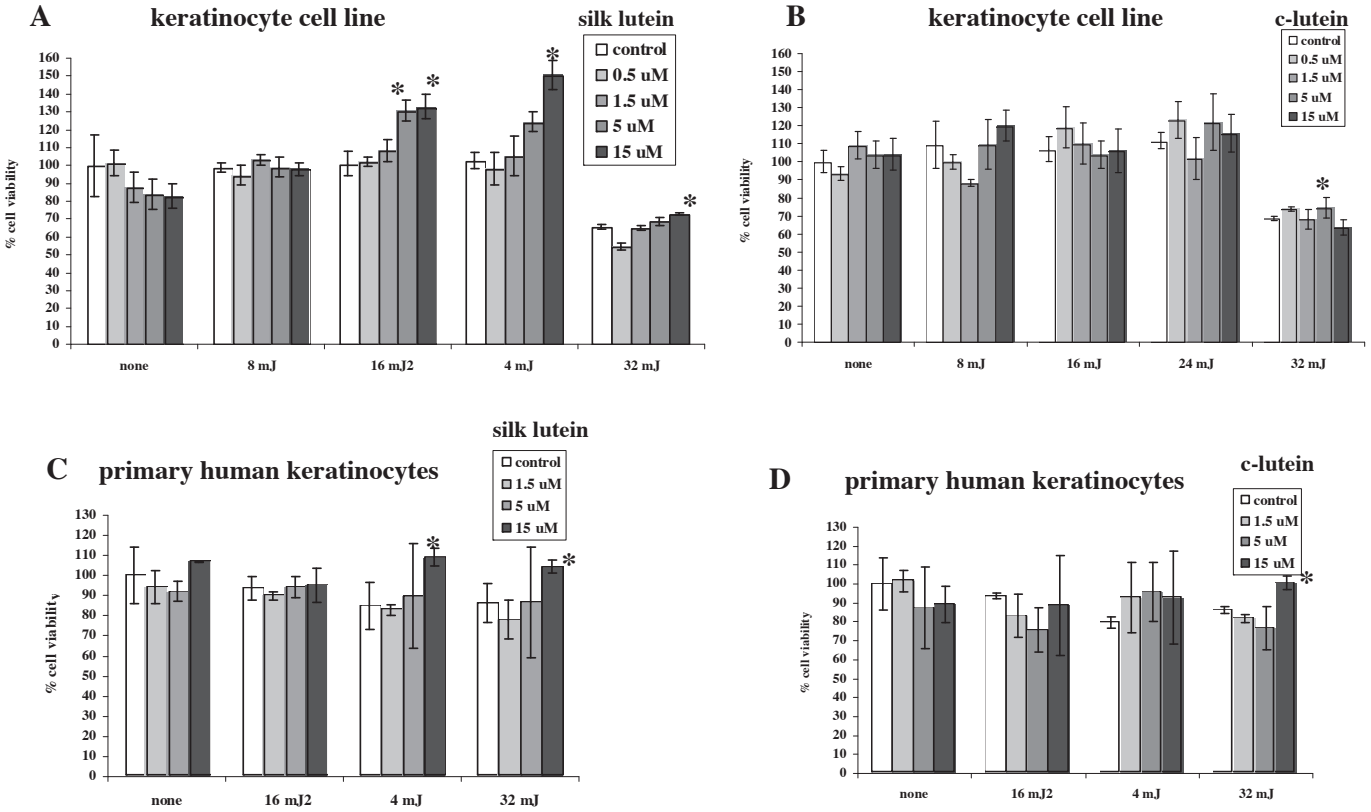

Figure 2 Effect of lutein on the viability of keratinocytes treated with UVB measured by MTT assay. Viability of keratinocyte cell line (A, B) and primary human keratinocytes (C, D) treated with 0.5 to 15 μM of silk lutein (A, C) or c-lutein (B, D) for 24 hours prior to irradiation with UVB at various doses ranging from 8 to 32 mJ/cm^2. Each bar represents the percentage of cell viability. Error bars are one standard deviation. *, $p < 0.05$

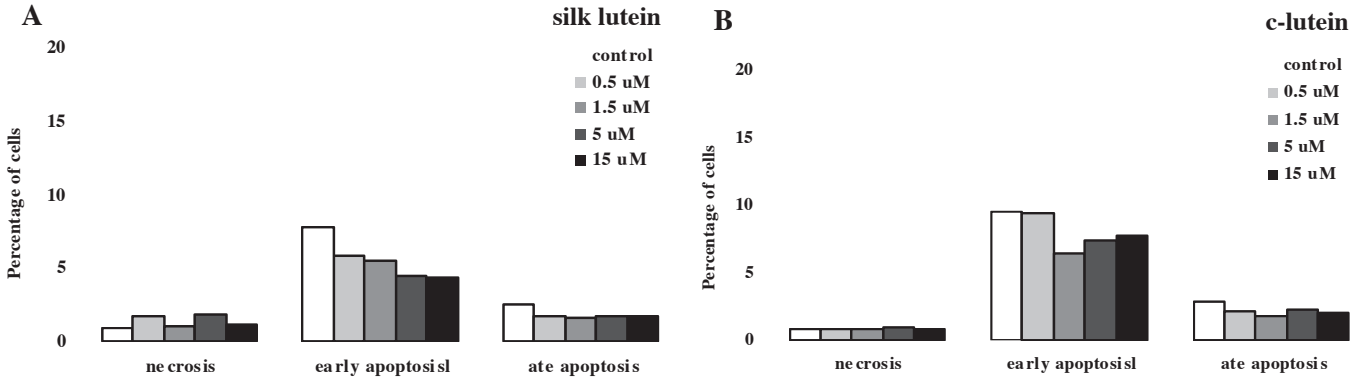

Figure 3 Effect of lutein on the apoptosis of keratinocytes measured by annexin V-FITC assay. Apoptosis of keratinocyte cell line treated with silk lutein (A) or c-lutein (B) for 24 hours at concentrations ranging from 0.5 to 15 μM. Each bar represents the percentage of cells undergoing apoptosis. Error bars are one standard deviation.

of concentrations had no effect on the proliferation of keratinocytes.

The keratinocytes treated with silk lutein and c-lutein followed by UVB irradiation from 16 mJ/cm^2 had more cell proliferation, particularly at 15 μM lutein, compared to cells without prior treatment with lutein (Figure 5A, 5B, 5C, 5D). Therefore treatment with lutein before UVB irradiation appears to help the proliferation of keratinocytes. The explanation may be that UVB irradiation resulted in some cell death, but 24 hours later the remaining cells continued to proliferate. The controlled keratinocytes without prior treatment with lutein had less proliferation.

DISCUSSION

The present study demonstrated the effect of silk lutein on human keratinocytes. Primary human keratinocytes were studied along with a keratinocyte cell line. This is because keratinocyte cell lines may have abnormal characteristics including aneuploidy, genetic instability, as well as having heterogeneous cell populations. Thus, they may not represent normal epidermis (van de Sandt et al., 1999). The present study, therefore, used primary human keratinocytes even though this source of normal skin biopsy is limited, particularly from adult normal skin, owing to ethical considerations.

The present findings demonstrated that silk lutein can decrease cell apoptosis caused by UVB-irradiation. It also showed that silk lutein increased the proliferation of keratinocytes that had been treated with UVB. The silk lutein in the present study was in a protein binding form and some of our present results were better than those from c-lutein of plant origins. In the preliminary studies on the doses of UVB only 8 to 32 mJ/cm^2 were tested, because the UVB doses of higher than 32 mJ/cm^2 caused death of most cells both in the absence and presence of lutein and c-lutein. This might be due to the pro-oxidative activity of caroteinoids at high doses of UV (Lutter et al., 2012).

A previous report showed that high dietary intake of lutein and zeaxanthin can reduce the incidence of squamous cell carcinoma of the skin (Heinen et al., 2007). Studies have shown that lutein and zeaxanthin are present in the skin and *in vivo* studies have claimed their efficacy against ultraviolet-induced skin damage (Roberts et al., 2009; Astner et al., 2007). Thus the present findings support this information as silk lutein decreased the number of early and late apoptosis of human keratinocytes exposed to UVB.

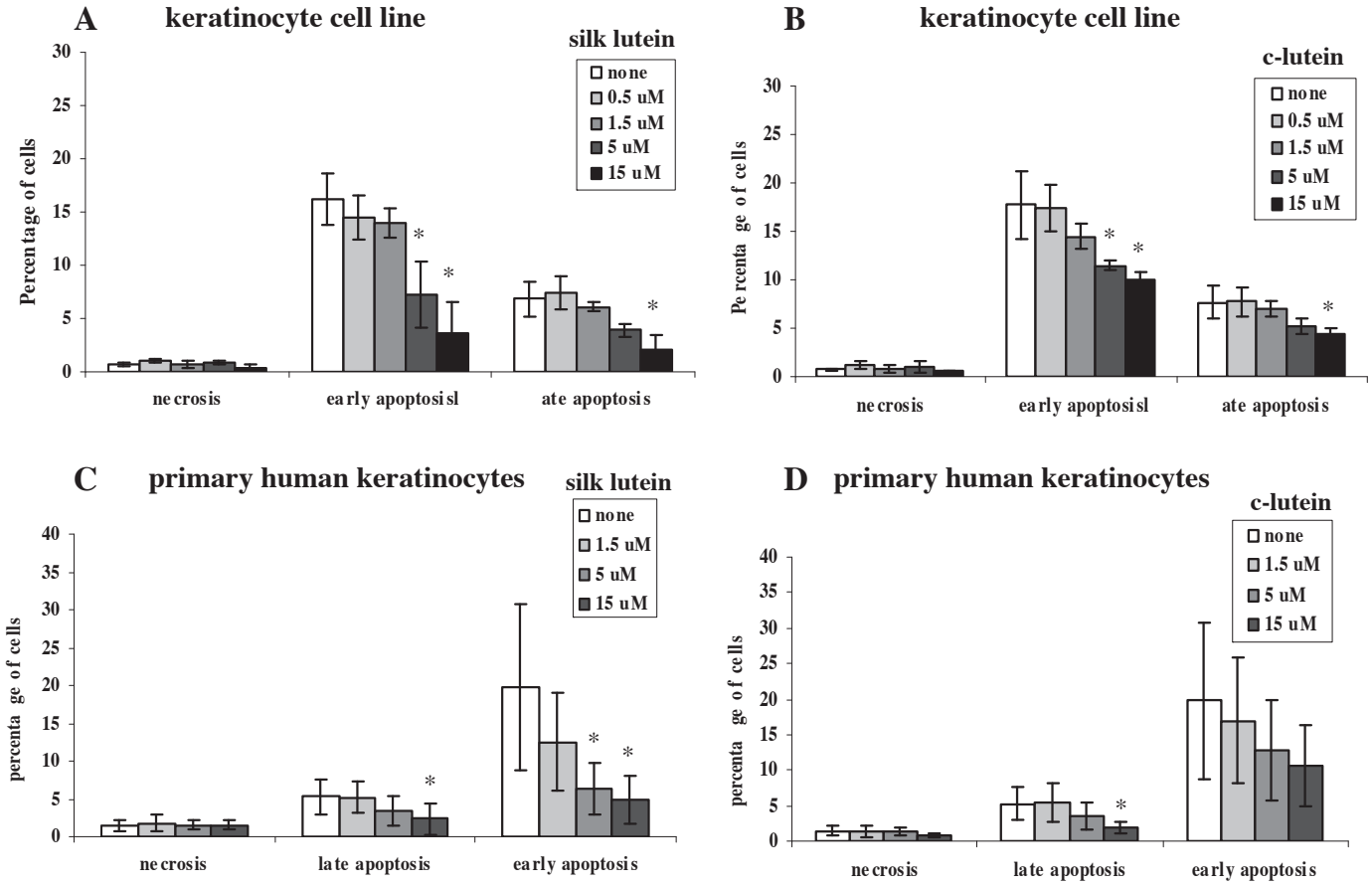

Figure 4 Effect of lutein on the apoptosis of keratinocytes treated with UBV measured by annexin V-FITC assay. Apoptosis of keratinocyte cell line (A, B) and primary human keratinocytes (C, D) treated with 0.5 to 15 μM of silk lutein (A, C) or c-lutein (B, D) for 24 hours prior to irradiation with UVB at 24 mJ/cm^2. Each bar represents the percentage of cells undergoing apoptosis. Error bars are one standard deviation. *, $p < 0.05$

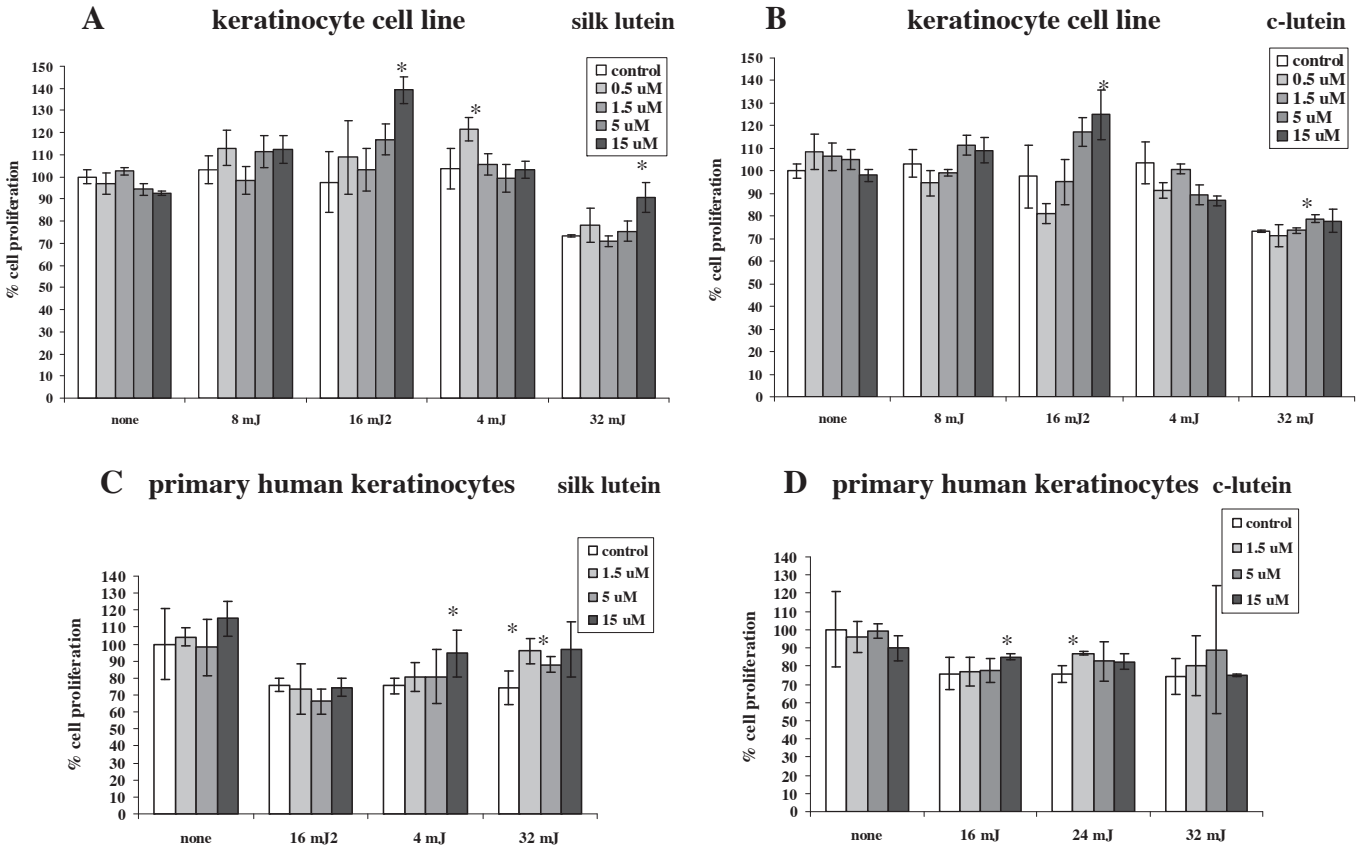

Figure 5 Effect of lutein on the proliferation of keratinocytes measured by BrdU-incorporation assay. Proliferation of keratinocyte cell line (A, B) and primary human keratinocytes (C, D) treated with 0.5 to 15 μM of silk lutein (A, C) or c-lutein (B, D) for 24 hours prior to irradiation with UVB at various doses ranging from 8 to 32 mJ/cm^2. Each bar represents the percentage of cell proliferation. Error bars are one standard deviation. *, $p < 0.05$

Although the number of keratinocytes evaluated by BrdU proliferation assay was found to be increased when they were treated with lutein prior to irradiation at 16-24 mJ/cm^2 of UVB, keratinocytes irradiated with other doses of UVB and non-irradiated keratinocytes had similar numbers of cells compared to cells that had not been treated with lutein. This could imply that lutein alone at the range of concentrations used did not stimulate keratinocyte proliferation. However, when the keratinocytes were irradiated with UVB, a number of cells died and the remaining cells continued to proliferate. Silk lutein at a range of concentrations used in this present study provides a protective effect for keratinocytes against UVB-induced damage. Therefore, silk lutein may have a significant benefit in term of skin protection against UVB-irradiation.

ACKNOWLEDGEMENTS

This work was supported by the Agriculture Research Development Agency (Public Organization), Thailand. The authors thank Miss Kwansuda Supalap and Miss Sanchawan Supalap for technical assistance.

REFERENCES

ASTNER S, WU A, CHEN J, PHILIPS N, RIUS-DIAZ F, PARRADO C, MIHM MC, GOUKASSIAN DA, PATHAK MA, GONZALEZ S (2007) Dietary lutein/zeaxanthin partially reduces photoaging and photocarcinogenesis in chronically UVB-irradiated Skh-1 hairless mice. Skin Pharmacol Physiol 20:283-291.

BAILEY RL, MILLER PE, MITCHELL DC, HARTMAN TJ, LAWRENCE FR, SEMPOS CT, SMICIKLAS-WRIGHT H (2009) Dietary screening tool identifies nutritional risk in older adults. Am J Clin Nutr 90:177-183.

CHANG S, ERDMAN SWJR, CLINTON SK, VADIVELOO M, STROM SS, YAMAMURA Y, DUPHORNE CM, SPITZ MR, AMOS AI, CONTOIS JH, GU X, BABAIAN RJ, SCARDINO PT, HURSTING SD (2005) Relationship between plasma carotenoids and prostate cancer. Nutr Cancer 53:127-134.

HARIKUMAR KB, NIMITA CV, PREETHI CK, KUTTAN R, SHANKARANARAYANA ML, DESHPANDE J (2008) Toxicity profile of lutein and lutein ester isolated from marigold flowers (*Tagetes erecta*). Int J Toxicol 27:1-9.

HEINEN MM, HUGHES MC, IBIEBELE TI, MARKS GC, GREEN AC, VAN DER POLS JC (2007) Intake of antioxidant nutrients and the risk of skin cancer. Eur J Cancer 43:2707-2716.

JEONG NH, SONG ES, LEE JM, LEE KB, KIM MK, YUN YM, LEE JK, SON SK, LEE JP, KIM JH, HUR SY, KWON YI (2009) Preoperative levels of plasma micronutrients are related to endometrial cancer risk. Acta Obstet Gynecol Scand 88:434-439.

JOHNSON JD (2009) Do carotenoids serve as transmembrane radical channels?. Free Radic Biol Med 47:321-323.

KOPCZYNSKI M, LENZER T, OUM K, SEEHUSEN J, SEIDEL MT, USHAKOV VG (2005) Ultrafast transient lens spectroscopy of various C_{40} carotenoids: lycopene, β-carotene, (3*R*,3′*R*)-zeaxanthin, (3*R*,3′*R*,6′*R*)-lutein, echinenone, canthaxanthin, and astaxanthin. Phys Chem Chem Phys 7:2793-2803.

LUTTER K, DE SPIRT S, KOCK S, KRONCKE KD, MARTIN HD, WAGENER T, STAHL W (2010) 3,3,-Dihydroxyisorenieratene prevents UV-induced

formation of reactive oxygen species and the release of protein-bound zinc ions in human skin fibroblast. Mol Nutr Food Res 54:285-291.

MAIANI G, CASTON MJ, CATASTA G, TOTI E, CAMBRODON IG, BYSTED A, GRANADO-LORENCIO F, OLMEDILLA-ALONSO B, KNUTHSEN P, VALOTI M, BOHM V, MAYER-MIEBACH E, BEHSNILIAN D, SCHLEMMER U (2009) Carotenoids: actual knowledge on food sources, intakes, stability and bioavailability and their protective role in humans. Mol Nutr Food Res 53 Suppl 2:S194-218.

PALOMBO P, FABRIZI G, RUOCCO V, RUOCCO E, FLUHR J, ROBERTS R, MORGANTI P (2007) Beneficial long-term effects of combined oral/topical antioxidant treatment with the carotenoids lutein and zeaxanthin on human skin: a double-blind, placebo-controlled study. Skin Pharmacol Physiol 20:199-210.

PELUCCHI C, DAL MASO L, MONTELLA M, PARPINEL M, NEGRI E, TALAMINI R, GIUDICE A, FRANCESCHI S, LA VECCHIA C (2008) Dietary intake of carotenoids and retinol and endometrial cancer risk in an Italian case-control study. Cancer Causes Control 19:1209-1215.

POLIDORI MC, CARRILLO JC, VERDE PE, SIES H, SIEGRIST J, STAHL W (2009) Plasma micronutrient status is improved after a 3-month dietary intervention with 5 daily portions of fruits and vegetables: implications for optimal antioxidant levels. Nutr J 8:10.

POLIVKA T, SUNDSTROM V (2004) Ultrafast dynamics of carotenoid excited states-from solution to natural artificial systems. Chem Rev 104:2021-2071.

ROBERTS RL, GREEN J, LEWIS B (2009) Lutein and zeaxanthin in eye and skin health. Clin Dermatol 27:195-201.

SANTOCONO M, ZURRIA M, BERRETTINI M, FEDELI D, FALCIONI G (2006) Influence of astaxanthin, zeaxanthin and lutein on DNA damage and repair in UVA-irradiated cells. J Photochem Photobiol B 85:205-215.

SANTOCONO M, ZURRIA M, BERRETTINI M, FEDELI D, FALCIONI G (2007) Lutein, zeaxanthin and astaxanthin protect against DNA damage in SK-N-SH human neuroblastoma cells induced by reactive nitrogen species. J Photochem Photobiol B 88:1-10.

TAMIMI RM, COLDITZ GA, HANKINSON SE (2009) Circulating carotenoids, mammographic density, and subsequent risk of breast cancer. Cancer Res 69:9323-9329.

THOMSON CA, STENDELL-HOLLIS NR, ROCK CL, CUSSLER EC, FLATT SW, PIERCE JP (2007) Plasma and dietary carotenoids are associated with reduced oxidative stress in women previously treated for breast cancer. Cancer Epidemiol Biomarkers Prev 16:2008-2015.

TREVITHICK-SUTTON CC, FOOTE CS, COLLINS M, TREVITHICK JR (2006) The retinal carotenoids zeaxanthin and lutein scavenge superoxide and hydroxyl radicals: a chemiluminescence and ESR study. Mol Vis 12:1127-1135.

VAN DE SANDT J, ROGUET R, COHEN C, ESDAILE D, PONEC M, CORSINI E, BARKER C, FUSENIG N, LIEBSCH M, BENFORD D, DE BRUGEROLLE DE FRAISSINETTE A, FARTASCH M. (1999) The use of human keratinocytes and human skin models for predicting skin irritation. In: The report and recommendations of ECVAM Workshop 38. Available at: http://ecvam.jrc.it/publication/WorkshopReport38.pdf. Accessed on 6 Feb 2012. ATLA 27:723-743.

YONG LC, PETERSEN MR, SIGURDSON AJ, SAMPSON LA, WARD EM (2009) High dietary antioxidant intakes are associated with decreased chromosome translocation frequency in airline pilots. Am J Clin Nutr 90:1402-1410.

Biol Res 46: 47-52, 2013

A simple and effective pressure culture system modified from a transwell cell culture system

Xuerong Sun[1,2], Xinguang Liu[1], Yuehong Zhang[2,3], Xielan¸Kuang[2], Bo Lv[4*] and Jian Ge[2*]

[1] Institute of Aging Research, Key Laboratory for Medical Molecular Diagnostics of Guangdong Province, Guangdong Medical College, Dongguan 523808, China
[2] State Key Laboratory of Ophthalmology, Zhongshan Ophthalmic Center, Sun Yat-sen University, Guangzhou 510060, China.
[3] Departments of Ophthalmology, First Municipal People's Hospital of Guangzhou, Affiliated Hospital of Guangzhou Medical College, Guangzhou, 510080, China.
[4] Department of Emergency and Critical Care Medicine, Guangdong General Hospital, Guangdong Academy of Medical Sciences, Guangzhou 510080, China.

ABSTRACT

Mechanical pressure plays an important role in many physiological and pathological processes. Mimicking the mechanical pressure present *in vitro* is necessary for related research, but usually requires expensive and complicated equipment. In this study we created a simple pressure culture system based on the transwell culture system. By cutting off the top rim of the transwell insert, the cells were compressed between the insert membrane and the well floor. The new pressure culture system was proven effective in that it induced cell morphological change, integrin β1 upregulation, actin polymerization and growth change in rat retinal ganglion cells, human nasopharyngeal carcinoma cells and mice embryonic fibroblasts. Though the pressure value is immeasurable and inhomogeneous, the easily available culture system still provides a choice for the laboratories that do not have access to the better, but much more expensive pressure culture equipment.

Key words: Mechanical pressure; Cell culture; Transwell culture system; cytoskeleton.

INTRODUCTION

Mechanical pressure stimuli exists and plays important roles in many physiological and pathological processes [1-4]. In glaucoma, intracranial hypertension and solid tumors, the somatic cells are exposed to an elevated hydrostatic pressure [5, 6]. In some physiological conditions, intervertebral discs and articular cartilage often bear a high mechanical burden, which probably includes both hydrostatic pressure and tensile strain. For vascular endothelial cells or the cells in the cavitas medullaris such as hemopoietic and mesenchymal stem cells, fluid shear stress has a great influence on proliferation, differentiation and other biological functions [7, 8]. Though hydrostatic pressure, mechanical strain and shear stress have different features, they all exert mechanical pressure on cells.

To facilitate the investigation of the biological role and mechanisms of mechanical pressure, it is necessary to establish this model *in vitro*. There has been a long history of pressure chamber inventions. Some pressure chambers were mounted into the microscopy to observe the depolymerization of spindle microtubules[9, 10], and some use the syringe – based pressure chamber to evaluate the ATP release from retina[11]. A tensegrity model has been established to explain the mechanism of cellular mechanotransduction, which considers cells and the extracellular matrix as a continuous network of fibers[12, 13].

Our lab has previously set up an elevated hydrostatic pressure model, which is mainly composed of an air-tight pressure chamber and a regulator which is connected to an additional power supply [14]. The model could provide a stable pressure *in vitro*, but it requires a huge incubator in which the pressure chamber is placed. Some other laboratories have established their own mechanical pressure models [15, 16], which are often complicated and not easily adoptable by others. Some commercial equipment also mimics mechanical pressure, but the equipment is often expensive and not available for many laboratories.

To establish an easily available pressure culture system, we made some modifications to the 6-well transwell culture system. The resulting hand-made pressure culture system is effective on rat retinal ganglion cell line 5 (RGC-5) cells, human nasopharyngeal carcinoma cell line (CNE-1) and mice embryonic fibroblasts (MEFs). This pressure culture system is simple and readily available for nearly every laboratory.

MATERIALS AND METHODS

Cell culture

The rat RGC-5 cell line was a gift from Prof. Zhikuan Yang in Zhongshan Ophthalmic Center, Sun Yat-sen University, and was cultured with high glucose Dulbecco's modified Eagle medium (DMEM medium) (Gibco, Grand Island, NY, USA) containing 10% fetal bovine serum (FBS; Hyclone, Logan, UT, USA). Mice MEFs were harvested from embryonic 13.5 days *C57/BL6* mice and cultured with DMEM medium containing 10% FBS. MEFs in 3 to 4 passages were used for this study. The CNE-1 cell line was cultured with 1640 medium (Gibco) containing 10% FBS. All these cells were passaged by trypsin digestion, serum neutralization, centrifugalization and re-plating as usual. The usage of experiment animals and the protocol of the study were approved by the local ethics committee.

*Corresponding author: Bo Lv. Department of Emergency and Critical Care Medicine, Guangdong General Hospital, Guangdong Academy of Medical Sciences, Guangzhou 510080, China. E-mail address: gdsylb@126.com; Tel: 86-20-83827812; Fax: 020-83827712

*Corresponding author: Jian Ge. State Key Laboratory of Ophthalmology, Zhongshan Ophthalmic Center, Sun Yet-sen University, Guangzhou 510060, China. E-mail address: gejian@mail.sysu.edu.cn; Tel: 86-20-8733 1374; Fax: 86-20-8733 3271.

Received: August 16, 2012. In Revised form: October 11, 2012. Accepted: December 17, 2012

Design of the pressure culture system

The pressure culture system was designed based on the transwell inserts (353102, BD Falcon) for 6-well plates. The bottom of the insert is sealed with cell-culture grade polyethylene terephthalate (PET) membranes (Figure 1). When placed into one well of the 6-well plate, the arcuated processes at the top of the insert lies right on the rim of the well. The insert and well together could be used as a non-contact co-culture system [17] (Figure 1C).

To establish the pressure culture system, we cut off the arcuated processes at the top of the insert so that the whole insert descended and the membrane at the bottom of the insert pressed directly on the floor of the well (Figure 1B, 1D). When cultured on the well floor, the cells are mechanically pressed by the PET membranes (Figure 1D).

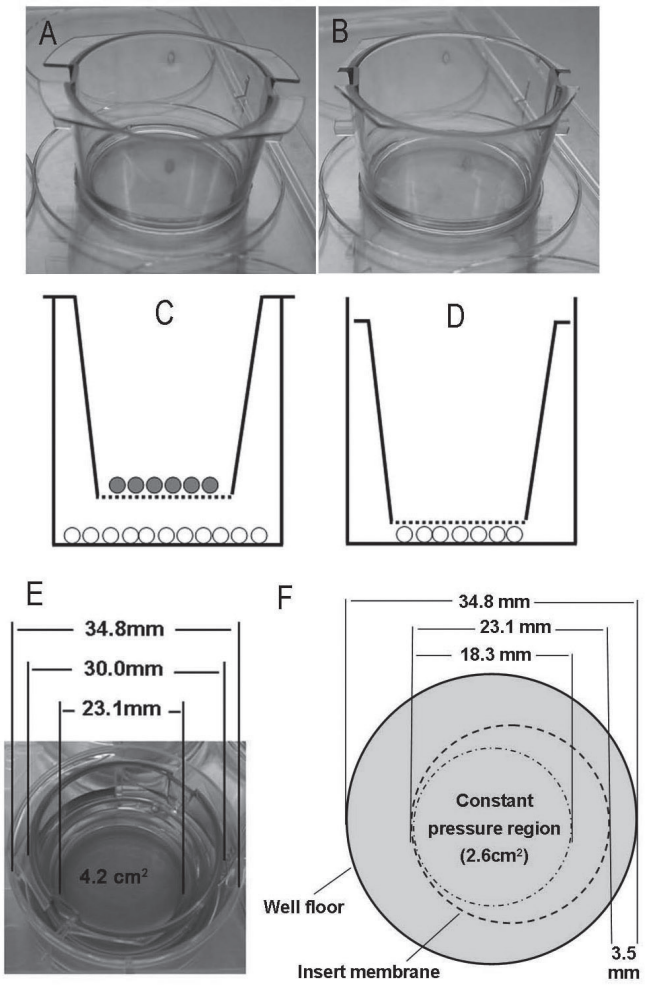

Figure 1: The pressure culture system modified from the transwell culture system. The transwell culture system is composed of an insert and a well, which can be used for co-culture of different types of cells (**A, C**). In figure **C** and **D**, the dotted line at the bottom of the insert represents the semi-permeable PET membrane. To establish the pressure culture, the rim at the top of the insert was cut off (**B**) so that the insert was placed directly on the well floor, where the cells (blank circle) were mechanically compressed (**D**). The membrane area that could be used for the pressure culture was 4.2 cm^2 (**E**). When the insert was randomly placed in the well, the 2.6 cm^2 circle in the center of the well floor was consistently in the range of the pressure culture (**F**).

In this study, to verify the pressure culture system 1×10^3 RGC-5, 1×10^3 CNE-1 and 2×10^3 MEF suspensions were seeded into 6-well plates, within an approximately 19 mm-diameter circle marked at the bottom center of the well with a pen. After allowing attachment for about 4-5 hours, the growth medium in each well was added up to 2.5 ml. When 24 hours had passed after cell seeding the modified inserts were put into the well, covering the circle line, to trigger the pressure culture. Meanwhile, 1.5 ml growth medium was added into the insert. The growth medium in the insert was fully replaced with fresh medium every day, and a similar volume of growth medium was replaced in the normal control group. After pressure culture for 6, 12, 24 or 72 hours, RGC-5, CNE-1 and MEFs were harvested for real-time quantitative reverse transcription PCR (qRT-PCR) detection or cell counting.

Staining of cell membrane with DiI

DiI (1,1′-dioctadecyl-3,3,3′,3′-tetramethylindocarbocyanine perchlorate, C1036, Beyotime, China) was reconstituted with DMSO into 2 mM stock solution. Before staining, DiI stock solution was diluted to 10 μM with fresh growth medium. To stain the cells, the growth medium in the 6-well plates was removed and the fresh medium containing DiI was added. Then the plates were incubated in 37 °C for 20 min. After washing with PBS solution 3 times, the cells were fixed with 4% paraformaldehyde for 15 min at room temperature. DAPI (C1002, Beyotime, China) was used to stain the nucleus. The cells were observed under a fluorescence microscope (Leica DM2500, Leica, Germany).

Real-time quantitative reverse transcription PCR

The procedure of qRT-PCR was similar to that we previously described with minimal modification [18]. Total RNA was extracted from RGC-5, CNE-1 and MEFs following the specification of RNeasy Mini Kit (Qiagen, Hilden, Germany). The likelihood of genomic DNA contamination was reduced with DNase I (Sigma, St. Louis, MO) treatment. cDNA was synthesized with a PrimeScript RT reagent kit (Takara, Tokyo, Japan). SYBR Premix Ex Taq (Takara) was used for quantitative PCR in an ABI Prism 7000 real-time PCR system. Glyceraldehyde-3- phosphate dehydrogenase (GAPDH) acted as the internal reference gene. The primer pairs for mice integrin β1 were: forward TTGCCTTGCTGCTGATTTG, reverse TTTCACCCGTGTCCCACTT, product 105 bp; for rat integrin β1 they were: forward AGTGAACAGCAACGGTGAAGC, reverse AGCAAGGCAAGGCCAATAAGA, product 126 bp; and for human integrin β1 they were: forward CAGTGAATGGGAACAACGAGG, reverse ATGCAAGGCCAATCAGAACAA, product 123 bp. The fold changes of integrin β1 relative to GAPDH were calculated as previously described [18].

Immunofluorescence detection

To facilitate immunofluorescence detection, RGC-5, CNE-1 or MEFs were seeded onto a 22 mm round cover slip to initiate the pressure culture. After 1 or 3 days these cells were fixed with 4% paraformaldehyde for 15 min at room temperature.

Expression of filamentous actin (F-actin) in these cells was detected following the specification of Actin-Tracker Green (Beyotime, China), which is FITC-labeled phalloidin. The tracker was 1:200 attenuated with PBS containing 0.1% Triton X-100 and 4% BSA, and then incubated with the cover slip for about 50 min at room temperature before detection by a fluorescence microscope (Leica DM2500).

Cell proliferation detection

Each well of a 6-well plate was seeded with 1×10^3 RGC-5 or CNE-1, or 2×10^3 MEFs cell suspension, up to 4 wells for each type, within a 19 mm circle as per the foregoing description. Of these, 2 wells were prepared for the pressure culture and 2 other wells served as the control. The pressure culture was initiated 24 hours after plating. After another 3 days the cells in each well were harvested with trypsin, and counted using a hemocytometer under an inverted microscope (Leica DMI3000 B, Leica). Since we noticed the attachment of some cells onto the transwell membrane in pressure culture, for the well of pressure culture the transwell membrane was also digested with trypsin and the liquid was harvested and counted together with the cell suspension of that well. The average cell number of the duplicate wells was regarded as the final result in that group. The cell number in each group was divided by the initial cell number to get the fold change. The experiment was repeated twice for each cell type.

Statistical analysis

Values were expressed as mean ± standard error (number of observations). Analysis of variance (ANOVA) or Student's t-test was used to test for significant differences, and $P<0.05$ was taken to be significant.

RESULTS

Parameter of the pressure culture system

The pressure culture system was composed of a transwell insert and a 6-well plate with some modifications described in Methods (Figure 1A-1D). The pressure came from the PET membrane attached at the bottom of the insert, which may exert mechanical tension on the cells.

The diameter of the PET membrane at the bottom of transwell inserts was 23.1 mm (Figure 1E- 1F). The cells were pressure-cultured between PET membrane and the well floor; thus, the maximum area that could be achieved for pressure culture was only the area of the PET membrane, which is about 4.2 cm^2 (Figure 1E). To facilitate seeding cells into the 4.2 cm^2 circle, a line along the inner circle of the insert can be drawn at the bottom of the well.

The inner diameter of the well was 34.8 mm, and the outer diameter of the insert top was 30.0 mm (Figure 1E). If the insert was placed randomly within the well, the mobilizable distance was 4.8 mm. Therefore, a round area (2.6 cm^2) with an 18.3 mm diameter in the center of the floor would be constantly within the range of pressure culture, wherever the inserts were placed (Figure 1F).

To get a preliminary impression of the pressure level, we detected the change of cell area after 3- or 7- day pressure culture. DiI is a kind of membrane-bound dye and was used to identify cell boundaries and thus to evaluate cell area. Normal culture did not induce obvious change on cell area. The results showed that after 3-day pressure culture, the cell area of CNE-1 and MEFs decreased. The effect became more evident after 7 days. Typical pictures are shown in Figure 2. Similar results were observed in 2 independent experiments.

Morphology change and actin cytoskeleton rearrangement under pressure culture

Three kinds of cells, specifically rat RGC-5, human CNE-1 and mice MEFs, were selected to evaluate the pressure culture

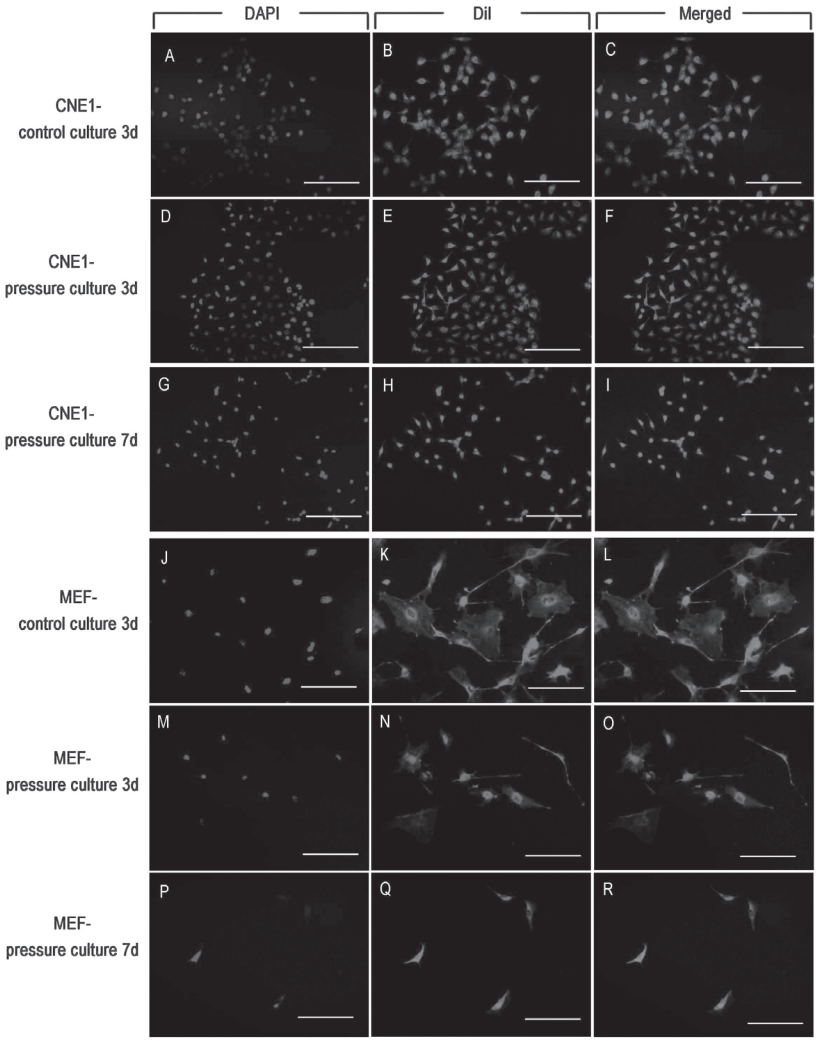

Figure 2: The effect of pressure culture on the cell area of CNE-1 and MEFs. DiI membrane dye was used to stain the cell membrane. It can be seen that after 3-day pressure culture, CNE-1 and MEFs became smaller than those in control culture. The effect became more evident after 7-day pressure culture. Bars represent 200 μm.

system. Before pressure culture, RGC-5 cells had a short-rod shape with a few thin processes, CNE-1 cells were polygonal with short processes, and MEFs were long and spindle-shaped. After being pressure cultured for 1 or 3 days, the three types of cells showed similar changes, including a thinner body and more processes, often with a clearer cell boundary (Figure 3A).

Actin is an extensive-expression protein in somatic cells and also a sensor of mechanical stress [19, 20]. Phalloidin is a toxin from the toadstool which binds specifically to polymerized actin filaments rather than to actin monomers [21]. FITC-labeled phalloidin was used to detect the distribution of actin filaments. Before pressure culture, RGC-5, CNE-1 and MEFs cells all displayed evident green fluorescence by phalloidin staining, suggesting the universal existence of filamentous actin. After pressure culture for 1 or 3 days, expression of filamentous actin in all these cells became brighter and denser (Figure 3B), which might be from the result of the transition of globular actin into filamentous actin [22]. Similar phenomena were observed in three independent experiments.

The effect of pressure culture on integrin β1 *expression*

Integrin β1 plays an important role in sensing mechanical pressure or stress [23]. To verify the effect of the pressure culture system, expression of integrin β1 was investigated by qRT-PCR before and after pressure culture. The results showed that after 6 hours of pressure culture, expression of integrin β1 increased dramatically and peaked at 12 hours in RGC-5 (Figure 4A). After 12 hours, integrin β1 expression gradually decreased. The expression of integrin β1 in CNE-1 and MEFs cells also increased evidently upon pressure culture and peaked at 6 hours, after which the expression level declined. By 72 hours, the expression of integrin β1 in MEFs was still significantly greater than that of the normal culture (Figure 4A).

To exclude the possible effect of PET membrane on integrin β1 expression from the pressure culture system, 2.0×10^4 RGC-5, CNE-1 or MEFs cell suspensions were seeded onto the insert membrane placed on the well floor. Meanwhile, 4.6×10^4 RGC-5, CNE-1 or MEFs cell suspensions were seeded into one well of a 6-well plate to achieve the same cell density. After 6 hours, qRT-PCR detection showed that integrin β1 expression was slightly less in the cells grown on the PET membrane than those grown on the well floor, but the difference was not significant (Figure 4B). The results suggested that upregulation of integrin β1 in the pressure culture should be attributed to mechanical pressure, not the membrane substrate.

The effect of pressure culture on cell proliferation

Cells grown under mechanical pressure usually display a changed growth rate [3]. To assess the effect of the transwell-based pressure culture on cell proliferation, cells were counted after 3 days of pressure culture. Compared to control groups in the normal culture, 3-day pressure culture induced a significant increase in CNE-1 growth, along with an evident decrease in MEFs (Figure 5). Pressure culture also promoted the proliferation of RGC-5 slightly.

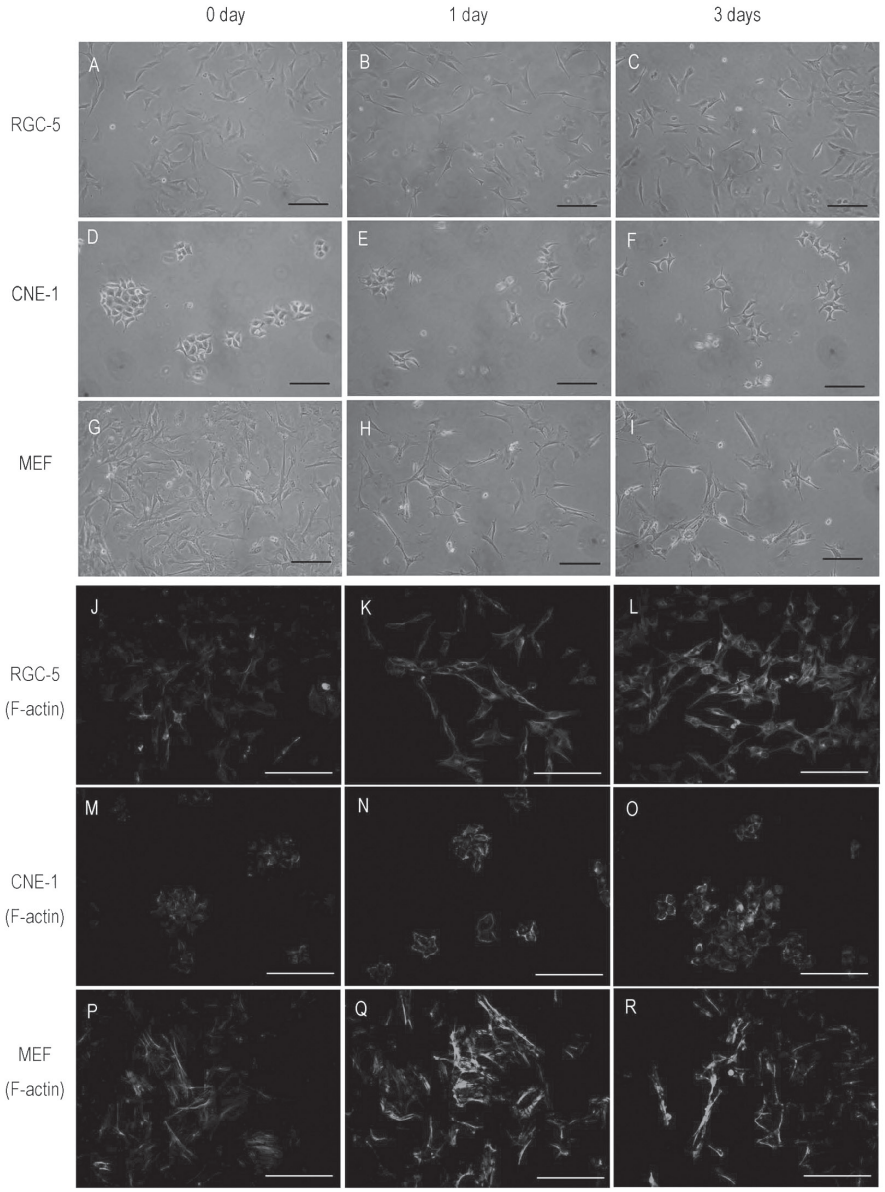

Figure 3: The morphology and actin cytoskeleton change in RGC-5, CNE-1 and MEFs under pressure culture. RGC-5, CNE-1 and MEFs cells were pressure cultured for 3 days. Compared to the normal culture (0 day), 1 day or 3 days pressure culture induced obvious changes in these cells, including more processes, thinner and longer soma and clearer boundaries (**A-I**). For the actin cytoskeleton, pressure culture induced an obvious increase of filamentous actin in the three cell types (**J-R**). Bars represent 200 μm.

DISCUSSION

This study showed that the pressure system was effective in that it induced morphological change, integrin β1 upregulation, and actin polymerization in rat-, human-, and mouse-derived cells, which included both normal somatic cells and tumor cells. The morphological changes included a thinner, longer cell body and more processes. These changes were different than those produced under hydrostatic-pressure or shear-stress cultures [14, 24]. One reason accounting for this might be that the pressure exerted on the cell surface in this study was not as uniform as in hydrostatic-pressure culture, or not as unidirectional as in shear-stress cultures. Integrin β1 upregulation was not long-lasting in this study, which might be due to a negative feedback regulation [25, 26].

The mechanical stimuli to which cells are usually subjected include hydrostatic pressure, shear stress and tensile strain [13]. In some reports, hydrostatic pressure induced actin depolymerization [14, 27], while shear stress and tensile strain induced actin reorganization or polymerization [22, 28]. In this study, cells were quiescently compressed between two objects, which induced an obvious increase of filamentous actin. Therefore, tensile strain might be the main stimulus in our pressure culture system.

The pressure culture system was modified from the transwell system of Becton, Dickinson and Company. The cells were mechanically compressed between the insert membranes and the well floor. Based on the principle, the transwell systems from other companies such as Coring, Millipore or Costar could also be easily modified into pressure culture systems by cutting off the rim of the insert so that the insert is directly placed on the well floor.

In this study, the membrane of the insert was made of polyethylene terephthalate (PET), which is transparent to facilitate observation. There are also insert membranes made of polycarbonate. These membrane materials are all cell-culture grade and appropriate for pressure cultures. Different membrane pore sizes can be chosen, such as 0.4μm, 1μm or 3μm. To guarantee the pressure effect, the membrane pore size should be smaller than the cell diameter, which depends on cell type, cell cycle progression and cell viability, among other factors.

The advantages of this pressure culture system are obvious. First, it is easy and available for every laboratory if they meet the conditions for cell culture. Second, the insert membrane is permeable to gasses such as carbon dioxide and oxygen, as well as molecular substances such as proteins; thus the condition of the pressure culture is almost completely the same as that of a normal culture, except for the pressure.

The shortcomings of the pressure culture system are also equally obvious. Most significantly, the pressure exerted on cells is inhomogeneous, immeasurable, and dynamically changing due to the growth of cells. Although we observed a decrease in cell area of CNE-1 and MEFs under pressure

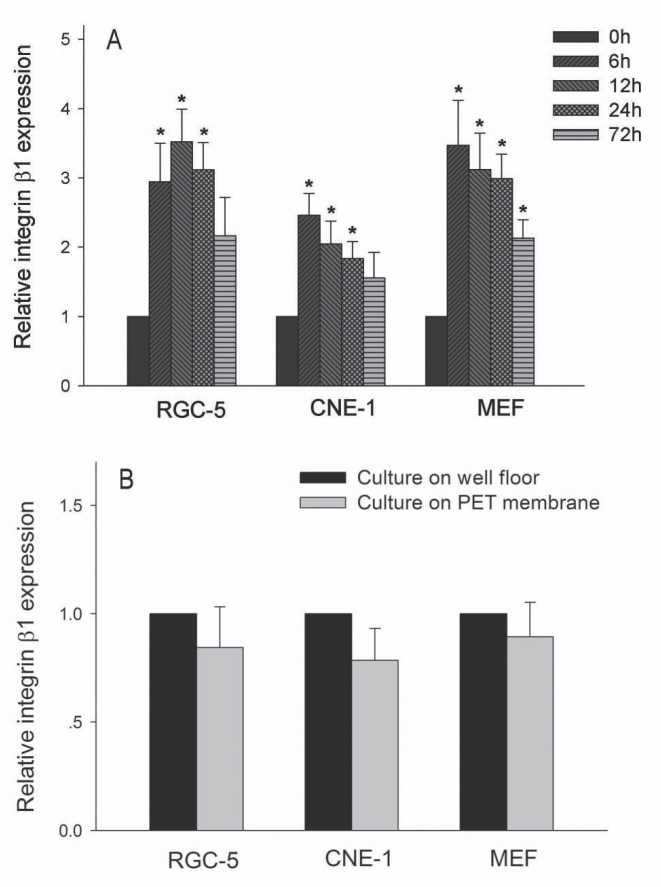

Figure 4: The effect of transwell-based pressure culture on integrin β1 expression. The mRNA level of integrin β1 was referred to GAPDH. **A** shows the relative integrin β1 expression in RGC-5, CNE-1 and MEFs before and after pressure culture. Expression level before pressure culture (0 h) was defined as 1. **B** shows the effect of membrane substrate on integrin β1 expression. Cells were grown on the well floor or on the insert membrane for 6 hours before for integrin β1 detection. The expression levels in well floor groups was defined as 1. It should be noted that culture on membrane only decreased integrin β1 expression slightly, but not significantly. Data were mean ± standard error from 3 independent experiments. * represents $P<0.05$ *vs.* 0 h.

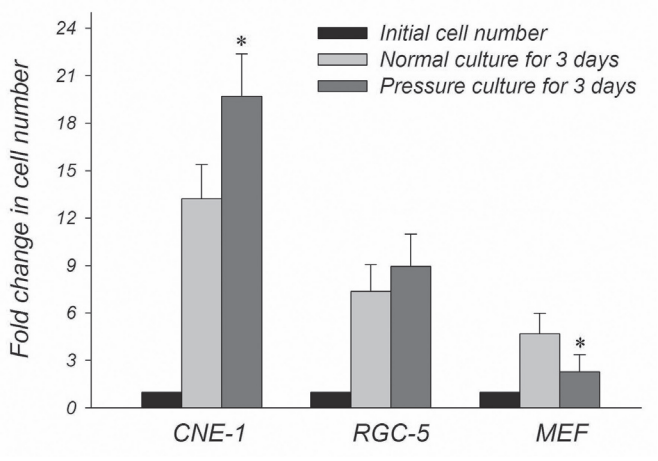

Figure 5: The effect of pressure culture on the proliferation of RGC-5, CNE-1 and MEFs. The initial cell number of each cell type (1×10^3 RGC-5, 1×10^3 CNE-1 and 2×10^3 MEFs) was defined as 1. Normal culture served as the control. 3-day pressure culture promoted the growth of CNE-1, while inhibited MEFs significantly. Data were obtained from 3 independent experiments. * represents $P<0.05$ *vs.* normal culture.

culture, the exact pressure level was unknown. Furthermore, the pressure exerted on each cell might be different. Many factors could affect the pressure level. The factors arising from cells include cell size, cell density and cell distribution, among others. The membrane material, membrane pore size, and nominal pore density car also influence the pressure level. Even the position in which the individual cell seeded or the placement of the insert might change the pressure level. Additionally, the pressure culture system can be used only for adherent cells, not for suspension cells.

Mechanical stimuli have great effects on cell proliferation. Elevated interstitial fluid pressure or mechanical strain may either increase or decrease cell growth, depending on cell type, stimuli amplitude, stimuli frequency, and other factors [3, 29]. The pressure culture in our study induced growth promotion on CNE-1 and RGC-5, while inducing evident inhibition on MEFs. It was reported that another kind of mouse fibroblast, 3T3-L1 grew faster under pressure of 5 MPa than at normal atmospheric pressure[30]. The difference might be due to the reason that the influence of mechanical pressure on cell proliferation is cell-type dependent[3]. 3T3-L1 is an established cell line and grows faster than MEFs. In current study, the MEFs were seeded at low density, which might also enhance the sensitivity to pressure stimulus.

In summary, we established an easily available pressure culture system which is effective for various kinds of cell types and can exert obvious influence on cell morphology and biological functions. Mechanical strain probably is the main component of the pressure.

ACKNOWLEDGMENTS

This work was supported by the National Natural Science Foundation of China (81170846, 81170327), the Fundamental Research Funds of State Key Laboratory of Ophthalmology (QN-1), the Medical Scientific Research Foundation of Guangdong Province (A2012420) and the Science & Technology Innovation Fund of Guangdong Medical College (STIF201102).

REFERENCES

1. AGHA R, et al. (2011) *A review of the role of mechanical forces in cutaneous wound healing.* J Surg Res. **171**(2): p. 700-8.
2. OH S, et al. (2010) *Role of elevated pressure in TRAIL-induced apoptosis in human lung carcinoma cells.* Apoptosis. **15**(12): p. 1517-28.
3. DIRESTA GR, et al. (2005) *Cell proliferation of cultured human cancer cells are affected by the elevated tumor pressures that exist in vivo.* Ann Biomed Eng. **33**(9): p. 1270-80.
4. LEVENTAL KR, et al. (2009) *Matrix crosslinking forces tumor progression by enhancing integrin signaling.* Cell. **139**(5): p. 891-906.
5. LUNT SJ, et al. (2008) *I nterstitial fluid pressure, vascularity and metastasis in ectopic, orthotopic and spontaneous tumours.* BMC Cancer. **8**: p. 2.
6. CAPRIOLI J and VARMA R (2011) *I ntraocular pressure: modulation as treatment for glaucoma.* Am J Ophthalmol. **152**(3): p. 340-344 e2.
7. THOMPSON WR, RUBIN CT and RUBIN J (2012) *Mechanical regulation of signaling pathways in bone.* Gene.
8. THILO F, et al. (2012) *Pulsatile atheroprone shear stress affects the expression of transient receptor potential channels in human endothelial cells.* Hypertension. **59**(6): p. 1232-40.
9. SALMON ED and ELLIS GW (1975) *A new miniature hydrostatic pressure chamber for microscopy. Strain-free optical glass windows facilitate phase-contrast and polarized-light microscopy of living cells. Optional fixture permits simultaneous control of pressure and temperature.* J Cell Biol. **65**(3): p. 587-602.
10. SALMON ED (1975) *Pressure-induced depolymerization of spindle microtubules. I. Changes in birefringence and spindle length.* J Cell Biol. **65**(3): p. 603-14.
11. REIGADA D, et al. (2008) *Elevated pressure triggers a physiological release of ATP from the retina: Possible role for pannexin hemichannels.* Neuroscience. **157**(2): p. 396-404.
12. INGBER DE (2006) *Cellular mechanotransduction: putting all the pieces together again.* Faseb J. **20**(7): p. 811-27.
13. MYERS KA, et al. (2007) *Hydrostatic pressure sensation in cells: integration into the tensegrity model.* Biochem Cell Biol. **85**(5): p. 543-51.
14. YANG X, et al. (2011) *Elevated pressure downregulates ZO-1 expression and disrupts cytoskeleton and focal adhesion in human trabecular meshwork cells.* Mol Vis. **17**: p. 2978-85.
15. JU WK, et al. (2009) *Elevated hydrostatic pressure triggers release of OPA1 and cytochrome C, and induces apoptotic cell death in differentiated RGC-5 cells.* Mol Vis. **15**: p. 120-34.
16. LEI Y, et al. (2011) *In vitro models for glaucoma research: effects of hydrostatic pressure.* Invest Ophthalmol Vis Sci. **52**(9): p. 6329-39.
17. SUN X, et al. (2011) *E13.5 retinal progenitors induce mouse bone marrow mesenchymal stromal cells to differentiate into retinal progenitor-like cells.* Cytotherapy. **13**(3): p. 294-303.
18. SUN X, et al. (2009) *Gene expression and differentiation characteristics in mice E13.5 and E17.5 neural retinal progenitors.* Mol Vis. **15**: p. 2503-14.
19. GARDEL ML, et al. (2010) *Mechanical integration of actin and adhesion dynamics in cell migration.* Annu Rev Cell Dev Biol. **26**: p. 315-33.
20. STRICKER J, FALZONE T and GARDEL ML (2010) *Mechanics of the F-actin cytoskeleton.* J Biomech **43**(1): p. 9-14.
21. COOPER JA (1987) *Effects of cytochalasin and phalloidin on actin.* J Cell Biol. **105**(4): p. 1473-8.
22. CIPOLLA MJ, GOKINA NI and OSOL G (2002) *Pressure-induced actin polymerization in vascular smooth muscle as a mechanism underlying myogenic behavior.* Faseb J. **16**(1): p. 72-6.
23. MCILHENNY SE, et al. (2010) *Linear shear conditioning improves vascular graft retention of adipose-derived stem cells by upregulation of the alpha5beta1 integrin.* Tissue Eng Part A. **16**(1): p. 245-55.
24. THOUMINE O, NEREM RM and GIRARD PR (1995) *Oscillatory shear stress and hydrostatic pressure modulate cell-matrix attachment proteins in cultured endothelial cells.* In Vitro Cell Dev Biol Anim. **31**(1): p. 45-54.
25. HUVENEERS S and DANEN EH (2009) *Adhesion signaling - crosstalk between integrins, Src and Rho.* J Cell Sci. **122**(Pt 8): p. 1059-69.
26. SHYY JY and CHIEN S (1997) *Role of integrins in cellular responses to mechanical stress and adhesion.* Curr Opin Cell Biol. **9**(5): p. 707-13.
27. TOKUDA S, et al. (2009) *Hydrostatic pressure regulates tight junctions, actin cytoskeleton and transcellular ion transport.* Biochem Biophys Res Commun. **390**(4): p. 1315-21.
28. ARNSDORF EJ, et al. (2009) *Mechanically induced osteogenic differentiation--the role of RhoA, ROCKII and cytoskeletal dynamics.* J Cell Sci. **122**(Pt 4): p. 546-53.
29. GAYER CP and BASSON MD (2009) *The effects of mechanical forces on intestinal physiology and pathology.* Cell Signal. **21**(8): p. 1237-44.
30. KOYAMA S, et al. (2005) *Effects of the piezo-tolerance of cultured deep-sea eel cells on survival rates, cell proliferation, and cytoskeletal structures.* Extremophiles. **9**(6): p. 449-60.

Biol Res 46: 53-57, 2013

The pioneering use of ISSR (Inter Simple Sequence Repeat) in Neotropical anurans: preliminary assessment of genetic diversity in populations of *Physalaemus cuvieri* (Amphibia, Leiuperidae)

Rafaela M. Moresco[1,3*], Thiago C. Maniglia[2], Classius De Oliveira[1] and Vladimir P. Margarido[3]

[1] Universidade Estadual Paulista (Unesp), Departamento de Biologia. Rua Cristóvão Colombo, 2265 - Jardim Nazareth. CEP 15054-000, São José do Rio Preto, São Paulo, Brazil. Phone: +55 17 3221 2387

[2] Universidade Tecnológica Federal do Paraná (UTFPR), Ciências Biológicas. Estrada para Boa Esperança, km 04 - Comunidade São Cristóvão. CEP 85660-000, Dois Vizinhos, Paraná, Brazil. Phone: +55 46 3536-8431

[3] Universidade Estadual do Oeste do Paraná (Unioeste), Centro de Ciências Biológicas e da Saúde. Rua Universitária, 2069 – Jardim Universitário. CEP 85819-110, Cascavel, Paraná, Brazil. Phone: +55 45 3220-3235

ABSTRACT

The greatest diversity of anurans in the world is in Brazil and one of the major challenges is to reconcile the accelerated economic development with strategies that aim to maintain this diversity in forest fragments, often representing ESUs of some biomes. This study aimed to obtain data that will support conservation projects through the pioneering use of ISSR analysis in Neotropical anurans, estimating the intra- and interpopulation genetic diversity of four populations of *P. cuvieri* (Paraná and São Paulo regions). Of the 65 loci scored 58 were polymorphic, with 0.797 intrapopulation variation and 0.203 interpopulation variation. The index of interpopulation genetic differentiation (F_{ST}) proved to be high among the population of Marmeleiro-PR and the three populations of SP ($F_{ST} > 0.288$); genetic dissimilarity was related to the geographical distance. The ISSR proved to be efficient and useful molecular markers in comparison with other markers most widely used for preliminary diagnosis of genetic diversity in populations of amphibians, and could be applied as a tool for future conservation projects, since they could identify potential ESUs and influence decisions on the preservation of fragments.

Key words: ESU; F_{ST}; Gene flow; Genetic structure; Molecular marker

INTRODUCTION

Amphibians are considered relatively poor dispersers and highly philopatric (Blaustein et al., 1994). Usually, anuran populations exhibit a high degree of spatial structure, mainly when interpopulation distances exceed several kilometers (Shaffer et al., 2000). Amphibians have become a focus for studies on the effect of habitat fragmentation on genetic diversity and population differentiation (Reh and Seitz, 1990; Hitchings and Beebee, 1998).

With more than 800 described species, Brazil has the highest species diversity of frogs in the world, with many endemic species (SBH, 2011). The barker frog *Physalaemus cuvieri* Fitzinger, 1826 occurs in Argentina, Brazil, Paraguay, Bolivia, Guyana and possibly in the southern plains of Venezuela. In Brazil *P. cuvieri* occurs in environments with distinct climatic characteristics, where the amount and distribution of rainfall and range of temperature differs, as in the Caatinga, Cerrado (Brazilian savannah) and Forest (Nimer, 1989). *Physalaemus cuvieri* is a very small Leiuperidae (about 3 cm of rostrum–anal length). It breeds in permanent, semi-permanent and temporary bodies of water; and the eggs are laid in foam nests attached to grass stems at the margin of the pond. Males of *Physalaemus cuvieri* call on the water surface, floating by the inflation of vocal sacs and lungs. Aggressive interactions among males are frequently observed, mainly during the period of high activity levels (Barreto and Andrade, 1995). Studies using genetic molecular markers (microsatellite and RAPD) to evaluate the variation and population genetic structure of *P. cuvieri* have shown relatively low dispersion rates, high habitat fidelity and specificity (Telles et al., 2006; Conte et al., 2011).

Currently in Brazil one of the greatest scientific challenges is to reconcile strategies that avoid the loss of an important part of biodiversity with economic development, mainly related to agricultural activities (Ewers, 2005). The Atlantic Forest and Cerrado were the most degraded biomes during this process of human occupation, making small and isolated fragments be the only current representatives of native vegetation as well as its characteristic fauna (Ranta et al., 1998; Oliveira and Marquis, 2002). These small fragments are still very important for maintaining the diversity of amphibians, since they serve as a refuge for animals during the dry season, as a day shelter during the breeding season, a foraging area and even as dispersal corridors (Silva and Rossa-Feres, 2007; Silva and Rossa-Feres, 2011). According to the same authors, these fragments collaborate with the maintenance of regional rainfall regimes, essential for the survival of most species of anurans.

One important component of biodiversity is genetic variability; with the popularization of molecular techniques it has become a tool for determining more accurately whether a population does or does not have the minimum attributes for maintenance or if it is at risk of extinction (Nei et al., 1975; Leberg, 1992). Thus molecular techniques have been used for several studies of anurans, and the most commonly used markers are allozymes (Spasic-Boskovic et al., 1999; Bisconti et al., 2011), RAPD (Telles et al., 2006; Silva et al., 2007),

*Author for correspondence: Rafaela Maria Moresco. Universidade Estadual Paulista (Unesp), Departamento de Biologia. Rua Cristóvão Colombo, 2265 - Jardim Nazareth. CEP 15054-000, São José do Rio Preto, São Paulo, Brazil. Phone: +55 17 3221 2387. E-mail: rafaelabiologia@yahoo.com.br

Received: August 21, 2012. In Revised form: November 26 , 2012. Accepted: January 9 ,2013

mitochondrial DNA (Vences et al., 2005; Funk et al., 2007) and microsatellites (Martínez-Solano and García-París, 2005; Conte et al., 2011).

ISSR (*Inter Simple Sequence Repeat*) analysis has recently been used, since it produces excellent results and also has very low cost compared to other techniques. In ISSR, fragments are amplified via PCR, obtaining dominant markers and using only one primer (anchored microsatellite sequences) composed of three or four repeating units of a microsatellite (often 18-20 base pairs) that may or may not have one to four degenerate nucleotides anchored in the 3 'or 5' ends (Zietkiewicz et al., 1994). The amplified genomic segment is the one that lies between two blocks of microsatellite. Thus a previous knowledge of the region to be amplified is not necessary, nor a time-consuming and expensive step of genomic library construction (or cloning and sequencing) as with microsatellite markers. The greater reproducibility is an advantage that makes the ISSR more promising than RAPD, due to the use of longer primers which allows the use of high annealing temperature (45-60 °C) leading to higher stringency (Reddy et al., 2002), and increasing the repeatability of experiments (for review, see Semagn et al., 2006).

The extinction of genetically unique populations has largely taken place since 1900 as a result of habitat destruction, pollution and overexploitation. The main agents that cause a species to lose genetic variability are the isolation of populations and the reduction of the population effective size. These reductions may result in a decline in fitness and eventual extinction (Carvalho and Hauser, 1998). The present study provides preliminary data of the pioneering use of the ISSR technique in Neotropical anurans to estimate the intra- and interpopulation genetic diversity in populations of *P. cuvieri*, and verify the effectiveness of this technique to generate data that may support proposals for the conservation of threatened forest fragments.

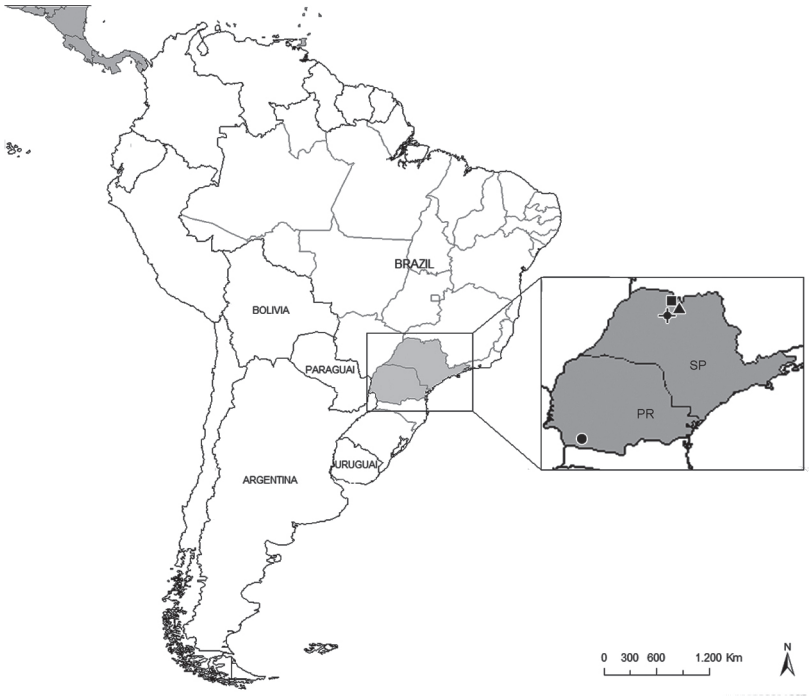

Figure 1: Map of sampling sites of *P. cuvieri* populations in Brazil: Marmeleiro-PR (●), Nova Itapirema-SP (-✦-), Eng. Schmidt-SP (▲) and Talhado-SP (■).

MATERIAL AND METHODS

Three populations of *P. cuvieri* from São Paulo (SP): Engenheiro Schmidt (20º51'58.45"S; 49º18'29.07"W), Nova Itapirema (21º05'60.00"S; 49º31'60.00"W), Talhado (20º40'51.01"S; 49º17'34.57"W), and a population from Paraná (PR): Marmeleiro (26º08'58.43"S; 53º01'31.77"W) were sampled (Fig. 1). Since this is a preliminary study for presenting new and useful information on the utility of ISSR marker to assess the genetic variability in Neotropical anurans, only five male individuals were collected from each population (we suggest increasing the sample size and the number of populations for inferences on the genetic structure and for conservation purposes); they were anesthetized and sacrificed in the laboratory by benzocaine saturation. Fragments of liver were removed and stored in 100% ethanol for DNA extraction, which was performed with *GenElute™ Mammalian Genomic DNA Miniprep Kit* (Sigma-Aldrich) following the manufacturer's instructions.

For the amplification of ISSR fragments, the following primers were previously selected and used $(GGAC)_3A$, $(GGAC)_3C$, $(GGAC)_3T$ and $(GGAC)_4$. The conditions for DNA amplification via PCR were as recommended by Fernandes-Matioli et al. (2000), with modifications. The amplification reaction mixture consisted of Tris-KCl, 2 mM $MgCl_2$, 0.92 mM primer, 0.38 mM dNTP, 1 U/ reaction Taq DNA polymerase, DNA (10 ng) and enough water to make up a volume of 13 µL. The amplification reactions were performed in Eppendorf Mastercycler Gradient thermocycler scheduled for 4 cycles of 45s at 94 °C, 1 min at 51 °C and 1 min at 72 °C, followed by 29 cycles of 45s at 94 °C, 1 min at 48 °C and 1 min at 72 °C. After the last cycle of amplification, the reaction mixture was cooled and maintained at 4 °C. Negative controls without DNA were included in each set of amplifications. After amplification, samples consisting of 7 µL of PCR reaction mixture were subjected to electrophoresis on 1.4% agarose gels and stained with ethidium bromide (0.2 µg/mL). Electrophoresis was performed in TBE buffer (Tris-borate), 5 $V.cm^{-1}$, for 4 hours; the amplified fragments were visualized under ultraviolet light and the gel was photographed for analysis. The size of the fragments was estimated by comparison with 100 bp ladder marker (Invitrogen ™). The fragments of ISSR were treated as dominant markers and judged as binary characters: present (1) or absent (0), so a binary matrix was produced and from it were estimated the indices of genetic diversity within and among populations. The accuracy of band assignment was studied by repeating in a minimum of five replicates; the bands were bright enough that presence/absence scoring was not confounded by simple intensity differences and the bands were distinct enough in size from the surrounding bands.

The pairwise genetic distance matrix between individuals was obtained by the Jaccard similarity index, and used to construct the Neighbor-Joining dendrogram with the program FreeTree and Mega 3.1. The scatter plot of principal coordinates was constructed

using the programs DistPCoA and Statistica 7.1. Genetic differentiation was examined by applying the Mantel test, with 10,000 permutations for the Jaccard similarity matrix using the Mantel-Struct 1.0 program. The analysis of molecular variance, expected heterozygosity and the value of genetic differentiation (F_{ST}) were obtained using the program Arlequin 3.5.1.2. The linear regression between F_{ST} and geographic distance was carried out using Statistica 7.1 using the data in Table 1.

RESULTS

Of the 65 loci scored 58 were polymorphic, with 0.797 intrapopulation variation and 0.203 interpopulation variation. The polymorphic *vs.* total number of loci per each primer was: 15/17 for the $(GGAC)_3A$ primer; 15/17 for the $(GGAC)_3C$ primer, 14/16 for the $(GGAC)_3T$ primer and 14/15 for the $(GGAC)_4$ primer. Primer $(GGAC)_3A$ produced a fragment of 250 bp uniquely from the population of Marmeleiro-PR and another fragment of 210 bp uniquely from populations of SP. The amplified fragments ranged from 200 to about 1,500 bp (Fig. 2A).

The dendrogram analysis identified two main groups whose compositions show that there is a clear relationship between genetic distance and geographical distance, and the population of Marmeleiro-PR proved to be differentiated from the other populations analyzed (Fig. 2B). The scatter plot of principal coordinates built with the two major eigenvectors (0.245 and 0.122 of variation, respectively), also obtained with the Jaccard similarity index, corroborates the dendrogram, since it shows that the population of Marmeleiro-PR is separated from the SP populations (Fig. 2C).

Genetic differentiation among populations of *P. cuvieri* quantified by the Mantel test showed no significant correlation only between the populations of Eng. Schmidt-SP and Talhado- SP (the smallest geographic distance), showing that these populations are not genetically differentiated (p = 0.473, r = -0.011 and $Z_{10,000} < Z$). Values of genetic dissimilarity, which is the genetic variability within and among populations, were also obtained through this test (Table 1). The intrapopulational genetic dissimilarity was almost the same for all populations, being 0.469 in the population of Marmeleiro-PR; 0.449 in Nova Itapirema-SP; 0.454 in Eng. Schmidt-SP and 0.446 in Talhado-SP. The expected heterozygosity was almost the same for all populations; 0.513 ± 0.101 in Marmeleiro-PR; 0.488 ± 0.101 in Nova Itapirema-SP; 0.457 ± 0.091 in Eng. Schmidt-SP and 0.506 ± 0.101 in Talhado-SP. The index of interpopulation genetic differentiation (F_{ST}) was high between populations of the two different regions PR/SP ($F_{ST} \geq 0.25$), moderate among the population of Nova Itapirema and the other two SP populations ($0.25 > F_{ST} \geq 0.05$), and not different among the populations of Schmidt and Talhado ($F_{ST} < 0.05$). These results corroborate the genetic difference among Marmeleiro-PR population and SP populations, and indicate that genetic dissimilarity is related to geographical distance, as the correlation between F_{ST} and geographic distance (p = 0.002, r = 0.966) (Table 1, Fig 3).

DISCUSSION

Although the studied populations of *P. cuvieri* are present in small preserved fragments of Atlantic Forest and Cerrado, the genetic variability present is high (around 0.45), and 0.797 of all variation is intrapopulation. A similar result was found by Telles et al. (2006) in a study with RAPD marker in 214 individuals from 18 populations of *P. cuvieri*, where most of the genetic variation was found among individuals of the same fragment (0.898). When the authors analyzed only the 6 local populations with more than 12 individuals (12 to 23 individuals), the result obtained was qualitatively similar, and indicated that unbalanced sample sizes and the relatively small sample size in some populations did not qualitatively affect the evaluation of overall population genetic structure (using AMOVA and Bayesian estimate of θ^B). In relation to the expected heterozygosity (H_e), our study showed high values ranging from 0.46 to 0.51. Similar results were obtained by Conte et al. (2011) using microsatellite markers in 85 individuals from 5 populations (14 to 21 individuals/populations), with high observed heterozygosities (H_o) ranging from 0.31 to 0.59 (and H_e ranging from 0.30 to 0.58). As already shown in other studies, forest fragments can contribute to the maintenance of species diversity of frogs (Silva and Rossa-

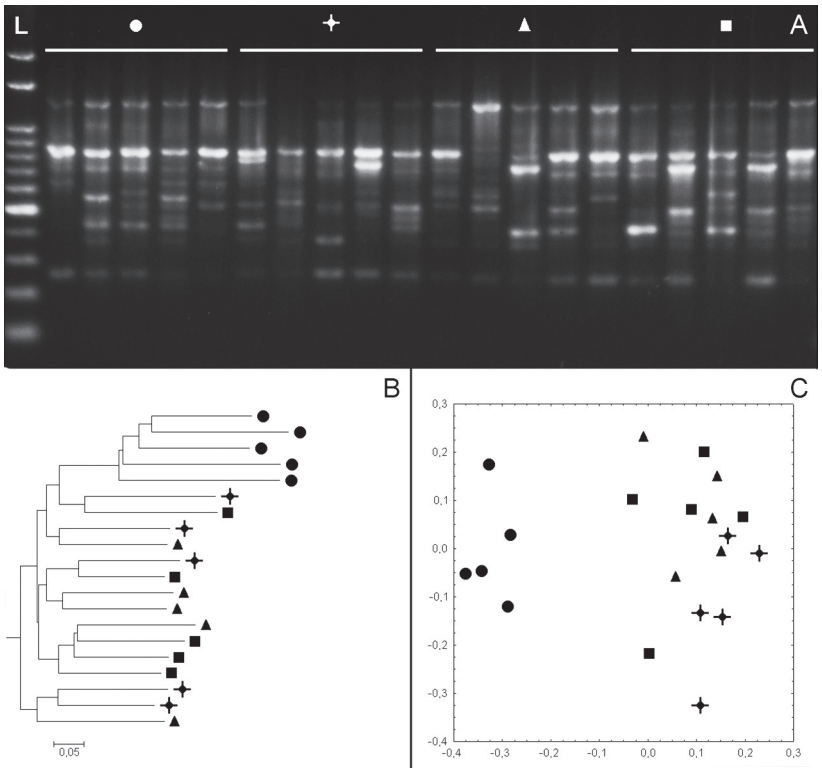

Figure 2: Analysis of P. cuvieri populations using ISSR markers: (A) *agarose gel electrophoresis* of PCR products obtained from the amplification of DNA samples using the primer (GGAC)3T; (B) Neighbor-joining dendrogram based on Jaccard similarity index with 10,000 bootstrap resamplings. (C) Scatter plot of main coordinates based on Jaccard similarity index. (L) 100 bp ladder, (●) Marmeleiro-PR, (✦) Nova Itapirema-SP, (▲) Eng. Schmidt-SP and (■) Talhado-SP.

TABLE 1

Pairwise comparisons of *Physalaemus cuvieri* populations.

Pairwise comparisons	Distance (Km)	F_{ST}	p	r	Z	$Z_{10\,000}$	Genetic dissimilarity
Marmeleiro-PR x Nova Itapirema-SP	663.88	0.359	0.007	0.861	15.849	13.900	0.634
Marmeleiro-PR x Eng. Schmidt-SP	699.08	0.292	0.009	0.759	14.854	13.383	0.594
Marmeleiro-PR x Talhado-SP	717.33	0.288	0.007	0.687	14.679	13.228	0.587
Nova Itapirema-SP x Eng. Schmidt-SP	35.40	0.072	0.114	0.185	11.871	11.611	0.475
Nova Itapirema-SP x Talhado-SP	53.42	0.058	0.183	0.145	11.668	11.446	0.467
Eng. Schmidt-SP x Talhado-SP	21.06	-0.005	0.473	-0.011	11.208	11.220	0.448

Approximate distance (km), interpopulation genetic differentiation index (F_{ST}), significance level (p), correlation of two matrices (r), robustness of the relation original data (Z) and after 10,000 permutations ($Z_{10\,000}$), genetic dissimilarity using Jaccard Coefficient.

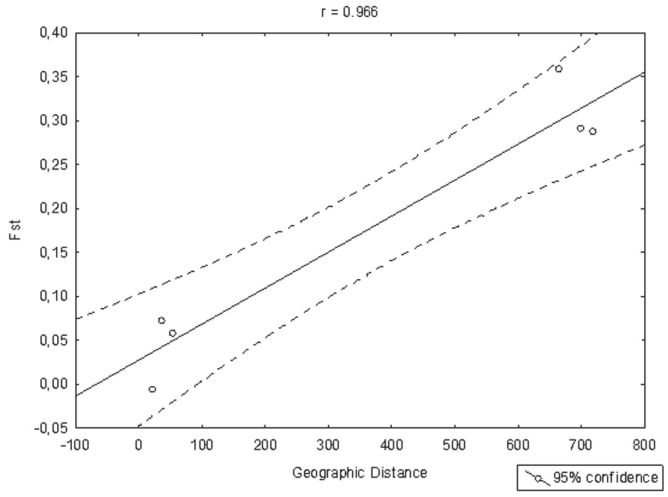

Figure 3: Linear regression between FST and geographic distance among P. cuvieri populations.

Feres, 2007; Silva and Rossa-Feres, 2011), and the present study supports that the genetic diversity can also be maintained, and thus the populations would be potentially more protected from the extinction factor due to environmental changes.

Gene flow is geographically restricted to nearby populations, indicated by F_{ST} that increases in direct proportion to the distance. In our study, this correlation was observed, where the highest F_{ST} occurred between populations of the two different regions PR/SP (distance ≥ 663.8 Km; Table I, Fig. 3). Similar results were obtained in *P. cuvieri* by Conte et al. (2011) using microsatellite markers, with high G_{ST} values ($G_{ST} \geq 0.20$) observed between populations isolated by long distances (ranging from 381 Km to 2936 Km). Telles et al. (2006), in RAPD studies with *P. cuvieri* at a much smaller spatial scale, indicate that genetic similarity among local populations tends to be slightly larger than expected by chance alone. Lampert et al. (2003), working with populations of *Physalaemus pustulosus* separated by 260 meters on average, that is, a very small range of spatial distance, showed strong positive correlation between genetic and geographic distances. Although genetic diversity can be produced by mutation, genetic drift and selection, the differentiation between populations tends to increase with the absence of gene flow, and these data can contribute to the identification of evolutionarily significant units (ESUs) (Varvio et al., 1986). The preservation of ESUs maximizes the potential for future evolutionary success of species or population groups of species (Hey et al., 2003). The use of ESUs as targets for conservation actions is increasing, so it is very important that preliminary studies identify quickly, accurately and correctly an ESU. In the present study it was possible to determine by the ISSR marker that the level of interpopulation genetic differentiation is high among the population of Marmeleiro-PR and other SP populations ($F_{ST} > 0.288$), suggesting that this population has a genetic composition quite different from the others.

The frequent occupation of many areas of agriculture and livestock has reduced many characteristic biomes of Brazil to small fragments, surrounded by a landscape highly modified and degraded with an edge effect greatly increased, which is reflected in changes of abiotic factors resulting from the abrupt transition between two adjacent ecosystems that affect population dynamics (Murcia, 1995; Rambaldi and Oliveira, 2003). Decreases in the potential for dispersal of species, the number of species and population size can also be observed, resulting in reduced genetic variability (Fahrig, 2003). According to Ohmer and Bishop (2011), studies from the last two decades indicate climate change and habitat loss as the factors most related to the worldwide decline of amphibians. Nevertheless, the small fragments are often the last remnants of a biota and play an important role in the preservation of these species (Silva et al., 2011).

As recommended by Fraser and Bernatchez (2001) and Aleixo (2009), the degree of vulnerability of an ESU should be assessed at the planning stage of conservation, to prevent a species listed as threatened from losing one of its ESUs before conservation action. The ISSR proved to be an efficient and useful molecular marker for the preliminary diagnosis of genetic diversity in populations of amphibians; it has a low cost, high repeatability and produces quick results, since it does not require prior knowledge of sequence to be amplified. Moreover, for the preliminary diagnosis of genetic diversity, the limited sample size should be compensated by a higher number of loci per sample. Thus it can be used as a tool for future conservation projects, helping in making decisions about the preservation of fragments, and identification of ESUs before they are threatened.

ACKNOWLEDGMENTS

To Conselho Nacional de Desenvolvimento Científico e Tecnológico (CNPq, Proc. 474596/2010-9) and to Coordenação de Aperfeiçoamento de Pessoal de Nível Superior (Capes) for the support of the research.

REFERENCES

ALEIXO A (2009) Conceitos de espécie e suas implicações para a conservação. Megadiversidade 5: 87-95.

BARRETO L, ANDRADE GV (1995) Aspects of the reproductive biology of *Physalaemus cuvieri* (Anura: Leptodactylidae) in notheastern Brazil. Amphibia-Reptilia 16: 67-76.

BISCONTI R, CANESTRELLI D, NASCETTI G (2011) Genetic diversity and evolutionary history of the Tyrrhenian treefrog *Hyla sarda* (Anura: Hylidae): adding pieces to the puzzle of Corsica-Sardinia biota. Biol J Linn Soc 103: 159-167.

BLAUSTEIN AR, WAKE DB, SOUSA WP (1994) Amphibian declines: Judging stability, persistence, and susceptibility of populations to local and global extinctions. Conserv Biol 8: 60-71.

CARVALHO GR, HAUSER L (1998) Advances in the molecular analysis of fish population structure. Ital J Zool 65: 21-33.

CONTE M, ZUCCHI MI, ANDRADE GV, SOUZA AP, RECCO-PIMENTEL SM (2011) Study of closely related species within the *Physalaemus cuvieri* group (Anura): contribution of microsatellite markers. Genet Mol Res 10: 1434-1444.

EWERS RM (2005) Are conservation and development compatible? Trends Ecol Evol 20: 159.

FAHRING L (2003) Effects of fragmentation on biodiversity. Annu Rev Ecol Syst 34: 487-515.

FERNANDES-MATIOLI FMC, MATIOLI SR, ALMEIDA-TOLEDO LF (2000) Species diversity and geographic distribution of *Gymnotus* (Pisces: Gymnotiformes) by nuclear $(GGAC)_n$ microsatellite analysis. Genet Mol Biol 23: 803-807.

FRASER DJ, BERNATCHEZ L (2001) Adaptive evolutionary conservation: towards a unified concept for defining conservation units. Mol Ecol 10: 2741-2752.

FUNK WC, CALDWELL JP, PEDEN CE, PADIAL JM, DE LA RIVA I, CANNATELLA DC (2007) Tests of biogeographic hypotheses for diversification in the Amazonian forest frog, *Physalaemus petersi*. Mol Phylogenet Evol 44: 825-837.

HEY J, WAPLES RS, ARNOLD ML, BUTLIN RK, HARRISON RG (2003) Understanding and confronting species uncertainty in biology and conservation. Trends Ecol Evol 18: 597-603.

HITCHINGS SP, BEEBEE TJC (1998) Loss of genetic diversity and fitness in Common Toad (*Bufo bufo*) populations isolated by inimical habitat. J Evol Biol 11: 269-283.

LAMPERT KP, RAND AS, MUELLER UG, RYAN MJ (2003) Fine-scale genetic pattern and evidence for sex-biased dispersal in the túngara frog, *Physalaemus pustulosus*. Mol Ecol 12, 3325-3334.

LEBERG PL (1992) Effects of population bottlenecks on genetic diversity as measured by allozyme eletrophoresis. Evolution 46: 477-494.

MARTÍNEZ-SOLANO IR, GARCÍA-PARÍS M (2005) The impact of historical and recent factors on genetic variability in a mountain frog: the case of *Rana iberica* (Anura: Ranidae). Anim Conserv 8: 431-441.

MURCIA C (1995) Edge effects in fragmented forests: implications for conservation. Trends Ecol Evol 10: 58-62.

NEI M, MARUYAMA T, CHAKRABORTY R (1975) The bottleneck effect and genetic variability in populations. Evolution 29: 1-10.

NIMER E (1989) *Climatologia do Brasil*. Rio de Janeiro: IBGE: Departamento de Recursos Naturais e Estudos Ambientais.

OHMER ME, BISHOP PJ (2011) Citation rate and perceived subject bias in the amphibian-decline literature. Conserv Biol 25: 195-199.

OLIVEIRA PS, MARQUIS RJ (2002) *The Cerrados of Brazil: ecology and natural history of a Neotropical Savanna*. New York: Columbia University Press.

RAMBALDI DM, OLIVEIRA DAS (2003) *Fragmentação de Ecossistemas: causas, efeitos sobre a biodiversidade e recomendações de políticas públicas*. Brasília: Ministério do Meio Ambiente.

RANTA P, BLOM T, NIEMELAÈ J, JOENSUU E, SIITONEN M (1998) The fragmented Atlantic rain forest of Brazil: size, shape and distribution of forest fragments. Biodivers Conserv 7, 385-403.

REDDY MP, SARLA N, SIDDIQ EA (2002) Inter simple sequence repeat (ISSR) polymorphism and its application in plant breeding. Euphytica 128: 9-17.

REH W, SEITZ A. (1990). The influence of land use on the genetic structure of populations of the common frog *Rana temporaria*. Biol Conserv 54: 239-249.

SBH (2011). *Sociedade Brasileira de Herpetologia: A Lista Brasileira de Anfíbios e Répteis*. See http://www.sbherpetologia.org.br/checklist/checklist_brasil.asp.

SEMAGN K, BJØRNSTAD Å, NDJIONDJOP MN (2006) An overview of molecular marker methods for plant. Afr J Biotechnol 5: 2540-2569.

SHAFFER HB, FELLERS GM, MAGEE A, VOSS SR (2000) The genetics of amphibian declines: population substructure and molecular differentiation in the Yosemite toad, *Bufo canorus* (Anura Bufonidae) based on single-strand conformation polymorphism analysis (SSCP) and mitochondrial DNA sequence data. Mol Ecol 9: 245-257.

SILVA DM, CRUZ AD, BASTOS RP, REIS RL, TELLES MPC, DINIZ-FILHO JAF (2007). Population structure of *Eupemphix nattereri* (Amphibia, Anura, Leiuperidae) from Central Brazil. Genet Mol Biol 30: 1161-1168.

SILVA FR, ROSSA-FERES DC (2007) Uso de fragmentos florestais por anuros (Amphibia) de área aberta na região noroeste de Estado de São Paulo. Biota Neotrop 7: 141-147.

SILVA FR, ROSSA-FERES DC (2011) Influence of terrestrial habitat isolation on the diversity and temporal distribution of anurans in an agricultural landscape. J Trop Ecol 27: 327-331.

SILVA FR, PRADO VHM ROSSA-FERES DC (2011) Value of small forest fragments to amphibians. Science 332: 1033.

SPASIC-BOSKOVIC O, KRIZMANIC I, VUJOSEVIC M (1999) Population composition and genetic variation of water frogs (Anura: Ranidae) from Yugoslavia. Caryologia 52: 9-20.

TELLES MPC, BASTOS RP, SOARES TN, RESENDE LV, DINIZ-FILHO JAF (2006) RAPD variation and population genetic structure of *Physalaemus cuvieri* (Anura: Leptodactylidae) in Central Brazil. Genetica 128: 323-332.

VARVIO SL, CHAKRABORTY R, NEI M (1986) Genetic variation in subdivided populations and conservation genetics. Heredity 57: 189-198.

VENCES M, THOMAS M, MEIJDEN A, CHIARI Y, VIEITES DR (2005) Comparative performance of the 16S rRNA gene in DNA barcoding of amphibians. Front Zool 2: 5.

ZIETKIEWICZ E, RAFALSKI A, LABUDA D (1994) Genome fingerprinting by simple sequence repeat (SSR)-anchored polymerase chain reaction amplification. Genomics 20: 176-183.

Biol Res 46: 59-67, 2013

Acclimatization to chronic intermittent hypoxia in mine workers: a challenge to mountain medicine in Chile

Jorge G. Farías[1,*,†], Daniel Jimenez[2,*], Jorge Osorio[2], Andrẹa B. Zepeda[1], Carolina A. Figueroa[1] and Victor M. Pulgar[3,4,†]

[1] Departamento de Ingeniería Química y Ciencias, Facultad de Ingeniería, Universidad de La Frontera, Temuco, Chile.
[2] Medicina de Altura Ltda. Santiago, Chile.
[3] Biomedical Research Infrastructure Center, Winston-Salem State University, Winston Salem, NC, USA.
[4] Department of Obstetrics and Gynecology, Wake Forest School of Medicine, Winston Salem, NC, USA.
[*] These authors contributed equally to this work.

ABSTRACT

In the past two decades, Chile has developed intense mining activity in the Andes mountain range, whose altitude is over 4,000 meters above sea level. It is estimated that a workforce population of over 55,000 is exposed to high altitude hypobaric hypoxia. The miners work under shift systems which vary from 4 to 20 days at the worksite followed by rest days at sea level, in a cycle repeated for several years. This Chronic Intermittent Hypoxia (CIH) constitutes an unusual condition for workers involving a series of changes at the physiological, cellular and molecular levels attempting to compensate for the decrease in the environmental partial pressure of oxygen (PO_2). The mine worker must become acclimatized to CIH, and consequently undergoes an acute acclimatization process when he reaches the worksite and an acute reverse process when he reaches sea level. We have observed that after a period of 3 to 8 years of CIH exposure workers acclimatize well, and evidence from our studies and those of others indicates that CIH induces acute and chronic multisystem adjustments which are effective in offsetting the reduced availability of oxygen at high altitudes. The aims of this review are to summarize findings of the physiological responses to CIH exposure, highlighting outstanding issues in the field.

Key words: High Altitude, Mine Workers, Intermittent Hypoxia, Acclimatization, Chilean Model.

1. GENERAL CONCEPTS

High altitude-induced hypobaric hypoxia involves a series of adaptive changes in multiple physiological systems in exposed individuals. Based in our findings and those of others, in this review we summarize the main physiological responses observed in mine workers intermittently exposed to hypobaric hypoxia. The literature on the occupational health of high-altitude exposed workers has been recently reviewed by Vearrier and Greenberg, 2011.

Hypobaric hypoxia occurs as a consequence of the low partial pressure of oxygen (PO_2) in the inspired air, resulting from the low barometric pressure found at high altitudes. A lower arterial PO_2 in turn initiates a physiological response attempting to maintain tissue oxygenation. One parameter used to determine respiratory response and the transport of oxygen in the blood to the tissues is percent hemoglobin saturation ($\%SaO_2$), which can be estimated with a portable device. At sea level values fluctuate between 95 and 97%; values below 90% SaO_2 are associated with pathological situations such as respiratory failure (Farias *et al*., 2006). An effect produced by exposure to hypobaric hypoxia is the well known Acute Mountain Sickness (AMS), whose symptoms include headaches, vomiting, fatigue, loss of appetite and sleep disturbances (Hackett *et al*., 1976, León-Velarde *et al*., 2010).

The acute response to hypoxia depends mainly on 4 factors: a) the altitude reached, i.e. the degree of hypobaric hypoxia, b) the rate of climb, c) individual susceptibility, and d) physical and environmental requirements in the ascent and arrival. It is known that upon exposure to 2,500 m altitude the problems associated with hypobaric hypoxia begin, with the consequent challenges for the individuals exposed (León-Velarde *et al*., 2005).

The lower availability of oxygen at high altitudes triggers physiological mechanisms that first seek to protect oxygen transport to the tissues, inducing mainly respiratory and cardiovascular adjustments. The increase in ventilation depends on the activity of the peripheral chemo receptors, particularly those located inside the carotid bodies that detect changes in arterial PO_2 and transmit sensorial information to regulate breathing (Prabhakar *et al*., 2000). Some data indicate that enzymes present in all mammalian cells, especially hydroxylases, are sensitive to moderate hypoxia and their activity may be controlled at several other levels, which provides flexibility to the physiological responses to hypoxia (Schofield and Ratcliff, 2004).

Important factors in personal susceptibility to hypoxia are the presence of sensitive oxygen sensors and effective physiological adaptations. Based on susceptibility to hypoxia, exposed individuals may be classified as good responders, who tolerate and acclimate without symptoms; a group with a low response and temporary minor symptoms that may limit performance; and poor responders, who display low sensitivity to hypoxia and ineffective compensatory physiological responses.

Residency in high altitude locations exposes humans to ambient hypobaric hypoxia, thus Chronic Hypoxia exposure

* Correspoding author: Jorge G. Farias, PhD, Email: jfarias@ufro.cl, Phone: +56-45-325472/592189, Fax: +56-45-325053 and Victor M. Pulgar, PhD. Email: vpulgar@wakehealth.edu, Phone: 1-336-716-5149, Fax: 1-336-716-6937

Received: September 12, 2012. In Revised form: December 28, 2012. Accepted: January 9, 2013

refers to groups of people who live for generations at high altitudes or are occasionally exposed to short periods (days) of normoxia. Acute Hypoxia refers to individuals who live at sea level and are exposed to high altitudes for only minutes, hours or days, as in the case of mountain climbers. Periodic intermittent exposure to high altitudes, as in the case of the Chilean miners who work at altitudes over 4,000 m is called Chronic Intermittent Hypoxia (CIH) (Richalet *et al*., 2002; Vargas *et al*, 1989; Farías *et al*., 2006). Mining workers at high altitudes must adjust to the requirements of hypobaric hypoxia for some days and then return to sea level, where they lose some of the acclimatization to hypoxia, depending on the time in normoxia. This model of exposure to hypobaric hypoxia, named the Chilean model or CIH exposure, has received increased attention in recent years (Casanegra *et al*., 1993; Chamorro *et al*., 1993; Jalil *et al*., 1994; Jimenez 1995; Richalet *et al*., 2002; Farias *et al*., 2006; Brito *et al*., 2007).

2. ACCLIMATIZATION TO INTERMITTENT EXPOSURE TO HIGH ALTITUDES

The term 'altitude acclimatization' describes the processes whereby lowland humans and animals respond to reduced PO_2 in the inspired air. It refers only to the changes in response to hypoxia seen as beneficial, as opposed to changes that are pathological and result in illness such as AMS (West *et al*., 2007; Vearrier and Greenberg, 2011). Altitude acclimatization involves a series of adaptive physiological adjustments that compensate for the reduction in ambient PO_2 (see Figure 1) and is the best strategy for the prevention of AMS (Forgey, 2006) Altitude acclimatization allows people to achieve their maximum physical and cognitive work performance possible for the altitude once they are acclimatized (Fulco *et al*., 2000).

2.1.. Physiological effects of intermittent hypobaric hypoxia.

Cyclical exposure to high altitude triggers responses throughout the route of oxygen, beginning with the carotid chemoreceptors and including ventilatory responses, pulmonary circulatory adjustments, the alveolar/capillary barrier, erythropoietin, hemoglobin, adjustments in the distribution of intra and extravascular fluid, changes in acid-base conditions, PO_2, PCO_2 and O_2 delivery at the cellular level, with modifications in the peripheral capillaries and mitochondrial enzyme optimization.

One type of intermittent exposure to hypobaric hypoxia occurs with exercise training at high altitude; endurance athletes have evolved different models of exposure with the ultimate goal of increasing athletic performance at sea level. The most used models are Live High (at altitude) and Training Low (at sea level) LH-TL, Live High-Train High LH-TH, Intermittent Hypoxic Exposure (IHE) and Intermittent Hypoxic Training (IHT) (Wilber, 2007). With the aim of using altitude acclimatization to enhance aerobic capacity via hypoxia-induced increases in serum erythropoietin and hemoglobin concentrations, athletes either live and/or sleep in hypoxia (natural or artificial). Also, by stimulating ventilation and better oxygen saturation, the increased aerobic capacity improves muscle oxygenation and increases exercise tolerance. Based on studies of maximum oxygen uptake (VO_2max) and

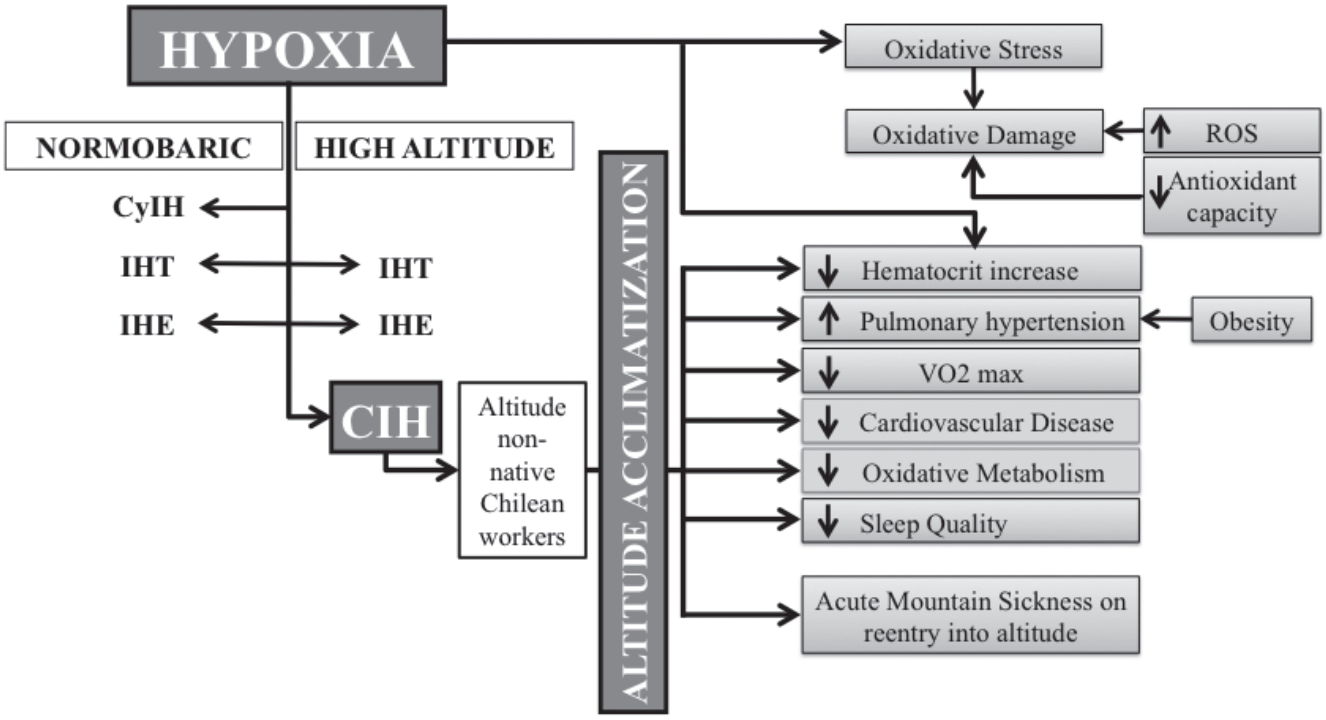

Figure 1. Physiological responses to hypoxia and effects of high altitude acclimatization. CyIH: Cyclic Intermittent Hypoxia. IHT: Intermittent Hypoxic Training. IHE: Intermittent Hypoxic Exposure. CIH: Chronic Intermittent Hypoxia. ROS: Reactive Oxygen Species. See text for details.

(maximum) power output, training at high altitude does not consistently result in increased exercise performance at sea level, with some evidence indicating benefits of training at high altitude on exercise performance at altitude (Vogt and Hoppeler, 2010). A great individual variability in responses has been observed and although some debate still exists in terms of the efficacy of the different models, combinations of them are being recently explored to improve results (see Millet *et al*., 2010 for review). From a research standpoint this experience has served to learn more about how hematological, aerobic and muscle responses are modulated by intermittent hypoxia (de Paula and Niebauer, 2012).

Other forms of intermittent exposure to hypoxia occur in several diseases such as chronic obstructive pulmonary disease, congestive heart failure, obesity-hypoventilation syndrome and obstructive sleep apnea, where hypoxia and normoxia occur at the same barometric pressure. This intermittent isobaric hypoxia is called recurrent or cyclic intermittent hypoxia (CyIH) (Gilmartin *et al*., 2008). The study of the relationships between CyIH and cardiovascular disease has seen significant progress; however the physiological mechanisms linking them remain unknown. Both animal (Fletcher *et al*., 1992; Brooks *et al*., 1997) and human (Peppard *et al*., 2002) models showed increases in arterial blood pressure after CIH exposure with enhanced chemosensitivity being invoked as a contributor to the CIH-induced increased blood pressure (Tamisier *et al*., 2009).

CIH exposure in no altitude native Chilean miners differs from the IHT/IHE and CyIH because it involves alternating between normobaric normoxia and hypobaric hypoxia. The CIH model has gathered interesting information about the characteristics of acclimatization to CIH, particularly in relation to the effects of hypoxia, but there is also evidence that hypobaria is playing a role. For example, studies showing different heart rate variability responses in normobaric hypoxia *versus* hypobaric hypoxia suggest that these two exposure conditions are clearly not equal stimuli to the cardiovascular and respiratory systems (Basualto-Alarcón *et al*., 2012).

The long term adjustments in CIH tend to resemble those in chronic hypoxia at the level of ventilatory and cardiovascular responses, red cell mass and cardiac β-adrenergic receptors, among others. Considering exposure to the same altitude however, there is a difference in the time needed to complete acclimatization. Whereas acclimatization to chronic hypoxia is achieved in few months, CIH acclimatization is achieved in years, with stabilization of biomedical variables being observed after 18 months of exposure (Richalet *et al*., 2002; Jimenez, 2003).

2.2. *Polycythemia and Pulmonary Hypertension*

Some of the body's first strategies when man or other animals not genetically adapted to high altitudes are subjected to hypoxia are expressed as metabolic, respiratory and cardiovascular adjustments. The increased production of red blood cells that improves oxygen transport capacity from the lungs to the tissues is one of them (Richalet, 1990). In the kidney, hypoxia stimulates the secretion of the hormone erythropoietin (after 2 to 3 hours of exposure to high altitude), which in turn stimulates the production of red blood cells by the bone marrow. This increase in erythropoiesis becomes the essential mechanism of long term acclimatization (Eckardt *et al*., 1989).

In a study performed in Chilean mine workers, Richalet *et al*., 2002 showed that hematocrit increased both at sea level and at high altitude after 12 and 19 months of CIH, and returned to pre-exposure values after 31 months of CIH exposure. The risk of polycythemia was lower than in chronic highlanders (Richalet *et al*., 2002). In another study of subjects exposed to CIH for 12 years or more to a 4 x 3 commuting system (4 days at altitude and 3 days at sea level) at 3,550 m altitude, hematocrit and hemoglobin reached lower values than for residents at altitude over 4,000 m (Brito *et al*., 2007).

According to the Venice Symposium Consensus, pulmonary hypertension (PH) is defined as a mean pulmonary artery pressure (PAP) > 25mm Hg in conjunction with right ventricle (RV) and right atrium (RA) enlargement (McLaughlin, 2004). PH is described as a marker of chronic exposure to high altitude-induced hypoxia; a direct relationship exists between PAP and the altitude reached (Peñaloza and Arias-Stella, 2007). The development of high-altitude PH is one of the main physiological changes observed in a poor response to hypoxia, and in people who permanently live at high altitudes the prevalence of PH increases from 5 to 10% (Leon-Velarde *et al*., 2005).

A 32-month prospective study performed in Chilean miners exposed to CIH in a 7 x 7 commuting system at 4,500 m a.s.l. showed that PAP increased in hypoxia, but further evidence of PH was not observed (Antezana *et al*., 2003). Moreover, values of PAP were lower than in subjects living permanently at high altitude (Richalet *et al*., 2002; Hultgren, 1997). Similar results were observed in a 24-month follow-up of workers exposed to CIH in a 28 x 28 commuting system at 3,700 m a.s.l. at Kumtor, Kyrgyzstan (Saryvaeb *et al*., 2003). However in subjects with more than 12 years of exposure to CIH, a 4% prevalence of PH was observed (Brito *et al*., 2007). Thus polycythemia and PH are some of the main chronic changes during exposure to chronic hypoxia and CIH at high altitude (Pasha and Newman, 2010; Leon-Velarde *et al*., 2010; Brito *et al*., 2007).

Obesity, defined as a body mass index above 30 kg/m^2, has been reported to be a risk factor for the development of PH at high altitude, and obesity-related hypoventilation has been reported to be the primary mediator of the increased risk for this disorder (Valencia *et al*., 2004).

2.3. *Physiological response to Exercise*

Exercise tests are often used to elucidate the effects of high altitude hypoxia on aerobic capacity. We used two different protocols of exercise to test the degree of acclimatization and the response to exercise during high altitude induced-CIH. The response to sub-maximal exercise (workload of 100 watts in a stationary bike) was used as a test of acclimatization. In mine workers exposed to CIH in a 7 x 7 commuting system at 4,500 m for a period of 2.5 years, blood pressure, heart rate and artery oxygen saturation during resting and during exercise were measured. CIH resulted in a useful degree of acclimatization that was maintained over a period of three years (Farías *et al*., 2006). Conversely, another group of workers exposed intermittently to high altitudes showed that the cardiovascular response to a sub-maximal exercise load does not change between the first and fourth day of shifts at high altitudes (Jalil *et al*., 1994). In order to test long term effects of CIH exposure

on exercise performance we used Aerobox sessions. Aerobox is a high-energy exercise regime that combines moves from a range of martial arts disciplines. Methodologically, the phases of a 45 min Aerobox training session are warm up, main phase (with the highest cardiovascular impact), localized phase (such as pushups and abdominal exercises) and recovery phase (this phase allows time for the blood vessels and the heart to resume their normal status).

Studies performed by Osorio in 2005 (unpublished) on 12 workers acclimatized to CIH performing Aerobox sessions at 4,000 m altitude indicated that the lowest level of oxygen saturation appears in the cardiovascular phase, with 83% SaO_2 (Table 1). Heart rate (HR) reached a higher level in the cardiovascular phase with 159 bpm. Considering that the heart rate at maximum exercise (HRmax) for this group is 172 bpm (Astrand, 1952; Fox *et al*., 1971; Richalet *et al*., 2002), HR during the cardiovascular phase reached 92%HRmax, a value considered adequate for training at maximum aerobic capacity (American College of Sports Medicine, 2000; Skinner *et al*., 2003). In the localized phase 59% HRmax was observed, indicating that the cardiac rhythm is within the physiological limits recommended for aerobic training (American College of Sports Medicine, 2000); Skinner *et al*., 2003). The high level of HR observed during exercise corresponds to a group trained and acclimatized to high altitudes.

Richalet *et al*., (2002) found that maximum oxygen consumption (VO_2max) decreased significantly with time of CIH exposure. Only part of this decrease can be attributed to the decrease in maximum heart rate induced by the downregulation of β-adrenergic and upregulation of muscarinic receptors (Richalet *et al*., 1992). A detraining effect of CIH exposure and/or sedentary living during the resting periods at sea level are probably also responsible for this effect (Richalet *et al*., 2002). A lack of physical activity during mining work could be another reason to explain the reduction in VO_2max.

2.4. Cardiovascular response

Andean mountain medicine has repeatedly shown that populations chronically exposed to altitude have low incidence of hypertension, atherosclerosis and myocardial infarction (Mortimer *et al*., 1977; Naeije, 2010). To what extent these characteristics depend on chronic hypoxia exposure, racial or nutritional factors has not yet been elucidated (Gamboa, 2003). Similarly, it has been recognized that long-term high-altitude hypoxia exposure protects the heart against ischemia / hypoxia injury, inducing a reduction of infarct size during acute ischemia. The relaxing effects of hypoxia on arterial smooth muscle cells may be proposed as contributors to this protection, as this vasodilatation tends to counteract polycythemia-induced blood viscosity (Hurtado, 1960).

Overall, the initial cardiovascular effects of altitude exposure involve an acute response associated with increased HR, blood pressure, cardiac output and myocardial contractility. Over time, during chronic hypoxia cardiac output decreases at levels lower than pre-exposure, accompanied by a decrease in sympathetic activity secondary to cardiac β-adrenergic receptor desensitization (Richalet, 1990).

Multiple mechanisms are involved in the cardioprotection induced by CIH. Hypobaric CIH preserves myocardial contractility and prevents apoptosis of cardiomyocytes (Beguin *et al*., 2007, Zhu *et al*., 2006, Dong et al., 2003, Zhang et al., 2004), increases coronary flow and myocardial capillary angiogenesis, activates ATP-sensitive K^+ channels and inhibits mitochondrial permeability transition pores (Zhong *et al*., 2002, Zhu *et al*., 2003). A rat model of CIH has also provided evidence that CIH attenuates β-adrenergic receptor activity by decreasing β-adrenergic receptor density and affinity in the right ventricle, and these alterations in the β-adrenergic receptor may contribute to cardiac protection in CIH (Guan *et al*., 2010).

In miners exposed to CIH for 31 months, blood pressure initially increased followed by a reduction, but remained slightly elevated compared to blood pressure measured at sea level; also a reduction in pulse and a slight dilation of the right ventricle were observed (Richalet *et al*., 2002; Farias *et al*., 2006). A study performed on Chilean soldiers exposed to CIH for more than 12 years revealed an increase in the amount of triglycerides and a reduction in LDL cholesterol (Brito *et al*., 2007).

Autonomic control in high altitude-exposed subjects has been studied using the non-invasive technique of power spectral analysis of HR (heart rate variability; HRV). Variables usually determined included power in the low (LF, 0.04-.0.15 Hz) and high (HF, 0.15-0.4 Hz) frequency ranges of the heart period spectrum, among others. Analyses showed an increase in the LH/HF ratio during acclimatization (Sevre *et al*., 2001). Since HF power is assumed to be a marker of parasympathetic activity and LF power to be a combination of both parasympathetic and sympathetic tonic activity, it has been concluded that the sympathetic tone is less reduced than the parasympathetic control of HR upon high-altitude exposure (Sevre *et al*., 2001; Cornolo *et al*., 2004).

2.5. Metabolic response and metabolic rate

High altitude-induced hypoxia alters the regulation of substrate metabolism favoring carbohydrate oxidation,

TABLE 1

Hemoglobin saturation (SaO_2, %) and heart rate (HR, bpm) values during Aerobox sessions at 4,000 m altitude in workers acclimatized to CIH.

		Aerobox Sessions (phases)			
	Resting	**Warming up**	**Main**	**Localized**	**Recovery**
SaO_2, %	90 ± 3	89 ± 2	83 ± 2	90 ± 6	92 ± 4
HR, bpm	83.5 ± 4.3	89.2 ± 5.6	159 ± 10	101 ± 9.6	90.6 ± 8.8

(mean ± SD, n=12)

as an adaptive mechanism to the limited ATP supply due to a diminished oxidative phosphorylation caused by the reduction in the available oxygen. Thus cells increase anaerobic glycolysis through positive regulation of the glycolytic enzymes and decrease the activity of some ATP consumers, e.g., Na^+-K^+ ATPase. Invariably acclimatization to high altitudes results in the increased use of blood sugar (Brooks *et al*., 1991). It has also been demonstrated that acclimatization to hypobaric hypoxia selectively reduces key enzymes responsible for lipid oxidation in heart, liver and skeletal muscle. Therefore, the greater dependency on blood sugar than on lipid metabolism probably contributes to the maintenance of homeostasis by optimizing the energy performance per unit of oxygen (Kennedy *et al*., 2001). We have studied the relationships between oxidative mitochondrial phosphorylation and oxygen consumption during chronic or intermittent hypobaric hypoxia exposure. Using a rat model of exposure to simulated conditions of continuous or intermittent high altitude (Farías *et al*. 2005a, Farías *et al*., 2005b) we observed a greater inhibition of oxygen consumption in spermatid cells in chronic versus intermittent hypobaric hypoxia (inhibition of 80% *vs*. 57%, respectively), in the presence of the mitochondrial H^+-ATPase inhibitor oligomycin. Similar oxygen consumption in both hypoxic treatments was observed after uncoupling of the oxidative phosphorylation, suggesting that continuous chronic hypobaric hypoxia is associated with an uncoupling of oxidative phosphorylation.

Basal metabolic rate (BMR) increases during the first days of exposure to high altitudes, apparently depending on the altitude reached. Increases of 6% and 10% have been found at altitudes of 3,650 and 3,800 m, respectively. As the days progress BMR decreases, but does not reach sea level values. For mountaineers who climb for 10 to 18 hours a day in high altitudes, the largest proportion of their energy comes from fats, and glycogen is only used for short and high-intensity exercises. However, after 18 days at the moderate altitude of 4,300 m, Young *et al.* (1982) found that the muscular glycogen at rest was lower than at sea level. Apparently, there are no data available about the deposits of muscular and hepatic glycogen at extreme altitudes, but with many more days of intensive work and adequate caloric consumption, it would not be surprising to find this reduced in liver and muscle (Young *et al.*, 1982). These findings suggest that in humans from sea level chronically exposed to high altitudes, fat is the principal fuel for exercise and the re-synthesis of the muscular glycogen can be reduced. It is not clear whether this is an effect of altitude or lower food consumption during hypoxia exposure. An elevated metabolism in rats (Rennie *et al.*, 1977) and humans (Costill *et al.*, 1977) has also been observed, indicating a saving of muscular glycogen, probably through the inhibition of the enzymes phosphofructokinase and pyruvate dehydrogenase.

2.6. Sleep quality

Travel to altitude is associated with a reduction in sleep quality (Anholm *et al*., 1992). These symptoms can be relieved with descent, simulated descent in a hyperbaric chamber or by enhancing room air with oxygen (West, 2002). In addition, travel to altitude results in a temporary reduction of rapid eye movement (REM) sleep that appears to improve with acclimatization (Anholm *et al*., 1992; Przybylowski *et al*., 2003). In the study performed by Richalet *et al*., (2002) with Chilean miners, sleep quality was altered during the first two nights at high altitude (worse on the second night) and did not ameliorate with time of exposure. In workers acclimatized to CIH a poorer sleep quality at 3,800 m than at sea level was observed. In this study some of the changes observed between sea level and altitude were: greater number of arousals (10.4 *vs.* 28.7), higher apneas/hypopneas index (5.8 *vs.* 10.1), and greater oxygen desaturation and periodic breathing (zero *vs.* 9.8) (Vargas *et al*., 2002). Supplemental oxygen partially reduced these differences between sea level and high altitude.

There is great concern regarding exposure to altitude of obstructive sleep apnea (OSA) syndrome carriers, since their cyclical reduction in $\%SaO_2$ during sleep is exacerbated by environmental hypobaric hypoxia. $\%SaO_2$ is low during sleep in altitude, and whereas the development of AMS has been shown to be partially associated with low mean $\%SaO_2$ in sleep (Burgess *et al*., 2004), positive airway pressure has been shown to prevent the occurrence of AMS (Johnson *et al*., 2010). Thus it is considered that untreated obstructive sleep apnea is a condition incompatible with altitude. In turn, the effects observed, including excessive daytime sleepiness and impaired daytime function, can affect job performance.

In terms of the respiratory mechanisms contributing to AMS, it has been long recognized that the ventilatory response is reduced in people susceptible to AMS (Hackett et al., 1982). Recently, in a group of people exposed to experimental hypoxia (FIO_2 = 80% SaO_2), the acute hypoxic ventilatory response at 5 min (HVR5min) was greater in individuals not susceptible to AMS compared to susceptible individuals (Nespoulet *et al*., 2012). These results support the hypothesis of low chemoreceptor sensitivity as a marker of AMS predisposition (Moore *et al*., 1986), suggesting high chemo sensitivity as a protective factor for AMS.

2.7. Oxidative stress

Reactive oxygen species (ROS) are produced by diverse cellular processes and are considered to have beneficial and harmful effects. Moderate concentrations of ROS mediate their beneficial effects such as cellular defense against infections, control of vascular tone, ventilation and erythropoietin production, the induction of mitogenic responses and modulation of several transduction signaling pathways. Overproduction of ROS leads to their harmful effects due to oxidative stress (for reviews see Dröge, 2002 and Valko *et al*., 2007).

Several reports indicate that exposure to high altitude hypobaric hypoxia causes oxidative cellular damage. This cellular oxidative stress appears directly related to the altitude level and an increased production of ROS seems to be responsible for these effects (Dosek *et al*., 2007). Concomitantly, oxygen enrichment of room air is increasingly being used in work stations at high altitude (West, 2002, 2003) and since the production of ROS is favored at higher oxygen supply (Dosek *et al*., 2007; González *et al*., 2002), oxidative stress may be an even more important factor in high altitude exposed workers.

The main cause of oxidative stress is the lower availability of O_2 to be reduced to H_2O by the enzyme cytochrome oxidase in the mitochondrial respiratory chain. This produces an accumulation of electrons that in the absence of sufficient oxygen as final acceptor will form superoxide anion (O_2^-) which in turn produces hydrogen peroxide (H_2O_2) and the

hydroxyl radical (OH^-) after reacting with water (Maiti *et al.*, 2006). The accumulation of these reduced equivalents formed principally in complexes I and III of the electron transport chain is known as "reductive stress" and can favor self-oxidation of one or more mitochondrial complexes, such as the redox pair ubiquinone–biquinol, as well as increasing the $NADH/NAD^+$ ratio (Dosek *et al.*, 2007). The accumulation of free radicals of coenzyme Q, called ubisemiquinone, causes the transfer of its unpaired electron to oxygen, generating the superoxide radical anion ($\cdot O_2^-$). Although ($\cdot O_2^-$) by itself is not particularly harmful, it is a precursor of the highly reactive hydroxyl radical (OH^-) and, through irreversible condensation with nitric acid, forms peroxynitrite (ONOO) (Manukhina *et al*., 2006). Oxidative damage may also be produced by reductions in the antioxidant capacity, and it has been established that during hypoxia the cellular systems of redox defense are affected. Antioxidant enzyme activities such as superoxide dismutase (SOD), glutathione reductase (GSR) and glutathione peroxidase (GPX) are reduced (Maiti *et al.*, 2006). Other molecular events that also favor oxidative stress induced by hypobaric hypoxia are the xanthine dehydrogenase/oxidase system and the inducible isoform of nitric acid synthase (iNOS). The former has been described as a strong ROS generator in high altitude conditions, as hypoxic cells generate greater amounts of ATP and cAMP by the action of adenylyl kinase from two ADP. iNOS is up-regulated during acclimatization, thus altering the balance of ROS/NO, which recovers as time elapses (Dosek *et al*., 2007). The alteration in this balance may be related to the microcirculatory changes caused by hypobaric hypoxia expressed in AMS and cerebral and pulmonary edemas (Dosek *et al.*, 2007). Finally, other factors that contribute to the development of oxidative stress are exercise, UV radiation (which penetrates the epidermis with greater aggressiveness in high-altitude zones), lack of antioxidant supplements in the diet and the oxidation of catecholamines (adrenaline, noradrenaline and dopamine), which increases with altitude (Askew, 2002). The high reactivity and oxidant properties characteristic of ROS and free radicals result in overall damage that affects main cell components including carbohydrates, proteins, lipids and even DNA (Blokhina *et al.*, 2003).

Little is known about the level of real oxidative damage suffered by cell structures of the organs and tissues exposed to a situation of high altitude. Moller *et al*., (2001) exposed 12 healthy individuals to an altitude of 4,559 m, which caused a significant increase in the rupture of the DNA chain measured in the urine. The damage was prominent in endonuclease-III sites. Also, when a group of humans were exposed simultaneously to an altitude of 2,700 m and cold conditions, the peroxide lipid levels and the DNA damaged chain in the urine increased up to 23% at 6,000 m and up to 79% at 8,848 m, indicating that the oxidative stress increases with escalating altitude (Joanny *et al*., 2001). Thus, studies performed on humans consistently describe that high altitude hypoxia causes oxidative damage to lipids, proteins, and DNA chains. This damage may be due to the increase in the production of ROS and/or to the reduced antioxidant capacity. Given their high content in unsaturated fatty acids, cell membranes constitute a main target of ROS, with lipoperoxidation being usually observed upon exposure to hypoxia (Behn *et al*., 2007). In animal models, CIH (12 hrs per day, simulated 4,000 m altitude for 6 months) increases lipoperoxidation and carbonyl derivatives in skeletal muscle (Radak *et al*., 1994, 1997). However, short exposure for 5 days to 7,576 m elevation causes an increase in lipoperoxidation in plasma in rats (Kumar *et al*., 1999). Maiti *et al*. (2006) also reported that exposure of 3 and 7 days to 6,100 m significantly increases ROS levels and lipoperoxidation in various brain regions. It appears that the effects of oxidative stress are systemic, as suggested by Nakanishi *et al*. (1995), who reported that exposure to 5,000 m resulted in increased serum levels of malonydialdehyde in lungs, liver, heart and kidneys in rats, whereas exposition to a simulated altitude of 9,000 m causes increases in lipid peroxidation of selected rat brain membranes (Rauchová *et al*., 2012).

As previously stated, exposure to high altitudes reduces activity and expression levels of antioxidant enzymes; consequently the disruption in the efficiency of the antioxidant systems due to the increase in ROS production by hypobaric hypoxia leads to oxidative damage of macromolecules (Dosek *et al*., 2007). A reduction in the activity of superoxide dismutase (SOD) content in skeletal muscle has been reported in rats exposed to intermittent hypobaric hypoxia (Radak *et al*., 1994). Reduction in the activity of glutathione peroxidase (GPX) has also been shown in the liver of rats exposed to high altitude (Nakanishi *et al*., 1995), whereas Imai *et al*. (1995) compared GPX activity of high altitude residents (4,000 m) to individuals from sea level, finding that high-altitude dwellers had lower levels of GPX activity. Nevertheless, it has been observed that catalase (CAT), SOD and also the heat shock proteins lead to the stabilization of cell membranes and restriction of apoptosis, alleviating the oxidative effect when subjected to hypobaric hypoxia (Manukhina *et al*., 2006). Rat myocardia cells, for example, presented high levels of SOD and CAT after CIH exposure to 3,500 m (Ning *et al*., 2000). Additionally, our studies of expression and activity of glutathione reductase (GR) in CIH found no differences in GR expression, but lower activity in testes and epididymis in CIH exposed rats (Farias *et al*. 2010). However, we observed that melatonin decreased lipid peroxidation in heart, kidneys and lung under CIH conditions, but melatonin did not exhibit any protective effect in liver, testis, epididymis sperm count (Farias *et al*., 2012). It is generally accepted that testicular and seminal ROS levels are important in terms of the deleterious effects of hypoxia on male fertility (Reyes *et al*., 2012).

In view of the pathological roles played by increased ROS generation, the supplementation of antioxidants seems a good detoxification strategy to improve tissue function under hypobaric hypoxia. In our rat model we observed that exogenous administration of ascorbic acid and blueberry extract restored GR activity, reduced lipoperoxidation and hypospermatogenesis typical of hypobaric hypoxic exposure (Farias *et al*., 2010; Zepeda *et al*., 2012). However, the clinical translation of antioxidant therapies has proven difficult, as few benefits and even harmful effects (Dotan *et al*., 2009) have been observed in clinical trials aimed to reduce oxidative stress by antioxidant supplementation (Armitage *et al*., 2009; Villanueva and Kross, 2012).

3. FINAL CONSIDERATIONS

Exposure to chronic and intermittent hypobaric hypoxia is a biomedical condition unique in the world and represents a great challenge for miners such as Chilean mine workers.

Studies leading to the elaboration of strategies to prevent and revert the negative physiological effects brought about by exposure to high altitudes are highly desirable. Specifically, urgent new challenges for the future are: a) Acute Mountain Sickness on the first day of the re-ascent after 3-7 days of rest; this condition affects people with signs of good acclimatization, oxygen saturation, without polycythemia or hypertension, despite years of exposure to CIH, b) Prevention or control of disturbance of quality of sleep, periodic breathing, oxygen desaturation, sleep fragmentation and /or total sleep, c) Causes of polycythemia in CIH, d) Biological parameters that define a suitable physiological intermittent hypoxia acclimatization to altitudes between 3,000 and 5,500 m, e) Long-term monitoring of pulmonary artery pressure, f) Aging biomarkers of CIH, g) Hypoxia tolerance test to identify, at sea level, before the climb, the good responders to hypoxia and susceptibility to severe AMS, and h) Best strategies to mitigate the effects of CIH, based on nutrients, sleep hygiene, supplemental oxygenation, commuting patterns, ergonomic jobs adjustments, etc. The determination of markers that can identify in advance the good and bad responders to this environmental condition (Richalet *et al*., 2012; Burtscher *et al*., 2008), as well as markers of health condition of workers chronically exposed will greatly contribute to the health of miners who have to work intermittently under different shift schemes at work sites over 4,000 m altitude. in the Andes mountain range.

ACKNOWLEDGEMENTS

The authors are sincerely thankful for the support provided by DIUFRO grant DI12-2007 and CONICYT PhD Fellowship Program.

REFERENCES

AMERICAN COLLEGE OF SPORTS MEDICINE (2000) ACSM's guidelines for exercise testing and prescription. 6:145.

ANHOLM JD, POWLES AC, DOWNEY R, 3RD, HOUSTON CS, SUTTON JR, BONNET MH, et al. (1992) Operation Everest II: arterial oxygen saturation and sleep at extreme simulated altitude. Am Rev Respir Dis 145(4 Pt 1):817-826.

ANTEZANA AM (2003) Cardiovascular changes in chronic intermittent hypoxia. In Health & Height, Viscor G, Ricart A, Leal C, edit Publicacions Universitat Barcelona, pp151-155

ASKEW E (2002) Work at high altitude and oxidative stress: antioxidants nutrients. Toxicology 180(2):107-119.

ARANEDA O, GARCÍA C, LAGOS N, QUIROGA G, CAJIGAL J, SALAZAR MP, BEHN C (2005) Lung oxidative stress as related to exercise and altitude. Lipid peroxidation evidence in exhaled breath condensate: a possible predictor of acute mountain sickness Eur J Appl Physiol. 95:383-390.

ARMITAGE ME, WINGLER K, SCHMIDT HH, LA M.(2009) Translating the oxidative stress hypothesis into the clinic: NOX versus NOS. J Mol Med (Berl). 87(11):1071-1076.

BASUALTO-ALARCÓN C, RODAS G, GALILEA P, RIERA J, PAGÉS T, RICARTE A, TORRELLA J, BEHN C, VISCOR G (2012) Cardiorespiratory parameters during submaximal exercise under acute exposure to normobaric and hypobaric hypoxia. Apunts Med Esport. 47(174):65-72

BEGUIN PC, BELAIDI E, GODIN-RIBUOT D, LEVY P, RIBUOT C (2007) Intermittent hypoxia-induced delayed cardioprotection is mediated by PKC and triggered by p38 MAP kinase and Erk1/2. J Mol Cell Cardiol 42: 343-351.

BEHN C, ARANEDA OF, LLANOS AJ, CELEDÓN G, GONZÁLEZ G (2007) Hypoxia-related lipid peroxidation: evidences, implications and approaches. Respir Physiol Neurobiol 158:143-150.

BLOKHINA O, VIROLAINEN E, FAGERSTEDT K (2003) Antioxidants, oxidative damage and oxygen deprivation stress: a review. Ann Bot 91(2):179-194.

BRITO J, SIQUES P, LEÓN-VELARDE F, DE LA CRUZ JJ, LOPEZ V, HERRUZO R (2007) Chronic intermittent hypoxia at high altitude exposure for over 12 years: assessment of hematological cardiovascular, and renal effects. High Alt Med Biol 8(3):236-244.

BROOKS D, HORNER RL, KOZAR LF, RENDER-TEIXEIRA CL, PHILLIPSON EA (1997) Obstructive sleep apnea as a cause of systemic hypertension. Evidence from a canine model. J Clin Invest 99:106-*109*.

BUSTOS-OBREGÓN E, RIVEROS J, MAURER I (2005) Función espermática post-hipoxia simulada en ratón. Cienc Trab 7(16):56-60.

BROOKS GA, BUTTERFIELD GE, WOLFE RR, GROVES BM, MAZZEO RS, SUTTON JR, WOLFEL EE, REEVES JT (1991) Increased dependence on blood glucose after acclimatization to 4,300 m. J Appl Physiol 70:919-927.

BURTSCHER M, SZUBSKI C, FAULHABER M (2008) Prediction of the susceptibility to AMS in simulated altitude. Sleep Breath. 12(2):103-108.

CASANEGRA P, JALIL J, BRAUN S, CHAMORRO G, RODRÍGUEZ R, ILIC JP, MORALES M, LISBOA C, SALDIAS F, BEROIZA T (1993) Periodic physical work at high altitude mining: long term evaluation of exercise responses under one specific working cycle. In: Hypoxia and Molecular Medicine. Sutton J, Houston C, Coates G, editors. Queen City Printers Inc. Vermont, USA, pp 296.

CHAMORRO G, BRAUN S, JALIL J, ILIC JP, BEROIZA T, CASANEGRA P, RODRÍGUEZ R (1993) High altitude mining: influence of working cycle on changes in pulmonary pressure. In: Hypoxia and Molecular Medicine. Sutton J, Houston C, Coates G, eds. Queen City Printers Inc. Vermont, USA, pp 296.

COSTILL DL, COYLE E, DALSKY G, EVANS W, FINK W, HOOPES D (1977) Effects of elevated plasma FFA and insulin on muscle glycogen usage during exercise. J Appl Physiol 43:695-699.

CORNOLO J, MOLLARD P, BRUGNIAUX JV, ROBACH P, RICHALET JP (2004) Autonomic control of the cardiovascular system during acclimatization to high altitude: effects of sildenafil. J Appl Physiol 97: 935-940.

DE PAULA P, NIEBAUER J (2012) Effects of high altitude training on exercise capacity: fact or myth. Sleep Breath 16(1):233-239.

DONG JW, ZHU HF, ZHU WZ, DING HL, MA TM, ZHOU ZN (2003) Intermittent hypoxia attenuates ischemia/reperfusion induced apoptosis in cardiac myocytes. Cell Res 13:385-391.

DOSEK A, OHNOB H, ACSA Z, TAYLOR A, RADAK Z (2007) High altitude and oxidative stress Respir Physiol Neurobiol 158:128-131.

DOTAN Y, PINCHUK I, LICHTENBERG D, LESHNO M (2009) Decision analysis supports the paradigm that indiscriminate supplementation of vitamin E does more harm than good. Arterioscler Thromb Vasc Biol 29:1304-1309.

ECKARDT KU, BOUTELLIER U, KURTZ A, SCHOPEN M, KOLLER EA, BAUER W (1989) Rate of erythropoietin in humans in response to acute hypobaric hypoxia. J Appl Physiol. 6(4):1785-1788.

FARÍAS JG, BUSTOS-OBREGON E, ORELLANA R, BUCAREY, JL, QUIROZ E, REYES JG (2005a) Effects of chronic hypobaric hypoxia on testis histology and round spermatid oxidative metabolism. Andrologia 37:47-52.

FARÍAS JG, BUSTOS-OBREGÓN R, REYES J (2005b). Increase in testicular tTemperature and vascularization induced by hypobaric hypoxia in rats. J Androl 26(6):693-697.

FARÍAS JG, OSORIO J, SOTO G, BRITO J, SIQUÉS P, REYES J (2006). Sustained acclimatization in Chilean mine workers subjected to chronic intermittent hypoxia. High Alt Med Biol 7(4):302-306.

FARÍAS JG, PUEBLA M, ACEVEDO A, TAPIA P, GUTIERREZ E, ZEPEDA A, CALAF G, JUANTOK C, REYES, J (2010) Oxidative stress in testis and epididymis under intermittent hypobaric hypoxia in rats: protective role of antioxidant supplementation. J Androl 31(3):314-321.

FARÍAS JG, ZEPEDA AB, CALAF G (2012) Melatonin protects the heart, lungs and kidneys from oxidative stress under intermittent hypobaric hypoxia in rats. Biol Res 45:81-85.

FLETCHER EC, LESSKE J, QIAN W, MILLER CC, 3RD, UNGER T *(1992) Repetitive, episodic hypoxia causes diurnal elevation of blood pressure in rats*. Hypertension 19:555-*561*.

FORGEY WW (2006). High-altitude illness. In: Wilderness Medical Society: Practice Guidelines for Wilderness Emergency Care. W. W. Forgey, ed. Guilford, New York; pp. 46-53.

FULCO CS, ROCK PB, AND CYMERMAN (2000) Improving athletic performance: is altitude residence or altitude training helpful? Aviat Space Environ Med 71:162-171.

GAMBOA R (2003) Circulación Sistémica. in "El Resto Fisiológico de vivir en los Andes". Monge C, León-Velarde F, Eds. IFEA UPCH. Lima. Peru. 2003. pp. 119-132.

GILMARTIN GS, TAMISIER R, CURLEY M, WEISS JW (2008) Ventilatory, hemodynamic, sympathetic nervous system, and vascular reactivity changes after recurrent nocturnal sustained hypoxia in humans. Am J Physiol Heart Circ Physiol 295(2):H778-H785.

GONZÁLEZ C, SANZ-ALFAYATE G, AGAPITO T, GÓMEZ-NIÑO A, ROCHER A AND OBESO A (2002) Significance of ROS in oxygen sensing in cell systems with sensitivity to physiological hypoxia. Respir Physiol Neurobiol. 132(1):17-41.

GUAN Y, GAO L, MA H, LI Q, ZHANG H, YUAN F, ZHOU Z, ZHANG Y (2010) Chronic intermittent hypobaric hypoxia decreases-adrenoceptor activity in right ventricular papillary muscle. Am J Physiol Heart Circ Physiol. 298:H1267-H1272.

HACKETT PH, RENNIE D, HOFMEISTER SE, GROVER RF, GROVER EB, REEVES JT (1982) Fluid retention and relative hypoventilation in acute mountain sickness. Respiration 43(5):321-9.

HACKETT PH, RENNIE ID, LEVINE HD (1976) The incidence, importance, and prophylaxis of acute mountain sickness. Lancet 2(7996):1149-1154.

HULTGREN H (1997) High Altitude Medicine. H.N. Hultgren pub., San Francisco, USA, pp. 68–69.

HURTADO A (1960) Some clinical aspects of life at high altitudes. Ann Intern Med. 53:247-258.

IMAI H, KASHIWAZAKI H, SUZUKI T, KABUTO M, HIMENO S, WATANABE C, MOJI K, KIM SW, RIVERA JO, TAKEMOTO T (1995) Selenium levels and glutathione peroxidase activities in blood in an andean high-altitude population. J Nutr Sci Vitaminol (Tokyo) 41:349-361.

JALIL J, BRAUN S, CHAMORRO G, CASANEGRA P, SALDÍAS F, BEROÍZA T, FORADORI A, RODRÍGUEZ R, MORALES M (1994) Cardiovascular response to exercise at high altitude in workers chronically exposed to intermittent hypobaric hypoxia. Rev Med Chil. 122(10):1120-1125.

JIMÉNEZ D (1995) High altitude intermittent chronic exposure to hypoxia. In Hypoxia and the Brain. Sutton JR, Houston CS, Coates G, eds. Burlington, Vt, USA. p. 284-291.

JIMÉNEZ D (2003) Mountain medicine for sustainable high altitude mining. In: Health Environment and Sustainable Development, Copper 2003. Lagos G, Warner A, Sanchez M, eds. MetSoc, Quebec, Canada. Vol 2:459-468.

JOANNY P, STEINBERG J, ROBACH P, RICHALET JP, GORTAN C, GARDETTE B, JAMMES Y (2001). Operation Everest III (Comex'97): the effect of simulated sever hypobaric hypoxia on lipid peroxidation and antioxidant defence systems in human blood at rest and after maximal exercise. Resuscitation 49:307-314.

KENNEDY SL, STANLEY WC, PANCHAL AR, MAZZEO RS (2001) Alterations in enzymes involved in fat metabolism after acute and chronic altitude exposure. J Appl Physiol 90:17-22.

KUMAR D, BANSAL A, THOMAS P, SAIRAM M, SHARMA S, MONGIA S, SINGH S, SELVAMURTHY S (1999). Biochemical and immunological changes on oral glutamate feeding in male albino rats. Int J Biometeorol. 42:201-204.

LEÓN-VELARDE F, MAGGIORINI M, REEVES JT, ALDASHEV A, ASMUS I, BERNARDI L, GE RL, HACKETT P, KOBAYASHI T, MOORE LG, PENALOZA D, RICHALET JP, ROACH R, WU T, VARGAS E, ZUBIETA-CASTILLO G AND ZUBIETA-CALLEJA G (2005) Consensus statement on chronic and subacute high altitude diseases. High Alt Med Biol. 6(2):147-1157

LEÓN-VELARDE F, VILLAFUERTE FC, RICHALET JP (2010) Chronic mountain sickness and the heart. Prog Cardiovasc Dis. 52(6):540-9.

MAITI P, SINGH S, SHARMA A, MUTHURAJU S, BANERJEE P AND ILAVAZHAGAN G (2006) Hypobaric hypoxia induces oxidative stress in rat brain. Neurochem Int. 49(8):709–716.

MCLAUGHLIN VV, RICH S (2004) Pulmonary hypertension. Curr Probl Cardiol. 29(10):575-634.

MEERSON FZ, MALYSHEV IYU, ZAMOTINSKY AV (1992). Differences in adaptive stabilization of structures in response to stress and hypoxia relate with the accumulation of hsp70 isoforms. Mol Cell Biochem. 111: 87-95.

MILLET GP, ROELS B, SCHMITT L, WOORONS X, RICHALET JP (2010) Combining hypoxic methods for peak performance. Sports Med. 40(1):1-25.

MOLLER P, LOFT S, LUNDBY C, OLSEN N (2001) Acute hypoxia and hypoxic exercise induce DNA strand breaks and oxidative DNA damage in humans. FASEB J. 15(7):1181-1186.

MOORE LG, HARRISON GL, MCCULLOUGH RE, MCCULLOUGH RG, MICCO AJ, TUCKER A, WEIL JV, REEVES JT (1986) Low acute hypoxic ventilatory response and hypoxic depression in acute altitude sickness. J Appl Physiol. 60(4):1407-12.

MORTIMER EA JR, MONSON RR, MACMAHON B (1977) Reduction in mortality from coronary heart disease in men residing at high altitude. N Engl J Med. 296(11):581-5.

NAEIJE R (2010) Physiological adaptations of the cardiovascular system to high altitude. Prog Cardiovasc Dis. 52:456-466.

NAKANISHI K, TAJIMA F, NAKAMURA A, YAGURA S, OOKAWARA T, YAMASHITA H, SUZUKI K, TANIGUCHI N, OHNO H (1995) Antioxidant system in hypobaric-hypoxia in rats. J Physiol. 489:869-876.

NESPOULET H, WUYAM B, TAMISIER R, SAUNIER C, MONNERET D, REMY J, CHABRE O, PÉPIN JL, LÉVY P (2012) Altitude illness is related to low hypoxic chemoresponse and low oxygenation during sleep. Eur Respir J. 40(3):673-80.

NING Z, YI Z, QI-ZHI F, ZHAO-NIAN Z (2000) Intermittent hypoxia exposure-induced heat-shock protein 70 expression increases resistance of rat heart to ischemic injury. Acta Pharmacol Sin. 21(5):467-472.

PASHA MA AND NEWMAN JH (2010). High-altitude disorders: pulmonary hypertension: pulmonary vascular disease: the global perspective. Chest 137(6 Suppl):13S-19S.

PEÑALOZA D AND ARIAS-STELLA J (2007) The heart and pulmonary circulation at high altitudes. Healthy highlanders and Chronic Mountain Sickness. Circulation 115:1132-1146.

PEPPARD PE, YOUNG T, PALTA M, SKATRUD J *(2002) Prospective study of the association between sleep-disordered breathing and hypertension.* N Engl J Med 342:1378-*1384.*

PRABHAKAR NR (2000) Oxygen sensing in the carotid body chemoreceptors. J Appl Physiol 88: 2287–2295.

PRZYBYLOWSKI T, ASHIRBAEV A, LE ROUX J, ZIELIŃSKI J (2003) Sleep and breathing at altitude of 3800 m-the acclimatization effect. Pneumonol Alergol Pol 71(5-6):213-220.

RADAK Z, LEE K, CHOI W, SUNOO S, KIZAKI T, OH-ISHI S, SUZUKI K, TANIGUCHI N, OHNO H, ASANO K (1994). Oxidative stress induced by intermittent exposure at a simulated altitude of 4000m decreases mitochondrial superoxide dismutase content in soleus muscle of rats. Eur J Appl Physiol Occup Physiol 69:392-395.

RADAK Z, ASANO K, LEE KC, OHNO H, NAKAMURA A, NAKAMOTO H, GOTO S (1997) High altitude training increases reactive carbonyl derivatives but not lipid peroxidation in skeletal muscle of rats. Free Radic Biol Med 22:1109-1114.

RAUCHOVÁ M, VOKURKOVÁ J, KOUDELOVÁ J (2012) Hypoxia-induced lipid peroxidation in the brain during postnatal ontogenesis. Physiol Res. 61 (Suppl. 1): S89-S101.

RENNIE JJ AND HOLLOSZY JO (1977) Inhibition of glucose uptake and glycogenolysis by availability of oleate in well oxygenated perfused skeletal muscle. Biochem J 168:161-170.

REYES JG, FARÍAS JG, HENRIQUEZ-OLAVARRIETA S, MADRID E, PARRAGA M, ZEPEDA AB, MORENO RD (2012) The hypoxic testicle: physiology and pathophysiology. Oxid Med Cell Longev, vol. 2012, Article ID 929285, 15 pages. doi:10.1155/2012/929285

RICHALET JP (1990) The heart and adrenergic system in hypoxia. In: Hypoxia: The Adaptations. Edited by J.R. Sutton, G. Coates, and J.E. Remmers. Toronto, Philadelphia: B.C. Decker Inc., p. 13-21

RICHALET JP, KACIMI R, ANTEZANA AM (1992) The control of chronotropic function in hypobaric hypoxia. Int J Sports Med 13:S22–S24.

RICHALET JP, LARMIGNAT P, POITRINE E, LETOURNEL M, CANOUÏ-POITRINE F (2012) Physiological risk factors for severe high-altitude illness: a prospective cohort study. Am J Respir Crit Care Med 185(2):192-198.

RICHALET JP, VARGAS M, JIMÉNEZ D, ANTEZANA AM, HUDSON C, CORTÉS G, OSORIO J, LEÓN G (2002) Chilean miners commuting from sea level to 4500 m: A prospective study. High Alt Med Biol 3:159–166.

SARYBAEV A, PALASIEWICZ G, USUPBAEVA D, PLYWACZEWSKI R, MARIPOV A, SYDYKOV A, MIRRAKHIMOV M, LE ROUX H, KADYROV T, ZIELINSKI J (2003) Effects of intermittent exposure to high altitude on pulmonary hemodynamics: a prospective study. High Alt Med Biol 4 (4):455-463.

SEVRE K, BENDZ B, HANKO E, NAKSTAD AR, HAUGE A, KÅSIN JI, LEFRANDT JD, SMIT AJ, EIDE I, ROSTRUP M (2001) Reduced autonomic activity during stepwise exposure to high altitude. Acta Physiol Scand 173(4):409-17.

SCHOFIELD C. AND RATCLIFFE P (2004) Oxygen sensing by HIF hidrolases. Nat Rev Mol Cell Biol. 5: 343-354.

SKINNER JS, GASKILL SE, RANKINEN T, LEÓN AS, RAO DC, WILMORE JH, BOUCHARD C (2003) Heart rate versus %VO_2max: age, sex, race, initial fitness, and training response-HERITAGE. Med Sci Sports Exerc. 35(11):1908-1913.

TAMISIER R, GILMARTIN G, LAUNOIS S, PÉPIN J, NESPOULET H, THOMAS R, LÉVY P, AND WEISS J (2009) A new model of chronic intermittent hypoxia in humans: effect on ventilation, sleep, and blood pressure. J Appl Physiol. 107(1):17-24.

VARGAS E. VILLENA M (1989) La vie humaine en haute altitude: mythes et realités. Bull Soc Pathol Exot Filiales 82(5):701-19.

VALENCIA-FLORES M, REBOLLAR V, SANTIAGO V, OREA A, RODRÍGUEZ C, RESENDIZ M (2004). Prevalence of pulmonary hypertension and its association with respiratory disturbances in obese patients living at moderately high altitude. Int J Obes Relat Metab Disord 28:1174- 1180.

VALKO M, LEIBFRITZ D, MONCOL J, CRONIN MT, MAZUR M, TELSER J (2007) Free radicals and antioxidants in normal physiological functions and human disease. Int J Biochem Cell Biol. 39(1):44-84.

VEARRIER D AND GREENBERG MI (2011) Occupational health of miners at altitude: adverse health effects, toxic exposures, pre-placement screening, acclimatization, and worker surveillance. Clin Toxicol (Phila) 49(7):629-640.

VILLANUEVA C, KROSS RD (2012) Antioxidant-induced stress. Int J Mol Sci. 13:2091-2109.

VOGT M, HOPPELER H (2010) Is hypoxia training good for muscles and exercise performance?. Prog Cardiovasc Dis 52(6):525-33.

VARGAS M, LASSO J, RIVEROS A, HUDSON C, JIMÉNEZ D (2002) Polysomnography in acclimatized workers to intermittent hypoxia, comparison of sea level, altitude 3,800 m and oxygen supplementary effect. High Alt Med Biol 3(1):97-137

WEST JB (2002) Commuting to high altitude: value of oxygen enrichment of room air. High Alt Med Biol 2:223-235.

WEST JB (2003) Improving oxygenation at high altitude: acclimatization and O_2 enrichment. High Alt Med Biol 4:389-398.

WEST JB, SCHOENE R, MILLEDGE J (2007) High Altitude Medicine and Physiology. Hodder Arnold. pag 39,40.

WILBER RL (2007) Application of altitude/hypoxic training by elite athletes. Med Sci Sports Exerc. 39 (9):1610-1624.

YOUNG A J, EVANS WJ, CYMERMAN A, PANDOLF KB, KNAPIK JJ, MAHER JT (1982) Sparing effect of chronic high altitude exposure on muscle glycogen utilization during exercise. J Appl Physiol 52:857-862.

ZEPEDA A, AGUAYO LG, FUENTEALBA J, et al (2012) Blueberry extracts protect testis from hypobaric hypoxia induced oxidative stress in rats. Oxid Med Cell Longev (2012) Article ID 975870, 7 pages, doi:10.1155/2012/975870

ZHANG Y, ZHONG N, GIA J, ZHOU Z (2004) Effects of chronic intermittent hypoxia on the hemodynamics of systemic circulation in rats. Jpn J Physiol 54:171-174.

ZHONG N, ZHANG Y, ZHU HF, WANG JC, FANG QZ, ZHOU ZN (2002) Myocardial capillary angiogenesis and coronary flow in ischemia tolerance rat by adaptation to intermittent high altitude hypoxia. Acta Pharmacol Sin 23:305-310.

ZHU HF, DONG JW, ZHU WZ, DING HL, ZHOU ZN (2003) ATP-dependent potassium channels involved in the cardiac protection induced by intermittent hypoxia against ischemia/reperfusion injury. Life Sci 73:1275-1287.

ZHU WZ, XIE Y, CHEN L, YANG HT, ZHOU ZN (2006) Intermittent high altitude hypoxia inhibits opening of mitochondrial permeability transition pores against reperfusion injury. J Mol Cell Cardiol 40:96-106.

Biol Res 46: 69-74, 2013

Quantitative analysis of nucleolar chromatin distribution in the complex convoluted nucleoli of *Didinium nasutum* (Ciliophora)

Olga G. Leonova[1], Bella P. Karajan[2], Yuri F. Ivlev[3], Julia L. Ivanova[1], Sergei O. Skarlato[2] and Vladimir I. Popenko[1*]

[1] Engelhardt Institute of Molecular Biology, Russian Academy of Sciences, Vavilov str. 32, Moscow 119991, Russia
[2] Institute of Cytology, Russian Academy of Sciences, Tikhoretsky av. 4, St. Petersburg 194064, Russia
[3] Severtsov Institute of Ecology and Evolution, Russian Academy of Sciences, Leninsky av. 33, Moscow 119071, Russia

ABSTRACT

We have earlier shown that the typical *Didinium nasutum* nucleolus is a complex convoluted branched domain, comprising a dense fibrillar component located at the periphery of the nucleolus and a granular component located in the central part. Here our main interest was to study quantitatively the spatial distribution of nucleolar chromatin structures in these convoluted nucleoli. There are no "classical" fibrillar centers in *D.nasutum* nucleoli. The spatial distribution of nucleolar chromatin bodies, which play the role of nucleolar organizers in the macronucleus of *D.nasutum,* was studied using 3D reconstructions based on serial ultrathin sections. The relative number of nucleolar chromatin bodies was determined in macronuclei of recently fed, starved *D.nasutum* cells and in resting cysts. This parameter is shown to correlate with the activity of the nucleolus. However, the relative number of nucleolar chromatin bodies in different regions of the same convoluted nucleolus is approximately the same. This finding suggests equal activity in different parts of the nucleolar domain and indicates the existence of some molecular mechanism enabling it to synchronize this activity in *D. nasutum* nucleoli. Our data show that *D. nasutum* nucleoli display bipartite structure. All nucleolar chromatin bodies are shown to be located outside of nucleoli, at the periphery of the fibrillar component.

Key words*:* 3D reconstruction; ciliates; electron microscopy; macronucleus; nucleoli

INTRODUCTION

The nucleolus is a highly dynamic subnuclear domain where ribosomal RNA (rRNA) synthesis, rRNA processing and assembly of ribosomal subunits take place. In a typical cell nucleus nucleoli are formed around the ribosomal DNA (rDNA) repeats arranged around the nucleolar-organizing regions (NORs) on one or several chromosomes (Scheer and Hock, 1999; Carmo-Fonseca et al., 2000, Raska et al., 2006). In some cells such as the slime mold *Dictyostelium* and amphibian oocytes, the nucleoli are formed around extrachromosomal rDNA (Raikov, 1989; Thiebaud, 1979).

Extensive electron microscopic studies revealed the same general principles of nucleolar organization in the vast majority of species studied. Three main constituent parts of nucleoli, usually arrayed more or less concentrically, can be distinguished in the nucleus: (1) the fibrillar centers, (2) the dense fibrillar component, and (3) the granular component (Mosgoeller, 2004; Thiry et al., 2011). On ultrathin sections, the fibrillar centers have a rounded shape and are formed by densely packed fibrillar material. In the interphase nucleus, these centers are apparently the equivalent of NORs of individual chromosomes (Goessens, 1984; Zatsepina et al., 1988). Transcription of ribosomal genes presumably takes place at the border of fibrillar centers and the dense fibrillar component, whereas the surrounding dense fibrillar component corresponds to the nucleolar regions where maturation of pre-rRNA transcripts occurs (Cheutin et al., 2004; Guillot et al., 2005). The last stages of assembly of pre-ribosomal particles preceding their transport to the cytoplasm take place in the granular component. This organization of the nucleolus implies that the vector of rRNA processing is directed from the inner part of the nucleolus to its periphery (Fromont-Racine et al., 2003; Nazar, 2004; Derenzini et al., 2006).

Thiry et al. (2005, 2011) carried out a detailed comparative examination of the nucleolar ultrastructure in various eukaryotic species and came to the conclusion that tripartite nucleoli containing all three components are only typical of amniotic vertebrates; in all other eukaryotes bipartite nucleoli are present. In such nucleoli only two nucleolar compartments can be unambiguously identified: a fibrillar zone, surrounded by a granular zone (review, Thiry and Lafontaine, 2005).

In contrast to higher organisms, nucleolar domains of single-celled protists have received much less attention. The most promising models for these studies can be found among ciliates. Ciliated protists contain two morphologically and functionally different types of nuclei in a single cell - micro- and macronuclei. The micronuclei are inert diploid germ line nuclei which lack nucleoli, whereas the macronuclei are transcriptionally active somatic nuclei with prominent nucleolar compartments (see Raikov, 1995).

All ciliate species studied so far can be divided into two groups: the ciliates with macronuclear DNAs of subchromosomal size (up to several hundred kbp), and those with gene-sized (0.4 to 20 kbp) macronuclear DNAs which show the characters of mini-chromosomes. Thus macronuclei provide opportunity for studies of spatial organization of nucleoli in the absence of typical chromosomes.

The macronucleus of the ciliate *Didinium nasutum* (Fig. 1) contains DNA of subchromosomal size (Popenko et al., 2007). The nucleolar domains in this somatic nucleus are

*Corresponding author: Vladimir I. Popenko PhD, DrSci, Laboratory of Cell Biology, Engelhardt Institute of Molecular Biology, Russian Academy of Sciences, Vavilov str. 32, Moscow 119991, Russia. Tel: +7-499-1359804. Fax: +7-495-1351405. E-mail: popenko@eimb.ru

Received: November 26, 2012. In Revised form: January 14, 2013. Accepted: January 17, 2013

distributed among numerous compact chromatin bodies 90-250 nm in diameter (Karajan et al., 1995). 3D reconstructions based on serial ultrathin sections clearly show that nucleoli are complex convoluted, branched structures in which the fibrillar component is located at the periphery, while the granular part is in the central part of the nucleolus (Leonova et al., 2006; Popenko et al., 2008). Results from these studies led us to suggest that in *D. nasutum* processing of rRNAs occurs from the periphery of the nucleolus to its center. In many ciliate species, NORs look like chromatin bodies partially or completely surrounded by the fibrillar component of the nucleolus (Sabaneyeva, 1997; Sabaneyeva et al., 1984, see also references in Raikov, 1995). It has been also shown by autoradiography that NORs in *D. nasutum* are represented by chromatin bodies located both inside and at the boundary of nucleoli (Karadzhan, 1987).

Numerous reports in the literature demonstrate that nucleolar activity in both ciliates and higher eukaryotic cells reduces drastically under unfavorable conditions such as starvation (see references in Raikov, 1995; Engberg, 1985; Mayer and Grummt, 2005; Boulon et al., 2010). The aim of this research is to determine the exact spatial localization of nucleolar chromatin bodies in convoluted interphase *D. nasutum* nucleoli on the ultrastructural level and to compare the relative number of such bodies in the nucleoli of recently fed cells, starved cells, resting cysts and in different parts of convoluted nucleoli. To address these issues, we used 3D reconstructions to study localization of all the chromatin bodies, which corresponded to NORs by morphological criteria.

METHODS

The laboratory strain of *Didinium nasutum* was grown at room temperature in lettuce medium and fed with *Paramecium caudatum* as described earlier (Leonova et al., 2006). Ciliates cultivated in the excess of food were fixed for electron microscopy 5-7 min after the last feeding ("fed" ciliates). Part of the ciliate culture was transferred into food-free culture medium and fixed 30 h later ("starved" cells). Resting cysts of *D. nasutum* were obtained and fixed as described in (Karajan et al., 2003).

Both fed and starved cells were fixed with 2.5% glutaraldehyde in 0.1 M phosphate buffer (pH 7.5) for 1 h at room temperature, dehydrated in a graded series of alcohol and embedded in Epon-Araldite mixture. Serial ultrathin sections were obtained with an LKB III ultratome (LKB Products, Stockholm-Bromma, Sweden) and stained with uranyl acetate and lead citrate using the standard procedure. The specimens were examined in a JEM-100CX electron microscope (JEOL Ltd., Tokyo, Japan).

A regressive staining of sections with uranyl acetate –EDTA– lead citrate, which selectively contrasts ribonucleoproteins, was performed as described elsewhere (Bernhard, 1969).

Negatives of serial sections of macronucleus (20–30 items, 50-70 nm thick) were scanned at a final resolution of 480 pixels per 1 μm of a section. The 3D reconstruction was carried out using the STERM software developed by the authors (Leonova et al., 2006). During reconstruction we took into account only structures larger than 50 nm in size. Six regions of macronuclei of five fed cells (reconstructed volumes varied from 48 to 418 μm^3) and four regions of four starved cells (56 to 220 μm^3) were reconstructed. Average values were compared using a 2-tailed Student's *t*-test. The relative number of NORs, i.e. the number of nucleolar chromatin bodies per $1\mu m^2$ of the nucleolar surface, was calculated in 3D reconstructions by division of the number of nucleolar bodies by the area of adjacent nucleolar surface.

RESULTS

The macronucleus of recently fed interphase *D. nasutum* cells contains numerous conspicuous nucleoli that are evenly distributed throughout the nucleoplasm (Fig. 2a). The dense fibrillar component mainly occurs in the form of discrete bands or trabecules on the surface of the nucleoli, while the granular component lies inside the nucleoli, filling the space between trabeculae of the fibrillar component more or less uniformly. Figures 2b and 3 display 3D reconstructions of the macronuclear region, corresponding to the ultrathin section shown in Figure 2a. In order to give a clear idea of nucleolar topology and reduce the overlapping of nucleolar structures, the granular component in 3D reconstructions was omitted.

3D reconstructions show that the nucleoli, which normally look in single sections like individual separate structures, have actually been assembled into large convoluted nucleolar networks (Figs 2b, 3). Chromatin bodies of irregular shape and 0.09-0.25 μm in size are uniformly distributed in the macronucleus (Figs 2a, 4a). Those of these bodies which are thought to correspond to NORs were determined in individual ultrathin sections by morphological criteria. Such chromatin bodies are located either inside the nucleolus, fully surrounded by the dense fibrillar component (Fig. 4b), or at the periphery of nucleoli and connected with the fibrillar component by visible chromatin threads or fibers (Figs 4a, c). These threads and fibers are of deoxyribonucleoprotein nature, since they appeared bleached in sections stained according to Bernhard's method (Bernhard, 1969), which selectively reveals ribonucleoproteins (Figs 4d, e).

3D reconstructions show that all nucleolar chromatin bodies - putative NORs are located outside the nucleoli, in the nucleoplasm. No chromatin bodies were located in the inner part of the nucleoli or inside the fibrillar component. Even the chromatin bodies that seem to be located inside the nucleolus in single sections (Fig. 4b) were in fact located at the periphery, in the cavities of the fibrillar component (Fig. 3).

The structure of nucleoli in starved cells fixed 30 h after feeding is strikingly different from that of recently fed cells (Fig. 5a). No chromatin bodies are observed inside the nucleoli in these starved cells. 3D reconstructions (Figs 5b) show that all nucleolar chromatin bodies are located at the periphery of the nucleoli, in the nucleoplasm.

The number of NORs in the nucleoli is known to indicate the activity of ribosomal protein synthesis in both proliferating and non-proliferating cells (Jozsa et al., 1993). In *D. nasutum* we could not determine the exact number of nucleolar bodies per nucleolus, since most of the branched interphase nucleoli exceeded the boundaries of the reconstructed region and had an intricate shape. Therefore, we calculated the relative number of nucleolar bodies per 1 μm^2 area of the nucleolar surface and compared this parameter in recently fed and starved cells. In fed *D. nasutum*, the relative number of nucleolar bodies was 5.29 ± 0.49 (M ± SD, averaged over six

reconstructions from five cells). In the starved cells, it was equal to 3.58 ± 0.62 (M ± SD, four reconstructions from four cells), i.e. 1.52 times lower (statistically significant at $p<0.001$). The latter finding correlates well with the lower activity of the macronucleus in the starved cells (Engberg, 1985, Raikov, 1995). In addition, in resting *D. nasutum* cysts we detected no chromatin bodies either inside the nucleoli or at their periphery (Fig. 6). Thus there is a good correlation between the relative number of nucleolar chromatin bodies and the activity of the nucleolus.

To answer the question of whether the activity in various parts of complex convoluted *D. nasutum* nucleoli is different, we calculated the relative number of nucleolar chromatin bodies for the whole nucleolus and for its different parts. These values were found to be very close. For example, in the convoluted nucleolus of fed ciliates, shown in Figure 4, the mean number of nucleolar chromatin bodies per 1μm^2 was equal to 5.57, while it varied from 5.37 to 5.8 in different parts of it (Table 1). For the nucleolus from starved *D. nasutum* cell (Fig. 5), the mean relative number was 3.71 and the range was 3.4 - 3.85 for the four different parts of it (Table 2). The coefficient of variation in these two examples and other seven reconstructions (not shown) was less than 10%. These data make it safe to conclude that the activity of the various parts of complex interphase *D. nasutum* nucleoli is approximately the same.

DISCUSSION

Our 3D reconstructions based on serial ultrathin sections, image analysis and computer-aided modeling clearly show that all compact chromatin bodies in the macronucleus of *D. nasutum* are located outside the nucleoli, in the nucleoplasm, both in recently fed and starved cells. In ciliates macronuclear rDNAs are preferentially replicated before the

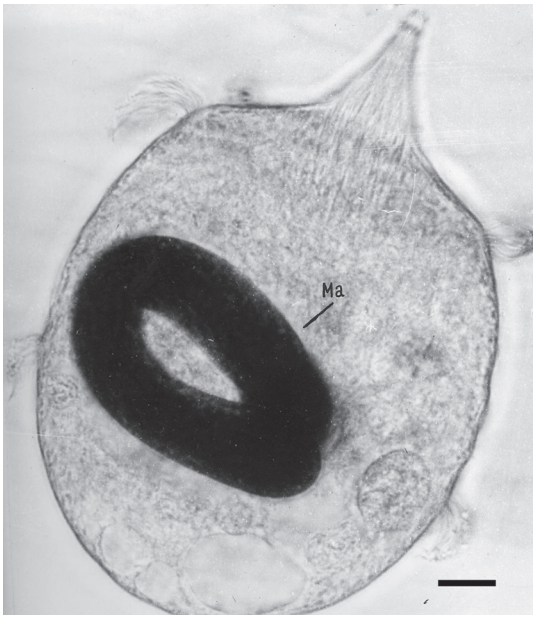

Figure 1. *Didinium nasutum* in the light microscope. Feulgen staining. Ma – macronucleus. Scale bar, 10 μm.

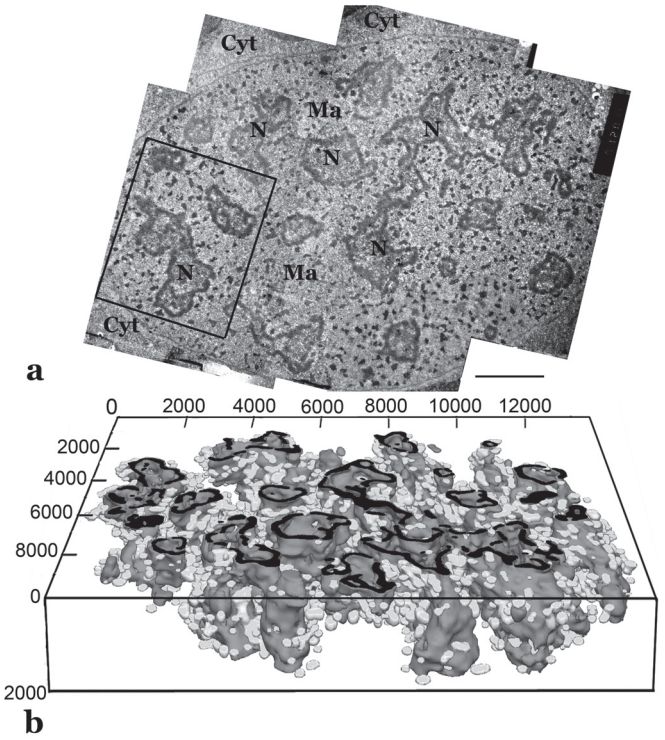

Figure 2. Nucleoli in recently fed *Didinium nasutum* cells. a – an ultrathin section of a macronucleus. Numerous conspicuous large nucleoli are evenly distributed throughout the nucleoplasm. Ma – nucleoplasm of macronucleus, Cyt – cytoplasm, N – nucleoli. Scale bar, 2 μm. b - 3D reconstruction of the macronuclear region cross-sectioned at the level corresponding to the section in Figure 1a. Only the fibrillar component and nucleolar bodies are shown. The fibrillar component in the cross section plane is tinted black to compare with the corresponding structures in Figure 1a. The distances are shown in nm.

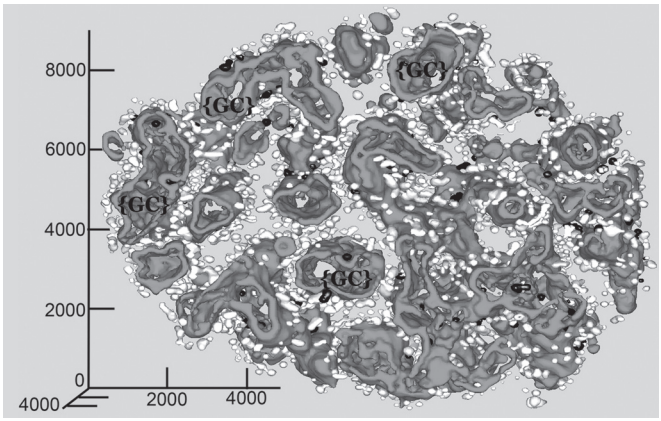

Figure 3. Top view of a 3D reconstruction of network-like branched nucleoli in fed D. nasutum cells. Only the fibrillar component (grey color) and nucleolar chromatin bodies (black and white colors) are shown. Chromatin bodies, which were completely surrounded by the fibrillar component in individual sections, are colored black. The intranucleolar space where the granular component was located is designated as {GC}. The distances are shown in nm.

bulk of macronuclear DNA (Engberg, 1985). It was shown autoradiographically by Karadzhan (1987) that chromatin bodies at the periphery or inside the *D. nasutum* nucleoli were labeled at the beginning of the S-phase. Since no other chromatin structures resembling the nucleolar fibrillar centers were detected in ultrathin sections of *D. nasutum*, we considered these perinucleolar chromatin bodies as putative NORs. This approach is quite consistent with the data of many authors, who reported that NORs in ciliates can look like chromatin bodies, completely or partially surrounded by the

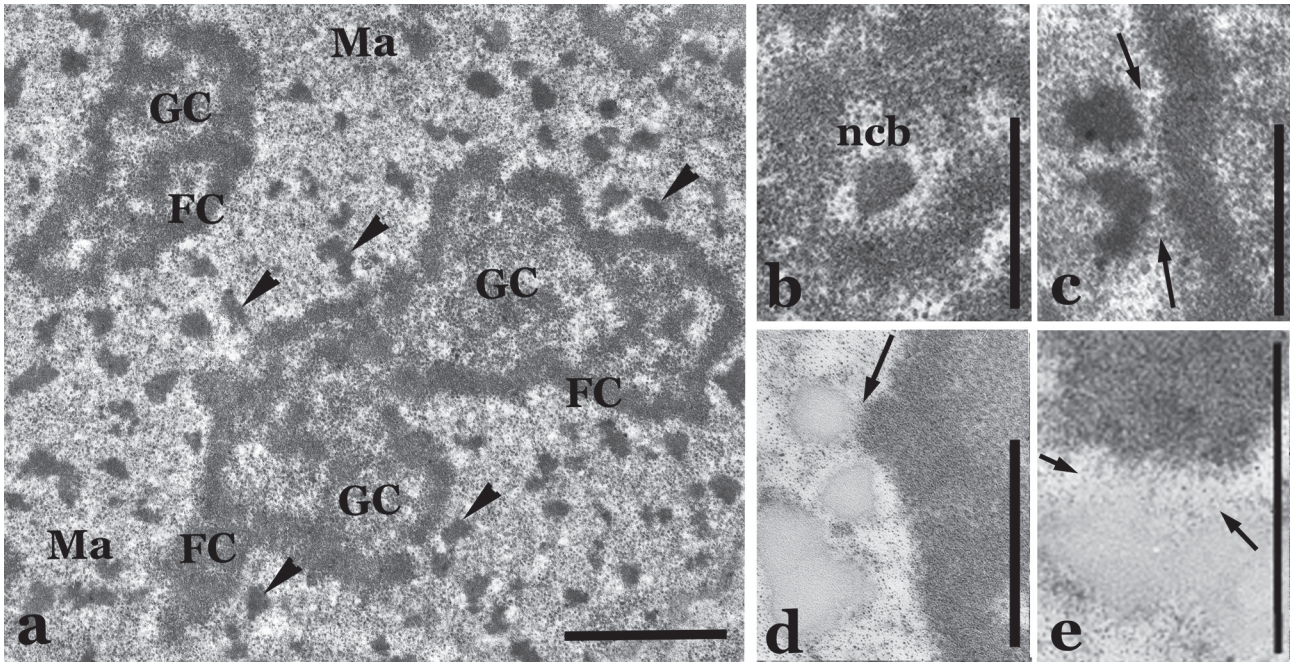

Figure 4. Nucleolar chromatin bodies in recently fed D. nasutum cells. a – a fragment of Figure 1a at higher magnification (part of the large convoluted branchy nucleolus). The dense fibrillar component is located at the periphery and looks like discrete bands or trabecules. The granular component is in the inner part of the nucleolus. Arrowheads – chromatin bodies connected with the fibrillar component by visible chromatin threads, Ma – nucleoplasm of the macronucleus, FC – the fibrillar component, GC – the granular component. b – nucleolar chromatin body (ncb) located inside the nucleolus at higher magnification. c - nucleolar chromatin bodies located in nucleoplasm at the periphery of nucleoli and connected with the fibrillar component by visible chromatin threads (arrows). d, e- a regressive staining of sections with uranyl acetate – EDTA – lead citrate. RNPs are selectively contrasted. The chromatin threads (arrows) remain unstained. Scale bars, 1 μm (a), 0.5 μm (b – e).

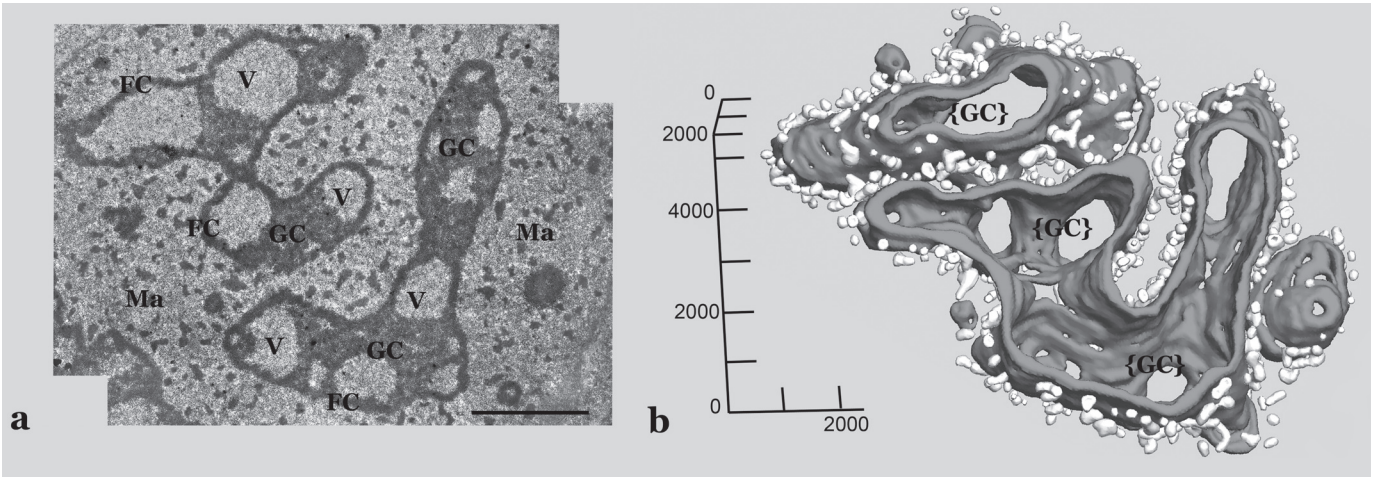

Figure 5. Nucleoli in starved D. nasutum cells. a – a single section of typical macronuclear region. Large vacuoles (V) appear in the granular component of nucleoli. No chromatin bodies are observed inside the nucleoli. Ma –macronucleus, FC – the fibrillar component, GC – the granular component. Scale bar, 2 μm. b –3D reconstruction of network-like branched nucleolus in fed D. nasutum cells. The fibrillar component is tinted grey, nucleolar chromatin bodies – white. The granular component is not shown. The intranucleolar space where the granular component was located is designated as {GC}. The distances are shown in nm.

fibrillar component (references in Raikov, 1995; Sabaneyeva 1984, 1997). Results of the present study clearly show that "intranucleolar" chromatin bodies are not really localized within the constituent parts of nucleoli. In fact, the so-called intranucleolar chromatin bodies appear to represent nucleolar chromatin bodies in cavities of the complex branched nucleoli. Together with the fact that the granular component is located in the inner part of convoluted nucleoli, these data strongly suggest that the vector of rRNA processing in *D. nasutum* is directed from the periphery to the central part of the nucleolus.

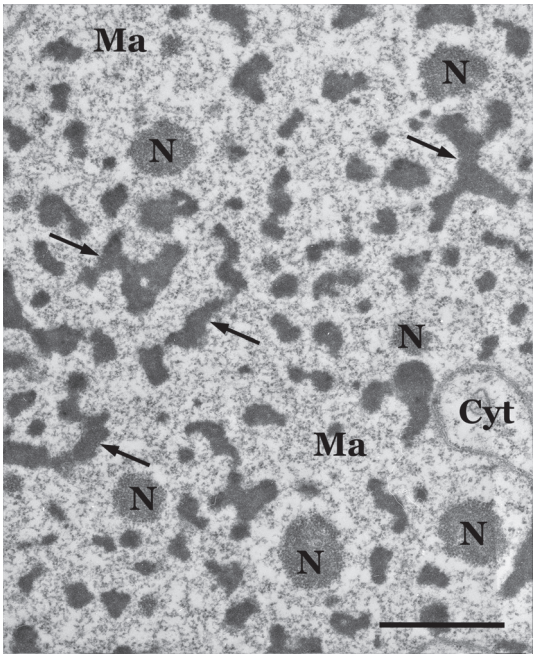

Figure 6. Fragment of the macronucleus of D. nasutum cyst. Arrows point to chromatin fibers of aggregated chromatin bodies. N – nucleoli, Ma – nucleoplasm of macronucleus, Cyt – cytoplasm. Scale bar, 1 μm.

Our results are in a good agreement with the findings of Postberg et al. (2006) in the macronucleus of *Stylonychia lemnae*, which displays gene-sized mini-chromosomes. In this ciliate rDNAs are found to occur adjacent to, but outside the nucleoli. Thus transcription, or at least its initiation, should start within the outer domains of condensed chromatin and the subsequent processing of rRNA should occur in the interior of nucleolar domains. It was assumed that the absence of typical chromosomes determines this alternative spatial organization of the nucleolus (Postberg et al., 2006). Our data show that nucleoli within macronuclei with subchromosomal DNAs (*D. nasutum*) can also conduct rRNA processing in thr opposite direction compared to the "classical" nucleoli of Metazoa.

We have demonstrated that the relative number of nucleolar bodies in the branched *D. nasutum* nucleoli correlates with the functional state of these ciliates. The relative number in recently fed cells was 1.52 times greater than in starved cells. Moreover, no chromatin bodies connected with nucleolar structures were observed in cysts. These results are in accordance with the fact that the number of NORs in the nucleoli indicates the activity of ribosomal protein synthesis in both proliferating and non-proliferating cells (Jozsa et al., 1993). However, the relative number of nucleolar chromatin bodies in the whole convoluted nucleolus and in different parts of it appeared to be the same (Tables 1, 2). Thus in *D. nasutum*, the synthetic activity in various parts of complex interphase nucleoli is approximately the same. It is tempting to speculate

TABLE 1

Nucleolar chromatin bodies in a complex convoluted nucleolus in recently fed D. nasutum ciliates.

Parameter	Reconstructed convoluted network-like nucleolus as a whole	Fragments of the same convoluted nucleolus			
		1	2	3	4
Number of nucleolar chromatin bodies	2433	175	1145	105	8
Area of fibrillar component outside, μm^2	436.55	32.47	211.62	18.139	1.488
Relative quantity of nucleolar chromatin bodies per 1 μm^2 of fibrillar component outside	5.57	5.52	5.41	5.8	5.37

TABLE 2

Nucleolar chromatin bodies in a complex convoluted nucleolus of starved D. nasutum ciliates.

Parameter	Reconstructed convoluted nucleolus as a whole	Fragments of the same convoluted nucleolus			
		1	2	3	4
Number of nucleolar chromatin bodies	537	18	9	32	1
Area of fibrillar component outside, μm^2	144.64	5.29	2.52	8.54	0.26
Relative quantity of nucleolar chromatin bodies per 1 μm^2 of fibrillar component outside	3.71	3.4	3.57	3.75	3.85

that a specific molecular mechanism exists in *D. nasutum* which synchronizes the rRNA synthesis in different parts of the interphase nucleoli.

The classical fibrillar centers in nucleoli of higher eukaryotes are structures with low electron density composed of fine fibrils 7-10 nm in diameter (Goessens, 1984). According to Thiry at al. (2011), typical tripartite nucleoli containing all three main components (i.e. fibrillar center, dense fibrillar component and granular component) are only found in amniotic vertebrates (Thiry and Lafontaine, 2005; Thiry et al., 2011). In other eukaryotes the nucleoli are usually bicompartmentalized, where only two nucleolar compartments –fibrillar and granular components– are unambiguously identified. The absence of classical fibrillar centers in *D. nasutum* nucleoli is in agreement with these data.

In summary, we infer that both gene- and subchromosomal-size atypical chromosomes of macronuclei which lack centromeres can determine an alternative spatial organization of vectorial synthesis and processing of rRNA in ciliates.

ACKNOWLEGEMENTS

The authors are grateful to V.A. Grigoryev for technical assistance, Dr. John G. Holt (USA) for valuable criticism and proofreading of the text. This work was supported by grants no. 11-04-01967a to V.I.P and no.10-04-00943a to S.O.S from the Russian Foundation for Basic Research.

REFERENCES

BERNHARD W (1969) A new staining procedure for electron microscopical cytology. J Ultrastr Res 27:250-265.

BOULON S, WESTMAN BJ, HUTTEN S, BOISVERT F-M, LAMOND AI (2010). The Nucleolus under Stress. Mol Cell 40:216–227.

CARNO-FONSECA M, MENDES-SOARES L, CAMPOS I (2000) To be or not to be in the nucleolus. Nature Cell Biol 2:107–112.

CHEUTIN T, MISTELI T, DUNDR M (2004) Dynamics of nucleolar components. In: The nucleolus. Kluwer Academic/Plenium Publishers, New York, pp. 29-40.

DERENZINI M, PASQUINELLI G, ODONOHUE MF, PLOTON D, THIRY M (2006) Structural and functional organization of ribosomal genes within the mammalian cell nucleolus. J Histochem Cytochem 54:131-145.

ENGBERG J (1985) The ribosomal RNA genes of *Tetrahymena*: structure and function. Europ J Cell Biol 36:133-151.

FROMONT-RACINE M, SENGER B, SAVEANU C, FASIOLO F (2003) Ribosome assembly in eukaryotes. Gene 313**:**17-42.

GOESSENS G (1984). Nucleolar structure. Int Rev Cytol 87:107-158.

GUILLOT PV, MARTIN S, POMBO A (2005) The organization of transcription in the nucleus of mammalian cells. In: Vision of the cell nucleus. California, Amer. Sci. Publ., pp. 95-105.

JOZSA L, KANNUS P, JARVINEN M, ISOLA J, KVIST M, LEHTO M (1993) Atrophy and regeneration of rat calf muscles cause reversible changes in the number of nucleolar organizer regions. Evidence that also in nonproliferating cells the number of NORs is a marker of protein synthesis activity. Lab Invest 69:231–237.

KARADZHAN BP (1987) Replication of rDNA in the cell cycle of the ciliate *Didinium nasutum*. Autoradiographic data. Doklady Akad Nauk SSSR 296:984-986.

KARAJAN BP, POPENKO VI, RAIKOV IB (1995) Organization of transcriptionally inactive chromatin of interphase macronucleus of the ciliate *Didinium nasutum*. Acta Protozool 34:135-141.

KARAJAN BP, POPENKO VI, LEONOVA OG (2003) Fine structure of nucleoli in the ciliate *Didinium nasutum.* Protistology 3:87-94.

LEONOVA OG, KARAJAN BP, IVLEV YF, IVANOVA JL, POPENKO VI (2006). Nucleolar apparatus in the macronucleus of *Didinium nasutum* (Ciliata): EM and 3D reconstruction. Protist 157:391-400.

MAYER C, GRUMMT I (2005) Cellular Stress and Nucleolar Function. Cell Cycle 4:1036-1038.

MOSGOELLER W (2004) Nucleolar ultrastructure in vertebrate. In: The nucleolus. Kluwer Acad./Plenium Publ., New York., pp. 10-20.

NAZAR RN (2004) Ribosomal RNA processing and ribosome biogenesis in eukaryotes. IUBMB Life. 56:457-465.

POPENKO VI, KARAJAN BP, LEONOVA OG, IVANOVA YL (2007) Chromomeric level of chromatin organization in the macronuclei of ciliates. Tsitologiya 49:785-786.

POPENKO VI, KARAJAN BP, LEONOVA OG, SKARLATO SO, IVLEV YF, IVANOVA YL (2008) Three-dimensional structure of the ciliate *Didinium nasutum* nucleoli. Molecular Biology 42:455–461.

POSTBERG J, ALEXANDROVA O, LIPPS HJ **(**2006) Synthesis of pre-rRNA and mRNA is directed to a chromatin-poor compartment in the macronucleus of the spirotrichous ciliate *Stylonychia lemnae*. Chromosome Res 14:161–175.

RAIKOV IB (1989) Nuclear genome of the protozoa. Progress in Protistology 3:21-86.

RAIKOV IB (1995) Structure and genetic organization of the polyploid macronucleus of ciliates: a comparative review. Acta Protozool 34:151-171.

RASKA I, SHAW PJ, CMARKO D (2006) New insights into nucleolar architecture and activity. Int Rev Cytol 255:177–135.

SABANEYEVA EV, RAUTIAN MS, RODIONOV AV (1984) Demostration of active nucleolar organizers in the macronucleus of the ciliate *Tetrahymena pyriformis* by staining with silver nitrate. Tsitologiia 26:849-852 (in Russian with Englsh summary).

SABANEYEVA E (1997) Extrachromosomal nucleolar apparatus in the macronucleus of the ciliate *Paramecium putrinum*: LM, EM and Confocal Microscopy Studies. Arch Protistenkd 148: 365-373

SCHEER U, HOCK R (1999) Structure and function of the nucleolus. Curr Opin Cell Biol 11:385-390.

THIEBAUD CH (1979) Quantitative determination of amplified rDNA and its distribution during oogenesis in *Xenopus laevis*. Chromosoma 73:37-44.

THIRY M, LAFONTAINE DLJ (2005). Birth of a nucleolus: the evolution of nucleolar compartments. Trends Cell Biol 15:194-199.

THIRY M, LAMAYE F, LAFONTAINE DLJ (2011) The nucleolus. When two became three. Nucleus 2:289-293.

ZATSEPINA OV, HOZAK P, BABAJANYAN D, CHENTSOV Y (1988). Quantitative ultrastructural study of nucleolus-organizing regions at some stages of the cell cycle (G0-period, G2-period, mitosis). Biol Cell 62:211-218.

Biol Res 46: 75-78, 2013

High gender –specific susceptibility to curare– a neuromuscular blocking agent

Santosh K. Maurya, Muthu Periasamy[1] and Naresh C. Bal[2]

[1] Davis Heart and Lung Research Institute, Ohio State University, Columbus, Ohio, USA
[2] Department of Physiology and Cell Biology, The Ohio State University, College of Medicine, Columbus, OH 43210, United States.

ABSTRACT

Curare, a selective skeletal muscle relaxant, has been used clinically to reduce shivering and as an anesthetic auxiliary in abdominal surgery. It is also widely used in animal experiments to block neuromuscular junction activity. Effective doses of curare diminish muscle contraction without affecting brain function, but at higher doses it is known to be lethal. However, the exact dose of curare initiating muscle relaxation *vs.* lethal effect has not been fully characterized in mice. In this study we carefully examined the dose-response for achieving muscle inactivity over lethality in both male and female mice (C57BL6/J). The most striking finding of this study is that female mice were highly susceptible to curare; both the ED_{50} and LD_{50} were at least 3-fold lower than male littermates. This study shows that gender-specific differences can be an important factor when administering skeletal muscle relaxants, particularly curare or other analogous agents targeted to the neuromuscular junction.

Key terms. Curare, dose response, gender, muscle activity, oxygen consumption.

INTRODUCTION

Curare has long been used by the Indians of South America as an arrow poison for hunting wild game (Bisset, 1992). After it became known that curare affects voluntary muscles selectively without affecting the brain and heart it was widely used in modern medicine as an auxiliary in general anesthesia, frequently with cyclopropane (Anderson, 2010; Lee, 2003). Curare has recently been used in humans to reduce shivering (Hovland et al., 2006), and is also used in animal experimentation to block shivering (Hovland et al., 2006; Kashimura et al., 1992; Nonogaki et al., 1991), to diagnose myasthenia gravis (a muscle disease) (Biesecker and Koffler, 1988; Somnier and Trojaborg, 1993) and to manipulate neurosysnaptic transmission (Witoonpanich et al., 1989) etc. Curare acts as a neuromuscular blocking agent by binding to the acetylcholine receptor (AChR) at the neuromuscular junction and preventing nerve impulses from activating skeletal muscles (Bowman, 2006). Although high doses of curare are lethal, low doses are well tolerated and the effect is completely reversible (Clement, 1978). However, it is not known if curare has a gender-specific effect on physical activity and whole body metabolic rate. In this study we therefore examined the dose-dependent effects of curare on both male and female mice littermates by monitoring physical activity, core body temperature (Tc), whole animal oxygen consumption, circadian rhythm and feeding behavior.

METHODS

Experimental Animals: Age-matched (12-18 weeks old) male and female mice (C57BL/6J) littermates were housed at a temperature of 22±1 °C with a 12:12-h light: dark cycle and relative humidity about 50%. Diet (2014, Harlan Teklad) and water was provided *ad libitum*. The study protocol was approved by the Ohio State University Institutional Animal Care and Use Committee. All of the animal procedures were carried out at our AAALAC-accredited animal facility and conducted in accordance with *the Guide for the Care and Use of Laboratory Animals*.

Curare dose response: Tubocurarine hydrochloride (curare with better solubility profile) was purchased from Sigma-Aldrich, St. Louis, MO. Curare solution (0.9% NaCl solution) was administered intraperitonially in various quantities as reported in **Table 1**. The mice were individually monitored for at least 30 minutes after treatment for drug effect. Dose and percentage of death were fitted into a dose-response graph in GraphPad Prism 3.0 software to calculate the LD_{50} (dose at which 50% of the mice died). From the dose-response curves an effective sub-lethal dose (ED_i), at which mice became immobile for few minutes, was determined for both male and female mice.

Monitoring of circadian rhythm and basal metabolic rate (BMR): To determine if administration of curare affects the metabolic rate in male and female mice differently, we measured oxygen consumption (VO_2), RER (respiratory exchange ratio) and physical activity (measured by infrared sensors installed around each housing cage). These experiments were performed at 25±1.0 °C using a Comprehensive Lab Animal Monitoring System **(oxymax/CLAMS)** equipped with a temperature-controlled environmental chamber from Columbus Instruments, Columbus, OH, USA. The mice were given ED_i at 10AM following 18 hours acclimatization at 25±1.0 °C and metabolic measurements were recorded.

Core body Temperature measurement in mice exposed to cold: Core body temperature (Tc) was measured by thermal transponders (IPTT300, Bio Medic Data System, Seaford, DE). Mice were administered with ED_i of curare and allowed to recover for 30 minutes and then challenged with 4 °C. Tc, oxygen consumption and physical activity were continuously monitored using oxymax/ CLAMS.

Corresponding author: Naresh C. Bal, PhD, Or, Muthu Periasamy, PhD, 304 Hamilton Hall, 1645 Neil Ave, Columbus, OH 43210. Fax: 614-292-4888; Email: bal.8@osu.edu or, periasamy.1@osu.edu.

Received: November 30, 2012. In Revised form: January 17, 2013. Accepted: February 1, 2013

TABLE 1

Dose-dependent effect of curare (tubocurarine) on male and female mice

Dose (mg/kg)	Female			Male		
	Total animals tested	Mortality	Immobility	Total animals tested	Mortality	Immobility
0.04	10	0	0	10	0	0
0.05	10	0	0	10	0	0
0.06	10	0	3	10	0	0
0.08	11	0	4	10	0	0
0.1	10	2	7	10	0	0
0.2	11	5	11	10	0	1
0.3	10	6	10	10	0	3
0.4	11	9	11	10	2	6
0.5	10	9	10	7	2	6
0.6	10	10	10	8	5	8
0.8				10	8	10
1				9	9	9

Statistical analysis: Mortality data were analyzed using student't' test (nonparametric) using Graph pad Prism software and $p < 0.05$ was considered significant.

RESULTS

We were interested in studying the role of muscle shivering over non-shivering thermogenic (NST) mechanisms contributing to heat production and Tc maintenance (Bal et al., 2012). Therefore we chose to utilize curare, which has been shown to reduce shivering (Hovland et al., 2006; Kashimura et al., 1992). We first set out to optimize the dose that would minimize shivering by using different doses of curare in both male and female mice. Interestingly, the LD_{50} of curare for the female mice was very low (0.22 mg/kg) as compared to male mice (0.75 mg/kg) (Figure 1A). At doses below LD_{50}, curare completely immobilizes the mice for ~10 minutes, after which mice can be used for experimental studies with maximal inhibition of shivering for the next ~5 hours. The ED_{50} for achieving complete immobility was calculated to be 0.38 mg/kg for males, while that for the female mice was 0.01 mg/kg (Figure 1A). The difference in percentage mortality between male and female groups was found to be statistically significant by applying a student't' test ($p=0.003$). The number of animals used in this study for each dose of curare and number of animals affected is presented in Table 1. These data suggest that females are highly susceptible to curare and one-third dose for males is sufficient to achieve complete immobility. Therefore, for all the remaining studies reported here, we chose 0.4 mg/kg for male and 0.1 mg/kg for female mice as their respective effective dose to achieve immobility (ED_i). The immobility induced at these doses (0.4 mg/kg for male and 0.1 mg/kg for female mice) was completely reversible within ~10 minutes.

Administration of **c**urare causes an immediate effect on physical activity and mice are immobilized for a short period. Therefore, we studied if curare has a long-lasting effect on metabolism (measured as whole body O_2 consumption) and physical activity on both male and female mice. O_2 consumption remained unchanged regardless of gender and dose administered (ED_i). Following curare (ED_i) administration, physical activity remained low for ~3 hours both in males (Figure 2A) and in females (Figure 2B). Other parameters, including Tc, respiratory exchange ratio (RER or respiratory quotient), energy expenditure measured at 25±1 °C did not show any significant difference (Supplemental Figure). At ED_i, both male and female mice were able to tolerate the acute cold challenge of 4 °C (maintained Tc around 37.0 °C) and were able to upregulate their metabolism to meet the thermogenic demands during cold stress, which is reflected in the increase in O_2 consumption (Figure 2C and 2D).

DISCUSSION

Curare has been used as a muscle relaxant in clinical surgery until recently, when safer alternatives became available. Many of these newer muscle relaxants have similar chemical structures/moieties and also have an analogous mode of action through AChR (Bowman, 2006). Although widely used as a muscle relaxant in clinical surgery, gender-specific differences have not been reported previously. However, it was recently administered in a female patient to reduce shivering (Hovland et al., 2006) and one report suggested that female patients should receive a lower dose of curare (Bennett, 1968), indicating that gender-specific differences may exist. This is the first study to report that female mice are more sensitive to curare at a concentration three fold (LD_{50}) lower than males, but the exact mechanism is unclear. We used reproductively mature mice; the reproductive cycle of the female mice and their hormonal status were not considered. However, we expect that there is very little chance of overlap between the reproductive cycles of the 103 female mice used in the present study. Therefore, the role of reproductive hormones in the observed sensitivity of female mice to curare can be ruled out. This difference between males and females might

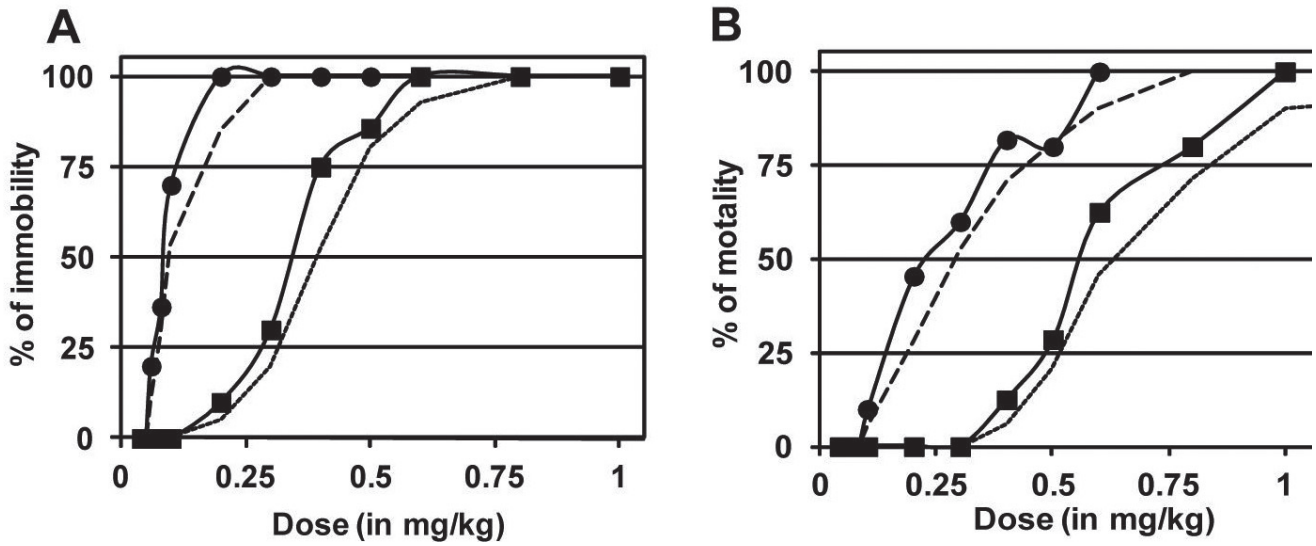

Figure 1: Comparison of curare dose response for male *vs.* female mice. (A) Immobility curve and **(B)** survival curve. Solid circles represent female mice and solid squares are the male mice. Dashed and dotted lines are the trend lines for females and males, respectively.

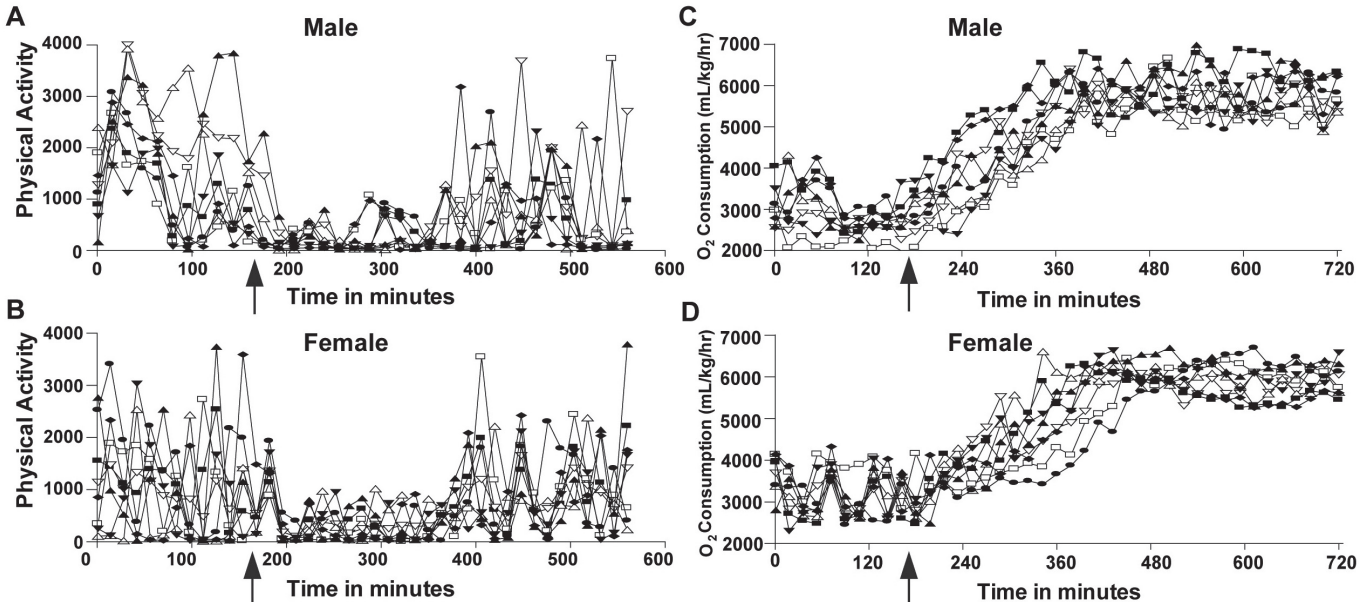

Figure 2: Physiological and metabolic effects of curare. Effect on physical activity of male mice **(A)** and physical activity of female mice **(B)** at 25±1.0 °C. Effect on VO_2 in male mice **(C)** and female mice **(D)** upon acute cold challenge. Individual data on 8 male and female mice are presented. The time of administration of curare is indicated by arrows. In **C** and **D** the cold challenge was started 30 minutes after curare administration.

be due to intrinsic gender-specific differences in recruitment and activation of neuromuscular junctions (Green et al., 1984; Simoneau et al., 1985) and/or gender-specific differences in ability of clearance of the drug from the body. Although the rate of metabolic clearance of curare in mice is not known, clearance for another plant-derived alkaloid, strychnine, has been reported to be slower in female mice, which may be the basis of higher sensitivity of female mice towards these alkaloids (Durkin, 2010). Another interesting finding of this study is that the ED_{50} and LD_{50} for curare are close. Therefore, the curare dose for a given experiment should be chosen carefully to avoid lethality-induced differential results. Our study highlights the importance of a gender-specific difference in the curare dose-response relationship. Therefore it calls for careful reevaluation of dose response in females before administering muscle relaxants including curare-like molecules.

ACKNOWLEDGEMENTS

This work was supported in part by National Institutes of Health Grant R01 HL64014 to M. P. N.C.B. was supported by a postdoctoral fellowship from the American Heart Association.

REFERENCES

ANDERSON R. (2010). A TORTURED PATH: Curare's Journey from Poison Darts to Paralysis by Design. Mol Interventions 10:252-258.

BAL NC, MAURYA SK, SOPARIWALA DH, SAHOO SK, GUPTA SC, SHAIKH SA, PANT M, ROWLAND LA, BOMBARDIER E, GOONASEKERA SA, TUPLING AR, MOLKENTIN JD, PERIASAMY M. (2012). Sarcolipin is a newly identified regulator of muscle-based thermogenesis in mammals. Nat Med 18:1575-9.

BENNETT AE. (1968). The history of the introduction of curare into medicine. Anesth Analg 47:484-92.

BIESECKER G, KOFFLER D. (1988). Resistance to experimental autoimmune myasthenia gravis in genetically inbred rats. Association with decreased amounts of in situ acetylcholine receptor-antibody complexes. J Immunol 140:3406-10.

BISSET NG. (1992). War and hunting poisons of the New World. Part 1. Notes on the early history of curare. J Ethnopharmacol 36:1-26.

BOWMAN WC. (2006). Neuromuscular block. Br J Pharmacol 147:S277-86.

CLEMENT JG. (1978). Effect of ethanol, pentobarbital and morphine on the toxicity of hemicholinium-3 and d-tubocurarine in mice. Arch Int Pharmacodyn Ther 236:60-5.

DURKIN PR. (2010). Strychnine: Human Health and Ecological Risk Assessment. USDA/Forest Service, Southern Region, 1720 Peachtree RD, NW Atlanta, Georgia 30309

GREEN HJ, FRASER IG, RANNEY DA. (1984). Male and female differences in enzyme activities of energy metabolism in vastus lateralis muscle. J Neurol Sci 65:323-31.

HOVLAND A, NIELSEN EW, KLUVER J, SALVESEN R. (2006). EEG should be performed during induced hypothermia. Resuscitation 68:143-6.

KASHIMURA O, SAKAI A, YANAGIDAIRA Y, UEDA G. (1992). Thermogenesis induced by inhibition of shivering during cold exposure in exercise-trained rats. Aviat Space Environ Med 63:1082-6.

LEE C. (2003). Conformation, action, and mechanism of action of neuromuscular blocking muscle relaxants. Pharmacol Ther 98:143-69.

NONOGAKI K, IGUCHI A, YATOMI A, UEMURA K, MIURA H, TAMAGAWA T, ISHIGURO T, SAKAMOTO N. (1991). Dissociation of hyperthermic and hyperglycemic effects of central prostaglandin F2 alpha. Prostaglandins 41:451-62.

SIMONEAU JA, LORTIE G, BOULAY MR, THIBAULT MC, THERIAULT G, BOUCHARD C. (1985). Skeletal muscle histochemical and biochemical characteristics in sedentary male and female subjects. Can J Physiol Pharmacol 63:30-5.

SOMNIER FE, TROJABORG W. (1993). Neurophysiological evaluation in myasthenia gravis. A comprehensive study of a complete patient population. Electroencephalogr Clin Neurophysiol 89:73-87.

WITOONPANICH R, VEJJAJIVA A, LIMPISVASTI S. (1989). Regional curare test in the study of neuromuscular transmission in hyperthyroidism. J Med Assoc Thai 72:187-91.

Biol Res 46: 79-85, 2013

Physiological behavior of bean (*phaseolus vulgaris l.*) Seedlings under metal stress

Fikriye Zengin

ABSTRACT

The effects of nickel, cobalt, chromium and zinc on the content of vitamins A, E and C, malondialdehyde (MDA), chlorophyll and carotenoids were investigated in bean seedlings (*Phaseolus vulgaris* L.) grown in Hoagland solution Control and heavy metal-treated plants were grown for ten days in Hoagland solution. Vitamin A, E, and C content were measured in primary leaves by high performance liquid chromatographic (HPLC). MDA, chlorophyll and carotenoids were measured in leaves by spectrophotometer. In heavy metal treated plants, the levels of MDA, vitamins A, E and C and carotenoids significantly increased, while chlorophyll content decreased in leaves of seedlings. The results indicate that heavy metals caused an oxidative stress in bean plants. The strongest effect on vitamins A, E and C, MDA, chlorophyll and carotenoids was found in plants exposed to nickel, followed by the sequence cobalt > chromium> zinc.

Key Words: Heavy metal, vitamins A, E and C, MDA, chlorophyll and carotenoids

INTRODUCTION

Heavy metals released from industrial units, metallurgical operations and mining activities pose a threat to the environment. The retention of high concentrations of heavy metals in the environment exerts toxic effects on fauna and flora (Mishra and Tripathi, 2008). Some of these heavy metals, such as As, Cd, Hg, Pb or Se, are not essential, since they do not perform any known physiological function in plants. Others, such as Co, Cu, Fe, Mn, Mo, Ni and Zn, are essential elements required for normal growth and metabolism of plants. These latter elements can easily lead to poisoning when their concentration rises to supra-optimal values. Heavy metal phytotoxicity may result from alterations of numerous physiological processes caused at the cellular/molecular level such as inactivating enzymes, blocking functional groups of metabolically important molecules, displacing or substituting essential elements and disrupting membrane integrity (Rascio and Navarri-Izzo, 2011).

Redox-active (Cu, Fe) and non-redox-active (Cd, Ni, As) metals may catalyze, directly or indirectly, the formation of free radicals (FR) and reactive oxygen species (ROS) such as superoxide radicals (O_2^-), hydrogen peroxide (H_2O_2) and hydroxyl radicals (OH^-), which generate oxidative stress and cause cell damage by inducing lipid peroxidation, protein oxidation, enzyme inhibition and DNA damage (Sharma and Dietz, 2009). Tolerant plants have evolved different antioxidative mechanisms involving enzymes such as superoxide dismutase (SOD), catalase (CAT) and ascorbate peroxidase (APX), or small metabolites such as ascorbic acid (ASA), phenolics and carotenoids to prevent and counteract the increase in and effects of ROS (Kelman et al., 2009). A second group of antioxidants includes several vitamins and nutritional trace minerals that can reduce oxidative stress by directly scavenging free radicals and by interfering with free radical-producing mechanisms. For example, vitamin A (retinyl esters and all-trans retinols) and E (α-tocopherol) preserve against the development of oxidative damage (Sies and Stahl, 1995). There are many studies on the antioxidant properties of plants exposed to various stress factors (Havaux and Kloppstech, 2001). However, studies related to the effect of heavy metal-generated stress on vitamin levels of plants are limited. Some studies showed that lead and mercury caused an increase in ascorbic acid and α-tocopherol levels in two *Oryza sativa* cultivars (Mishra and Choudhuri, 1999), and mercury exposure of *Bacopa monnieri* increased the ascorbic acid levels in this plant (Sarita et al., 1996). Demirevska-Kepova et al. (2006) reported that the content of oxidized ascorbate increased during Cd exposure in *Hordeum vulgare* plants.

An excess of metals has deleterious effects on the content and functionality of the photosynthetic pigments (Broadley et al. 2007). This can be caused by the inhibition of pigment synthesis (Prasad and Prasad 1987), the formation of metal-substituted chlorophylls of reduced functionality (Küpper et al. 1996), or direct oxidative damage to the pigments (Oláh et al. 2010). The amount of chlorophyll was reduced in *Triticum aestivum* L. (Gajewska et al., 2006) exposed to Ni, and in *Phaseolus vulgaris* L. cv. Anupama (Chatterjee et al. 2006) exposed to Co.

The aim of the present study was to investigate the effects of four heavy cations, namely nickel, cobalt, chromium and zinc, on the content of vitamins A, E and C, chlorophyll, carotenoids and MDA in bean *(Phaseolus vulgaris* L.) seedlings.

MATERIALS AND METHODS

In this study, 7-day old bean seedlings (*Phaseolus vulgaris* L.) were used. Stock solutions of nickel ($NiCl_2.6H_2O$), cobalt ($CoCl_2.6H_2O$), chromium ($CrCl_3.6H_2O$) and zinc ($ZnCl_2.H_2O$) were prepared at concentrations of 0.1, 0.3, 0.5 mM Ni; 0.5, 0.7 and 1.0 mM Co; 0.5, 0.7 and 1mM Cr and 1.5, 2.0 and 2.5 mM Zn. The recovery rates of standards were determined as 96.8% for vitamin A, 96.7 % for vitamin E and 95.5% for vitamin C. Separation times, using a flow rate of 1 ml/min, were 3.2 min for vitamin A, 3.6 for vitamin C and 5.6 min for vitamin E.

The bean seeds were surface sterilized in $HgCl_2$ for 2 min, washed in distilled water and germinated between wet paper

Corresponding author: Fikriye Zengin, Department of Science Education, Firat University, Elazig 23119, Turkey. Tel: [+90] 424-237-0000/Ext.4812, Fax: [+90] 424-233-0062, E-mail: fzengin@firat.edu.tr fkzengin@gmail.com

Received: November 11, 2012. In Revised form: February 2, 2013. Accepted: February 22, 2013

towels at 25 ºC in the dark for 3 days. Subsequently plants cultivated hydroponically in a growth chamber at a light intensity of 4500 photon/sec/m^2 (16 h light/ 8 h). During this period day/night temperatures were 25 ºC. After 7 days, plants were transferred to Hoagland solution containing 0 mM (control) and various amounts of nickel, cobalt, chromium or zinc. After 10 days of heavy metal treatment, seedlings were used for vitamin A, E and C, chlorophyll, carotenoids and MDA determinations.

The extraction of vitamin A and E was done according to Catignani (1983) and Miller et al. (1984). Leaf tissues were homogenized in ethanol and the homogenate was centrifuged at 4500xg for 5 min. The supernatant was treated with n-hexane. Vitamin A and E were extracted twice in hexane phase and the collected extract was dried in liquid nitrogen. The dried extract was solubilized in 0.5 ml methanol for HPLC. Injections were made in duplicate for each sample. The quantification was according to (Catignani, 1983; Miller et al., 1984) utilizing absorption spectra of 326 and 296 nm for vitamin A and E, respectively. HPLC separations were accomplished at room temperature with a Perkin-Elmer liquid chromatography system (Series 1100) consisting of a sample injection valve (Cotati 7125) with a 20 µl sample loop, an ultra-violet (UV) spectrophotometric detector (Cecil 68174), an integrator (HP 3395) and a Techsphere ODS-2 packed (5 µm particle and 80 ºA pore size) column (250 x 4.6 ID) with a methanol: acetonitrile: chloroform (47: 42: 11, v/v) mobile phase at 1 ml min^{-1} flow rate. The extraction of vitamin C was done according to Cerhata et al. (1994) Leaf tissues were homogenized in perchloric acid and volume was adjusted to 1 ml by adding ddH_2O. The mixture was centrifuged at 4500 x for 5 min at 4 ºC. The supernatant was filtered as above and the vitamin C level was determined using the method of Tavazzi et al. (1992) by HPLC, utilizing a column (250 x 4.6 ID) packed with Li-60 reversed-phase material (10 µm particle size) with mobile phase (3.7 mM phosphate buffer, pH 4.0) at 1 ml min^{-1} flow rate.

The level of lipid peroxidation was measured in terms of MDA content, a product of lipid peroxidation. Leaf samples (0.5 g) were homogenized in 10 ml of 0.1% TCA. The homogenate was centrifuged at 15,000g for 5 min. To as 1.0 ml aliquot of the supernatant 4.0 mL of 0.5% TBA in 20% TCA was added. The mixture was heated at 95 ^{0}C for 30 min and then quickly cooled in an ice bath. After centrifugation at 10,000g for 10 min, the absorbance of the supernatant was recorded at 532 nm. The value for non-specific absorption at 600 nm was subtracted. The Following formula should be added after the MDA equivalent was calculated as follows (Heath and Packer 1968).

$$\text{MDA (nmol/mL FW)} = [(A532-A600)/155,000] \times 10^6$$

For the purpose of identifying the amount of photosynthetic pigments, about 1 g of fresh leaf tissue was obtained from the seedlings and extracted. The absorbance of these extracts was measured separately at 645 nm and 633 nm wavelengths in a blind manner. To determine absorbance, quartz tubes with a volume of 1 cm^3 were utilized. Using the absorbance values, chlorophyll a+b and carotenoid content were calculated as mg/g FW (Witham et al. 1971).

All experiments were repeated three times. Statistical analysis was performed using the SPSS (version 10.0) program. In order to detect the significance of differences ($p<0.01$ or $p<0.05$) of variables, a multiple comparison (LSD) test was performed. All values are expressed as mean ± 1 SE.

RESULTS

Figs 1-7 summarize the results for the effects of selected heavy metals (Ni, Co, Cr, and Zn) on vitamins, chlorophyll, carotenoids and MDA in primary leaves of bean seedlings. Significant increases of the content of vitamins, chlorophyll, carotenoids and MDA ($p<0.05$ or $p<0.01$) were detected after ten day exposure to the heavy metals.

In nickel-treated seedlings the amount of vitamin was significantly greater than in control seedlings ($p<0.05$). Vitamin A content in the primary leaves increased noticeably at 0.1, 0.3 and 0.5 mM nickel concentrations (Fig. 1A). Vitamin A content in leaves increased by 14.1%, 15.8% and 18.4%, respectively, compared to control seedlings ($p<0.05$). Nickel caused the increase of vitamin E between 12-18% ($p<0.05$) (Fig. 1B). These seedlings had significantly greater vitamin C content than control seedlings (Fig. 1C). Vitamin C content in seedlings increased noticeably at 0.1, 0.3 and 0.5 mM nickel concentrations. With 0.1, 0.3 and 0.5 mM nickel concentrations, vitamin C contents were increased a dose-dependent manner (7.5%, 13.6%, and 19.7%).

In cobalt treated seedlings vitamin content was significantly more effective than in control seedlings ($p<0.01$). The vitamin content of seedlings increased with increasing concentration of this metal (Fig. 2A, 2B, 2C). In seedlings treated with 0.5, 0.7 and 1 mM cobalt, vitamin A content increased by 12.3%, 14.9%, and 17.5%, respectively, compared to control plants ($p<0.01$). In seedlings treated with 0.5, 0.7 and 1 mM cobalt, vitamin E content increased by 10.2%, 13.1%, and 17.1%, respectively, compared to control plants ($p<0.01$) (Fig 2B). Vitamin C content of seedlings was increased by 4.6%, 10.3% and 14.6% compared to controls (Fig 2C).

Vitamin A, E, and C content of the seedling increased with increasing concentration of chromium (Fig. 3A, 3B, 3C). Chromium caused the increase of vitamin A between 10.5-16.7% ($p<0.05$) (Fig. 3A). In chromium-treated seedlings the vitamin E content was significantly greater than in control seedlings ($p<0.01$) (Fig 3B). In seedlings treated with 0.5, 0.7 and 1.0 mM chromium, vitamin C content increased by 7.51%, 12.2%, and 15%, respectively, compared to control plants ($p<0.01$) (Fig 3C).

The increase of zinc concentration in seedlings caused significant vitamin accumulation. In seedlings treated with 1.5, 2.0 and 2.5 mM zinc; vitamin A content increased by 9.6%, 12.7%, and 14.1%, respectively, compared to control plants ($p<0.01$) (Fig 4A). These seedlings had significantly greater vitamin E content than control seedlings (Fig. 4B). Vitamin E content in seedlings increased noticeably (5.9%, 9.1% and 12.2%) at 1.5, 2.0 and 2.5 mM zinc concentrations. The increase of zinc concentration in primary leaves caused significant vitamin C accumulation. In primary leaves treated with 1.5, 2.0 and 2.5 mM zinc, vitamin C content increased by 4.2%, 8.9%, and 13.1%, respectively, compared to control plants ($p<0.01$) (Fig. 4C).

The effect of heavy metals on MDA content is presented in Figure 5. Significant increases in MDA content in *bean* plants were observed in the experiments. MDA content increased linearly with increased heavy metal levels in the solution. The MDA content was increased by 47.2%, 55.4%, and 66.3% at 0.1,

0.3 and 0.5 mM Ni, 41.8%, 49.1% and 53.6% at 0.5, 0.7 and 1.0 mM Co, 27.2%, 31.8% and 42.7% at 0.5, 0.7 and 1.0 mM Cr, 20%, 26.3% and 30.9% at 1.5, 2.0,2.5 mM Zn, respectively

The chlorophyll content in the plants was significantly affected by heavy metal treatment (Fig. 6). For example, chlorophyll contents in leaves decreased by 25.6%, 23.1%, 21.2% and 19.3% at 0.5 mM Ni, 1 mM Co, 1 mM Cr and 2.5 mM Zn, respectively, compared to the control seedlings ($p<0.05$).

Carotenoids decreased significantly with increasing concentrations of heavy metals (Fig. 7). For example, carotenoids increased by 15%, 23.1% and 27.3% at at 0.1, 0.3 and 0.5 mM Ni, 8%, 13.5% and 17% at 1.5, 2.0 and 2.5 mM Zn respectively.

DISCUSSION

Many abiotic stresses, including exposures to heavy metals, can cause damage to plant cells either directly or indirectly through the burst of ROS. Plant cells are able to respond to elevated levels of ROS by activating their antioxidant defense system (Dazy et al., 2008). It is well known that exposure of plants to heavy metals induces the generation of active oxygen species (AOS), which are harmful to plants (Zenk, 1996). The injury of plant cells caused by heavy metals is, to a great extent, related to the destruction of the balance between the generation and detoxification of AOS. Plants possess the protective mechanisms to scavenge the toxic AOS, but the ability to balance between the generation and detoxification of AOS varies greatly among different plant species (Pang et al., 2003). Heavy metal treatment could enhance the activities of antioxidant vitamins. Plants contain a wide range of vitamins that are essential not only for human metabolism but also for plants, because of their redox chemistry and role as cofactors, and some of them also have strong antioxidant potential. The antioxidant vitamins that have been the focus of most attention in plants are carotenoids (pro-vitamin A), ascorbate (vitamin C) and tocochromanols (vitamin E, including both tocopherols and tocotrienols) (Asensi-Fabado and Munné- Bosch 2010). We

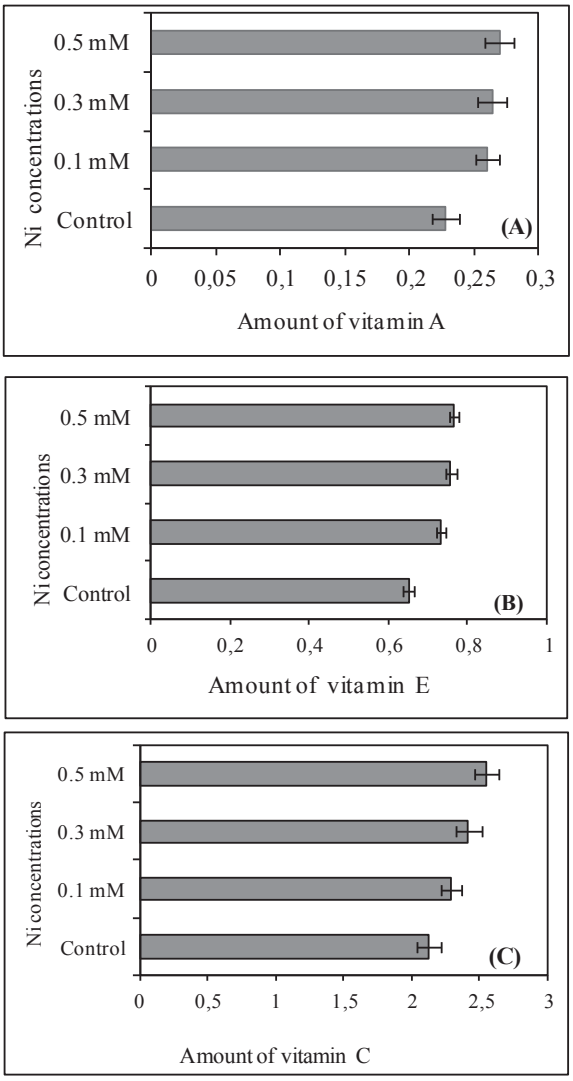

Figure 1. (A) Vitamin A [μg/g], **(B)** Vitamin E [μg/g fw] and **(C)** Vitamin C [μg/g] content in the primary leaves of bean seedlings applying different concentrations of nickel. Error bars indicate ± 1 SE.

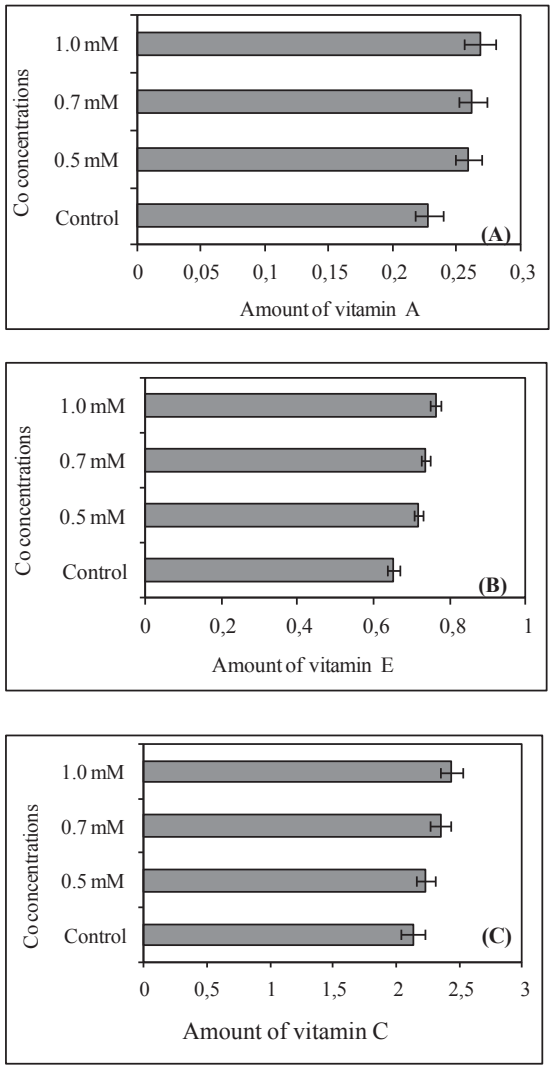

Figure 2. (A) Vitamin A [μg/g], **(B)** Vitamin E [μg/g fw] and **(C)** Vitamin C [μg/g] content in the primary leaves of bean seedlings applying different concentrations of cobalt. Error bars indicate ± 1 SE.

found that all four metals caused a significant ($p<0.01$, $p<0.05$) increase in vitamins A, E and C.

It was determined that all four metals caused a significant ($p<0.01$, $p<0.05$) increase in vitamin E. Increasing levels of α-tocopherol has been found in *Arabidopsis thaliana* under Cu and Cd stress (Collin et al., 2008). Yusuf et al. (2010) reported that the content of total tocopherol increased during salt, heavy metal and osmotic stress in *Brassica juncea* plants. Vitamin E includes tocopherols, one of the most powerful antioxidants, and tocotrienols (Schneider, 2005). Tocopherols have been suggested to play a major role in maintenance and protection of the photosynthetic machinery. There is clearly a correlation between the degree of stress and tocopherol concentration (Munné-Bosch and Alegre, 2002a). Gajewska and Sklodowska (2007) and Collin et al. (2008) have suggested that increased tocopherol content confers enhanced tolerance to plants against drought and heavy metal (Ni, Cu, Cd) stress. Tocopherols are able to quench physically or scavenge chemically $^1O_2$ (Krieger-Liszkay and Trebst, 2006). Fryer (1992) suggested that the changes in α-tocopherol during plant responses to environmental stress are characterized by two phases. In the first phase, there is an increase in tocopherol synthesis, which is followed by a second phase of net tocopherol loss. Initial enhanced tocopherol levels contribute to protection by reducing by ROS levels and inhibiting lipid peroxidation, thus avoiding oxidative damage. When the stress is too severe, tocopherol degradation exceeds its synthesis and levels decrease (phase II). Consequently, lipid peroxidation increases and cell death occurs if α-tocopherol deficiency cannot be compensated for by another mechanism of protection. In stress-tolerant plants, only the first phase is apparent (unless stress is too severe), while only the second phase is usually observed in stress-sensitive plants (Munné-Bosch, 2005).

In the present study, exposure to heavy metal (Ni, Co, Cr, Zn) level in the growth medium resulted in increased vitamin C in bean plants. The exposure of *Bacopa monnieri*

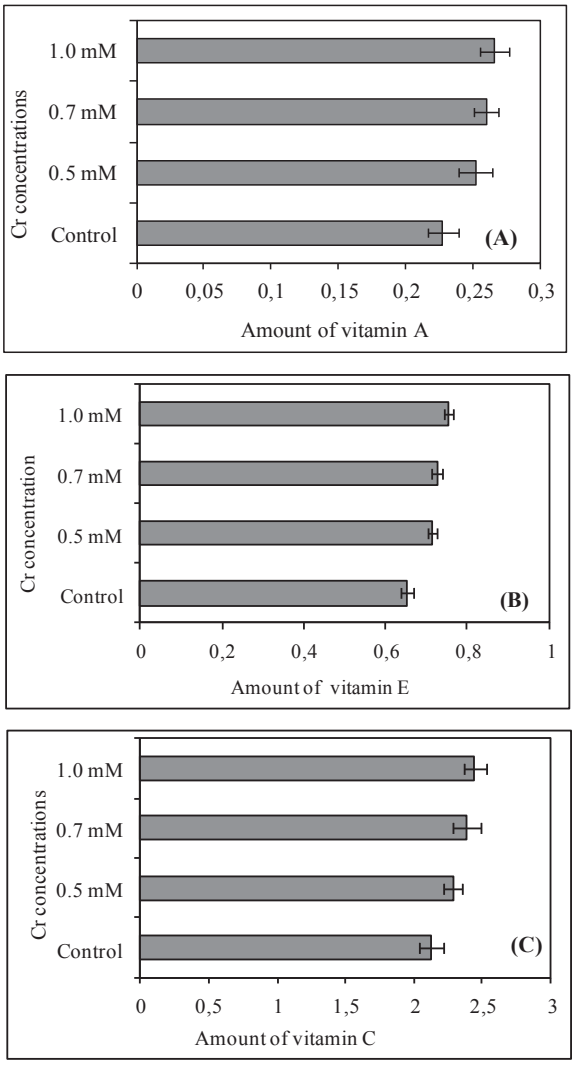

Figure 3. (A) Vitamin A [μg/g], **(B)** Vitamin E [μg/g fw)] and **(C)** Vitamin C [μg/g] content in the primary leaves of bean seedlings applying different concentrations of chromium. Error bars indicate ± 1 SE.

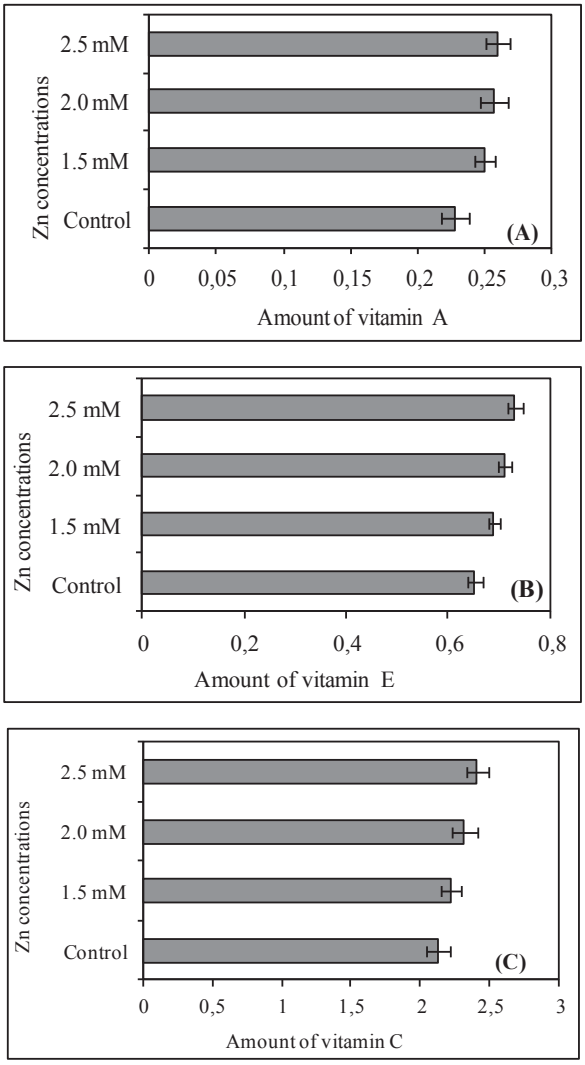

Figure 4. (A) Vitamin A [μg/g], **(B)** Vitamin E [μg/g fw] and **(C)** Vitamin C [μg/g] content in the primary leaves of bean seedlings applying different concentrations of zinc. Error bars indicate ± 1 SE.

to various concentrations of mercury for 14 days caused an increase in ascorbic acid levels (Sarita et al., 1996). ASA is the most abundant antioxidant in plants and plays a role in responding to oxidative stress (Chao et al., 2010). Besides, it participates in a variety of processes, including photosynthesis, photoprotection, the cell cycle, cell-wall growth and cell expansion, synthesis of ethylene, gibberellins, anthocyanins, and hydroxyproline. ASA is found in the thylakoid lumen and stroma of chloroplasts (Asada, 1999), α-tocopherol and β-carotene are found in the lipid matrix, and associated with protein domains in the tylakoid membrane (Munné-Bosch and Alegre, 2002a), which provides a protective effect of ASA on α-tocopherol and β-carotene oxidation, likely by scavenging and/or preventing the formation of OH^-. Exposure to heavy metal (Ni, Co, Cr, Zn) levels in the growth medium resulted in increased vitamin A of bean plants (Fig 1A, 2A, 3A, 4A). Vitamin A (retinol) is the most effective naturally occurring quencher of singlet oxygen; it is a radical scavenger and an effective chain-breaking antioxidant (Alpsoy et al., 2009). Vitamin E is a potent lipid-soluble antioxidant, with the ability to quench free radicals directly, and functions as a membrane stabilizer (Clarke et al., 2008). Carotenoids, ubiquinols, selenium (Se), copper (Cu) and flavonoids are also included in this group of nutritional antioxidants (Surai, 2003).

The level of MDA content has been considered as an indicator of oxidative stress. MDA is the decomposition product of polyunsaturated fatty acids of biomembranes and its increase shows that plants are under high-level antioxidant stress. Cell membrane stability has been used freqently to discriminate stress tolerant and sensitive cultivars of many crops (Hou et al., 2007). In the experiments, MDA concentration increased linearly with increased heavy metal (Ni, Co, Cr, Zn) levels in the solution. Similar results were obtained with *S. polyrrhiza* L. (Upadhyay, 2010) and *Ceratophyllum demersum* L. (Devi and Prasad, 1998). Thus increased MDA content shows the generality of oxidative stress and this may be one of the potential mechanisms by which toxicity due to heavy metals is manifested in plant tissues (Gupta et al., 2009).

Inhibition of photosynthetic pigment biosynthesis is one of the primary events in plants during heavy metal stress and decreases in photosynthetic pigment content have also been reported in many plants under heavy metal stress (Cenkci et al., 2010). It was suggested that heavy metals could interfere with chlorophyll biosynthesis either through the direct inhibition of enzymatic steps or through the substitution of the central Mg ion (Cenkci et al., 2010; Pourraut et al., 2011). Carotenoids serve as antioxidants against free radicals and photochemical damage (Sengar et al., 2008). Thus less effect on carotenoids might represent its supportive role against oxidative stress.

CONCLUSIONS

In the present study, exposure to heavy metals affected different parameters of bean: vitamin, MDA, chlorophyll and carotenoid content. Exposure of ten-day-old bean seedlings to nickel, cobalt, chromium and zinc increased vitamin, MDA and carotenoid contents. Chlorophyll content decreased with heavy metal (Ni, Co, Cr, Zn) treatment in comparison to the control.

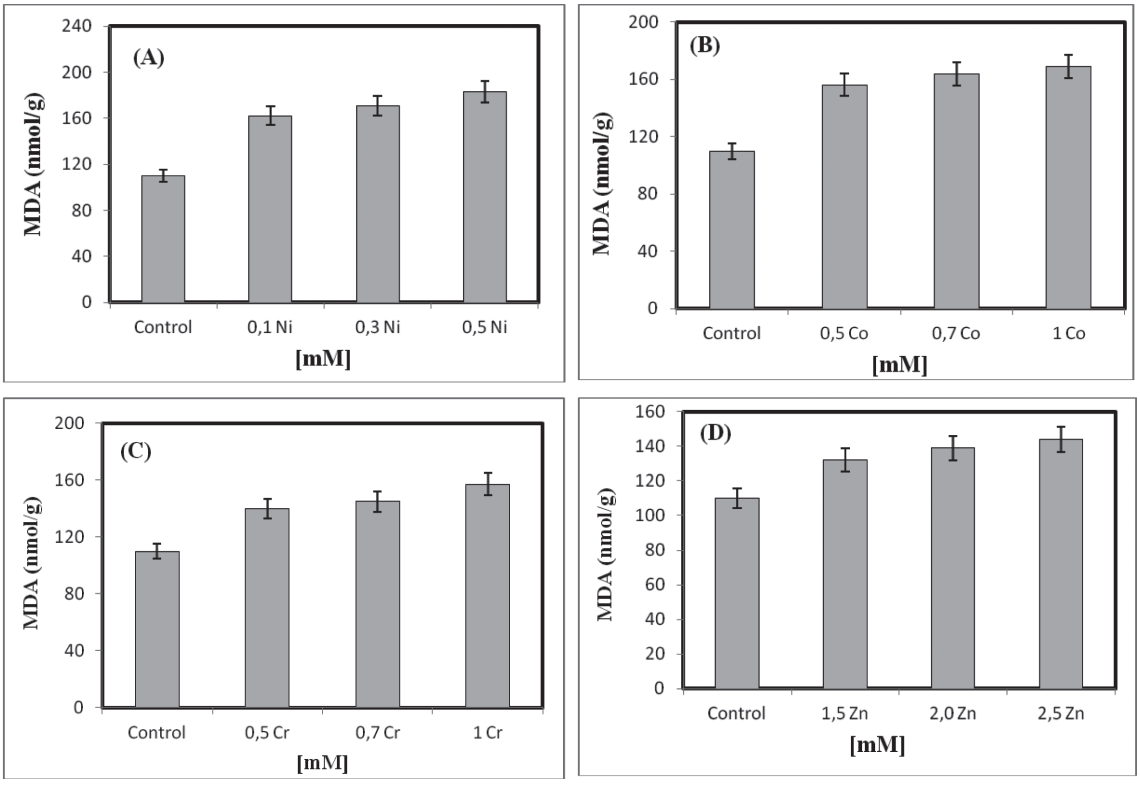

Figure 5. MDA content [nmol g^{-1} fw] in the leaves of bean seedlings at various concentrations of heavy metals. **(A)** Nickel, **(B)** Cobalt, **(C)** Chromium, **(D)** Zinc. Error bars indicate ± 1 SE.

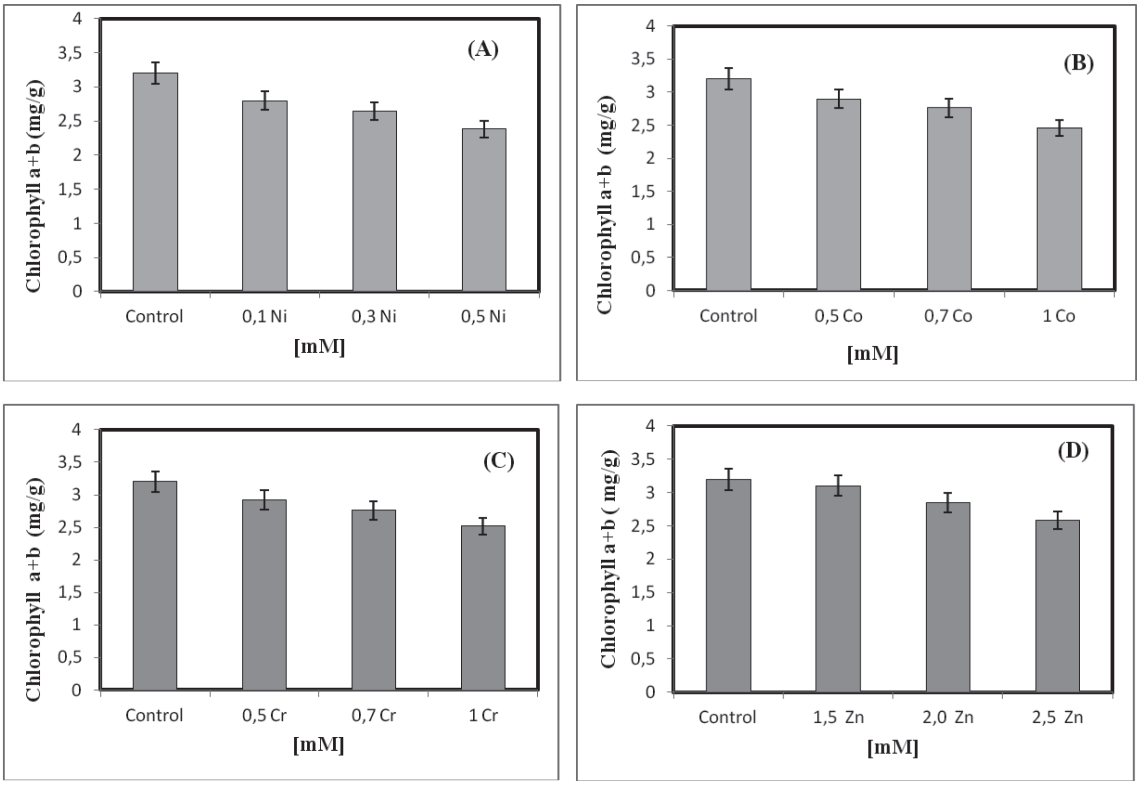

Figure 6. Chlorophyll (a+b) content [µmol/l fw] in the leaves of bean seedlings at various concentrations of heavy metals. **(A)** Nickel, **(B)** Cobalt, **(C)** Chromium, **(D)** Zinc. Error bars indicate ± 1 SE.

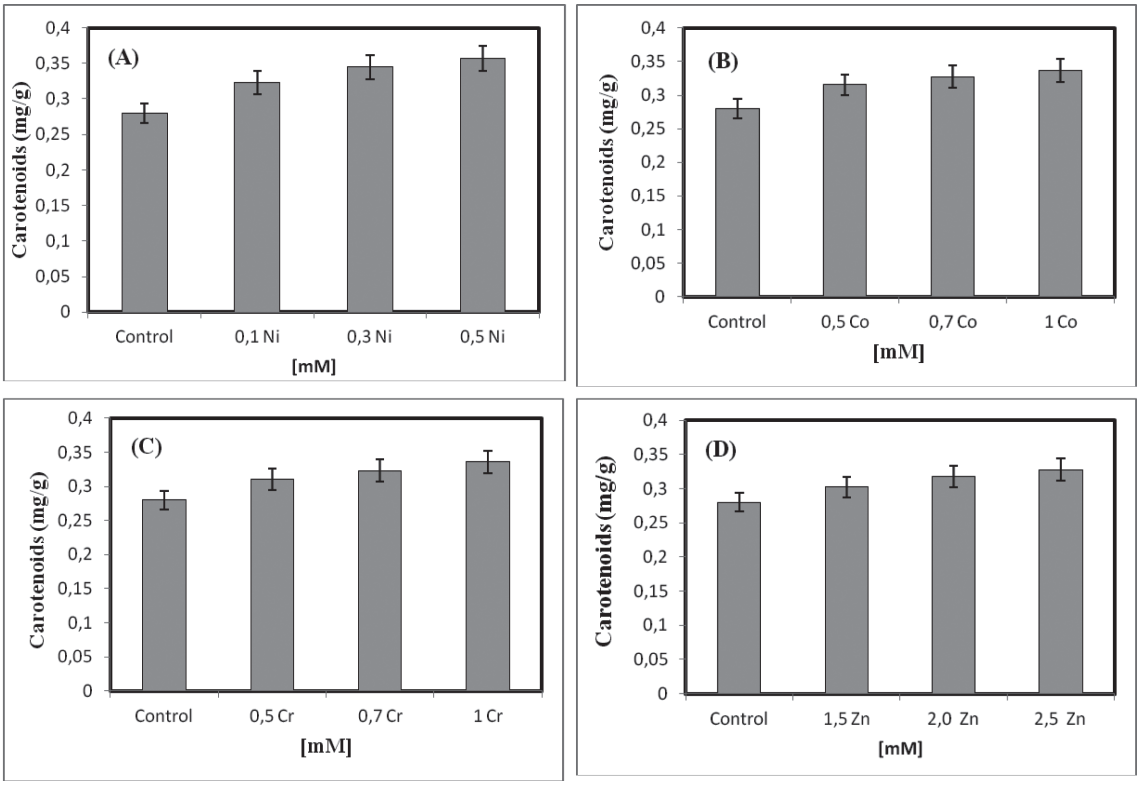

Figure 7. Carotenoid content [µmol g^{-1} fw] in the leaves bean seedlings at various concentrations of heavy metals. **(A)** Nickel, **(B)** Cobalt, **(C)** Chromium, **(D)** Zinc. Error bars indicate ± 1 SE.

The greatest effects were produced in plants exposed to nickel, followed by the sequence cobalt> chromium>zinc.

REFERENCES

ALPSOY L, YILDIRIM A, AGAR G (2009) The antioxidant effects of vitamin A, C and E on aflatoxin B1-induced oxidative stress in human lymphocytes. Tox Ind Healt 25(2): 121–7.

ASADA K (1999) The water- water cycle in chloroplasts: scavenging of active oxygens and dissipation of excess photons. Annu Rev Plant Physiol Plant Mol Biol 50: 601-639.

ASENSI-FABADO MA, MUNNÉ- BOSCH S (2010) Vitamins in plants: occurance, biosynthesis and antioxidant function. Trends in Plant Science15: 582-592.

BROADLEY MR, WHITE PJ, HAMMOND JP, ZELKO I, LUX A (2007) Zinc in plants. New Phytol 173:677–702

CATIGNANI GL (1983) Simultaneous determination of retinol and tocopherol in serum of plasma by liquid chromatography. Clin Chem 2914: 708-712.

CENKCI S, CIGERCI IH, YILDIZ M, OZAY C, BOZDAG A, TERZI H (2010) Lead contamination reduces chlorophyll biosynthesis and genome template stability in Brassica rapa L. Environ Exp Bot 67: 467–473.

CERHATA D, BAUEROV A, GINTER E (1994) Determination of ascorbic acid in blood serum using high-performance liquid chromatography and its correlation with spectrophometric. Caska-Slov-Farm 43 (4): 166-168.

CHAO YY, HONG CY, KAO CH (2010) The decline in ascorbic acid content is associated with cadmium toxicity of rice seedlings. Plant Physiol Biochem 48: 374-381.

CHATTERJEE C, RAJEEV G, DUBE BK (2006) Physiological and biochemical responses of French bean to excess cobalt. Journal of Plant Nutrition 29: 127–136.

CLARKE MW, BURNETT JR, CROFT KD (2008) Vitamin E in human health and disease. Crit Rev Clin Lab Sci 45(5): 417–50.

COLLIN VC, EYMERY F, GENTY B, REY P, HAVAUX M (2008) Vitamin E is essential for the tolerance of Arabidopsis thaliana to metal-induced oxidative stress. Plant Cell and Environment 31: 244-257.

DAZY M, BÉRAUD E, COTELLE S, MEUX E, MASFARAUD JF, FÉRARD VF (2008) Antioxidant enzyme activities as effected by trivalent and hexavalent chromium species in Fontinalis antipyretica. Hedw 73: 281-290.

DEMIREVSKA-KEPOVA K, SIMOVA-STOILOVA L, STOYANOVA ZP, FELLER U (2006) Cadmium stress in barley: growth, leaf pigment, and protein composition and detoxification of reactive oxygen species. J Plant Nutr 29: 451-468.

DEVI SR, PRASAD MNV (1998) Copper toxicity in Ceratophyllum demersum L. Coontail, a free floating macrophyte: response of antioxidant enzyme sand antioxidants. Plant Sci 138: 157–165.

FRYER MJ (1992) The antioxidant effects of thylakoid vitamin E (α-tocopherol). Plant Cell Environ 15: 381-392.

GAJEWSKA E, SKLODOWSK M, SALABA, MAZUR J (2006) Effect of nickel on antioxidative enzyme activities, proline, chlorophyll contents in wheat shoots. Biol Plan 50(4):653-659.

GAJEWSKA E, SKLODOWSK M (2007) Relations between tocopherol, chlorophyll and lipid peroxides contents in shoots of Ni-treated wheat. J Plant Physiol 164: 364-366.

GUPTA DK, NICOLOSO FT, SCHETINGER MRC, ROSSATO LV, PEREIRA LB, CASTRO GY,

SRIVASTAVA S, TRIPATHII RD (2009) Antioxidant defence mechanism in hydroponically grown Zea mays seedlings under moderate lead stress. J Hazard Mater 172 (1): 479–484.

HAVAUX M, KLOPPSTECH K (2001) The protective functions of carotenoid and flavanoid pigments against excess visible radiation at chilling temperature investigated in Arabidopsis npq and tt mutants. Planta 213: 953-966.

HEATH RL, PACKER L (1968) Photoperoxidation in isolated chloroplasts. I. Kinetics and Stoichiometry of fatty acid peroxidation. Arch Biochem Biophys 125: 189–198.

HOU W, CHEN X, SONG G, WANG Q, CHANG CC (2007) Effect of copper and cadmium on heavy metal polluted water body restoration by duckweed (Lemna minor). Plant Physiol Biochem 45: 62–69.

KELMAN D, BEN-AMOTZ A, BERMAN-FRANK I (2009) Carotenoids provide the major antioxidant defence in the globally significant N_2-fixing marine cyanobacterium Trichodesmium. Environ Microb 11: 1897-1908.

KRIEGER-LISZKAY A, TREBST A (2006) Tocopherol is the scavenger of singlet oxygen produced by the triplet states of chlorophyll a in the photosystem II reaction center. J Exp Bot 57: 1677-1684.

KUPPER H, KUPPER F, SPILLER M (1996) Environmental relevance of heavy metal-substituted chlorophylls using the example of water plants. J Exp Bot 47: 259–266.

MILLER KW, LORR NA, YANG CS (1984) Simultaneous of plasma retinol α tocoferol, lycopere, α-carotene, and β-carotene by high performance liquid chromatography. Analytical Biochem 138: 340-345

MISHRA A, CHOUDHURI MA (1999) Monitoring or phytotoxicity of lead and mercury from germination and early seedling growth induces two rice cultivars. Water Air and Soil Pollut 114 (3/4): 339-346

MISHRA VK, TRIPATHI BD (2008) Concurrent removal and accumulation of heavy metals by the three aquatic macrophytes. Bioresour Technol 99: 7091–7097.

MUNNÉ-BOSCH S, ALEGRE L (2002a) The function of tocopherols and tocotrienols in plants. Crit Rev Plant Sci 21: 31-57.

MUNNÉ-BOSCH S (2005) The role of α-tocopherol in plant stress tolerance. J Plant Physiology 16: 743-748.

OLAH V, LAKATOS G, BERTOK C, KANALAS P, SZOLLOSIZ E, KIS J, MESZAROS I (2010) Short-term chromium (VI) stress induces different photosynthetic responses in two duckweed species, *Lemna gibba* L. and *Lemna minor* L. PHOTOSYNTHETICA 48: 513–520.

PANG J, CHAN GSY, ZHANG J, LIANG J, WONG MH (2003) Physiological aspects of vetiver grass for rehabilitation in abandoned metalliferous mine waste. Chemosp52: 1559-1570.

POURRAUT B, SHAHID M, DUMAT C, WINTERTON P, PINELLI E (2011). Lead uptake, toxicity and detoxification in plants. Rev Environ Contam Toxicol 213: 113–136.

PRASAD DDK, PRASAD ARK (1987) Altered delta-aminolevulinic-acid metabolism by lead and mercury in germinating seedlings of bajra (*Pennisetum typhoideum*). J Plant Phys 127:241–249.

RASCIO N, NAVARRI-IZZO F (2011) Heavy metal hyperaccumulating plants: How and why do they do it? And what makes them so interesting. Plant Science 180: 169–181.

SARITA S, MANISHA G, PRAKASH C (1996) Bioaccumulation and biochemical effects of mercury in the plant *Bacopa monnieri* L. Environ Toxi and Wat Quality 11(2): 105-112.

SCHNEIDER C (2005) Chemistry and biology of vitamin E. Mol Nutr Food Res 49: 7-30.

SENGAR RK, GAUTAM M, SENGAR RK, GRAG SK, SENGAR K, CHAUDHARY R (2008) Lead stress effects on physiobiochemical activities of higher plants. Rev Environ Contam Toxicol 196: 73–93.

SHARMA SS, DIETZ KJ (2009) The relationship between metal toxicity and cellular redox imbalance. Trends Plant Sci 14: 43-50.

SIES H, STAHL W (1995) Vitamins E and C, β-carotene, and other carotenoids as antioxidants. Am J Clin Nutr 62(6): 1315S–21S.

SURAI PF (2003) Antioxidant systems in the animal body. In: Surai PF, editor. Natural antioxidants in avian nutrition and reproduction. UK: Nottingham Univers Press; 1-25.

TAVAZZI B, LAZZARINO G, DI-PIERRO D, GIARDINA B (1992) Malondialdyde production and ascorbate decrease are associated to the reperfusions of the isolated postischemic rat heart free- radic. Biol Med 13 (1): 75-78.

UPADHYAY R (2010) Zinc reduce scopper toxicity induced oxidative stres by promoting antioxidant defense in freshly grown aquatic duck weed Spirodela polyrrhiza L. J Hazard Mater 17 (1–3): 1081–1084.

WITHAM FH, BLAYDES DF, DEWLIN RM (1971) Experiments in Plant Physiology. Von Nostrand Reinhold Company, New York, pp. 55–56.

ZENK MH (1996) Heavy metal detoxification in higher plants a review. Gene 179: 21-30.

YUSUF KA, KUMAR D, RAJWANSHI R, STRASSER RJ, TSIMILLI-MICHAIL M, GOVINDJEE M, SARIN NB (2010) Overexpression of γ-tocopherol methyl transferase gene in transgenic Brassica juncea plants alleviates abiotic stress: Physiological and chlorophyll a fluorescence measurements. Biochimica et Biophysica Acta 1797: 1428-1438.

Biol Res 46: 87-95, 2013

Antitumor function and mechanism of phycoerythrin from *Porphyra haitanensis*

Qunwen Pan, Meizhen Chen*, Juan Li, Yan Wu, Chao Zhen, Bin Liang

Department of Biology and Guangdong provincial key laboratory of Marine Biotechnology, Shantou University, Shantou, Guangdong 515063, China

ABSTRACT

The anti-tumor effect of R-Phycoerythrin (R-PE) from *Porphyra haitanensis* was studied using cell line HeLa as an *in vitro* model and Sarcoma-180 (S180) tumor-bearing mice as an *in vivo* model. The results showed that the combination treatment of R-PE and photodynamic therapy PDT) significantly inhibited the growth of HeLa cells up to 81.5%, with a fair dose-effect relationship, but did not inhibit endothelial cells. The annexin v-fitc/PI fluorescence staining experiments demonstrated that at doses between 0~60μg/mL, apoptosis cells and later stage apoptosis cells or necrosis cells increased significantly as the R-PE dosage increased. DNA electrophoresis showed that after R-PE+PDT treatment of HeLa cells for 24 hours, a light "smear" band between 100~400bp appeared to indicate the degradation of genomic DNA. The QRT-PCR results showed that R-PE+PDT treatment increased caspase-3 and caspase-10 gene expression and decreased the Bcl-2 gene expression level significantly as the R-PE dose increased, implying that R-PE promoted HeLa cell apoptosis. Compared with untreated S180 tumor-bearing mice, R-PE injection significantly inhibited the growth of S180 in tumor-bearing mice up to 41.3% at a dose of 300mg·kg^{-1}. Simultaneously, the significant increase of superoxide dismutase (SOD) activity in serum ($p < 0.01$) and the decrease of the malondialdehyde (MDA) level in liver suggests that R-PE improved the anti-oxidant ability of the S180 tumor-bearing mice, which may related to its antitumor effect. In addition, the R-PE caused a significant increase ($p < 0.05$) in the spleen index and thymus index, and a significant increase ($p < 0.01$) in lymphocyte proliferation, NK cell kill activity and the TNF-α level in the serum of S180 tumor-bearing mice. These results strongly suggest that the antitumor effect of R-PE from *Porphyra haitanensis* functioned by increasing the immunity and antioxidant ability of S180 tumor-bearing mice, promoting apoptosis by increasing protease gene expression and TNF-α secretion.

1. INTRODUCTION

Phycoerythrin (PE) is an oligomeric protein formed in a $(\alpha\beta)_6$ hexamer in an annular architecture. The two different subunits, α and β, have molecular weights of 17 to 21 KDa.. Each α subunit contains 2 phycoerthrobilin (PEB) chromophores which link to Cys82 and Cys139 by a thioester bond. Each β subunit contains two PEBs linking to Cys82 and Cys158 and one phycourobilin (PUB) linking to two cysteines, Cys50 and Cys61. The PE hexamers can pile up to form rods which allow the pigment molecules to play an important role in light absorption, storage and transmission. The PE purified from *Porphyra haitanensis* belongs to *R* type PE (R-PE), with characteristic absorption peak of 498 nm from its linked PUB which allows it to play a photosensitive role (1-4).

Photodynamic therapy (PDT), the activation of a tumor-localized photosensitizer by light, is generally applied as a single modality for the treatment of a variety of solid tumors, and has received regulatory approval. Its dominant mechanism of action is the local generation of cytotoxic singlet oxygen, which causes the destruction of tumor cells and damage to the tumor microvasculature. PE is an attractive photosensitizer because of its good fluorescence characteristics (2 PEB, 1 PUB) (5-8); it has drawn considerable attention because of its low phototoxicity. Ling Hu et al. (9) studied the survival rate of the normal liver cell line HL7702 and liver cancer cell line HepG2 after treatment with 25~200 μg/mL of the β subunit of PE. Comparison of PE in four different treatments, PE subunit alone (PE-sub), PE subunit with liposome package (PE-sub-lip), PE subunit with laser irradiation (PE-sub-PDT) and PE subunit with liposome package and laser irritation (PE-sub-lip-PDT), demonstrated that the use of the liposome carrier increased the PE-sub accumulation in the cells and enhanced its PDT effect on HepG2.

Caspase is a special family of proteases which play a central role in programmed cell apoptosis (10). Caspases can degrade anti-apoptotic protein and induce the release of mitochondrial cytochrome C. At the same time, caspase-mediated degradation can weaken the function of DNAase inhibitor ICAD (inhibitor of caspase DNAase), thus increasing intracellular Ca^{2+} concentration, activating DNAase and encouraging the fragmentation of DNA as depicted in Fig. 1 (11-14).

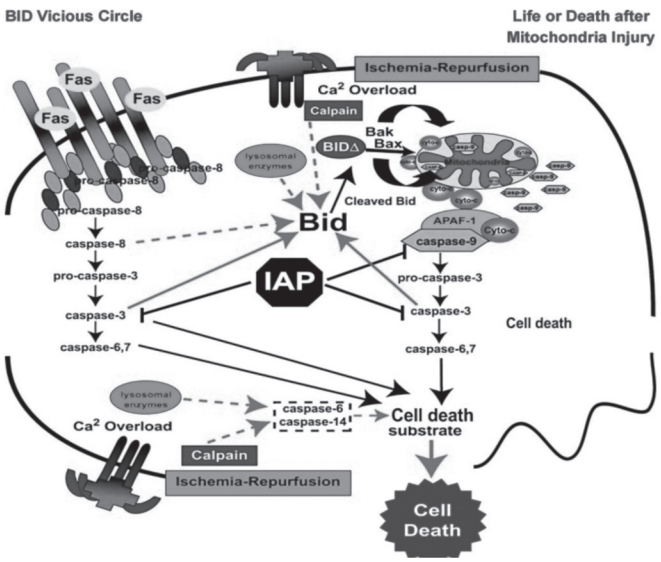

*Corresponding author: Prof. Mei-Zhen Chen. Department of Biology, School of Science. Shantou University. Shantou, Guangdong, China 515063. Tel: +86-754-86502918. Fax: +86-754-86502767. E-mail: chenmz@stu.edu.cn

Received: September 24, 2012. In Revised form: Februayr 2, 2013. Accepted: February 5, 2013

Fig. 1. Graphic summary of events after global brain ischemia during reperfusion. The activation of major, caspase-dependant apoptosis pathways, the possible cross-talk between necrosis-inducing cytoplasmic-lysosomal proteases and their possible interaction with Bcl-2 and caspase protein families are depicted (12).

The objective of this investigation was to study the *in vivo* and *in vitro* anti-tumor effect of R-PE from *Porphyra haitanensis*. The results showed that R-PE had a strong *in vivo* and *in vitro* anti-tumor effect, and that PDT can improve the *in vitro* anti-tumor effect of R-PE. These results may provide a basis for developing the PE into a photosensitive drug for cancer therapy.

2. MATERIALS AND METHODS

PE from *Porphyra haitanenis* (R-PE), with food grade purity (A565/A280>0.7) and drug class purity (A565/A280>2.0) was obtained in the laboratory. The cervical carcinoma cell line HeLa, mouse ascitic tumor cell line S180 and KM mice (qualified number: SCXKG Fujian 2004-0001) were obtained from the animal center of Xiamen University, Xiamen, China. Concanavalin (ConA) and MTT was purchased from Sigma (St Louis, MO, USA).

2.1. Extraction and purification of phycoerythrin

Fresh *Porphyra haitanenis* was washed with 1 M PBS buffer (pH 6.8). One volume of washed algal mass was resuspended in fifteen volumes of the same buffer and subjected to repeated freeze-thaw cycles of -20 °C and 4 °C for the release of PE. Purification was done by two-step ammounium sulphate precipitation (25% and 55%) followed by chromatography using a gel sephadex G-100 column (60cm×2cm) pre-equilibrated and eluted with 10mM PBS buffer (pH 7.0). The flow rate was maintained at 45ml·h^{-1}. Elute was collected and run through a DEAE-Cellulose ion exchange column (30cm×2cm) pre-equilibrated with 20mM PBS buffer (pH6.0). The R-PE rich fraction was eluted at 0.2M NaCl. The R-PE was stored at -20 °C. At each stage of purification the R-PE purity and molecular weight were determined by 12% SDS-PAGE (Fig. 1). The R-PE purity measured as the ratio of OD565/OD280 was also determined at each stage of purification (Table 2). The UV-vis overlay spectrum for purified R-PE is shown in Fig. 2.

2.2. R-PE PDT effect on HeLa cells

2.2.1. Cell culture

Cervical carcinoma line HeLa was routinely grown in Dulbecco's Modified Eagle's medium (DMEM) supplemented with 10% fetal bovine serum and 1% penicillin/streptomycin and kept in an atmosphere of 95% air and 5% CO_2 in a 37 °C humidified incubator.

2.2.2. PDT

In total, 5×10^4 /mL cells were inoculated in 96-well plates with serum-free DMEM and treated with 0, 3.5, 7, 15, 30 or 60μg/mL R-PE for 4h before laser irradiation. The PDT excitation wavelength was 632.8 nm and energy intensity was 12.5 J/cm^2 laser light; the two kinds of cells were cultured in DMEM containing 10% serum for 24h and 48h, respectively. Each concentration was repeated 6 times, along with a blank control (without R-PE or laser light irradiation) and a positive control group (treated with 20μg/mL 5-fluorouracil). The survival rate of the PDT-treated HeLa cell lines was analyzed using the 3-(4, 5-dimethylthiazol-2-yl)-2,5-diphenyltetrazolium bromide assay.

$$\text{Cell survival rate (\%)} = OD_{\text{experimental group}} / OD_{\text{blank group}} \times 100\%$$

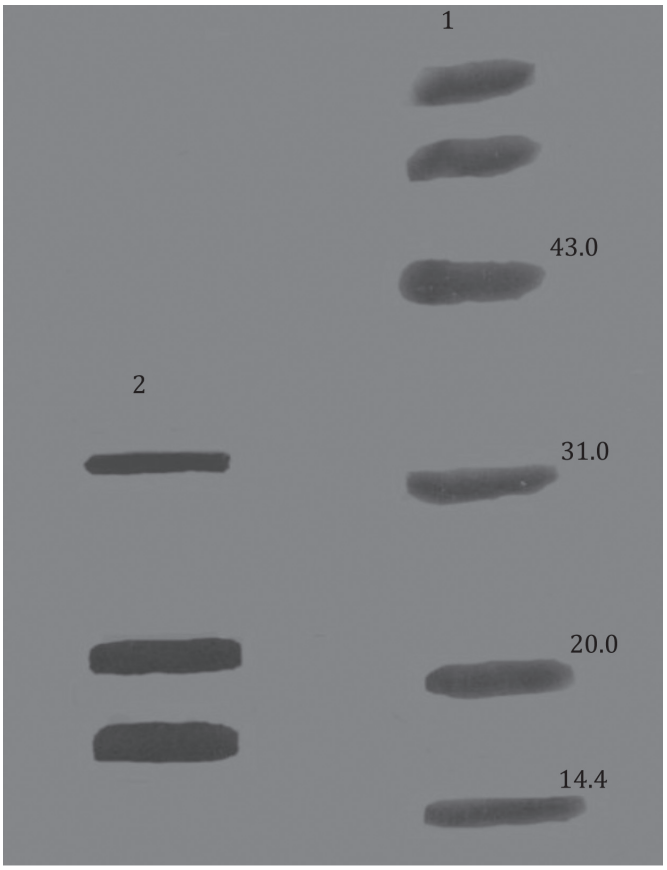

Fig.1. Molecular weight determination of *Porphyra haitanensis* R-PE on 12% SDS-PAGE. Lines:1, protein molecular mass standard in kDa; 2,R-PE purified from *Porphyra haitanensis* (purity, A565/A280=3.3)

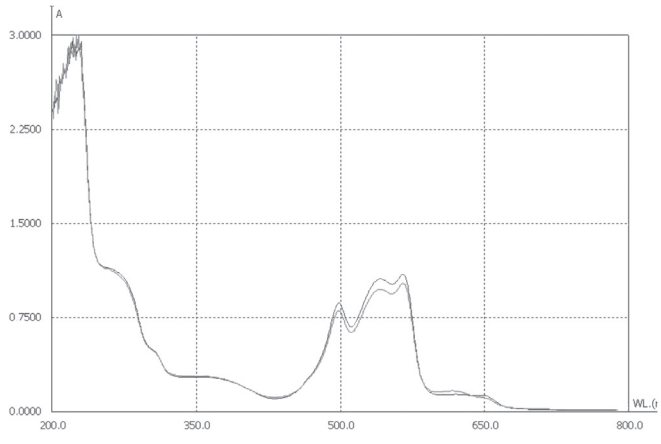

Fig.2. UV-vis overlay spectrum of R-PE

2.2.3. Cell apoptotic analysis by Annexin V-FITC / PI double fluorescent

At the exponential phase stage, 5×10^5 /mL cells were inoculated in 24-well plates with serum-free DMEM and treated with 0, 15, 30 or 60 μg/mL R-PE for 4h before laser irradiation. The PDT excitation wavelength was 632.8nm and energy intensity was 12.5 J/cm^2 laser light. The negative control and positive control groups were set up with treatments of 15, 30 or 60 μg/mL R-PE and with 20 μg/mL 5-fluorouracil. The cells were cultured in DMEM containing 10% serum for 24h. After the cells were washed with cold 10 mM PBS, Annexin V-FITC / PI double fluorescence dyeing liquid was added and the plates were placed in the dark for 15 min. The morphology of the HeLa cells was examined under a fluorescence microscope.

2.2.4. RNA isolation and cDNA synthesis

Total RNA was extracted from HeLa cells treated with 0, 15, 30 or 60 μg/mL R-PE for 4h before laser irradiation, using an RNAiso plus kit according to the manufacturer's instructions. Each concentration was repeated 3 times. The extracted RNA was treated with RNase-Free DNase to remove contaminating DNA, and cDNA was synthesized using the PrimeScript RT Reagent Kit following the manufacturer's instructions.

2.2.5. mRNA expression of caspase and Bcl-2

Caspase and Bcl-2 cDNA were amplified from the extracted total RNA (2 μg) using primers caspase-F, caspase-R and Bcl-2-F, Bcl-2-R, respectively (Table 1), under the following conditions: pre-denaturation at 95 °C for 2 min, 30 cycles of 95 °C for 30s, 60 °C for 30s, followed by a final elongation at 74 °C for 5 min. As an internal control, a crab beta-actin cDNA fragment was amplified with primers beta-actin-F and beta-actin-R (Table 1) and the same PCR amplification conditions.

TABLE 1

Nucleotide sequence of primers

primer	Sequence(5′- 3′)
Caspase-3-F	GGTTCATCCAGTCGCTTTG
Caspase-3-R	GCTTTCCACCGTTGTCTC
Caspase-10-F	GTATCAGGCTACCCAGTCC
Beta-actin-F	GTTGCGTTACACCCTTTC
Beta-actin-R	CTTGCCACTTCCACTGTC
Bcl-2-R	GTTCTTCGACTCGCTCAC

2. 3. Anti-tumor activity of R-PE on S180 tumor-bearing mice

2.3.1. Model establishment of S180 sarcoma

S180 tumor cells in mice were reproduced by ascites serial passage 3 times, 7 days per passage. S180 tumor cells were extracted from the last tumor-bearing mice under sterile conditions. The cell concentration was adjusted to 1.4×10^7 /mL with cold sterile saline, then 0.2 mL cell suspension fluid was inoculated in the left fore oxter of the mice.

2.3.2. Experimental design Male mice (28±2 g/mouse) were used in the experiments. Seventy two mice were arranged into six groups (n = 12): The blank group served as a normal control and received distilled water at level of 0.2 ml/day for 9 days. The model group served as an S180 sarcoma group and received distilled water at level of 0.2 ml/day for 9 days. The positive drug group served as an S180 sarcoma group and received 5-FU (20 mg·Kg^{-1}bw·d^{-1}) (15) for 9 days. The R-PE low-dose group served as an S180 sarcoma group and received R-PE (100 mg·Kg^{-1}bw·d^{-1}). The R-PE middle-dose group served as an S180 sarcoma group and received R-PE (200 mg·Kg^{-1}bw·d^{-1}). The R-PE high-dose group served as an S180 sarcoma group and received R-PE (300 mg·Kg^{-1}bw·d^{-1}). The mice were weighed every other day. At the end of the 9-day treatment, mice were sacrificed. Blood was collected using the eye socket and centrifuged at 1000×g for 10min. Serum was collected for antioxidative experiments and analyzed for TNF-αcontent. Liver and spleen were excised and used for antioxidative and cellular immunity experiments.

2.3.3. Tumor inhibitory rate and immune organ index

The tumor inhibitory rate and the immune organ index were calculated with the following formulae:

Tumor inhibitory rate (%) = tumor weight of text group / tumor weight of blank group×100%
Immune organ index (mg/10g) = weight of organs(mg) / weight of mouse(10g)×100%

TABLE 2

Total protein concentration and spectroscopic purity of *Porphyra haitanensis* R-PE at each stage of purification

Purification step	Purity (OD_{565}/OD_{280})	Quantity (mg)	Yield (mg/g)	Recovery (%)
Crude repeated freeze-thaw extract	0.56	342.6	11.42	
Two step salting-out extraction	1.39	173.4	5.78	50.60
SephadexG-100 chromatography	2.45	58.11	1.94	33.51
ion-exchange chromatography	3.30	50.42	1.68	86.69

2.3.4. SOD activity and MDA content analysis

SOD enzyme activity and the MDA content in liver and serum were determined using the commercial kit according to the manufacturer's instructions.

2.3.5. Splenic lymphocyte proliferation capacity of tumor-bearing mice

Spleen cells were prepared in sterile conditions and were diluted to 2×10^6/mL with the complete culture medium. The cell suspension liquid was inoculated in 96-well plates, 200 μL per well, 4 wells with each treatment group; three of them with 5μL 200 mg/ml ConA (final concentration 5 mg/l) and one well set as blank control with 5μL of the same complete culture medium. The plates were incubated for 3d. 100 μL of supernatant liquid per well was taken 4h before the end of the incubation. After adding 20 μL of MTT solution (5mg/ml), the plates were incubated for 4 more hours. The proliferation capacity of spleen lymphocytes was analyzed using 3-(4,5-dimethylthiazol-2-yl)-2,5-diphenyltetrazolium bromide assay (16,17).

Lymphocyte proliferation capacity (%) = ($OD_{ConA\ treated\ group}$ - $OD_{control\ group}$)

2.3.6. Natural killing activity of NK cells

Spleen cells were prepared in sterile conditions as the effector cell and were diluted to 2×10^7/mL with the complete culture medium. HeLa cells were prepared as the target cell and were diluted to 2×10^5/mL with the complete culture medium. 100 μL of the target cell suspension liquid was inoculated in 96-well plates and 4 wells for each treatment group and cultivated for 8h. The isopycnic effector cells were added in three wells per group, adjusting the ratio of effector cells to target cells to 100 to 1. The remaining wells were set as two control groups of the target cell and the effector cell wells. The cells were incubated in an incubator at 37 °C with 5% CO_2 for 4h. Cell survival rate was determined by MTT assay(18) using the following formula.

Natural killing activity of NK cells (%)=[$OD_{target\ cell\ group}$ - ($OD_{target\ cell\ treated\ with\ effector\ cell\ group}$-$OD_{effector\ cell\ group}$)]/ $OD_{target\ cell\ group}$

2.3.7. TNF-α secretion capacity of the spleen cells

TNF-α secretion capacity of the spleen cells in mice was determined using enzyme-linked immunosorbent assay (ELISA) according to manufacturer instructions.

2.3.8. Histopathology

The tumor specimens were examined microscopically after routine preparation (19). The tumor-bearing mice treated with 5-FU and different concentrations of R-PE were sacrificed 9 days after establishment of the S180 sarcoma model. Tumors were fixed using 10% neutral buffered formalin solution for 24h and then dehydrated in a series of different concentrations of ethanol, infiltrated with xylene and paraffin and embedded in paraplast. The specimens were serially sectioned (6 μm thickness) with a microtome and stained on microscope slides using haematoxylin and eosin (H&E). The stained slides were observed and photographed using a fluorescence microscope (20).

2.3.9. Statistical analysis

Data were expressed as mean ± 1 SD for at least three experiments. Student's t-test was used to compare data. The data with $P<0.05$ were considered to be statistically significant.

3. RESULTS

3.1. Extraction and purification of R-PE

The purity and homogeneity of the R-PE extracted from *Porphyra haitanensis* were examined using spectroscopic methods and denaturing gel electrophoresis (Table 2 and Figs. 1 and 2). The purified protein had three subunits, α, β and γ, corresponding to molecular weights of 18, 23 and 33KDa, and had its absorbance maximum at 565nm wavelength.

3.2. R-PE PDT effect on HeLa cells

In order to study R-PE as a photosensitizer on HeLa cells and its cell toxicity in normal cells, we treated cells with different purity and concentrations of R-PE for 4h and irradiated them with 12.5 J/cm2 of HE-NE laser. As shown in Table 3, at a concentration of 60 μg/mL and purity ratio of 3.3, the combination of 4h incubation with the R-PE and laser irradiation resulted in cytotoxicity, where 18.6% ±0.59% of the HeLa cells survived, which is 34% ±0.32% ($n=6$, $p<0.01$) less than the same treatment but without laser irradiation and 1.5% ±0.12% less than 5-FU group. The half lethal dose of R-PE (purity 2.45) for the R-PE+PDT treatment was approximately 15 μg/mL. At this concentration the survival rate of HeLa reached 73.5% ±1.63% without laser irradiation. Cell death induced by R-PE on normal endothelial cells after R-PE+PDT treatment was examined at 3.5-60 μg/mL of R-PE. The results showed that R-PE has low cell toxicity on normal cells and good tumor-targeting characteristics.

As shown in Table 4, when R-PE was incubated with the cells during rinsing with PBS and cells were then irradiated with laser, no cytotoxicity was observed. These results revealed that the laser irradiation (12.5 J/cm2) alone produced no cytotoxicity.

3.3. Apoptotic analysis of R-PE+PDT-treated cells

To investigate the R-PE+PDT effect on cell apoptosis, HeLa cells treated with R-PE alone and the combination of PDT and different concentrations of R-PE (15, 30 or 60 μg/mL) were harvested for morphological observation. As shown in Fig. 3, the blank group of HeLa cells showed tight connections (Figs 3a, 3e); after R-PE treatment the cells became more separated and loosely arranged with increasing concentration of R-PE (Figs.3b, 3c, 3d). The combination treatments of R-PE and PDT changed HeLa cells into oval cells in suspension. A large number of cells lysed (Fig. 3h) after the treatment with the highest concentration of R-PE (60 μg/mL) and PDT.

For morphological observation of the PDT-treated cells, the cells were stained with annexin V-FITC and propidium iodide and examined under a fluorescence microscope. The

green fluorescent spots represent viable apoptotic cells and the red fluorescent spots represent non-viable apoptotic cells. As shown in Fig. 4, the non-viable apoptotic cells increased as the concentration of the R-PE increased (Fig. 4b, 4c, 4d), and the additional PDT treatment significantly enhanced the effect.

3.4. Expression of caspase-3, casapse-10 and Bcl-2 mRNA

Expressions of Caspase-3, Caspase-10 and Bcl-2 mRNA were determined using RT-PCR. As shown in Fig. 5, with increasing concentrations of R-PE Caspase-3 and the Caspase-10 mRNA transcription increased. In contrast, Bcl-2 mRNA transcription decreased as the concentration of R-PE increased.

A quantitative real-time PCR assay was carried out to determine the transcript levels of Caspase-3, Caspase-10 and Bcl-2 in HeLa cells after R-PE+PDT treatment. Caspase-3 mRNA expression increased with increasing concentration of R-PE. At the concentration of 60 μg/mL R-PE Caspase-3 mRNA increased 22.1-fold in comparison to the control (Fig. 6A). However, the transcript levels of Caspase-10 mRNA were unchanged until the concentration of R-PE reached 60μg/mL, where the Caspase-10 mRNA expression increased 8.45-fold in comparison to the control (Fig. 6C). In contrast, Bcl-2 mRNA decreased significantly with increasing concentration of R-PE. At the concentration of 60μg/mL, Bcl-2 mRNA expression decreased 0.15-fold compared to the control (Fig. 6B). All these results were consistent with results shown in Fig. 5.

3.5. Inhibitory effect of R-PE on S180 tumor-burdened mice

As shown in Table 5, the inhibition effect of R-PE on S180 had an obviouse dose effect. The R-PE in the high dose group ($300mg \cdot Kg^{-1}bw \cdot d^{-1}$) showed much greater tumor inhibition rate, 41.3%±1.22% (n=12, $p<0.01$), than the 7.89±0.44 in the 5-FU

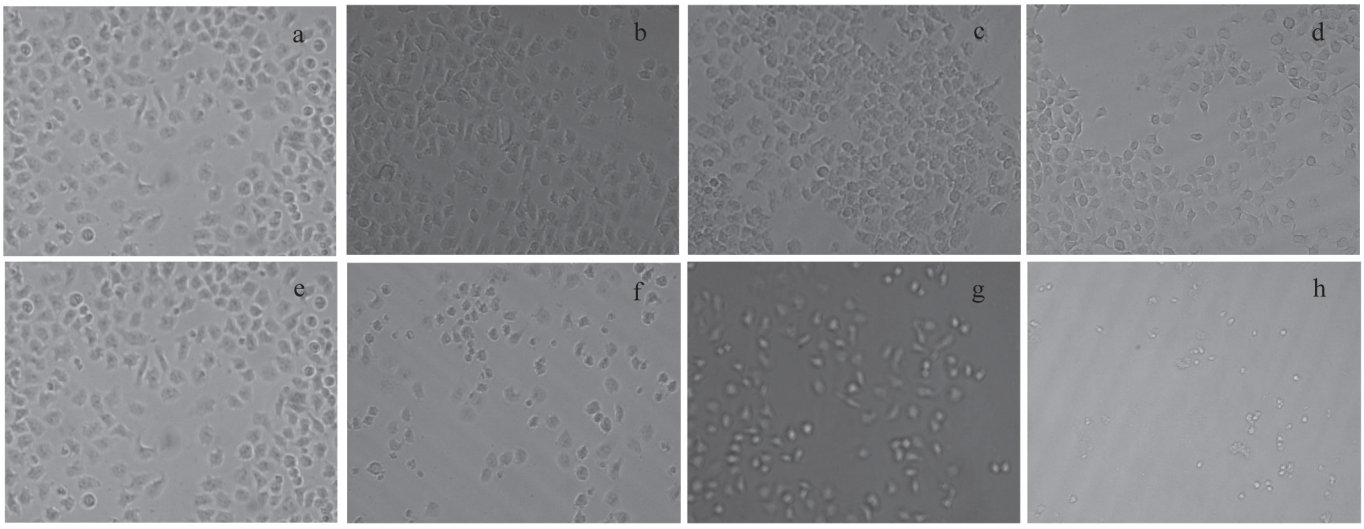

Fig.3. Cell morphological observations. (a), (e)blank group; (b), (c), (d)15, 30, 60μg/mL of R-PE treated group; (f), (g), (h)PDT treated with 15, 30, 60μg/mL R-PE group. Irradiation dose of PDT was 12.5J/cm^2

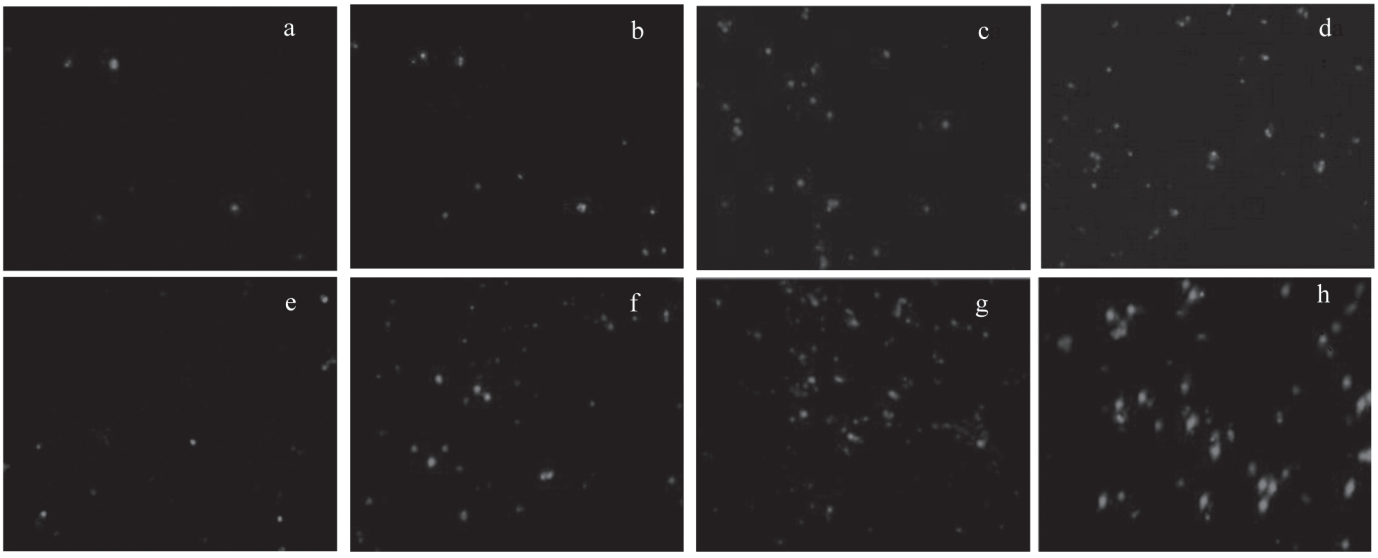

Fig. 4. Cell apoptotic analysis by Annexin V-FITC / PI double fluorescent.(a), (e) blank group; (b), (c), (d) 15, 30, 60μg/mL of R-PE treated group; (f), (g), (h)PDT treated with 15, 30, 60μg/mL R-PE group. Irradiation dose of PDT was 12.5J/cm^2

TABLE 3

PDT effect of R-PE on HeLa cell line. n=6. Mean ± SD. The blank group was the control. *P<0.01 *vs.* control

Group	Cell survival rate(%)					
	HeLa cells				Endothelial cells	
	24h	PDT(24h)	48h	PDT(48h)	24h	48h
Blank	100.0±0.00	100.0±0.00	100.0±0.00	100.0±0.00	100.0±0.00	100.0±0.00
5-FU	23.9±3.47	22.1±4.12	19.3±1.56	20.1±0.47	38.9±0.31	32.6±1.87
Concentration of R-PE (μg/ml), purity ratio 0.56						
3.5	97.9±0.31	96.3±1.42	94.8±3.11	93.9±1.44	97.8±0.06	98.1±0.04
7.0	94.8±1.33	90.3±1.53	90.7±0.89	74.6±3.71	96.3±0.0,9	98.2±0.14
15	87.9±0.24	86.4±1.41	84.5±1.81	71.8±2.99*	96.4± 0.07	97.3±0.05
30	86.9±1.22	72.9±3.11	83.3±1.76	59.4±2.22*	94.5±0.05	97.7±0.35
60	82.1±0.40	59.1±7.87	78.2±0.59	47.1±0.79*	90.0±0.06	93.8±0.25
Concentration of R-PE (μg/ml), purity ratio 2.45						
3.5	93.4±2.36	84.7 ±0.18	89.1±2.16	83.5±0.89	98.3±0.12	98.7±0.04
7	82.7±5.01	71.6±0.67*	84.2±2.08	71.9±0.51*	97.2±0.22	98.1±0.10
15	74.9±10.9	52.4±2.72*	73.5±1.63	48.2±1.30*	97.5±0.09	97.8±0.11
30	69.9±4.64*	33.9±0.75*	58.6±1.14*	29.3±0.27*	96.7±0.15	96.9±0.08
60	57.4±2.20*	20.9±0.86*	52.5±0.91*	18.6±0.59*	92.1±0.08	95.8±0.32

Irradiation dose of PDT was 12.5J/cm^2

TABLE. 4

HeLa cell survival rate irradiated with laser

n=6. Mean ± SD

Laser intensity(J/cm^2)	Cell survival rate (%)	
	24h	48h
0.00	100.00±0.00	100.00±0.00
12.50	97.20±2.38	98.70±3.12

Irradiation dose of PDT was 12.5J/cm^2

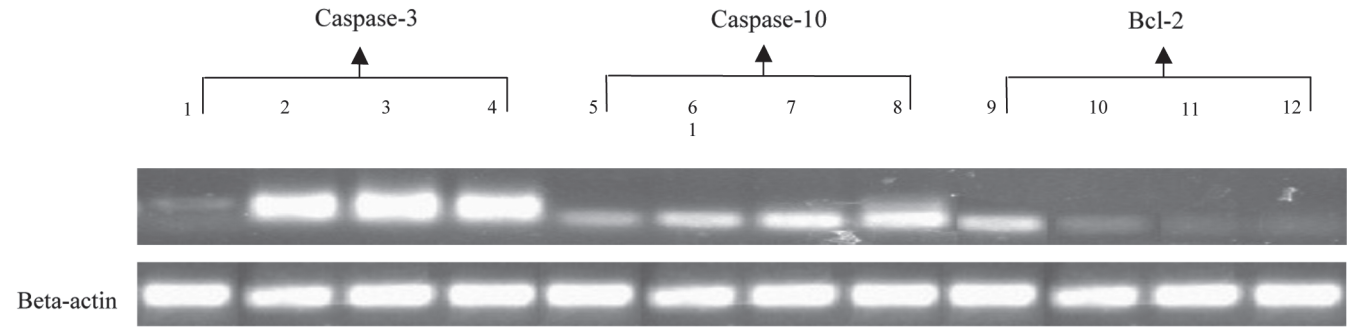

Fig. 5. Detection of Caspase-3, Caspase-10 and Bcl-2 mRNA transcripts in PDT-treated HeLa cells. Total RNA was isolated from HeLa cells for RT-PCR analysis using the Caspase-3, Caspase-10 and Bcl-2 gene-specific primers. The Beta-actin gene was used as a control. Line 1-4, 5-8 and 9-10 all represent 0, 15, 30 and 60 μg/mL R-PE PDT-treated HeLa cells.

($20mg \cdot Kg^{-1}bw \cdot d^{-1}$) treatment group. Furthermore, R-PE appeared to have a significant protection role rather than a harmful role to immune organs of tumor-bearing mice in 5-FU treatment.

In comparison to the model group, R-PE significantly improved SOD enzyme activity and reduced the content of MDA in mice. SOD enzyme activity in the R-PE treatment group was greater than the blank group and reached 109.24±30.89 U/mL.

As shown in Table 5, R-PE increased the rate of lymphocyte production. The lymphocyte prolifiration ratio increased by 66.7%±4.47% for the R-PE high dose group. Furthermore, the R-PE high dose group significantly improved the killing activity of NK cells (n=12, $p<0.01$) on HeLa cells, up to 41.13%±3.74%.

R-PE also significantly irritated the secretion of TNF-αby mononuclear macrophages in tumor-bearing mice (n=12, $p<0.01$).

3.6. Histopathology of the S180 sarcoma sections of the mice

As shown in Fig. 7, the tumor cells in the model group were mononucleated or multinucleated in a large dense patch. Tumor giant cells and the nucleus were hyperchromatic, nuclear division was easy to see and small tumor cells were observed in the cytoplasm .The tumor infiltration of the soft tissue was deep, and less fibrous tissues were observed in the tumor tissue. In contrast, the tumor cells in R-PE treatment group were arranged loosely, and tumor giant cells decreased significantly. Very little tumor infiltration of tumor biopsies was observed. The fibrous tissue increased significantly as the concentration of R-PE increased. A large number of lymphocytes and macrophages were observed to infiltrate into the tumor tissue to kill the tumor cells. Therefore, R-PE showed significant antitumor effect and obviously had a dose effect.

TABLE. 5

Effect of R-PE on the immune ability of mice bearing S180 sarcoma

Group	Normal	Model	5-FU	R-PE(LD)	R-PE(MD)	R-PE(HD)
Inhibition rate (%)	—	—	7.89±0.44	15.11±0.46	32.11±1.39	41.30±1.22[b]
Liver index(mg/10g)	474.49±19.11	539.17±39.31	567.86±25.43	539.48±25.46	564.50±139.59	572.61±12.11
Spleen index(mg/10g)	41.71±1.74	62.21±2.75	52.19±3.10	61.90±1.75	69.67±2.02	76.46±2.46[b]
Thymus index(mg/10g)	36.58±2.12	24.33±1.56	15.89±0.91[b]	35.57±2.31[b]	28.90±1.26	27.09±2.40
serum						
SOD(U/mL)	102.43±13.30	82.67±7.30	57.77±8.34[b]	85.49±9.18	86.40±8.33	109.20±10.89[bb]
MDA (mmol/mL)	4.33±0.41	8.54±0.37[aa]	7.01±1.49	6.77±1.09	6.57±0.19	6.57±0.35
Liver						
SOD(U/mgprot)	280.82±18.22	263.58±12.42	253.48±12.66	267.12±10.46	278.09±11.17	289.64±18.58
MDA(nmol/mgprot)	8.40±0.53	10.90±0.34	8.35±0.24	6.87±0.28	5.40±0.57[b]	4.70±0.18[bb]
Lymphocyte proliferation (%)	60.47±6.43	13.88±1.20[a a]	23.32±2.71[b]	47.90±1.40[b]	51.42±3.12[b b]	66.71±4.47[b b]
NK cells killed activity(%)	25.32±2.31	18.19±1.45[a]	13.70±1.54	21.73±1.93	28.57±2.69[b]	41.09±3.74[b b]
TNF-a level (ng/L)	76.51±1.95	81.10±5.29	92.12±2.96	101.20±0.53[b]	111.2±1.24[b b]	118.50±0.16[b b]

Values are expressed as mean ± SD for twelve mice in each group. One-way ANOVA repeated measures with Duncan's multiple range test was used to calculate statistical significance.

[a] Indicates statistical significance of $p < 0.05$ compared to the Normal group;

[aa] $p < 0.01$ compared to the Normal group;

[b] $p < 0.05$ compared to the Model group.

[b b] $p < 0.01$ compared to the Model group.

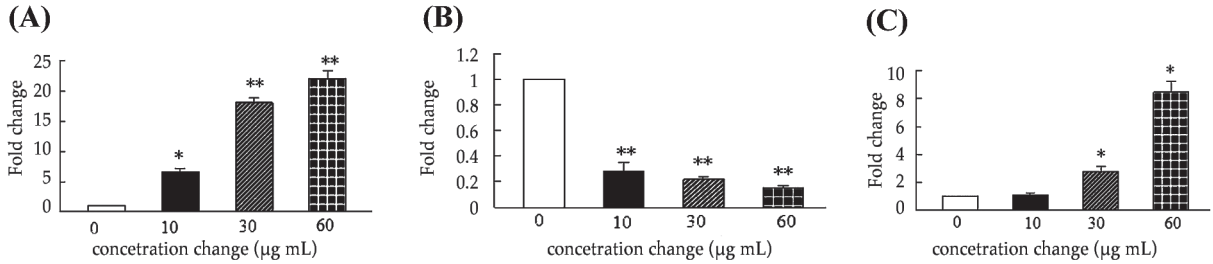

Fig. 6 Quantitative real-time PCR analysis of Caspase-3(A), Caspase-10 (C)and Bcl-2 (B)mRNA transcripts in PDT-treated HeLa cell after treated with 0, 10, 30 and 60μg/mL R-PE.Caspase-3, Caspase-10 and Bcl-2 mRNA levels were normalized with beta-actin mRNA levels. Bars represented the mean±SD (n=3) .significant differences between R-PE PDT-treated and the control were indicated with one ($p < 0.05$) or two ($p < 0.01$) asterisks.

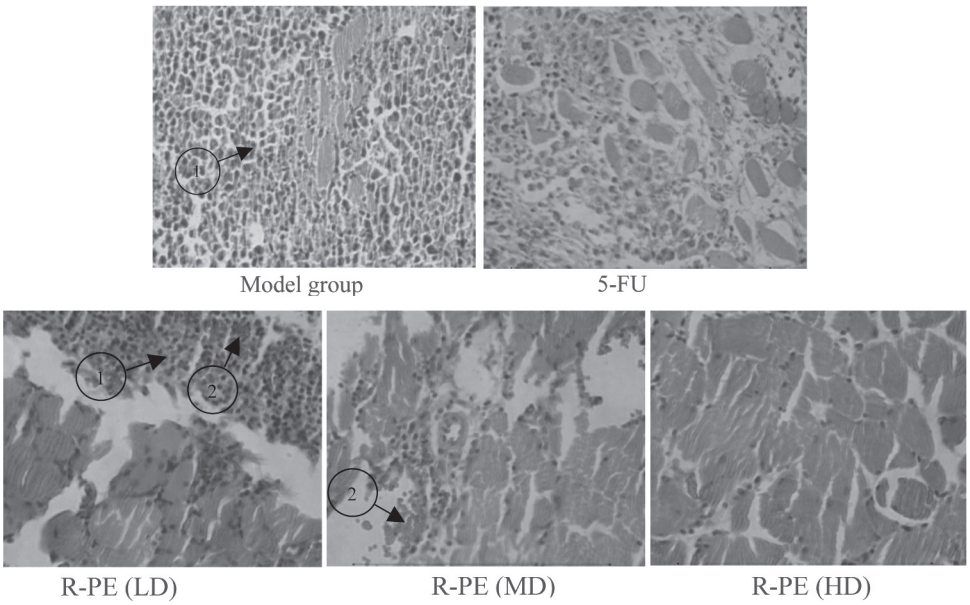

Fig. 7 Histopathology and cytopathology of the S180sarcoma sections of the mice (tissues were stained with H&E, 200×). (arrow 1) S180 sarcoma cells, (arrow 2) lymphocyte and phagocyte cells.

4. DISCUSSION

Phycoerythrin fluorescence properties are a consequence of interactions between covalently bound bilin chromophores and the apoprotein (21). Phycoerythrin was found to be sensitive to heat and light in aqueous solution and has strong fluorescence properties *in vitro*. Under laser irradiation (22), R-PE can absorb and transmit the light to the surrounding oxygen and produce singlet and reactive oxygen species components. These light reaction products can kill cancer cells (23). Antitumor drugs screening by cancer cells has been widely adopted. *In vitro* experiments showed that R-PE has a significant inhibition on HeLa cells; this effect is obviously dose dependent and additional PDT treatment can obviously improve the effect.

Cell apoptosis is a kind of energy dependence and programmed cell death. Caspase, a member of the aspartic acid specific homocysteine protease (caspase) family, can degrade the antiapoptotic protein and induce the release of cytochrome C of mitocondria. Caspase can also reduce the inhibitory effect of DNAase by ICAD (inhabitor of caspase DNAase) and improve the [Ca^{2+}] density of cells and activate the DNases, thus inducing cell apoptosis (24, 25). On the contrary, Bcl-2 protein can inhibit cell apoptosis by reducing membrane permeability of the mitochondria and preventing the release of cytochrome C (26). *In vitro* characterization studies revealed that exposure with R-PE to 632.8 nm laser light produced significant cytotoxicity on HeLa cells in a concentration-dependent manner. QRT-PCR studies showed that R-PE promoted the mRNA expression of caspase-3 and caspase-10, but inhibited the mRNA expression of Bcl-2 in a concentration-dependent manner.

It is generally acknowledged that cellular immunity plays a leading role in anti-tumor immunity. Cellular immunity is mediated by sensitized T cells and lymphatic factor; its characteristic is the inflammation caused by cell infiltrating, and lymphocyte T cells, macrophages, and the mechanism of NK cells are the important effect cells (27). *In vivo*, R-PE can improve lymphocyte proliferation capacity, the kill activity of NK cells of tumor-bearing mice and inhibit tumor growth.

Tumor necrosis factor a (TNF-a) secreted by mononuclear macrophages can combine with TNFR I to induce cell apoptosis by the death structure domain of the cell. It can also increase the membrane surface molecules of cell apoptosis (FAS) to express and through the FAS/FASL pathway induce the cell apoptosis. Meanwhile, TNF-a can inhibit the angiogenesis of the tumor and obviously increased the kill activity of the LAK cells, tumor infiltrating lymphocyte cells and NK cells (28). The results from this study demonstrated that the anti-tumor effect of R-PE resulted through its anti-oxidative activity, improving apoptosis protease gene expression, immunity enhancement and promoting the secretion of the TNF-α. Therefore R-PE could be a potential drug in the prevention of cancer.

ACKNOWLEDGMENTS

This work was sponsored by the Industry-University-Research Collaboration program of Guangdong Province (No. 2010B090400461), Science and Technology Program of Guangdong Province and Shantou City(Nos. 2010B020201015 & 2011-156).

REFERENCES

1 GlAZER A (1985) Light harvesting by phycobilisomes. Annual Review of Biophysics and Biophysical Chemistry 14: 47-77

2. ASHA, PARMA NIRA J, KUMAR SING H, AUANI KAUS HAL, DATTA MADAMWAR (2011) Characterization of an intact phycoerythrin and its cleaved 14KDa functional subunit from marine cyanobacterium phormidium sp. A27DM. Process Biochemistry 46: 1793-1799

3. CONTRERAS MARTEL C, MARTINEZ OYANEDEL J, BUNSTER M, LEGRAND P, PIRAS C, VERNEDE X, FONTECILLA CAMPS J (2001) Crystallization and 2.2Aresolution structure of R-phycoerythrin

from Gracilaria chilensis: a case of perfect hemihedral twinning. Acta Crystallographica Section D: Biological Crystallography 57: 52–60.
4. SUN L, WANG SM, GONG XQ, ETAL (2009) Isolation, purification and characteristics of R-phycoerythrin from a marine macroalga heterosiphonia japonica.Protein Expres Purif 64(2): 146-154
5. SIBATA CH, COLUSSI VC, OLEINICK NL, KINSELLA TJ (2001) Photodynamic therapy in oncology. Exp Opin Pharmacother 2: 917–927.
6. HENDERSON BW, GOLLNICK SO (2003) Mechanistic principles of photodynamic therapy. In: Vo-DinH T, editor. Biomedical photonics Handbook. Boca Raton (FL): CRC Press 36.1–36.27
7. HUANG B, WANG GC, ZENG CK, LI ZG (2002) The experimental research of R-phycoerythrin subunits on cancer treatment.A new photosensitizer in PDT. Cancer Biother Radiopharm 17: 35–42
8. TRIESSC HEIJN M, BAAS P, SCHELLENS JHM, STEWRT FA (2006) Photodynamic therapy in oncology. Oncologist 11: 1034-1044
9. LING HU, BEI HUANG, MAN MAN ZUO, RUI YONG GUO, HAO WEI (2008) Preparation of the phycoerythrin subunit liposome in a Photodynamic experiment on liver cancer cells. Acta Pharmacol Sin 29(12): 1539-1546
10. GONZALO RODRÍGUEZ BERRIGUETE BS, LAURA GALVIS BS, BENITO FRAILE PHD, ETC (2012) Imnunoreactivity to caspase-3,caspase-7,caspase-8 and caspase-9 forms is frequently lost in human prostate tumors.Human pathology 43: 229-237
11. AN CHIN CHENG, TZOU CHI HUANG, CHING SHU LAI, MIN HSIUNG PAN (2005) Induction of apoptosis by luteolin through cleavage of Bcl-2 family in human leukemia HL-60 cells. European Journal of Pharmacology 509: 1-10
12. MARYLA KRAJIEWSKA, ROBERT E, ROSENTHAL, JOWITA MIKOLJICZYK, HENNING R, STENNICKE, ETAL (2004) Early processing of Bid and caspase-6,-8, -10, -14 in the canine brain during cardiac arrest and resuscitation. Experimental Neurology 189: 261-279
13. TAPAS K, MAKAR, DAVID TRISLER, CHRISTOPHER T, BEVER, JAMES E, GOOLSBY, ETAL (2008) Stem cell based delivery of IFN-β reduces relapses in experimental autoimmune encephalomyelitis. Journal of Neuroimmunology 196: 67-81
14. PAUL TAWA, ANDRE GIROUX, ERICH GRIMM, YONGXIN HAN, DONALD W, NICHOLSON, STEVEN , XANTHOUDAKIS (2006) Correlating the fractional inhibition of caspase-3 in NT2 cells with apoptotic markers using an active-caspase-3 enzyme-linked immunosorbent assay. Analytical Biochemistry 350: 32-40
15. GEFEI ZHOU, WEN XU SHENG, WEN HONG YAO, CHANG HAI WANG (2006) Effect of low molecular λ-carrageenan from chondrugs ocellatus on antitumor H-22 activity of 5-FU. Pharmacological Research 53: 129-134
16. QING LI, YUKIYO HIRATA, SHUNAI PIAO, MASAYASU MINAMI (2000) Immunotoxicity of N,N-diethylaniline in mice: effect on natural killer activity, cytotoxic T lymphocyte activity, lymphocyte proliferation response and cellular components the spleen. Toxicology 150: 179-189
17. CESAR TEIJON, ROSA OLMO, MARIA DOLORES BLANCO, ARTURO ROMERO, JOSE MARIA TEIJON (2003) Effects of lead administration at low doses by different routes on rat spleens. Study of response of splenic lymphocytes and tissue lysozyme. Toxicology 191: 245-258
18. IVAN ZANONI, FRANCESCA GRANUCCI, MARIA FOTI, PAOLA RICCIARDI, CASTAGNOLI (2007) Self-tolerance dendritic cell(DC)-mediated activation and tissue distribution of natural killer (NK) cells. Immunology Letters 110: 6-17
19. MONTIRONI R, VAN DER KUWAST T, BOCCON-GIBOD L, BONO AV, BOCCON-GIBOD L (2003) Handling and pathology reporting of radical prostatectomy specimens. Eururol 44(6): 626-636
20. LAWRENCE A, LACEY, DARLENE F, HOFFMANN, BRIAN FEDERICI A (2011) Histopathology and effect on development of the phopGV on larvae of the potato tubermoth, phthorimaea operculella(Lepidoptera:G elechiidae). Journal of invertebrate pathology 108: 52-55
21. ANDERSON LK, GROSSMAN AR (1990) Structure and light-regulated expression of phycoerythrin genes in wild-type and phycobilisome assembly mutants of synechocystis sp. Strain PCC 6701. J Bacteriol 172: 1297-1305
22. SANJIV K, MISHRA, ANUPAMA SHRIVASTAV, IMRANPANCHA, IE (2010) Effect of preservatives for good grade C-phycoerythrin, isolated from marine cyanobacteria Pseudanabaena sp. International Journal of Biological macromolecules 47: 597-602.
23. HE JA, HU YZ, JIANG L J (1997) Photodynamic action of phycobiliproteins: In situ generation of reactive oxygen species. Biochimica et Biophysica Acta-Bioenergetics 1320: 165-174.
24. GIRI A, NARASU M L (2000) Production of podophyllotoxin from podophyllum hex and rum: a potential natural product for clinically useful anticancer drugs. Cytotechnology 34: 17-26
25. LOGUE SE, MARTIN ST (2008) Caspase activation cascades in apoptosis. Biochem Soc Trans 36: 1-9
26. KIM NEWTON, ANDREAS STRASSER (1998) The Bcl-2 family and cell death regulation. Current opinion in Genetics & Development 8: 68-75
27. JEFF J, SUBLESKI, ROBERT H, WILTROUT, JONATHAN M, WEISS (2009) Application of tissue-specific NK and NKT cell activity for tumor immunotherapy. Journal of Autoimmunity 33: 275-281
28. MICHAEL KARPUSAS, TERESA G, CACHERO, FANG QIAN, ANN BORIACK-SJODIN, COLLEEN MULLEN, ETAL (2002) Crystal Structure of Extracellular Human BAFF, a TNF family that stimulates B Lymphocytes. J.Mol.Biol 315:1145-1154